BERICHTE
aus dem Fachbereich Geowissenschaften
der Universität Bremen

Nr. 152

Karwath, B.

ECOLOGICAL STUDIES ON LIVING AND FOSSIL CALCAREOUS DINOFLAGELLATES OF THE EQUATORIAL AND TROPICAL ATLANTIC OCEAN

Berichte, Fachbereich Geowissenschaften, Universität Bremen, No. 152,
175 pages, Bremen 2000

ISSN 0931-0800

BERICHTE
aus dem Fachbereich Geowissenschaften
der Universität Bremen

Nr. 152

Karwath, B.

ECOLOGICAL STUDIES ON LIVING AND FOSSIL CALCAREOUS DINOFLAGELLATES OF THE EQUATORIAL AND TROPICAL ATLANTIC OCEAN

Berichte, Fachbereich Geowissenschaften, Universität Bremen, No. 152,
175 pages, Bremen 2000

ISSN 0931-0800

The "Berichte aus dem Fachbereich Geowissenschaften" are produced at irregular intervals by the Department of Geosciences, Bremen University.

They serve for the publication of experimental works, Ph.D.-theses and scientific contributions made by members of the department.

Reports can be ordered from:

Gisela Boelen

Sonderforschungsbereich 261

Universität Bremen

Postfach 330 440

D 28334 BREMEN

Phone: (49) 421 218-4124

Fax: (49) 421 218-3116

e-mail: eggerich@uni-bremen.de

Citation:

Karwath, B.

Ecological studies on living and fossil calcareous dinoflagellates of the equatorial and tropical Atlantic Ocean.

Berichte, Fachbereich Geowissenschaften, Universität Bremen, No. 152, 175 pages, Bremen, 2000.

ISSN 0931-0800

ECOLOGICAL STUDIES ON LIVING AND FOSSIL CALCAREOUS DINOFLAGELLATES OF THE EQUATORIAL AND TROPICAL ATLANTIC OCEAN

Dissertation

zur Erlangung des Doktorgrades
Fachbereich Geowissenschaften
Universität Bremen

vorgelegt von
Britta Karwath
Bremen, 1999

Tag des Kolloquiums

05.11.1999

Gutachter:

1. Prof. Dr. H. Willems
2. Prof. Dr. V. Smetacek

Prüfer:

1. Prof. Dr. G. Wefer
2. Prof. Dr. K. Herterich

ACKNOWLEDGEMENTS

I wish to express my gratitude to Prof. Dr. Helmut Willems for the initiation and supervision of this dissertation and his advice throughout this work.

My gratitude also goes to my advisor Dr. Dorothea Janofske for many animating discussions, her enthusiasm and general support.

Thanks also go to the technicians of the work group without whose help and experience this dissertation would not have been possible. Special mention is due to Monika Kirsch, Angelika Freesemann and Anja Meyer, whose dedication and encouragement went above and beyond the call of duty.

I am grateful to all the cruise participants of the *RV Meteor* expeditions M 34-4, M38-1 and M41-4, particularly Volker Ratmeyer and Gerhard Fischer who provided their CTD data so freely. Dr. Gerard J.M. Versteegh (Netherlands Institute for Sea Research, NIOZ, Netherlands) provided insights that improved this thesis. A general "thank you" also goes to all the members (past and present) of the AG Willems, especially those who have laboured onboard the RV Meteor day and night, taking samples and Dirk Krautwig for his extraordinary help with the Temperature and Light Gradient Box.

My gratitude goes to Sabine Gerhardt and Anja Meyer for being there when I needed them most and also to Frank Thiess and his family for giving their support to me for such a long time. I thank all my friends and family for their warmth and help, particularly my sister Bettina and her husband Adam Price. Their quick and thorough correction of my English is highly appreciated, though I reserve the right to claim any mistakes exclusively as my own. My gratitude goes to my parents for everything parents could give.

This work was financed by the Deutsche Forschungsgemeinschaft (Wi 725/7; 'Morphogenese und Produktivität kalkiger Dinoflagellaten unter kontrollierten Zuchtbedingungen') and was supported by the Sonderforschungsbereich 261 'Der Südatlantik im Spätquartär: Rekonstruktion von Stoffhaushalt und Stromsystemen' and the Graduiertenkolleg 'Stoff-Flüsse in marinen Geosystemen' at the Universität Bremen.

SUMMARY

Pelagic dinoflagellates that form calcareous skeletal elements are part of the calcareous phytoplankton in warm and temperate waters. These calcareous dinoflagellates have only recently been subjected to closer study, both concerning their cyst-theca relationship, their distribution in the plankton and their sedimentary signal. Their environmental affinities are largely unknown. The major objective of this dissertation is to add to the basic knowledge about marine calcareous dinoflagellates in these matters since such information is needed to enable the evaluation of the applicability of this phytoplankton group as a possible palaeoenvironmental indicator.

To this end, several biological and palaeontological approaches were used. Especially for these studies, various preparatory and experimental methods had to be developed. These included the design of a temperature gradient box (TGB) in co-operation with the Department of Production Engineering at the University of Bremen, a light gradient box (LGB), their operation during culture experiments, and the surrounding set-up. The gradient boxes allowed the simultaneous culturing of phytoplankton under different temperature and irradiance conditions. Other newly developed methods dealt with the onboard isolation and culture of calcareous dinoflagellates and the quantification of the skeletal remains of these organisms from plankton and sediment material.

At the centre of attention was *Thoracosphaera heimii* (Lohmannn) Kamptner, which was chosen for its dominance of the calcareous dinoflagellate assemblage within both the plankton and the sediment (Dale, 1992a; Kerntopf, 1997; Höll, 1998). This prevalence of *T. heimii* in the calcareous dinoflagellate associations can be explained by the predominantly vegetative-coccoid nature of this species: in contrast to other calcareous dinoflagellates, most of the cells in a culture of *T. heimii* form a calcareous skeleton (Tangen et al., 1982; Inouye and Pienaar, 1983). Other reasons why *T. heimii* was selected were the already established taxonomic position (Tangen et al., 1982), the known life-cycle (Tangen et al., 1982; Inouye and Pienaar, 1983) and the availability of the species as strains from culture collections. Later, fresh strains of *T. heimii* gained from onboard isolation were added to the stock of accessible cultures and also used to conduct laboratory experiments on the reaction of the species to environmental change. Due to the basically geological formulation of the problem, the attention was focused on the fossilisable calcareous stage of *T. heimii*.

The first manuscript (see chap. 3.1) deals with one of the basic environmental affinities of *T. heimii*, the temperature related growth range. The growth range was established for two

strains with the use of the TGB in a temperature gradient from 8°C to 34°C under different nutrient levels. During these experiments, the cultures were growing from 14°C to 27°C. At low temperatures, exponential growth lasts for a very long time (over 50 days) but is very efficient. The most stable of the strains (A603) showed highest final yield at 16°C which was five times higher than at 27°C, even though the growth rate is the highest at 27°C. The response curve of growth rates during exponential phase *vs.* temperature of all experiments was not unimodal. Growth rates rise with increasing temperatures and reach maximal values at 27°C. Despite different nutrient levels, growth rate and final yield at 27°C are approximately the same. Mean diameters of *T. heimii* shells were measured (n=300) in the different cultures to check whether a temperature dependence exists. Results show that there is no clear relation to growth temperature. The calcification of *T. heimii* shells, however, is inversely related to temperature.

In a further step (second manuscript; see chap. 3.2), the spatial distribution of *T. heimii* was surveyed in the upper water column (10 m to 200 m) of the equatorial and tropical Atlantic Ocean. Samples were taken during two *RV Meteor* cruises (M38-1 and M41-4) in January / February 1997 and May / June 1998. The study distinguishes between *T. heimii* shells with cell content (further referred to as 'calcified *T. heimii* cells') and without cell content (further referred to as '*T. heimii* shells'). This distinction is made to see if a special part of the water column is preferred by the species, and if this is the case, which water layer is subsequently represented by *T. heimii* in the fossil record. The vertical distribution of calcified *T. heimii* cells has shown a preferred water depth between 50 m and 100 m. The maximum occurrences of calcified *T. heimii* cells coincide with relatively lower temperatures and relatively higher salinities than those of surface water conditions.

In the third manuscript (see chap. 3.3), the more detailed depth profiles of cruise M41-4 were chosen to take a closer look at the vertical distribution of calcified *T. heimii* cells in relation to density, chlorophyll *a* and light intensity at the given depths. The results from this study were compared with experiments dealing with the reaction of two *T. heimii* strains to different light intensities (10 $\mu Em^{-2}s^{-1}$ to 800 $\mu Em^{-2}s^{-1}$, photosynthetically active radiation, PAR) under controlled laboratory conditions (22.5°C). The results of the field studies show strong peaks of *T. heimii* within the deep chlorophyll maximum (DCM) at or below 1% PAR of surface irradiation. This distribution pattern is not caused by cell accumulations above a density gradient, since the maxima occur in some cases together with the DCM below the pycnocline. The laboratory studies have indicated that *T. heimii* is highly adaptable to high and low irradiances. However, the species is also able to produce as many or more cells at

40 $\mu Em^{-2}s^{-1}$ (equalling about 1% PAR of surface irradiance in the waters examined) as at 500 $\mu Em^{-2}s^{-1}$ (about 10 m water depth under clear skies) under the same nutritional conditions. All in all the results have shown that though *T. heimii* is not totally restricted to the DCM, the species prefers this niche and is well adapted to an existence within the deeper levels of the euphotic zone.

Three of the most common calcareous dinoflagellates in the equatorial and tropical Atlantic Ocean apart from *T. heimii* were examined in the fourth contribution to this dissertation (see chap. 3.4). These species (*Calciodinellum albatrosianum* (Kamptner) n. comb., *Leonella granifera* (Fütterer) n. gen., *Pernambugia tuberosa* (Kamptner) n. gen.) were previously recorded only from sediment samples, the motile stages are described here for the first time. In a similar investigation to those made with *T. heimii*, the horizontal and vertical distribution of *C. albatrosianum*, *L. granifera* and *P. tuberosa* was studied in surface water samples (*RV Meteor* cruise M41-4). The occurrences of these three species could be connected to oceanic environments with SST above 22°C. They appear under upwelling as well as oligotrophic conditions and show a less clear pattern than *T. heimii*.

The fifth and final manuscript (see chap. 3.5) deals with the palaeoenvironmental information gained from calcareous dinoflagellates in Late Quaternary sediments. Two gravity cores recovered from the eastern and western tropical Atlantic Ocean were compared with regards to their changing content of calcareous dinoflagellates. The assemblage within the cores is dominated by *T. heimii*. Accumulation rates of calcareous dinoflagellates during the last 140 ka were much higher in the oligotrophic western region than in beneath the highly productive water masses in the east. The increase of calcareous dinoflagellate production (mostly *T. heimii*) in both areas can be related to relatively stratified oligotrophic conditions of the upper water column in the west.

All of the various aspects investigated during this dissertation, from culture experiments through plankton research to examination of Quaternary sediments, hint directly and indirectly at the link of *T. heimii* to open ocean and stratified conditions in the upper water column. This relative stratification is the basis for the formation of a well developed DCM (Kirk, 1983). Since *T. heimii* is a species with a strong preference for this water layer, this species could be developed as a useful tool in environmental reconstructions of the lower euphotic zone such as nutricline dynamics and palaeoproductivity.

TABLE OF CONTENTS

1. Introduction

In recent years, much effort has been put into research on the mechanisms that regulate the CO_2 content in the atmosphere and thus influence the world's climate, both in geological times and in the present. Special attention has been given to the primary production in the oceans, which is thought to influence the global climate system through photosynthetic processes (organic carbon pump). Some primary producers additionally influence the climate system by the formation of calcareous skeletal elements (inorganic carbon pump).

One of the major aims has been to establish proxies for primary production to allow reconstructions of the oceans' role as a CO_2 sink or as a CO_2 source, and thus the changing climate. Among the phototrophic calcareous nannoplankton, the group of the coccolithophorids has been widely used for palaeoceanographic reconstructions (e.g. Geitzenauer, 1969; McIntyre, 1967; Geitzenauer et al., 1977; Roth and Coulbourn, 1982 McIntyre and Molfino, 1996). Lately a further group of calcareous primary producers (dinoflagellates which form calcareous skeletal elements) have shown promise in their usefulness as palaeoceanographic indicators (Kerntopf, 1997; Höll, 1998; Zonneveld et al., in press; Vink et al., in press).

1.1 Dinoflagellates

Dinoflagellates (Dinoflagellata Bütschli 1885) Fensome et al. 1993) are a group of unicellular eucaryotic organisms and represent one of the major (marine) phytoplankton groups. The motile cells possess two dissimilar flagella, one is laterally directed (transverse flagellum), and the other is beating posteriorily (longitudinal flagellum). The flagella give the organism a unique forward rotating motion: the name "Dinoflagellata" proposed by Bütschli (1885) comes from the Greek *dinos* (whirling rotation) and the Latin *flagellum* (small whip).

The subdivision Dinokaryota sensu Fensome et al. (1993) includes dinoflagellates in which at least one stage in the life-cycle has a dinokaryon. A dinokaryon is defined by the authors as a "...nucleus in which the chromosomes are generally fibrillar [banded] in appearance (i.e. with unmasked DNA fibrils) and are more or less continuously condensed. Histones are absent." (Fensome et al., 1993, p.41). This subdivision contains the vast majority of dinoflagellates.

The class Dinophyceae Pascher 1914 includes dinoflagellates with a dinokaryon throughout their entire life-cycle. Motile cells are usually dominant in this class but life-cycles may include coccoid cells, filamentous stages, and cysts (Fensome et al., 1993).

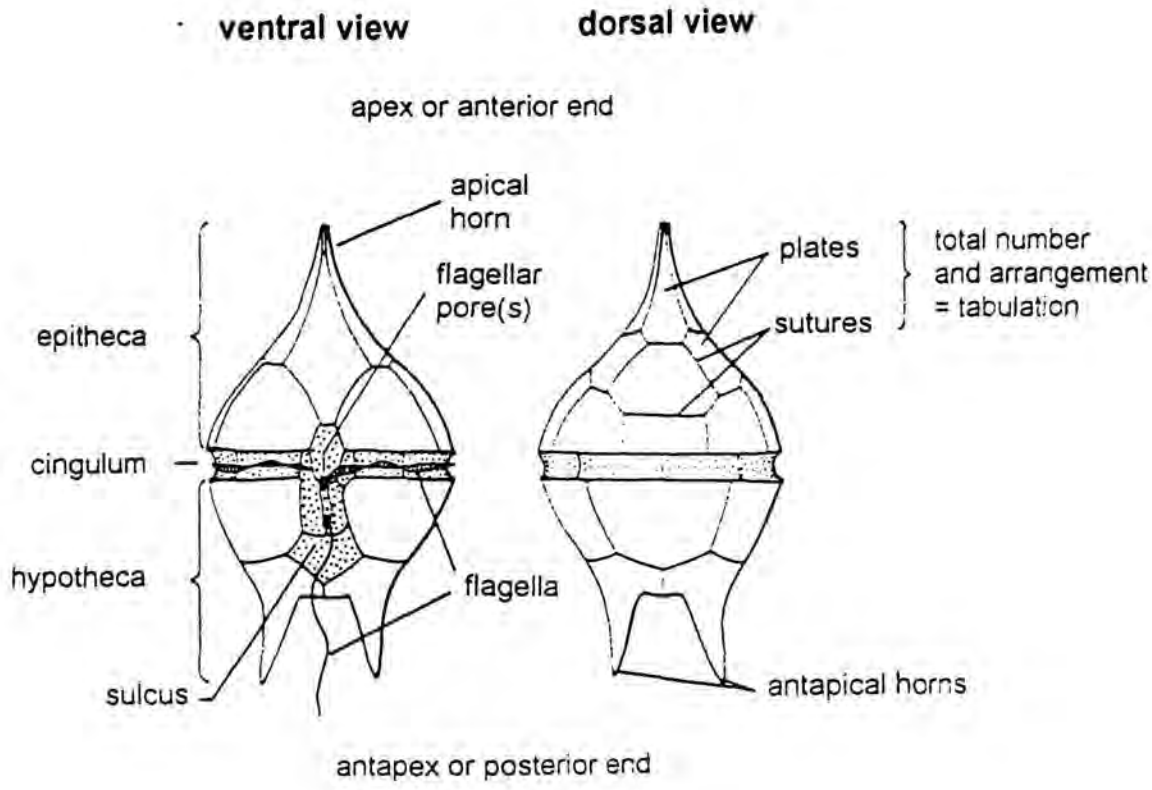

Fig.1: Principal features of the theca in a peridinialean dinoflagellate (after Evitt, 1985).

Skeletal elements are a typical feature of this group, although preservation in recent and fossil sediments is dependent on the material used. Cellulose, which is generally used for the skeletal elements of the motile stages during the life-cycle (theca, Fig.1), is not fossilisable due to rapid microbial decay. The motile stage is, with few exceptions (e.g. *Actiniscus pentasterias*; Hansen, 1993), usually devoid of geologically preservable structures (Evitt, 1985, Dale, 1992b). The wall of the non-motile cyst stage, however, generally contains more resistant material such as an organic sporopollenin-like material (dinosporin; Fensome et al., 1993) and/or calcareous elements (calcite; Wall et al., 1970). For brevity's sake, the species forming calcareous skeletal elements will be here referred to as calcareous dinoflagellates and those using dinosporin as organic dinoflagellates.

From the Triassic onwards calcareous dinoflagellates contribute in significant amounts to the microfossil content of marine sediments (Janofske, 1992), even to the point of being rock-forming (Willems, 1992). The majority of publications has dealt with the morphology, taxonomy, and biostratigraphy of this group and studies range from the Triassic to the Neogene (e.g. Willems, 1988; Janofske, 1992; Keupp et al., 1992; Versteegh, 1993; Keupp et

al., 1994; Hildebrand-Habel et al., 1999). Only few data are available on Quaternary and (sub) recent material (e.g. Wall and Dale, 1968; Wall et al., 1973; Fütterer, 1977; Gilbert and Clark, 1982; Janofske, 1996). Work on calcareous dinoflagellates concerning ecological aspects is even more rare, even though calcareous dinoflagellate remains are a potential source of (palaeo-) environmental information (e.g. Höll, 1998; Höll et al., 1998; Zonneveld et al., in press; Vink et al., in press). Presently, this opening field (i.e. ecological research on calcareous dinoflagellates) enjoys the growing interest of the scientific community dealing with calcareous nannoplankton and marine geology.

1.2 Objectives and presentation of results

The main objective of this dissertation is to contribute to the basic knowledge of calcareous dinoflagellates and to gain more data on the environmental affinities and ecology of these organisms, using both geological and biological approaches:

- Case study of the calcareous dinoflagellate *Thoracosphaera heimii* in both field and laboratory observations in comparison to temperature, light, salinity, and nutrients.
- Survey of the horizontal and vertical distribution of calcareous dinoflagellates in the photic zone in relation to environmental data.
- Examination of the variability of calcareous dinoflagellate associations in late Quaternary glacial / interglacial cycles in comparison to established proxies.

The goal of the case study of *T. heimii*, which constitutes the major part of this dissertation, is to get an impression of the environment inhabited by this pelagic calcareous dinoflagellate and thus to provide a data basis for the determination of *T. heimii*'s role as a proxy indicator for palaeoenvironmental reconstructions.

Results are presented in five chapters that correspond to manuscripts in press, submitted or in preparation as follows:

1. *Temperature effects on growth and cell size in the marine calcareous dinoflagellate* Thoracosphaera heimii

A temperature gradient box for the simultaneous testing of a wide range of temperatures on phytoplankton is presented. Two *T. heimii* strains were exposed to temperatures between 8°C and 34°C under different nutrient levels. Growth of the species was observed from 14°C

to 27°C, mean shell diameters show no clear relation to growth temperature. Calcification of *T. heimii* shells is inversely related to temperature.

2. *Spatial distribution of the marine calcareous dinoflagellate* Thoracosphaera heimii *in the upper water column of the tropic and equatorial Atlantic*

We examined the horizontal and vertical distribution patterns of *T. heimii* in the upper 10 m to 200 m of the water column of the study area in relation to temperature and salinity within two different seasons. This first survey has been made to determine which part of the water column is inhabited by *T. heimii* and is subsequently represented as a signal in the sedimentary record by the species. Highest quantities of *T. heimii* shells with cell content have been observed in water depths between 50 m and 100 m.

3. *On the ecology of marine calcareous dinoflagellates: A case study of* Thoracosphaera heimii *in field and laboratory observations*

We compare the vertical distribution of *T. heimii* within the photic zone to chlorophyll *a*, density, and irradiance measurements. The distribution patterns of the species in the field are discussed together with results from irradiance related growth experiments of *T. heimii*.

4. *Oceanic calcareous dinoflagellates of the equatorial Atlantic Ocean: cysts-theca relationship, taxonomy and aspects on ecology*

We present the cyst theca-relationship of three calcareous dinoflagellate species previously only recorded from sediment samples. Horizontal and vertical distribution of the calcareous cyst stages of the three species in surface water samples relate to sea surface temperatures above 22°C under upwelling as well as oligotrophic conditions.

5. *Palaeoenvironmental information gained from calcareous dinoflagellates: the late Quaternary eastern and western Tropical Atlantic Ocean in Comparison*

We compare sediment material including the last 140 ka from cores recovered below the highly productive equatorial divergence of the eastern Atlantic Ocean and the low productivity western tropical Atlantic Ocean. High calcareous dinoflagellate content coincides with low organic carbon accumulation rates and vice versa. Enhanced production of calcareous dinoflagellates can be correlated to periods of reduced palaeoproductivity probably related to relatively stratified conditions of the upper water column.

1.3 *Thoracosphaera heimii* (Lohmann 1920) Kamptner 1944

One of the main reasons we chose *T. heimii* as the subject for intensive study was the species' abundance: whereas organic dinoflagellates are predominant in boreal regions (Dale and Dale, 1992), in the subtropics and tropics the assemblages are mainly composed of calcareous dinoflagellates. The calcareous dinoflagellate associations in turn are often strongly dominated by *T. heimii* (Kerntopf, 1997; also chap. 3.5). Studies by Dale (1992a) on sediment trap material from the Equatorial Pacific Ocean and Equatorial Atlantic Ocean have revealed that the calcareous dinoflagellate association is mainly composed of "thoracosphaerids" (in this case *T. heimii* and *Thoracosphaera granifera* = *Leonella granifera*). In sediment samples taken from the Brazilian continental slope up to 1 % of the dry sediment is made up of calcareous dinoflagellates (see chap. 3.4, App.2, p.135), in this case 75 % of these calcareous dinoflagellates are made up of *T. heimii* (core GeoB 2204-2, 295 cm; see chap. 3.5, App.A, p.163).

Another reason why we chose *T. heimii* as a case study was that the systematic position had been established by Tangen et al. (1982) and confirmed by several other authors (Inouye and Pienaar, 1983; Jones et al., 1983; Bjørnland, 1990; Rowan and Powers, 1992). The systematic positions of the other extant pelagic calcareous dinoflagellates were not clear at that point in our studies. Furthermore, the life cycle of *T. heimii* had already been described in detail by Tangen et al. (1982) and Inouye and Pienaar (1983).

The prevalence of *T. heimii* in the calcareous dinoflagellate associations can be explained by the species' ability to produce large numbers of calcareous spheres in a relatively short period. Its position within the Dinophyceae is thus far unique: in contrast to other calcareous dinoflagellates, most of the cells produced by *T. heimii* form a calcareous skeleton (Tangen et al., 1982). This calcareous wall has been referred to as a "shell" rather than the more usual term "cyst" to stress that it is formed as a dominant vegetative-coccoid life-stage of the species and not as a resting stage (Inouye and Pienaar, 1983).

1.3.1 Taxonomy

In the past, the position of *T. heimii* in the marine calcareous nannoplankton has been under some discussion (Fütterer, 1976; Tappan, 1980; Dudley et al., 1980; Tangen et al., 1982; Inouye and Pienaar, 1983; Jones et al., 1983; Bjørnland, 1990).

To clear this, Tangen *et al.* (1982) undertook a detailed life-cycle analysis of *T. heimii*. They recognised a multiphase life-cycle with the formation of plano- and aplanospores. Aside from a mesocaryotic nucleus typical for dinoflagellates, the authors also reported that *T.*

heimii contains peridinin as the main carotinoid (see also Bjørnland,1990). The photosynthetic pigment peridinin is widespread among dinoflagellates (Jeffrey et al., 1975) and is restricted to this algal class (Taylor, 1987). Tangen *et al.* (1982) removed the genus from the Prymnesiophyceae where it had been placed by Tappan (1980), introducing it instead to a new order Thoracospherales Tangen 1982 into the Dinophyceae.

The fact that *T. heimii* shells are formed asexually, in contrast to the sexual formation generally believed to apply to cysts, and the fact that the calcified cell is the dominant stage, raised some problems in the systematics of what used to be called "thoracosphaerids". *T. heimii* is the type species of the subfamily Thoracosphaeraceae (Schiller 1930). The descriptions of this subfamily and the genus *Thoracosphaera* Kamptner 1927, however, apply to calcareous dinoflagellate cysts (Fütterer, 1976). Since the calcified cell of *T. heimii* is not a resting stage, as the term "cyst" often implies, and has been included in the order Thoracospherales Tangen 1982 as its only member, the term 'thoracosphaerid' would now describe one species only, and not an entire group of calcareous dinoflagellates. The calcareous dinoflagellate cysts, which had also been associated with the term 'thoracosphaerids', are currently under systematic revision (e.g. chap. 3.4).

Order **Thoracospherales** TANGEN in Tangen et al., 1982

Diagnosis Tangen et al. (1982, p. 210): "Marine planktonic dinophytes, photoautotrophic; predominant stage during vegetative life phase coccoid. Coccoid cell spherical, cell wall composed of calcium carbonate elements. Asexual reproduction by formation of aplanospores or planospores or by binary fission of a weakly calcified cell. Spore unarmoured; planospores biflagellate, with transverse and longitudinal grooves. Nucleus spherical, in all life stages with continually condensed chromosomes."

Family **Thoracosphaeraceae** (KAMPTNER, 1928) emend. TANGEN in Tangen et al., 1982

Diagnosis Tangen et al. (1982, p. 210): "Coccoid cell small, calcareous cell wall continuous, spherical, outer surface granular. An aperture in the cell wall formed in connection with spore formation. Calcareous shell formed near the cell surface. Planospores with undulating transverse flagellum and whip-like longitudinal flagellum, coccoid cells, planospores and aplanospores with chloroplasts."

Thoracosphaera (KAMPTNER, 1927)

Diagnosis (Kamptner, 1927; pp 180 – 181): "Testa sphaerroida, diametro 10 –20μ. Vertex flagelliferus pro maxima parte speciminum sine coccolithis. Coccolithi diametro 1-2 μ, alti 1-

2 µ, dense cohaerentes sine ullis interstitiis, lateribus invicern polygonaliter applanatis, foramine centrali."

Thoracosphaera heimii (LOHMANN, 1920) KAMPTNER, 1944

Observations made with the light microscope using polarised light and a gypsum plate have shown a symmetric extinction pattern in the calcareous shell of *T. heimii* (Pl.1, p. 11; chap. 3.4, p. 99; see also Janofske, 1996). Crystals of the shell wall are orientated with their crystallographic optic axis (c-axis) tangentially to the shell surface (Pl.1, Fig.8). A pseudopore is situated in the middle of the polygonal skeletal elements. Figs.9, 10 and 11 (Pl.1) show weakly, medium and well calcified cells, respectively.

The diameter of the calcareous *T. heimii* shell varies between 9 µm and 25 µm. The opening is circular and its diameter of 4 µm to 8 µm (Tangen et al., 1982) is about a third of the shell diameter (Fütterer, 1976). The single skeletal elements have an irregular, polygonal shape (Pl.1, Fig.1). Their width is about 0.8 µm to 2 µm and they are about 1 µm thick. The skeletal elements are made up of rhomboedric crystallites (Fütterer, 1976). A diagrammatic section through a cell covering of a calcified cell (Inouye and Pienaar, 1983) is shown in Fig.3.

The cell covering and size of an uncalcified non-motile cell is about the same as that of a calcified cell except for the absence of a calcium carbonate layer. The swimming cell has no thecal plates; it is about 7 µm wide and 9 µm long and has a slightly spiral, centrally situated girdle and both a transverse and longitudinal flagellum (Inouye and Pienaar, 1983; Pl.1, Fig.6).

1.3.2. Cell-cycles of *Thoracosphaera heimii*

Life-cycle analyses of *T. heimii* were made independently by Tangen et al. (1982) and Inouye and Pienaar (1983). While Tangen et al. (1982) put more emphasis on the systematic consequences of their findings; Inouye and Pienaar (1983) describe the microanatomy and the life cycles of *T. heimii* in greater detail. If not stated otherwise, the following text on life cycle analyses refers to the work of Inouye and Pienaar (1983).

T. heimii follows two main cell cycles (Fig.2). Central to these two cycles are spherical cells, covered with a thick perforated shell of calcium carbonate (Pl.1, Fig.1, Figs. 8 – 11; p.11). Nuclear division takes place within the shell, and, after opening of a circular lid, a binucleate cell is released (Pl.1, Figs.2 and 3).

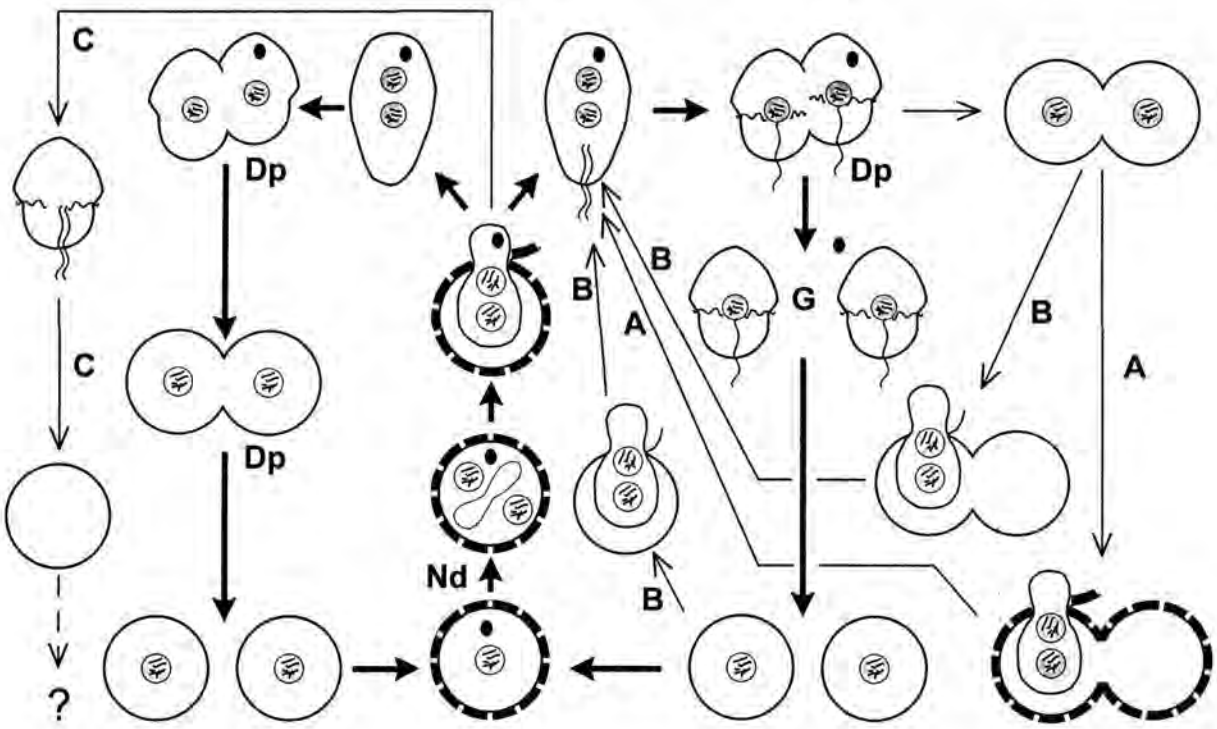

Fig.2: Life-cycles of *Thoracosphaera heimii*. Thick arrows show the main cell-cycles, thin arrows show the subcycles (A, B, C). G: gymnoidinium-like swarmers; Dp: divisional pair; Nd: Nuclear division. Calcified stages are marked with a thick broken outline. A red spot, if known, is symbolised by a black dot (after Inouye and Pienaar, 1983; see text for further details).

This lid, or opening, in the *T. heimii* shell is not delimited by a distinct permanent suture (Tangen et al., 1982) as in other skeletons (cysts) of calcareous dinoflagellates (e.g. chap. 3.4, *Calciodinellum albatrosianum, Leonella granifera, Pernambugia tuberosa*; pp. 106, 113, 120, 122). Tangen et al. (1982) postulate that a ring-shaped groove is formed from the inner shell surface. The shape of the edge of the opening indicates that the groove is formed by corrosion or dissolution of the calcium carbonate (Tangen et al., 1982). The region of the cell below the lid area begins to swell and the pressure causes the lid to open (Inouye and Pienaar, 1983).

The released binuclear cell is either biflagellate (Pl.1, Fig.5) or lacks flagella altogether. If it is biflagellate, the cell begins swimming shortly after release. The cell changes shape within a few minutes and continues to divide (Pl.1, Fig.4) into two *Gymnodinium*-like cells (Pl.1, Fig.6). Such a swimming divisional pair remains attached to each other for 2 to 25 min. After this time, separation into two *Gymnodinium*-like swarmers is complete.

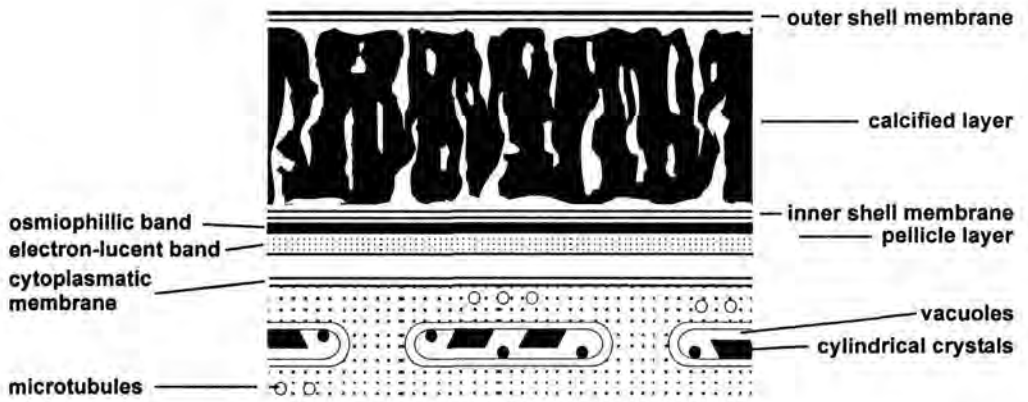

Fig.3: Schematic section through the wall of a calcified *Thoracosphaera heimii* cell (after Inouye and Pienaar, 1983).

These planospores swim from 3 min to several hours. The cells cease swimming, release their flagella and become spherical. Formation of a calcareous shell sets in: the process is finished after one to three days and concludes one of the two main cell cycles.

If a mature, spherical calcified cell releases a binuclear cell devoid of flagella, the released cell changes into a spherical divisional pair, also bearing no flagella (Pl.1, Fig.7). The divisional pair separates within 10 min into two daughter cells . These cells form a calcified shell and thus close the second main cell cycle of *T. heimii*.

Inouye and Pienaar (1983) describe several subcycles: The divisional pair does not separate completely and the resulting biglobular, binucleate cell calcifies (Pl.1, Fig.12). After maturity, a biflagellate cell is released (cycle A).

Some of the daughter cells formed from the separation of pairs and some twin divisional pairs without separation, do not calcify, but develop a thin envelope instead. On maturation, these cells also release swimming cells (cycle B). This cycle is usually observed in older cultures.

In a third subcycle (cycle C) the ellipsoidal cell released from a mature calcified cell changes its shape and forms only one *Gymnodinium*-like swimming cell with two longitudinal flagella. It does not separate into two planospores. The number of nuclei is uncertain. After a while it settles and becomes spherical. This has not actually been observed, but Inouye and Pienaar (1983) assume that calcification commences without the separation into two daughter cells.

Plate 1: SEM and LM micrographs of *Thoracosphaera heimii*

Fig.1: SEM micrograph of a calcareous *T. heimii* shell recovered from the sediment (core GeoB 2204-2, core depth: 159 cm). Scale bar represents 3 µm.

Figs.2 – 7: LM micrographs of strain GeoB86. Scale bars represent 10 µm.

Fig.2: A cell is being released from its shell (Figs.2 – 4). The lid is still attached to the shell.

Fig.3: The cell has left its shell. It is still deformed from its passage through the narrow opening.

Fig.4: The cell has changed into a non-motile divisional pair.

Fig.5: A newly released cell (motile). Cell division has not yet taken place. Direction of movement is to the upper right.

Fig.6: *Gymnodinium*-like swarmer. The arrow indicates the position of the cingulum. Direction of movement is to the upper right.

Fig.7: Non-motile stages. **a.** uncalcified aplanospore, the arrow indicates a red accumulation body. **b.** uncalcified aplanospore. **c.** calcified aplanospore.

Figs. 8 – 12: LM micrographs of calcified stages. - Polarised light and gypsum plate. Scale bars represent 10 µm.

Fig.8: Calcified aplanospore: thin section, strain A603 (photo courtesy of D. Janofske).

Figs.9 – 11: LM micrographs of aplanospores (strain GeoB86) in different states of calcification.

Fig.9: Weakly calcified.

Fig.10: Medium calcified.

Fig.11: Well calcified.

Fig.12: Biglobular calcified cell, strain A603 (photo courtesy of D. Janofske).

Plate 1

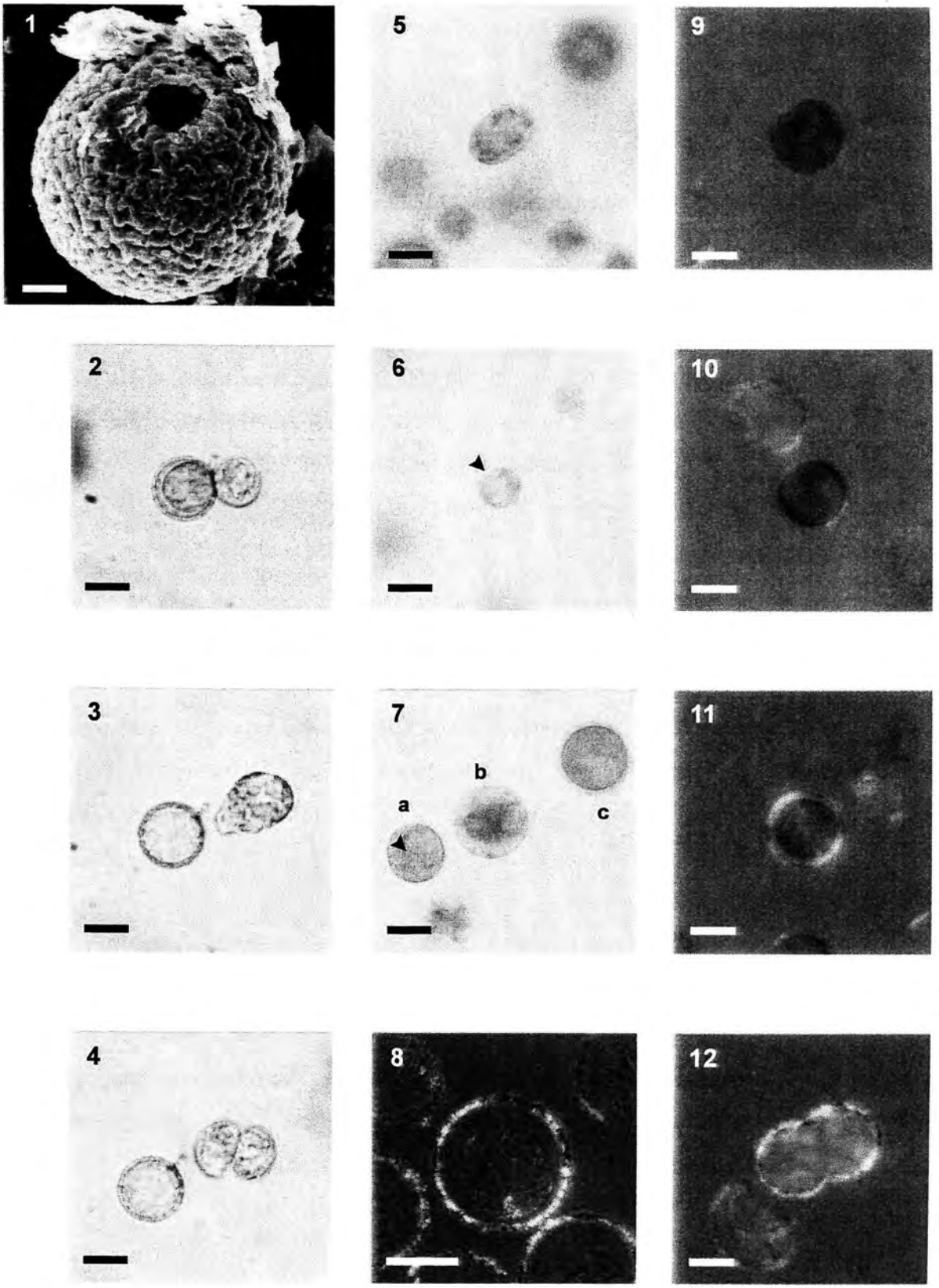

2. Material and Methods

For this interdisciplinary approach, it was necessary to develop several methodological solutions dealing with the isolation and culture of calcareous dinoflagellates, the set up of laboratory experiments, and the quantification of plankton and sediment material.

2.1 Plankton

2.1.1 Material

The sea water samples were taken during two Atlantic cruises of the RV Meteor in January / February 1997 (cruise M38-1) and May / June 1998 (cruise M41-4). Sample sites are shown in Fig.4. The samples were recovered in depths between 10 m to 100 m (M38-1) and 10 m to 200 m (M41-4) with a rosette sampler (Multi Wasserschöpfer MWS) using several 10 litre NISKIN™ bottles at each depth. Additional samples were taken with the ship's membrane pump from a water depth of 5 m. An overview of atmospheric and oceanographic conditions is given is Fig.4. A more detailed description is given in chapter 3.2, pp. 46 – 48.

The calcareous dinoflagellates gained from the plankton samples were used for a variety of studies. An overview is given in Fig.5.

2.1.2 Methods

Onboard filtration

The samples retrieved with the rosette were pre-filtered through a 100 µm mesh sieve (DIN 4188) and then filtered through 5 µm polycarbonate filters (diameter: 50 mm) using a vacuum pump system (Fig.6). The remaining 100 ml were stored in the dark together with the filters in 250 ml NALGENE™ polycarbonate flasks and fixed with 3 % to 4 % formaldehyde at a final concentration of 2 %.

The 10 µm to 100 µm fraction of the surface samples was separated with a filtration unit operated by the pump's pressure (Fig.7). Gauze (10 µm, 100 µm) was used for filtering, the material on the 10 µm filter was washed off into the sample. The gauze was repeatedly cleaned with freshwater in an ultrasound bath after each use. The remaining sample (1 litre) was filtered down to 100 ml using the vacuum pump system and 5 µm polycarbonate filters. Samples were then treated in the same fashion as the rosette material.

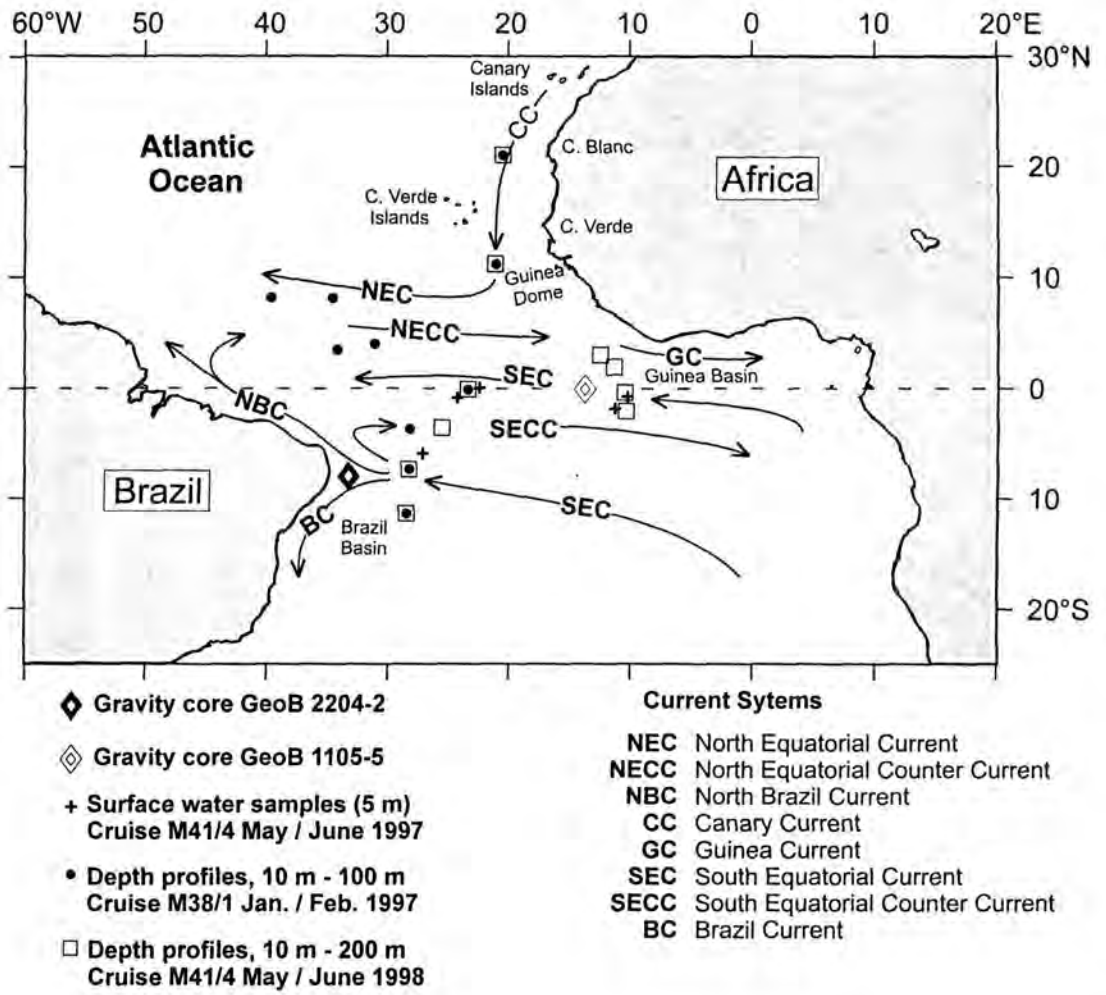

Fig. 4: Origin of the studied sediment and plankton material in relation to oceanographic current systems. See key for details.

Plankton Sample

Quantitative Studies	Culture →	Taxonomic Studies
Survey of horizontal and vertical distribution patterns	Study of the organisms' reactions to changing environmental conditions	Cyst-theca relationships
		Survival strategies
	Laboratory experiments:	Life cycle
Ecology		
	Temperature Salinity Nutrients Light	Ultrastructure

Fig.5: Overview of the different studies on calcareous dinoflagellates gained from seawater samples.

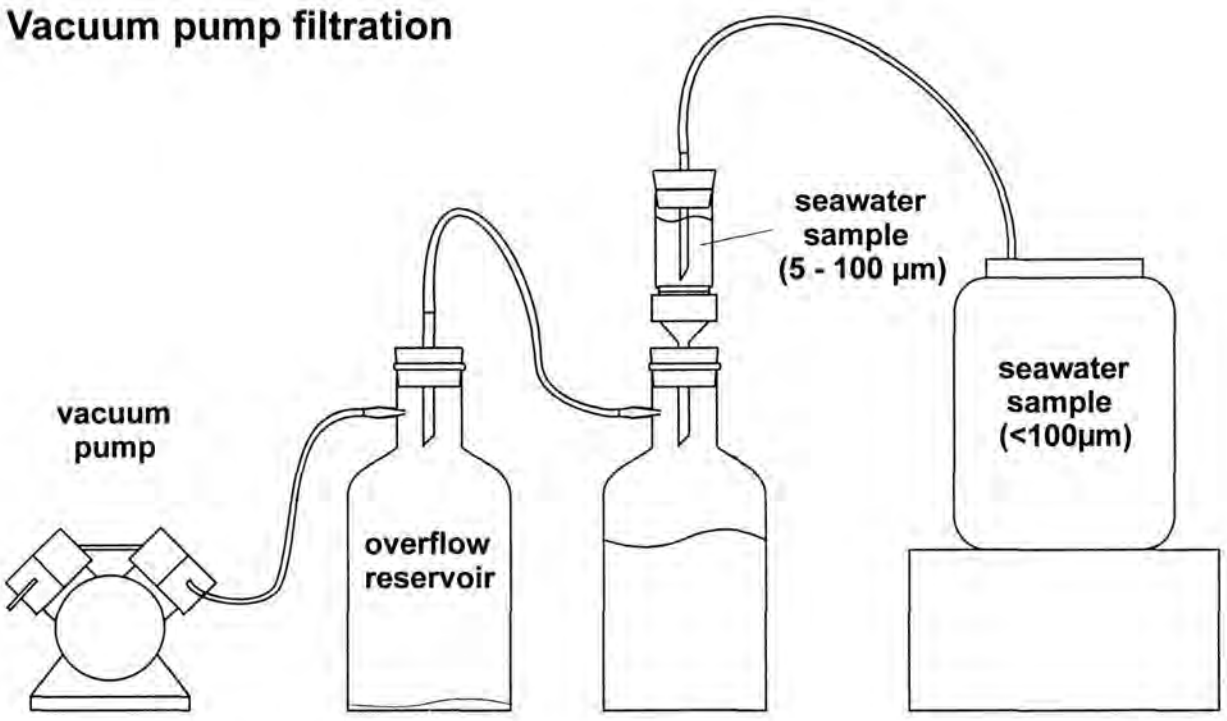

Fig.6: Vacuum pump filtration unit. The seawater was pre-filtered using a 100 µm mesh-sieve.

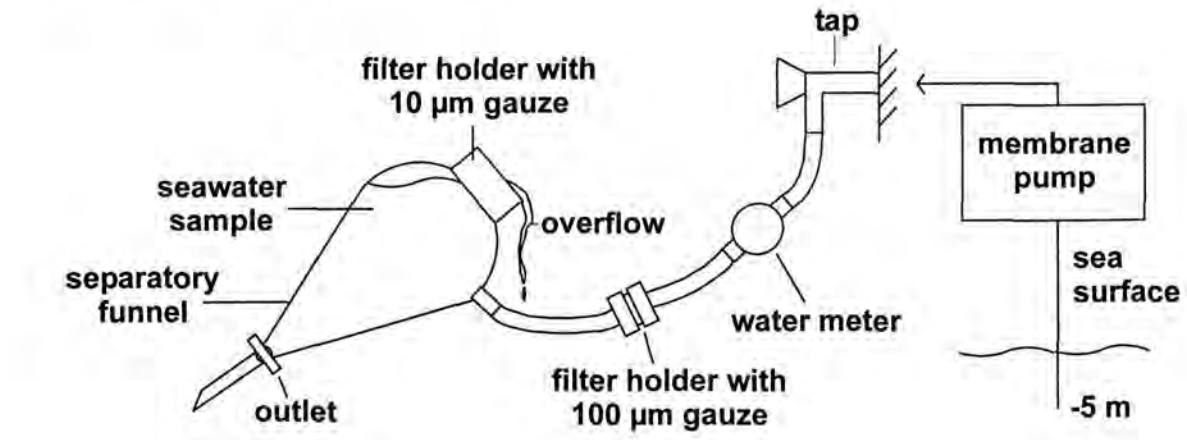

Fig.7: Membrane pump filtration unit. The filtration is operated by the pressure of the ship's membrane pump.

Onboard culturing

Prior to fixing the sample with formaldehyde, the plankton samples were scanned for living dinoflagellates. Both motile and calcareous stages were isolated with a capillary pipette using a Zeiss Axiovert 25 CFL inverted light microscope (ILM) at 100x to 400x magnification. The ILM is equipped with a polarisation unit to identify calcareous skeletal elements. Individual specimens were rinsed in polyterene CellWells™ with different culture media (without silica). We used f/2, (Guillard and Rhyther, 1962; 35 psu), K (Keller et al., 1987; 35 psu), filtered seawater of the respective sample (< 0.2 µm), and mixtures of filtered seawater and the mentioned culture media. Cultures were grown at room temperature using natural daylight as a light source.

Sample preparation

For the quantification of the plankton samples it was necessary to develop a method which allowed both easy and quick identification of the species to be studied as well as a distinction between calcareous cells with and without cell content. The last factor made the use of the light microscope (LM) imperative since the scanning electron microscope (SEM) allows only an outside view of the cell. The use of the LM in combination with a polarisation unit and a gypsum plate also allowed a quicker and easier identification of the oceanic calcareous dinoflagellate species studied during this dissertation (see also chap. 3.4, p. 99) than the use of the SEM would have. An overview of the sample preparation is given in the flow chart of Fig.8.

A portion of the fixed plankton sample was filtered through a cellulose-acetate filter (0.8 µm, diameter: 13 mm). The cellulose-acetate filters were chosen for their resistance to the chemicals used and for the fact that the originally opaque filters become transparent during preparation. The sample on the filter was rinsed with 1 ml artificial seawater and then allowed to react for 15 min with the DNA fluorochrome DAPI (4′,6-diamidino-2-phenylindole; Dann et al., 1979) to stain the nucleus.

At first we used a low viscosity resin (Spurr′s Resin; Spurr, 1969) to mount the filters on slides. The components of this resin are: vinylcyclohexene dioxide (ERL 4206; 5 g), diglycidyl ether v. polypropylene glycol (DER 736; 2.7 g), nonenylsuccinic anhydride (NSA; 13 g) and dimethylaminethanol (DMAE; 0.2 ml). Since water reacts with Spurr's Resin it was necessary to dehydrate the samples in an ethanol series (Fig.8). The filters are then removed from the holder and air-dried until nearly dry (if filters are dried completely they do not

Quantification of Plankton Material

seawater sample

⇩

filtration through a 0.8µm cellulose-acetate filter 

⇩

the sample is rinsed with 1 ml of artificial seawater 

⇩

DAPI is allowed to react with the sample for 15 minutes 

⇩

dehydration in an ethanol series
1 x 30, 50, 70, 80 and 90%,
2 x 95 % 10 minutes each and
2 x 100% ethanol 15 minutes **(1)** 

⇩

filters are removed from the holder and air-dried until only a slight wetness remains;
if dried completely the filters do not become transparent in the next step 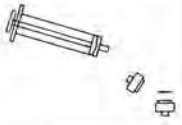

⇩

filters are mounted on microscope slides with a low viscosity resin in which they become transparent; filters are covered with a coverslip

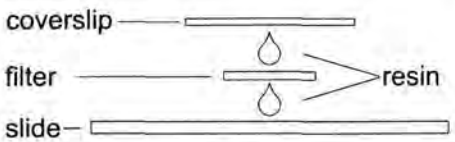

(1)

⇩

resin has to polymerise at least 8 hours at 70°C **(1)**

⇩

addition of 1 ml ethanol
to remove the saltwater **(2)** 

⇩

filters are mounted at about 60°C on microscope slides with glycerine-jelly in which they become transparent; filters are covered with a coverslip

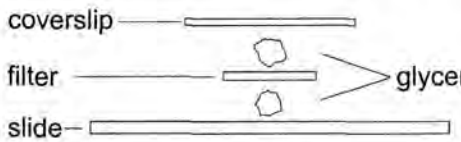

(2)

⇩

glycerine-jelly solidifies within 20 - 30 minutes; filters and coverslip are held into place during this time by a clamp; slide is cleaned and the sample is insulated from air with varnish **(2)**

Problems caused by method No. 1 :

A. Since water reacts with the resin, it has to be removed in a time intensive dehydration process.

B. Deformed filters can push up the cover slip and may cause air suction. Weighs or clamps used to hold the slips down adhere to the resin. The removal destroys the slide. **C.** The remaining ethanol in or on the filter may keep the resin from hardening or may turn to gas in the slide.

become transparent when mounted on the slide). Filters are then covered with a cover-slip. The resin has to polymerise at 70°C for at least 8 h.

The use of Spurr's Resin in this case was problematical: deformed filters can push up the cover-slip, which may cause air suction. Weighs or clamps used to hold the slips down, no matter how carefully placed, were in danger of adhering to the low viscosity resin and their removal destroyed the slide. Since the filters could not be allowed to dry completely, the remaining ethanol in or on the filter occasionally kept the resin from hardening or turned to gas in the slide, or both.

We abandoned the use of Spurr's Resin in favour of glycerine-jelly. Instead of dehydrating the sample, the salt water was simply removed by the addition of 1 ml ethanol. The glycerine-jelly was melted on the slide at about 60°C and the nearly dry filter was then embedded and covered with a cover-slip. The glycerine-jelly solidifies within 20 min to 30 min. During this time, filter and cover-slip were held into place by a clamp. The slide was cleaned with water and the sample insulated from air with varnish.

Sample evaluation

Samples were studied with a Zeiss Axiophot light microscope equipped with a polarisation unit and a gypsum plate. To distinguish between calcareous remains with and without cell content the material was viewed under ultra-violet light (Zeiss filter set 01, extinction BP, emission LP 377). The cell content was evident by the DAPI-stained nucleus. The entire slide was counted.

Depending on the sample volume available we tried to either view the equivalent of at least 10 L of sea water or continued our evaluation until 300 specimens were counted. To this end, several slides were prepared if necessary (chap. 3.2. Tabs.1, 2). This was not always possible, due to either low occurrence of calcareous dinoflagellates or loss of material during preparation.

2.2 Laboratory experiments

To allow phytoplankton experiments simultaneously under a wide range of temperatures, a temperature gradient box was developed in co-operation with the Department of Production Engineering at the University of Bremen.

Fig.8: Quantification of plankton material from seawater samples. Chemicals during preparation are changed by connecting different syringes to the filter holders.

Similar to the TGB, a light gradient box (LGB) was built to test the reaction of calcareous dinoflagellates to varying light intensities under constant temperature conditions (chap. 3.3, p. 70; see also Fig.10, p. 20).

2.2.1 Material

Three of the available *T. heimii* strains were chosen for the laboratory experiments. Strain A603 (syn.: L603; CCMP 1071) was obtained from the Provasoli-Guillard National Center of Marine Phytoplankton (CCMP), Bigelow Laboratory for Ocean Sciences. It was isolated in 1977 from the Sargasso Sea, North Atlantic Ocean (36°44.2'N; 69°20'W; Fig.9). A603 was the original isolate used by Tangen et al. (1982) to establish the systematic position of *T. heimii* in the phytoplankton. The strain has also been subject of various biochemical analyses confirming the affiliation of *T. heimii* to the Dinophyceae (Jones et al., 1983; Bjørnland, 1990; Rowan and Powers, 1992).

Strains GeoB79 and GeoB86 were isolated from plankton samples taken in 20 m water depth in the tropical South Atlantic (GeoB79: 07°30.01'S, 28°11.2'W; GeoB86: 03°52.1'S, 25°39.5'W; Fig.9) during RV Meteor cruise M38-1 in 1997. These two strains were chosen for their lack of contamination with other organisms.

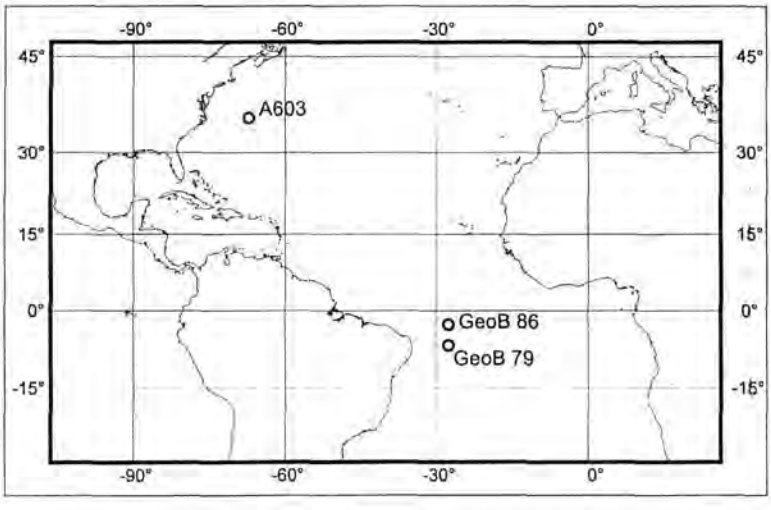

Fig.9: Origin of the studied strains. A603 was obtained from the Provasoli-Guillard National Center of Marine Phytoplankton (CCMP), Bigelow Laboratory for Ocean Sciences. It was isolated in 1977 from surface waters. Strains GeoB79 and GeoB86 were isolated from plankton samples taken in 20 m water depth during RV Meteor cruise M38-1 in 1997.

Cultures were maintained in growth chambers in polysterene culture plates (CellWells™) and 250 ml Erlenmeyer flasks at 20°C. Light with an irradiance of 80 $\mu Em^{-2}s^{-1}$ (Licor Li-250; Sensor: MQS S/N 007) was provided by cool white fluorescent tubes. The strains were kept in f/2 culture medium (Guillard and Ryther, 1962) without silica. Media were prepared with artificial seawater (hw Meersalz, Wiegand GmbH, Krefeld).

2.2.2 Methods

Equipment

Temperature studies

The temperature gradient box (TGB) allows the simultaneous culturing of phytoplankton strains in different temperature gradients. An aluminium alloy block was equipped with holes for culture tubes in four rows, thirty holes in each row. A steady state temperature gradient was set up in the longitudinal axis of the block by applying constant high and low temperatures to each end of the block. The culture tubes rested on a Plexiglas layer and were lit from underneath by nine cool white fluorescent tubes (Osram L18W/11-860). A more detailed description of this device is given in chap 3.1, pp. 32, 33.

Light intensity studies

The construction and use of the LGB (Fig.10) benefited greatly from the experience of the work with the TGB. Two cool white fluorescent lamps (Sylvania F58W/184, Biax™ S11W) were covered lengthways with different strengths of semi-transparent plastic film (Lee Filters 298.15 ND). Culture tubes were inserted in foamed plastic and were lit from underneath. Heat build-up in the box was a problem at first, but with the inclusion of several fans to cool the lamps, it was possible to avoid a temperature gradient. The whole construction was housed in an insulated box and is covered by lids. The windows in the air-conditioned room were darkened with opaque material so that the light intensity in the room with minimal illumination was only 12 $\mu Em^{-2}s^{-1}$ during measurements. The configuration of the LGB shown in Fig.10 allowed irradiance experiments between 10 $\mu Em^{-2}s^{-1}$ to 500 $\mu Em^{-2}s^{-1}$. To permit tests under light intensities of up to 800 $\mu Em^{-2}s^{-1}$ the light-reducing filter had to be removed.

Set up

The temperature related growth range of the *T. heimii* strains A603 (f/2) and GeoB86 (f/2; f/20) was tested. To this end the temperature gradient in the TGB was set from 8°C to 34°C.

Light Gradient Box

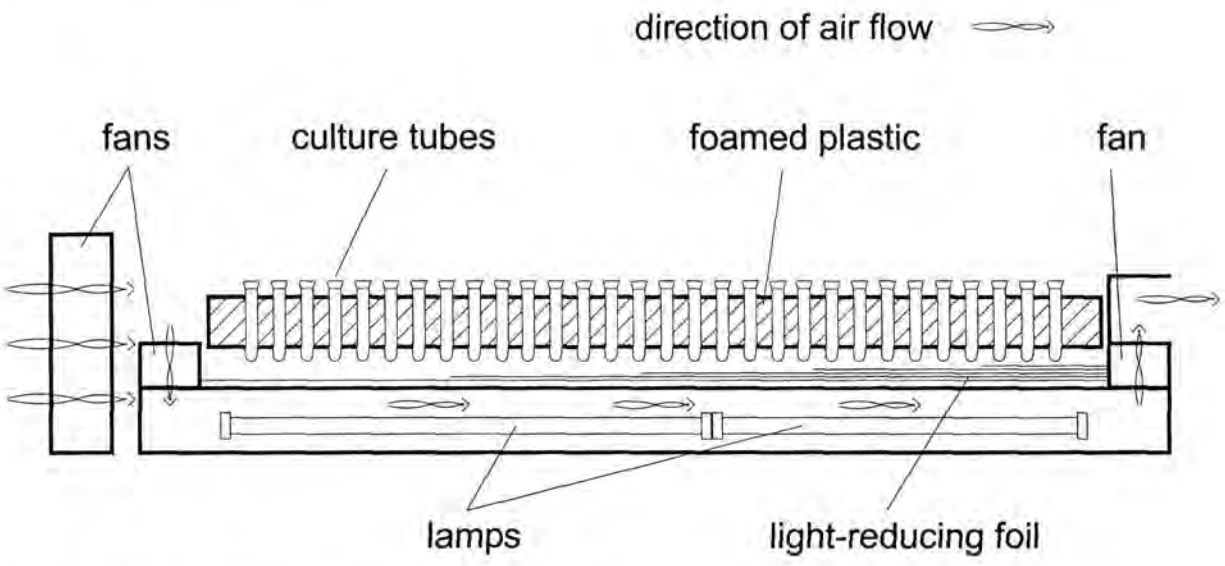

Fig.10: Schematic drawing of the Light Gradient Box.

Cultures were irradiated with 100 $\mu Em^{-2}s^{-1}$ in a 12 h : 12 h L/D cycle. Culture growth was monitored by daily *in vivo* chlorophyll *a* measurements (see also chaps. 3.1, 3.3).

Strains GeoB86 and GeoB79 were used for the experiments in the LGB. Temperature in the LGB was set at room temperature (22.5°C). Cultures were subjected to light intensities between 10 $\mu Em^{-2}s^{-1}$ and 800 $\mu Em^{-2}s^{-1}$ in a 12 h : 12 h L/D cycle. Reference cultures were kept in an incubator at 20°C under light irradiation of 80 $\mu Em^{-2}s^{-1}$.

During the experiments with both the TGB and the LGB, salinity and temperature measurements for each culture tube were taken in a two-week cycle. Evaporated water was refilled once or twice a week with demineralised autoclaved water to stabilise salinities.

Calculation of growth rates

The growth rate is a measure of velocity of growth, an index relating the process of multiplication of organic matter to time. Growth of a culture within a constant volume of unchanged medium is usually described by a sigmoid growth curve (Sorokin, 1973). Growth of most batch-cultures can be divided into several phases (e.g. *T. heimii*; Fig.11):

lag phase

exponential phase

declining phase

stationary phase

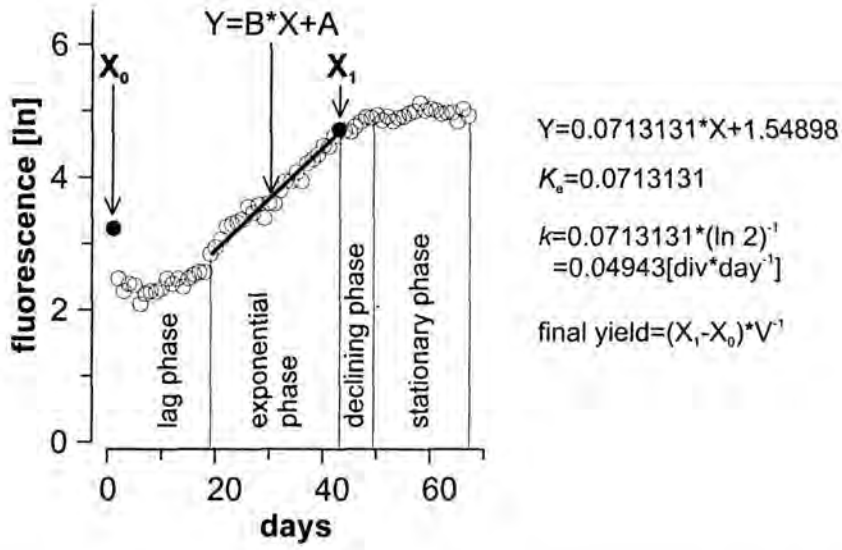

Fig.11: Calculation of growth rate: *Ke* is the slope of the exponential part of the growth curve calculated by linear regression analysis (linear fit: Y=B*X+A). Growth rate is also expressed as divisions per day (*k*). Calculation of final yield: The final yields of relative chlorophyll *a* ($yield_{RFD}$) and cell numbers ($yield_{CC}$) were calculated. X_0 equals the raw fluorescence data (RFD) after inoculation or the initial cell density. X_1 equals RFD or cell density on the last day of exponential growth. The cell density on the last day of exponential growth was calculated from RFD and the according cell count from the final day of the experiment, and the RFD from the last day of exponential growth. V is the culture media volume.

The lag phase has also been called the phase of adjustment (Winslow and Walker, 1939) or the acceleration phase (Monod, 1942). During the lag phase the growth rate is usually increasing, but net growth may also be absent during a portion of the phase or there may even be a decline in cell volume per unit volume of cell suspension (Sorokin, 1973).

During the exponential (Monod, 1942) growth phase the mass of cells doubles over each of the successive time intervals: the growth rate is constant during the entire exponential phase. This phase is thus uniquely suitable for growth rate determinations (Sorokin, 1973).

In the declining or the retardation phase of growth (Monod, 1942) the doubling time for the cell mass is increasing and this phase is generally unfit for growth rate measurements (Sorokin, 1973).

Within the stationary growth phase a stable concentration of cell mass per unit volume of cell suspension is maintained (Sorokin, 1973).

Usually, growth rates are calculated from cell counts per volume unit of culture media. Due to the sheer mass of material to be measured every day, we chose a faster alternative method. To this end, culture growth was monitored by daily *in vivo* chlorophyll *a* measurements. They were carried out with a laboratory fluorometer (TD-700, Turner Designs); cultures were mixed with a vortex stirrer before placing the tubes in the fluorometer. The results equal raw fluorescence data (RFD) and relate to standard cultures also measured *in vivo* prior to the experiments. Brand and Guillard (1981) have shown that the brief insertion of the culture (*T. heimii* was also tested) into the fluorometer each day does not affect its reproduction rate. In the present study, RFD were used to calculate growth rates during exponential phase after Brand and Guillard (1981) and Guillard (1973):

The logarithm of the RFD values to the base e was plotted against time (e.g. Fig.11). The beginning and end of the exponential phase was determined visually using a ruler as an aid. The slope of the curve between these two points was calculated by linear regression analysis. The slope calculation was done with the aid of the graphics program Grapher (Golden Software) using the linear fit:

$$Y = B*X+A$$

where X is a point on the x-axis, Y is the estimated response at X, B is the slope of the fitted line (growth constant K_e) and A is the intercept.

The growth constant K_e is the number of 'logarithm-to-base-e' units of increase per day:

$$K_e = \ln (X_1*X_0^{-1}) * (t_1-t_0)^{-1}$$

X_0 is the RFD at the beginning, X_1 the RFD at the end of the exponential growth phase. The according time is given by t_0 and t_1.

Growth rate is also expressed as divisions per day ('logarithm-to-base-2' units of increase per day), k; where:

$$k = \log_2 (X_1*X_0^{-1}) * (t_1-t_0)^{-1}$$

The expression K_e for the growth rate was converted into k by using the relationship between logarithms to two bases:

$$k\,[\text{div} * \text{day}^{-1}] = K_e * (\ln 2)^{-1}$$

During the light experiments, we encountered the problem that the relative chlorophyll *a* content per cell changes with different irradiances. This seems to be problematical in terms of the growth rate calculation because we did not use cell counts, but chlorophyll *a* measurements (RFD). However, since the rates are calculated from data of the exponential growth phase after the lag phase, and thus after acclimation to the ambient light, the slope of the exponential part of the curve should show the growth of the culture.

Calculation of the final yield and establishment of the cell density

Growth can also be expressed as yield (Fig.11). Yield is an expression of organic production and is usually given in terms of dry or fresh weight of the organic mass produced over a period of time per unit of volume (Sorokin, 1973). Instead of dry or fresh weight of the organic mass, we calculated the yield of relative chlorophyll *a* or cells produced over a period of time per unit of volume.

We calculated the final yield of relative chlorophyll *a* (RFD) after Sorokin (1973):

$$yield_{RFD} = (X_1 - X_0) * V^{-1}$$

were X_0 equals RFD after inoculation, X_1 equals RFD on the last day of exponential growth and V is the culture media volume. Cell counts were used for the second set of yield calculations ($yield_{CC}$). X_0 is the cell density on the last day of exponential growth. X_1 was calculated from RFD and the according cell count from the final day of the experiments and the RFD from the last day of exponential growth. We did not take cell counts on the last day of exponential growth since, in most cases, it only becomes apparent that the exponential phase has been finished after the declining phase has passed and the stationary phase has already been entered.

Cell numbers were established with a Thoma counting device (chamber depth 0.1 mm). Cells were counted in all squares with five refills of both chambers. If the cell density in the sample was too low it was concentrated by centrifugation. The average cell density per ml was calculated after:

$$cells * ml^{-1} = 1\ ml * V^{-1} * avg_C * Z^{-1}$$

where V is the chamber volume ($6.4*10^{-2}$ ml), avg_C is the average cell count (n=10), and Z is the concentration of the sample or subsample.

2.3 Sediment

2.3.1. Material

The two studied gravity cores were recovered during RV Meteor cruises M23-3 (Bleil et al., 1994) and M9-4 (Wefer et al., 1989) from the oligotrophic western tropical Atlantic (GeoB 2204-2; 8°32′S, 34°01′W; 2072 m water depth) and the divergence zone eastern equatorial Atlantic Ocean (GeoB 1105-4; 01°40′S, 12°26′W; 3225 m water depth). See also Fig.4.

The sediments of core 2204-2 consists mainly of foraminiferal-nannofossil ooze in the lower and nannofossil ooze in the upper part. The material of core 1105-4 consists of light to

dark grey nannofossil-foraminiferal ooze and siliceous nannofossil-foraminiferal ooze (chap. 3.5, p. 45).

The content of calcareous dinoflagellates (GeoB 2204-2; Karwath, 1995) were compared to data (e.g. total organic carbon) from the work of Rühlemann (1996) (chap. 3.5, p. 147). Age assessments of cores GeoB 2204-2 and GeoB 1105-4 were based on Dürkoop et al. (1997) and Wefer et al. (1996), respectively. The studied material encompassed the last 140 ka.

2.3.2. Methods

Sample preparation and evaluation

Samples were taken with either 5 ml or 10 ml syringes. The flow chart of Fig. 12 shows the preparatory process. Several trials with different preparatory techniques for both the SEM and the LM led to a decision in favour of the LM. All attempts of sample preparation for the SEM either led to fractionation of the material, or the covering of small particles with larger ones, or both, all of which precluded quantification. Light-optical methods allow to focus within different levels of the slide and the problem of particle covering is reduced to a minimum.

The factor of fractionation was minimised by the following methods:

GeoB 2204-2: Freeze drying of suspended sediment (H_2O, slightly ammoniacal) to achieve better particle separation. Suspension of 0.01 g (dry weight) sediment in 5 ml ethanol : H_2O (1 : 1, slightly ammoniacal). The sample was homogenised and allowed to rest for 0.5 min before removing 100 µl from 0.5 cm depth with an Eppendorf pipette. The subsample was dried on a coverslip at 90°C in an oven and mounted on a slide with Spurr's Resin (Karwath, 1995). Calcareous dinoflagellate counts see chap. 3.5, App.A, p. 163.

GeoB 1105-4: Generally the same. The sediment was dried in the oven overnight and 1g of sediment was suspended in 100 ml ethanol (40 %, slightly ammoniacal). Subsampling (50 µl – 100 µl) took place in depths between 0.5 to 1 cm, the subsample was dried at 70°C in an oven and mounted on a slide with Spurr's Resin (Höll, 1998). Calcareous dinoflagellate counts see chap. 3.5, App.B, p. 164.

Quantification of Sediment Material

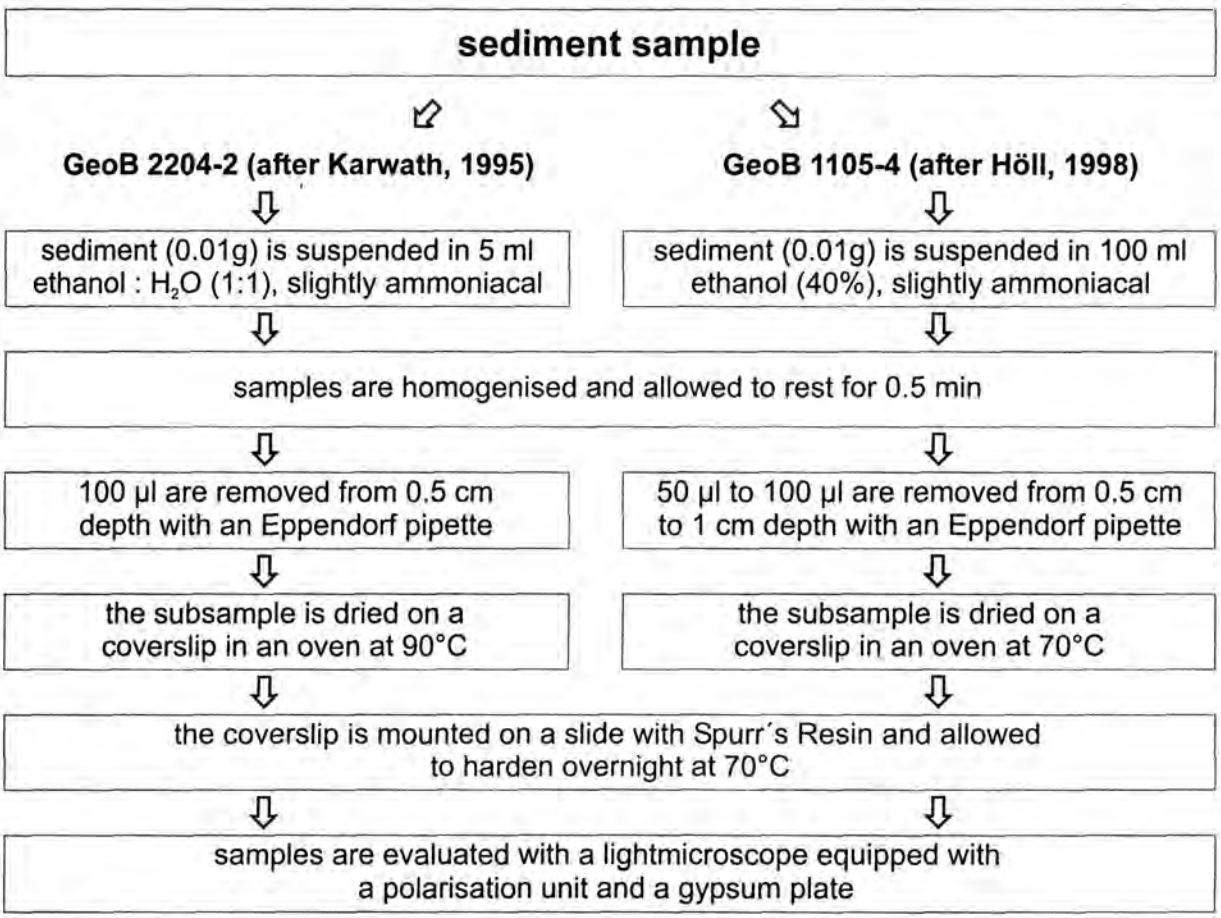

Fig.12: Flow chart of preparatory methods used during the quantification of calcareous dinoflagellates from sediment material.

3.

Manuscripts in press, submitted or in preparation

3.1

TEMPERATURE EFFECTS ON GROWTH AND CELL SIZE IN THE MARINE CALCAREOUS DINOFLAGELLATE *THORACOSPHAERA HEIMII*

(Marine Micropaleontology 39: 43-51. 2000)

TEMPERATURE EFFECTS ON GROWTH AND CELL SIZE IN THE MARINE CALCAREOUS DINOFLAGELLATE *THORACOSPHAERA HEIMII*

Britta Karwath[1]*, Dorothea Janofske[1], Frank Tietjen[2], Helmut Willems[1]

[1]Historische Geologie / Paläontologie, Fachbereich Geowissenschaften, Universität Bremen, Postfach 330 440, 28334 Bremen, Germany. Fax: 0421/218 4451

[2]Technische Thermodynamik / Wärme- und Stofftransport, Fachbereich Produktionstechnik, Postfach 330440, 28359 Bremen, Germany. Fax: 0421/218 7555

*e-mail corresponding author: karwath@micropal.uni-bremen.de

Abstract

Growth experiments were carried out on the marine calcareous dinoflagellate *Thoracosphaera heimii*. Two strains (A603, GeoB86) of the phototrophic, predominantly vegetative coccoid *T. heimii* were cultured at different temperature and nutrient levels. For the temperature experiment a gradient box was developed to allow the simultaneous testing of a wide range of temperatures on phytoplankton. During the investigations *T. heimii* was growing from 14°C to 27°C. Exponential growth rates do not show an unimodal response curve *vs.* temperature: values rise with increasing temperatures toward maximal growth rates around 27°C. At low temperatures exponential growth is extremely long (over 50 days). In f/2 culture medium *T. heimii* (A603) is less efficient at high temperatures than at low temperatures, final yield was about five times higher at 16°C than at 27°C. Growth rate and final yield at 27°C are approximately the same for all experiments despite different nutrient levels. Mean shell diameters show no clear relation to growth temperature. Calcification of *T. heimii* shells is inversely related to temperature.

Keywords: marine, calcareous dinoflagellates, growth, culture experiments, actuopalaeontology

Introduction

Dinoflagellates are a group of unicellular eukaryotic organisms which represent one of the major (marine) phytoplankton groups. Skeletal elements are a typical feature of this group (=

Pyrrhophyta; Fensome et al., 1993) although preservation in recent and fossil sediments is dependent on the material used. Cellulose, which is generally used for the skeletal elements (theca) of the motile stages during the life cycle, is not fossilisable due to rapid microbial decay. The wall of the cyst stage, however, generally contains more resistant material such as an organic sporopollenin-like material (dinosporin; Fensome et al., 1993) and/or calcareous elements (calcite; Wall et al. 1970).

During the last decades, research has focused on the fossilisable organic remains of dinoflagellates which are generally regarded as the preserved wall of cyst stages. Studies include, among other topics, research on (palaeo-) productivity, (palaeo-) environment and (palaeo-) oceanography (e.g. Turon, 1980; Lewis et al., 1990, Matthiessen, 1995; Höll et al., 1998; Höll et al. 1999). In contrast, information is rare on dinoflagellate taxa with calcareous skeletal elements and in particular the biology and ecology of pelagic taxa are largely unknown.

Research on various aspects of calcareous dinoflagellates from pelagic as well as neritic marine environments and from Recent as well as fossil sediments are being undertaken by members of the working group at the Department of Geoscience at the University of Bremen. Culture experiments on extant species are providing data on ultrastructure (Janofske, 1996), taxonomy (Montresor et al., 1997) and ecology (this study). Field work includes aspects of the distribution of extant species in the water column (Atlantic Ocean: Kerntopf, 1997; Karwath, 2000) and of their taphocoenosis in surface sediments and Quaternary sediments (Höll et al. 1998, Höll et al. 1999; Zonneveld et al. 1998). Data from fossil strata (Cretaceous: Hildebrand-Habel and Willems, 1997; K/T-boundary, Willems, 1996; Tertiary: Hildebrand-Habel and Willems, subm.) are revealing aspects of fossil taxa, their paleoecology and the evolution of this phytoplankton group.

Calcareous dinoflagellates have often been neglected in plankton studies due to their size of about 10 to 60 µm. They are too small to be included in foraminifera research and too large for nannoplankton studies. In palynological studies the use of acids during preparation automatically excludes calcareous dinoflagellates from consideration. During the last decade observations made on this group have hinted at a far more important role for calcareous dinoflagellates than formerly recognised (Dale, 1992a, b; Kerntopf, 1997; Höll et al., 1998; Höll et al., 1999).

Whereas in boreal regions Dale and Dale (1992) have shown a predominance of organic-walled dinoflagellate cysts, Dale (1992a) and Höll et al. (1998; 1999) have shown that assemblages of fossilisable dinoflagellate remains in the subtropics and tropics are mainly

composed of calcareous dinoflagellates. The high flux rates of calcareous dinoflagellates in these regions (Dale 1992a, b) suggest that they may form a significant contribution to the ocean carbon flux.

Recent investigations by Kerntopf (1997) and Höll et al. (1998; 1999) have shown that calcareous dinoflagellate associations in the tropics and subtropics are often overwhelmingly dominated by the phototrophic species *Thoracosphaera heimii*. Kerntopf (1997) described *T. heimii* as abundant offshore north-west Africa forming 2 – 12 % of the shelled phytoplankton. Studies by (Dale, 1992b) on sediment trap material from the Equatorial Pacific Ocean and Equatorial Atlantic Ocean have revealed that the calcareous dinoflagellate association is mostly composed of "thoracosphaerids" (in this case *T. heimii* and *Thoracosphaera granifera* = ?*Orthopithonella granifera*). Observations by Höll et al. (1998; 1999) from sediment core material (down to 140 ka) from the western and eastern tropical Atlantic Ocean have shown high contents of calcareous dinoflagellates and again, the dominance of *T. heimii* was overwhelming. This prevalence of *T. heimii* in the calcareous dinoflagellate associations can be explained by the species' ability to produce large numbers of calcareous spheres in a relatively short period of time. Its position within the Dinophyceae is unique: in the first study on the species' life- cycle Tangen et al. (1982) have shown that in contrast to other calcareous dinoflagellates most of the cells in a culture of *T. heimii* form a calcareous skeleton. This calcareous wall has been referred to as a "shell" rather than a "cyst" to stress that it is formed as a dominant vegetative-coccoid life-stage of the species and not as a resting stage (Inouye and Pienaar, 1983).

In spite of the abundance of the species and, in most cases, the dominance over other calcareous dinoflagellates, little is known to date about the environmental affinities of *T. heimii*.

In one of the first studies touching this topic Höll et al. (1999) compared the content of organic dinoflagellate remains in two sediment cores, one from below the highly productive eastern Atlantic equatorial divergence zone and another from the low productivity area of the western tropical Atlantic. In this endeavour to establish a new tool for palaeoenvironmental reconstructions, calcareous dinoflagellates (mostly *T. heimii*) show increased accumulation rates in the low productivity area in the western and lower accumulation rates in the high productivity region in the eastern South Atlantic. Organic dinoflagellates, on the other hand, follow an opposite pattern (Höll, 1998). Enhanced production of calcareous dinoflagellates in the investigated region and time interval were correlated to periods of reduced

palaeoproductivity probably related to relatively stratified conditions of the upper water column (Höll et al., 1999).

In view of these findings - and to improve on the data base available for the interpretation of *T. heimii* occurrences in the sediment - it is important to take a closer look at the recent environmental affinities. The aim of our investigations is to provide a sound basis for the use of *T. heimii*'s role as a proxy indicator of palaeoenvironmental conditions. The present study deals with the temperature related growth range of the *T. heimii* strains A603 (syn.: L603; CCMP 1071) and GeoB86 in growth experiments. A603 was the original isolate used by Tangen et al. (1982) to establish the taxonomic position of *T. heimii* in the phytoplankton. The strain has also been the subject of various biochemical analyses confirming the affiliation of *T. heimii* to the Dinophyceae (Jones et al., 1983; Bjørnland, 1990; Rowan and Powers, 1992). GeoB86 is an isolate from *RV Meteor* cruise M38-1 in 1997 carried out within the scope of the SFB 261 program "Der Südatlantik im Spätquartär: Rekonstruktion von Stoffhaushalt und Stromsystemen". For the growth experiments presented here a temperature gradient box (TGB) was developed. The device enabled us to test a wide range of temperatures on *T. heimii* cultures simultaneously.

The present study is the first publication on culturing experiments on temperature-related growth of calcareous dinoflagellates in a temperature gradient box (TGB) and deals with the basic technical aspects as well as the results of the first experiments. Comparable experiments with other pelagic and neritic species of calcareous dinoflagellates have already been carried out and will be the topic of future publications.

Material and Methods

Cultures

Strain A603 (syn.: L603; CCMP 1071) of *Thoracosphaera heimii* (Lohmann) Kamptner was obtained from the Provasoli-Guillard National Center for Culture of Marine Phytoplankton (CCMP), Bigelow Laboratory for Ocean Sciences. It was isolated in 1977 from the Sargasso Sea, North Atlantic Ocean (36°44.2'N; 69°20'W). Strain GeoB86 was isolated from a plankton sample taken in 20 m water depth in the Equatorial Atlantic (03°52.1'S; 25°39.5'W) during *RV Meteor* cruise M38-1 in 1997. The strains were maintained at the University of Bremen Department of Geoscience in growth chambers in polystyrene culture plates (CellWells) and 250 ml Erlenmeyer flasks at 24°C. Light with irradiance of 80 $\mu mol \cdot m^{-2} \cdot s^{-1}$ (2π - Photometer LI – 189; Sensor: Quantum 16244) was provided by cool white fluorescent tubes. Cultures were kept in f/2 and f/20 culture medium

(Guillard and Ryther, 1962) all without silica. Media were prepared with artificial seawater (hw Meersalz, Wiegand GmbH, Krefeld).

Equipment

The temperature gradient box (TGB) used for the growth experiments (Fig.1) was developed in co-operation with the Department of Production Engineering at the University of Bremen. This device allows the simultaneous culturing of phytoplankton strains in different temperature gradients.

An aluminium alloy block was equipped with holes for borosilicate culture tubes in four rows, thirty holes in each row. The tubes can hold a maximum of 40 ml culture medium and can be closed with stoppers. A steady state temperature gradient was set up in the longitudinal axis of the block by applying constant high and low temperatures to the opposite ends of the block. For this purpose, liquid containers are attached to each end of the block, which extends into the containers providing direct contact with the liquid. The liquids' temperatures were kept at constant levels by heating and cooling thermostats. To ensure a constant unidirectional heat flow and thus a steady-state temperature gradient through the length of the aluminium block the liquid containers as well as the block were insulated. The culture tubes rest on a Plexiglas layer and are lighted from below by nine cool white fluorescent tubes (Osram L18W/11-860).

The lamps were cooled by fans connected to the laboratory's air condition to avoid heat build up in the box. The upper protruding parts of the culture tubes are covered by insulation material. The whole construction is encased in a wooden housing and is covered by lids. For temperature control, twelve thermo-sensors (Pt 100/0, thermocouple, EandS Metronic) are positioned in the block at regular intervals. The sensors are connected via an interface (THERM 5500-2S AMR) to a computer and printer. Special recording software is used to record the temperature data (AMR WinControl 1.2.2). The temperature in the culture tubes was determined with a combined temperature and conductivity probe.

Temperature Gradient Box

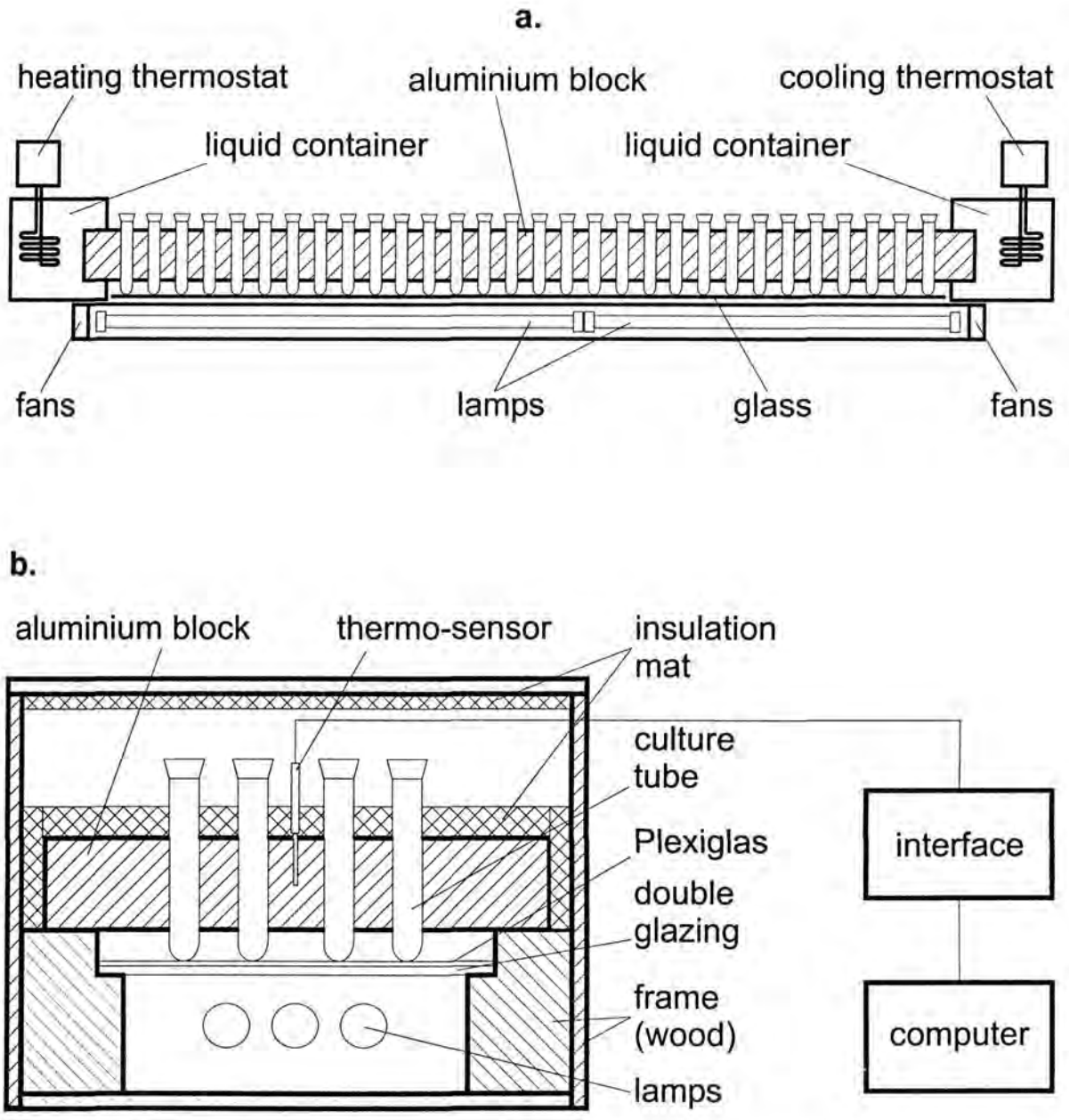

Fig.1: Schematic drawing of the temperature gradient box. (TGB) **a.:** Sectional drawing, longitudinal axis without frame and insulation. **b.:** Sectional drawing, lateral axis.

Growth Experiments

Set-up and Realisation

Fifteen holes in one of the rows of the TGB were set aside for each of the three experiments. The temperature gradient equalled 8° - 34°C. Cultures were irradiated with 100 $\mu mol \cdot m^{-2} \cdot s^{-1}$ in a 12h : 12h L/D cycle. Tab.1 shows, among other things, the strains, culture media, initial cell densities and the duration of the respective experiments. Cell numbers were established with a Thoma counting device (chamber depth 0.1 mm). Culture growth was monitored by daily *in vivo* chlorophyll *a* measurements. They were carried out with a laboratory fluorometer (TD-700, Turner Designs); cultures were mixed with a vortex stirrer before placing the tubes in the fluorometer. The results equal raw fluorescence data (RFD) and relate to standard cultures also measured *in vivo* prior to the experiments. RFD were used to calculate exponential growth rates for *T. heimii* after Brand and Guillard (1981) and Guillard (1973). Final yield was calculated after Sorokin (1973) $(X_1 - X_0) * V^{-1}$ where X_0 = RFD after innoculation, X_1 = RFD on the last day of exponential growth and V = culture media volume (30 ml) (Fig.3).

Salinity and temperature measurements for each culture tube were taken over a two-week cycle. Evaporated water was replaced once a week with demineralised autoclaved water to stabilise salinities.

Table 1: Set up of *Thoracosphaera heimii* growth experiments.

experiment No	strain	culture Medium			initial cell density	duration
		30 ml	[psu]	[pH]	$^{-1}$ml	[d]
#1	A603	f/2	33.8	8.35	5×10^3	74
#2	A603	f/20	34.1	8.27	3×10^3	81
#3	GeoB86	f/20	34.1	8.27	6×10^3	74

Sample Preparation

At the termination of the experiments, each culture was centrifuged down to 1 ml and fixed with 1 ml of 4 % formaldehyde solution in 2 ml Eppendorf cups. They were stored in the dark at room temperature. For preparation, the fixed material was mixed with a vortex stirrer. Of this sample, a drop of 40 µL was allowed to dry down to a wet film on a glass cover-slip. The cover-slip was then mounted on a microscope slide with glycerine jelly. Samples were insulated from air with varnish.

Sample Evaluation

Samples from Exp#1 were studied under a Zeiss Axiophot light microscope (LM). Size measurements were made at a 1000 fold magnification with an eyepiece micrometer with 0.98 µm divisions. The eyepiece micrometer was calibrated with a standard Zeiss micrometer slide. The diameters of at least 300 calcareous *T. heimii* shells were measured in cultures from 16° to 27°C (Fig.4), each sample was evaluated and an arithmetic mean established (n=300). In addition to the shell size studies, the degree of calcification of shells from Exp#1 was examined (Fig.5). This examination of the calcareous shells (size measurements and calcification) was done with the help of LM polarisation equipment (crossed nicols; gypsum plate) as described by Janofske (1996).

Results

Growth occurred from 14°C (Exp#1) to 27°C (Exp#3) (Fig.2). Maximal exponential growth rates (0.35 - 0.38 div * day $^{-1}$) were obtained at 26.9°C – 27°C. A second phase of exponential growth was only observed during Exp#3 at 19.5°C. For this culture the first exponential growth phase was used to calculate the growth rate.

Cultures from Exp#1 with f/2 have a generally higher final yield than the cultures grown in f/20 (Exp#2, Exp#3) except in the cultures grown at 26.9°C to 27.4°C, where the final yield shows very similar values in all three experiments (Fig.3). Highest final yield was observed at 14°C (Exp#1). During Exp#2 cultures at 14°C and 15.8°C did not reach the declining and stationary phase within the time frame of the experiments. No final yield was calculated for these cultures.

Shell sizes were evaluated for all cultures of Exp#1 and show a range from 9.9 µm to 21.7 µm (Fig.4). Most specimen have diameters between 13.8 µm to 17.7 µm. Distributions of the mean diameters (n = 300) in comparison to temperature are shown in Fig.4. Largest mean diameters were observed at 23.4°C.

Calcification degrees were divided into three levels: weakly calcified = crystals do not cover the entire sphere; medium calcified = the shell is fully formed with a very thin calcite layer; well calcified = fully formed shell with a strong wall. There are temperatures where shell calcification is particularly strong or weak (Fig.5). Samples show less than 50 % of well calcified shells at all temperatures except at 16°C (~75 %) and 25.1°C (~70 %). At 21.6°C well calcified shells are almost absent and ~60 % of shells are weakly calcified.

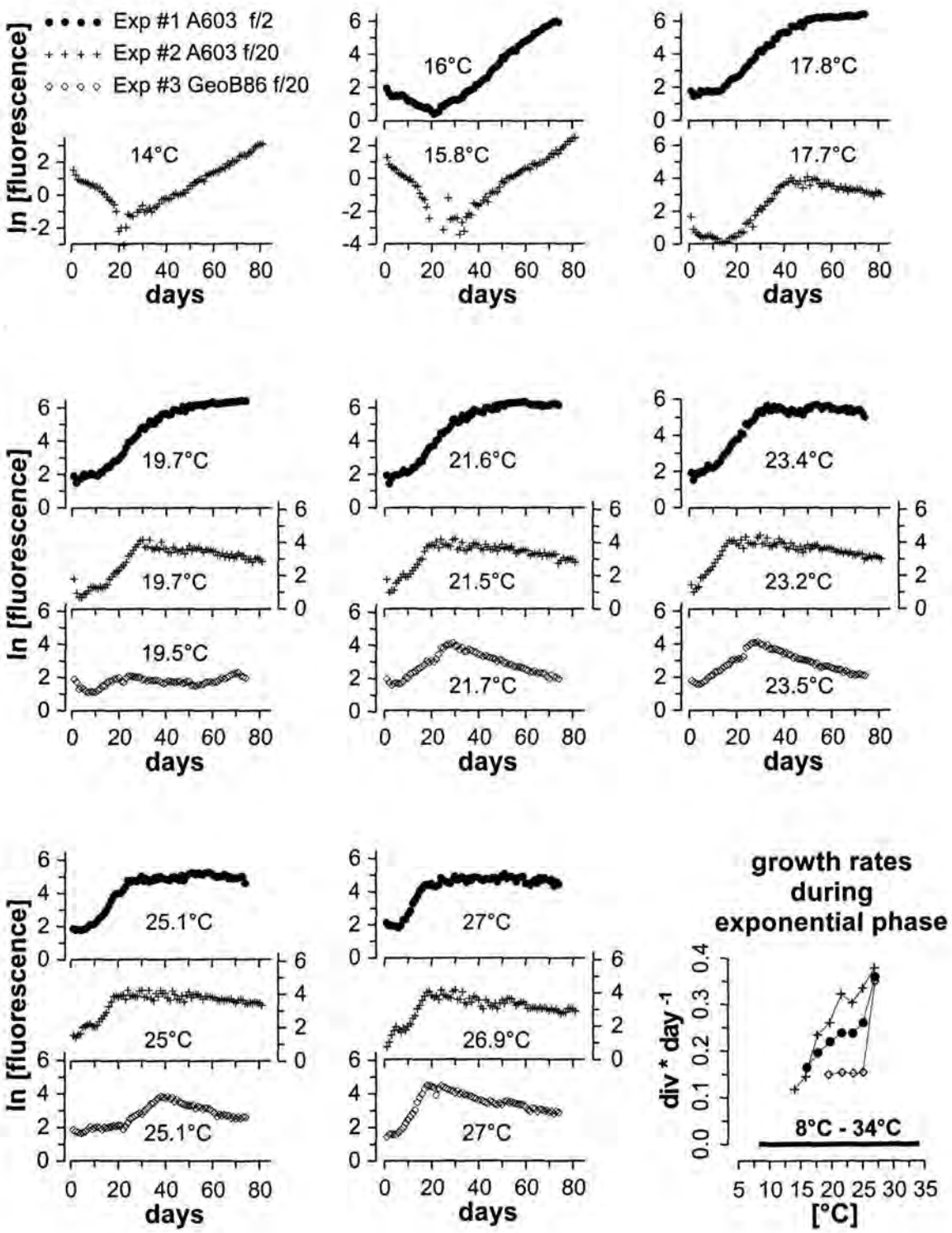

Fig.2: Growth of *Thoracosphaera heimii* in culture experiments. The bar in the growth rate diagram indicates the temperature range tested on the *T. heimii* clones; symbols in the graph indicate the temperatures at which growth occurred.

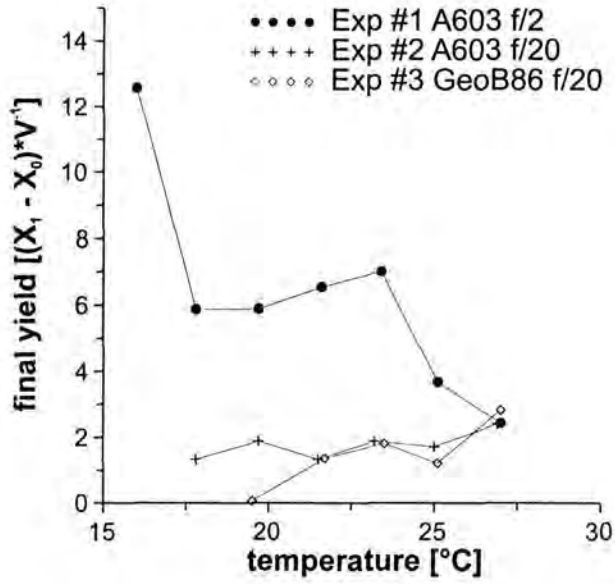

Fig.3: Final yield of *Thoracosphaera heimii* in Exp#1, 2 and 3. X_0 = fluorescence after inoculation; X_1 = fluorescence on the last day of exponential growth; V = culture media volume (30 ml).

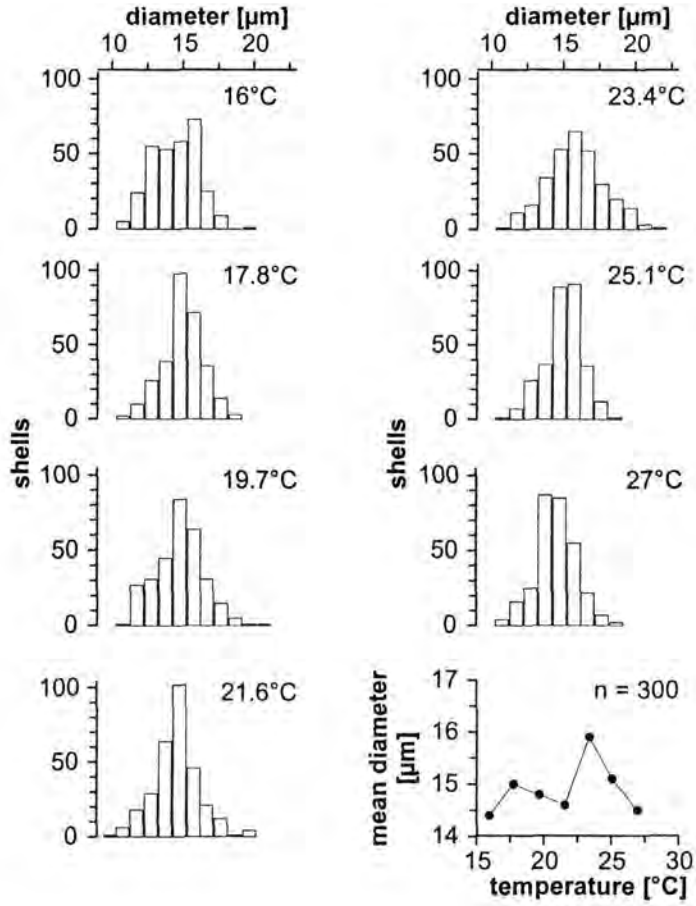

Fig.4: Shell diameters of *Thoracosphaera heimii* in Exp#1 and mean shell diameters *vs.* temperature.

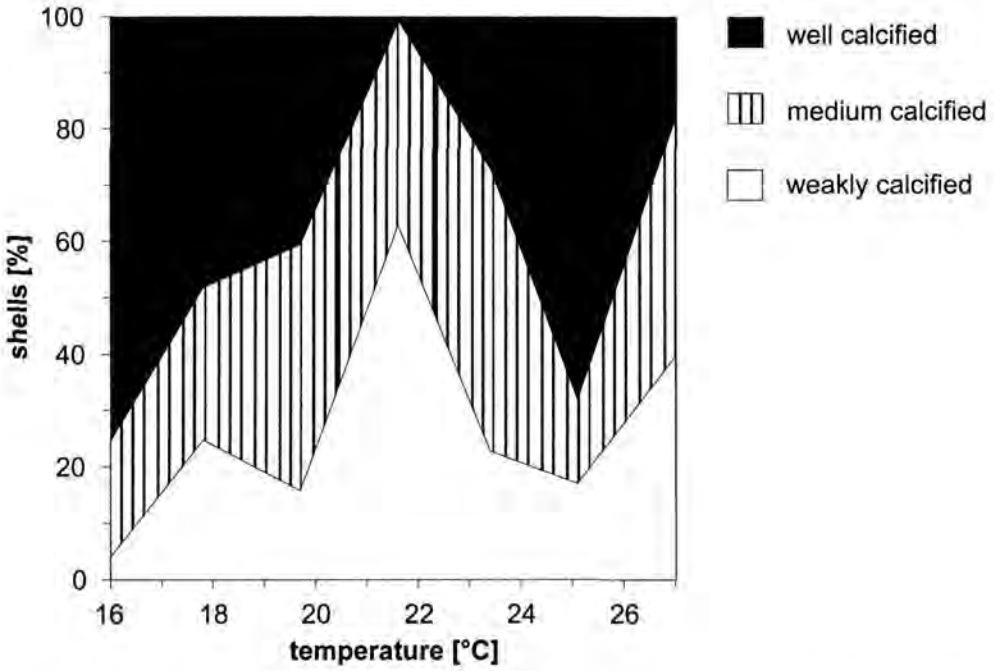

Fig.5: Distribution of weakly, medium and well calcified *Thoracosphaera heimii* shells *vs.* temperature in Exp#1 (100 % = 300 shells).

Discussion

Whereas it seems, that *T. heimii* is able to adapt to the lower temperatures of the tested gradient, cultures held in temperatures more than 27°C died rather quickly. It can be assumed that the point at which *T. heimii* is no longer successful in culture lies between 27°C and the next highest step in the temperature gradient of the presented experiments (28.6°C). During a first test run of the TGB *T. heimii* clone A603 was growing at 28.1°C in K culture medium without silica (Keller et al., 1987).

In the field *T. heimii* has been described as a cosmopolitan species of warm and temperate waters (Tangen et al., 1982). Kerntopf (1997) reported *T. heimii* in plankton samples off NW Africa with sea surface temperatures from 18°C to 29°C but did not distinguish between live and empty shells. Karwath et al. (2000) have obtained *T. heimii* shells with cell content from the tropical and equatorial Atlantic Ocean in waters ranging between 13.3°C and 28.7°C, though contents at high temperatures were very low. Maximum occurrences of *T. heimii* shells with cell content were observed between 18°C to 26.8°C at depths between 20 m to 100 m.

Growth rates of *T. heimii* observed during the experiments (0.08 – 0.38 div * day–1) fall for the most part within the range of low rates typical of dinoflagellates (0.16 – 1.28 div * day–1) reported by Tang (1996) but are well below the mean rate (0.577 div * day–1; n = 20; 15°C) established for *T. heimii* by Brand and Guillard (1981). Comparing the growth of the

strain A603 in two different media, f/20 (Exp#2) yields higher growth rates than f/2 (Exp#2). *T. heimii* growth rates during the present study do not show, as one might expect, an unimodal response curve *vs.* temperature. Values rise with increasing temperatures toward maximal growth rates around 27°C.

The high growth rates of *T. heimii* in all three experiments at 27°C do not necessarily result in the highest final yield of the respective experiment. Exp#2 and Exp#3 have their highest final yield at this temperature but during Exp#1 quite the opposite occurred: growth rates rise with increasing temperature but the final yield decreases with increasing temperature. The final yield at 27°C in all three experiments is about the same, even though there were more nutrients available during Exp#1.

During Exp#1 it is striking that *T. heimii* is able to produce the highest final yield with the lowest growth rate at the lowest temperature (16°C). The culture at 16°C has barely reached the declining phase after 52 days of exponential growth whereas the 27°C culture has an exponential phase of only 12 days. This means that *T. heimii* is able to grow higher amounts of cells (or chlorophyll) under the same nutritional conditions at lower temperatures than at high temperatures.

At the same time, shells grown at 16°C during Exp#1 have the highest percentage of well calcified cells (~75 %; Fig.5) and show the smallest mean diameter (Fig.4). Mean diameters of shells grown at 27°C are only marginally larger but evaluation shows only ~20 % well calcified shells. It is conceivable that due to the low division rates at 16°C the organism spends longer periods within the calcareous shell and thus forms stronger walls. Conversely with the relatively higher division rates at 27°C the organism does not seem to have enough time for the formation of a strong calcareous shell.

Other extreme values concerning the degree of calcification were observed at 21.6°C (well calcified shells ~ 1 %) and 25.1°C (well calcified shells ~70 %). These values do not correlate with special points in final yield, growth rate or shell size. The experiment was terminated for all cultures at the same time and the subsequently taken samples represent cultures in different stages of development. At the termination of Exp#1 cultures at low temperatures were still growing while cultures at high temperatures were already in the stationary phase or declining (Fig.2). To obtain more reliable data on calcification for possible use in palaeoenvironmental research the mineralisation process should be monitored by studying subsamples from each culture taken shortly after the exponential phase.

The results from the *T. heimii* growth experiments – especially the distribution of growth rates *vs.* temperature – of the present study did not meet with our expectations of growth of

the species in a temperature gradient. Whether other pelagic calcareous dinoflagellates show similar characteristics concerning growth rates and final yield *vs.* temperature or not will be compared in analogous experiments.

Acknowledgements

Financial support was provided by the Deutsche Forschungsgemeinschaft (Wi 725/7) and the SFB 261. We are indebted to an anonymous reviewer and Gerard Versteegh for critical remarks and discussion of an earlier version of the manuscript. We thank Dirk Krautwig for helping one of the authors (F.T.) with invaluable trouble-shooting and technical support during the completion of the temperature gradient box. The experiments would not have been possible without the help of Anja Meyer and we also thank Bettina and Adam Price for correcting the English.

References

Bjørnland, T., 1990. Chromatographic Separation and Spectrometric Characterization of Native Carotinoids from the Marine Dinoflagellate *Thoracosphaera heimii*. Biochem. Syst. Ecol., 18: 307-316.

Brand, L.E. and Guillard, R.R.L., 1981. A method for the precise determination of acclimated phytoplankton and reproduction rates. J. Plankton Res., 3 (2): 193-201.

Dale, B., 1992a. Dinoflagellate Contribution to the Open Ocean Sediment Flux. In: B. Dale and A. Dale (Editors), Dinoflagellate Contribution to the Deep Sea, Ocean Biocoenosis Series ed., Vol. No. 5. Woods Hole Oceanographic Institution, Woods Hole, pp. 1-32.

Dale, B., 1992b. Thoracosphaerids: Pelagic Fluxes. In: S. Honjo (ed.), Dinoflagellate Contibution to the Deep Sea, Ocean Biocoenosis Series ed., Vol. 5. Woods Hole Oceanographic Institution, Woods Hole, Massachusetts, pp. 33-43.

Dale, B. and Dale, A.L., 1992. Ocean Biocoenensis Series, 5: Dinoflagellate Contributions to the Deep Sea. Woods Hole Oceanographic Institution, Woods Hole, Massachusetts, 75 pp.

Fensome, R.A., Taylor, F.J.R., Norris, G., Sarjeant, W.A.S., Wharton, D.I., Williams, G.L. 1993. A classification of living and fossil dinoflagellates. Micropaleontology, Spec. Publ., 7: pp 351

Guillard, R.R.L., 1973. Division rates. In: Stein, J.R. (ed.) Handbook of Phycological Methods, Cambridge University Press, pp.289-311.

Guillard, R.R.L. and Ryther, J.H., 1962. Studies of marine planktonic diatoms. I. *Cyclotella*

nana Hustedt and *Detonula confervacea* Cleve, Can. J. Microbiol., 8: 229-239.

Hildebrand-Habel, T. and Willems, H., 1997. Calcareous dinoflagellate cysts from the Middle Coniacian to Upper Santonian chalk facies of Lägerdorf (N Germany). Cour. Forsch. - Inst. Senckenberg, 201: 177-199.

Hildebrand-Habel, T., Willems, H., (2000). Distribution of calcareous dinoflagellates from the Maastrichtian to early Miocene of DSDP Site 357 (Rio Grande Rise, western South Atlantic Ocean. Int. Journ. Earth Sciences 88 (4), 694-707.

Höll, C., 1998. Kalkige und organisch-wandige Dinoflagellaten-Zysten in Spätquartären Sedimenten des tropischen Atlantiks und ihre palökologische Auswertbarkeit. Berichte, Fachbereich Geowissenschaften, Universität Bremen, 127: pp.121.

Höll, C., Karwath, B., Rühlemann, C., Zonneveld, K.A.F. and Willems, H., 1999. Palaeoenvironmental information gained from calcareous dinoflagellates: The Late Quaternary eastern and western tropical Atlantic Ocean in comparison. Palaeogeogr. Palaeoclimatol. Palaeoecol. 146: 147-164.

Höll, C., Zonneveld, K.A.F. and Willems, H., 1998. On the ecology of calcareous dinoflagellates: The Quaternary eastern Equatorial Atlantic. Mar. Micropaleont., 33: 1-25.

Inouye, I. and Pienaar, R.N., 1983. Observations on the life cycle and microanatomy of *Thoracosphaera heimii* (Dinophyceae) with special reference to its systematic position. S. Afr. J. Bot., 2: 63-75.

Janofske, D., 1996. Ultrastructure types in Recent "calcispheres". Bull. Inst. Océanogr., Monaco, 14 (4): 295-305.

Jones, G.J., Nichols, P.D. and Johns, R.B., 1983. The Lipid Composition of *Thoracosphaera heimii*: Evidence for Inclusion in the Dinophyceae. J. Phycol., 19: 416-420.

Karwath, B., Janofske, D., Willems, H., (2000). Spatial distribution of the calcareous dinoflagellate Thoracosphaera heimii in the upper water column in the tropical and equatorial Atlantic. Int. Journ. Earth Sciences 88 (4), 668-679.

Keller, D.K., Selvin, R.C., Claus, W. and Guillard, R.R.L., 1987. Media for the culture of oceanic ultraplankton. J. Phycol., 23: 633-638.

Kerntopf, B., 1997. Dinoflagellate Distribution Patterns and Preservation in the Equatorial Atlantic and Offshore North-West Africa. Ber. Fachber. Geowiss., 103: 137pp.

Lewis, J., Dodge, J.D., Powell, A.J., 1990. Quaternary dinoflagellate cysts from the upwelling system offshore Peru, Hole 686B, ODP LEG 112. In: Suess R, von Huene et al. (eds.), Proceedings of the Ocean Drilling Program, Scientific Results, 112: 323-328.

Matthiessen, J., 1995. Distribution patterns of dinoflagellate cysts and other organic-walled microfossils in Recent Norwegian-Greenland Sea sediments. Mar. Micropaleont. 24: 307-334.

Montresor, M., Janofske, D., Willems, H., 1997. The cyst – theka relationship in *Calciodinellum operosum* emend. (Peridiniales, Dinophyceae) and a new approach for the study of calcareous cysts. J. Phycol., 33: 122-131.

Rowan, R. and Powers, D.A., 1992. Ribosomal RNA sequences and the diversity of symbiotic dinoflagellates (zooxanthellae). Proc. Natl. Acad. Sci. USA, 89: 3639-3643.

Sorokin, C., 1973. Dry weight, packed cell volume and optical density. In: Stein, J.R. (ed.) Handbook of Phycological Methods, Cambridge University Press, pp. 321-343.

Tang, E.P.Y., 1996. Why do dinoflagellates have lower growth rates? J. Phycol., 32: 80-84.

Tangen, K., Brand, L.E., Blackwelder, P.L. and Guillard, R.R., 1982. *Thoracopsheara heimii* (Lohmann) KAMPTNER is a dinophyte: observations on its morphology and life cycle. Mar. Micropaleont., 7: 193-212.

Turon, J.-L., 1980. Dinoflagellés dans les sédiments récents de l'Atlantique nord-oriental et leurs relations avec l'environment océanique. Application aux dépots Holocènes du Chenal de Rockall. Memoire Musée Naturelle d'Histoire, Paris B27: 269-282.

Wall, D., Guillard, R.R.L., Dale, B., Swift, E., Watabe, N., 1970. Calcitic resting cysts in *Peridinium trochoideum* (STEIN) LEMMERMANN, an autotrophic marine dinoflagellate. Phycologia 9 (2): 151-156

Willems, H., 1996. Calcareous dinocysts from the Geulhemmerberg K/T boundary section (Limburg, SE Netherlands). Geol. en Mijnb., 75: 215-231.

Zonneveld, K.A.F., Höll, C., Janofske, D., Karwath, B., Kerntopf, B. and Willems, H., (1999). Calcareous dinoflagellate resting cysts as paleo–environmental tools. In: Fischer, G., Wefer, G. (eds.) Proxies in Paleoceanography. Springer-Verlag, Berlin, Heidelberg, pp145-164.

3.2

SPATIAL DISTRIBUTION OF THE CALCAREOUS DINOFLAGELLATE *THORACOSPHAERA HEIMII* IN THE UPPER WATER COLUMN OF THE TROPICAL AND EQUATORIAL ATLANTIC

(International Journal of Earth Sciences 88 (4): 668-679. 2000)

SPATIAL DISTRIBUTION OF THE CALCAREOUS DINOFLAGELLATE *THORACOSPHAERA HEIMII* IN THE UPPER WATER COLUMN OF THE TROPICAL AND EQUATORIAL ATLANTIC

Britta Karwath*, Dorothea Janofske, Helmut Willems

Fachbereich-5 Geowissenschaften, Universität Bremen, Postfach 330 440, 28334 Bremen, Germany. Fax: 0421/2184451

*e-mail corresponding author: karwath@micropal.uni-bremen.de

Keywords: calcite, dinoflagellates, phytoplankton, Atlantic, actuopalaeontology

Abstract

The horizontal and vertical distribution of the phototrophic, calcareous dinoflagellate *Thoracosphaera heimii* in the upper part of the water column (10 to 200 m) of the equatorial and tropical Atlantic Ocean has been studied. This first survey has been made to determine which part of the water column is inhabited by *T. heimii* and subsequently represented as a signal in the sediment record by this species. The study concentrates on the fossilisable vegetative coccoid life-stage of the species and differentiates between *T. heimii* shells with cell content and empty ones. The highest quantities of *T. heimii* shells with cell content have been observed in water depths between 50 and 100 m and coincide with relatively lower temperatures and relatively higher salinities than respective surface conditions. We propose that in the tropical equatorial Atlantic the major part of the environmental signal given by *T. heimii* can be assumed to represent the deeper levels of the upper water column.

Introduction

Dinoflagellates are a group of unicellular eukaryotic organisms representing one of the major (marine) phytoplankton groups. During the last decades, research has focused on these fossilisable organic remains of dinoflagellates, generally regarded as the preserved wall of cyst stages. Studies include, among other topics, research on (palaeo-) productivity, (palaeo-) environment and (palaeo-) oceanography (e.g. Wall et al., 1977; Lewis et al., 1990;

Matthiessen, 1995; Höll et al., 1998; Höll et al., 1999). In contrast, information is rare on dinoflagellate taxa with calcareous skeletal elements. In particular, the biology and ecology of pelagic taxa are largely unknown.

Calcareous dinoflagellates have often been neglected in plankton studies due to their size of about 10 to 60 µm. They are too small to be included in foraminifera research and too large for nannoplankton studies. The use of acids during preparation automatically excludes calcareous dinoflagellates from consideration in palynological studies. During the last decade observations made on this group have hinted at a far more important role for calcareous dinoflagellates than formerly recognised (Dale, 1986; Dale, 1992a, b; Kerntopf, 1997; Höll et al., 1998; Höll et al., 1999).

Investigations in boreal regions by Dale and Dale (1992) have revealed a predominance of organic-walled dinoflagellate cysts. However, studies by Dale (1986), Dale (1992a) and Höll et al. (1998; 1999) have shown that dinoflagellate cyst assemblages in the subtropics and tropics are mainly composed of calcareous dinoflagellates. The high flux rates of calcareous dinoflagellates in the subtropics and tropics (Dale, 1992a, b) suggest that they may form a significant contribution to the ocean carbon flux.

Recent investigations by Kerntopf (1997) and Höll et al. (1998; 1999) have also shown that calcareous dinoflagellate associations in the tropics and subtropics are often overwhelmingly dominated by the phototrophic species *Thoracosphaera heimii*. Kerntopf (1997) described *T. heimii* as abundant off the north-west coast of Africa with 2 – 12 % of the shelled phytoplankton. Studies on sediment trap material from the Equatorial Pacific Ocean and the Equatorial Atlantic Ocean (Dale, 1992b) have revealed that the calcareous dinoflagellate flux is mostly composed of "thoracosphaerids" (in this case *T. heimii* and *Thoracosphaera granifera* = *?Orthopithonella granifera*). Observations by Höll et al. (1998; 1999) from sediment core material (down to 140 ka) from the western and eastern tropical Atlantic Ocean have shown high contents of calcareous dinoflagellates and again, the dominance of *T. heimii* was overwhelming. This prevalence of *T. heimii* in the calcareous dinoflagellate associations can be explained by the species' ability to produce large numbers of calcareous spheres in a relatively short period. Its position within the family of the Dinophyceae is thus far unique: in contrast to other calcareous dinoflagellates, most of the cells produced by *T. heimii* form a calcareous skeleton (Tangen, et al. 1982). This calcareous wall has been referred to as a "shell" rather than the more usual term "cyst". This is to stress that it is formed as a dominant vegetative-coccoid life-stage of the species and not as a resting stage (Inouye and Pienaar, 1983).

In spite of the abundance of the species and, in most cases, its dominance over other calcareous dinoflagellates, little is known to date about the environmental affinities of *T. heimii*.

In one of the first studies, Höll et al. (1999) compared the content of calcareous dinoflagellate remains in two sediment cores. One from below the highly productive eastern Atlantic equatorial divergence zone and another from the low productivity area of the western tropical Atlantic. In this endeavour to establish a new tool for palaeoenvironmental reconstructions, calcareous dinoflagellates (mostly *T. heimii*) show increased accumulation rates in the low productivity area in the western and lower accumulation rates in the high productivity region in the eastern South Atlantic. Organic dinoflagellates follow an opposite pattern (Höll, 1998). Enhanced production of calcareous dinoflagellates in the investigated region and time interval were correlated to periods of reduced palaeoproductivity probably related to relatively stratified conditions of the upper water column.

In order to improve the database available for interpretation of *T. heimii* occurrences in the sediment, and in view of these findings, it is important to determine which part of the water column is inhabited by *T. heimii*.

The aim of our investigations is to determine the value of *T. heimii* as a proxy for palaeoenvironmental conditions. The present study deals with the lateral and vertical distribution of the fossilisable vegetative-coccoid stage of *T. heimii* in the upper water column of the tropic and equatorial Atlantic in relation to the surrounding environmental parameters.

Oceanographic and Atmospheric Settings

The equatorial Atlantic is strongly influenced by the westward flow of the South Equatorial Current (SEC) and the eastward flow of the North and South Equatorial Counter Currents (NECC; SECC). North of the NECC lies the westward flowing North Equatorial Current (NEC). In the south, the SECC divides the SEC into separate streams, the stronger main branch to the south and a smaller but faster branch to the north. The SEC is part of the South Atlantic Subtropical Gyre (Peterson and Stramma 1991).

The upper-level current system of the eastern tropical Atlantic is characterised by the southward flowing Canary Current (CC) which eventually detaches itself from the continental slope and becomes the westward flowing NEC at 14° N (Voituriez, 1981; Hagen and Schemainda, 1984).

The Trade Winds and thus the seasonal migration of the Inner Tropical Convergence Zone (ITCZ) heavily influence the hydrographic conditions in the studied regions. The ITCZ is the

convergence zone of the prevailing Southeast and Northeast Trade Winds. There is a seasonal shift in the latitudinal position of the ITCZ: during boreal winter (January to April) the Northeast Trade Winds are at their strongest and move the ITCZ to its southernmost position near the equator. During boreal summer the Southeast Trade Winds gain dominance and shift the ITCZ toward its northernmost position (August). During this time, the SEC, driven by the Southeast Trade Winds, crosses the equator (Höflich, 1984; Philander and Pacanowski, 1986). In the following text, all seasons refer to the Northern Hemisphere.

Eastern Atlantic

Cape Blanc

In the study area off Cape Blanc (CB) the cold South-eastward bound CC detaches itself from the continental slope and entrains shelf water from the north and south offshore (Mittelstaedt, 1991). The open ocean waters are characterised by sea surface temperatures (SST) of about 21° to 22°C and low pigment concentrations (chlorophyll < 0.1 mg m^{-3}) (Van Camp et al. 1991). Over the shelf and along the entire coast nutrient-rich, newly upwelled cold waters are responsible for high chlorophyll concentrations and high primary production rates in all seasons (Van Camp et al., 1991; Longhurst et al., 1995).

Off CB upwelling conditions occur throughout the year influenced by the relatively steady and strong Trade Winds. Upwelling is most intense in spring, June/July and autumn (Mittelstaedt, 1991; Van Camp et al., 1991).

Cape Verde

The Guinea Dome - a permanent thermal (subthermoclinal) dome (Voituriez 1981; Hagen and Schemainda 1984) - has a homogeneous layer of warm water below the thermocline. This produces significant upwelling without the usual appearance of cold waters in its surface waters (Voituriez, 1981). The Dome is situated south of the Cape Verde Islands (mean position 12°N and 22°W) and is under strong influence of the seasonal migration of the ITCZ (Mittelsteadt, 1991).

The study area is under partial influence of the CC (Voituriez, 1981; Hagen and Schemainda, 1984). To the south of 10°N, the main influence in the area is the NECC, which is strong in summer and early fall. In winter and early spring the Trade Winds push the NECC southward and weaken the current. Upwelling occurs in the Cape Verde (CV) area during these months (Mittelstaedt, 1991).

Guinea Basin

During winter, the study area in the Guinea Basin is under influence of the NE Trades, which enhance both the NEC and the coastal Guinea Current (Philander and Pacanowski, 1986). In summer, the Southeast Trade Winds are very strong. This leads to a maximum development of the SEC and a maximum eastward advection of the NECC (Peterson and Stramma, 1991). Primary production is high (Longhurst et al., 1995) from July to September when equatorial upwelling occurs. SST's lie between 22° to 25°C (Voituriez and Herbland, 1977).

Western Atlantic

Western Equatorial Atlantic

Productivity in the Western Equatorial Atlantic is low (Longhurst et al., 1995). From March to April the pigment concentration (chlorophyll) is low (Monger et al., 1997) and the wind intensity is at a minimum. The westward NECC is weakened during this time (Philander and Pacanowski, 1986; Chepurin and Carton, 1997). Between the start of July and the end of September the ITCZ migrates northward which causes considerable intensification of the SEC south of 3° N. From August to December pigment concentrations start to increase (Monger et al., 1997). In January and February, the wind intensity along the equator weakens and pigment concentrations begin to recede (Monger et al., 1997).

Western Tropical Atlantic

The WTA region lies within the general area through which the NECC flows (5° to 10° N; Longhurst, 1993). The NECC lies under the meridional march of the ITCZ and is influenced during winter by the NE Trades. During summer, the stronger SE Trades dominate the area. Algal blooms in the Western and central region in the tropical Atlantic begin to develop when the continuous flow of the NECC originates at ~50° W.

By January the eastward flow of the NECC originates at only about 20° W (Carton, 1989). In the interval from January to March there are only a few scattered patches of 0.25 mg m^{-3} surface chlorophyll. Algal blooms in the western and eastern region from May to June reach values (0.25 to 1.0 mg m^{-3}) higher than background (Longhurst, 1993).

Material

The seawater samples examined in the present study were taken during two Atlantic cruises of the *R/V Meteor* in January/February 1997 (cruise M38-1) and May/June 1998

(cruise M41-4). The cruises were carried out within the scope of the SFB 261 program "Der Südatlantik im Spätquartär: Rekonstruktion von Stoffhaushalt und Stromsystemen" at the Universität Bremen. Sample sites are shown in Fig.1. Seawater samples were taken at depths between 10 m to 100 m (M38-1) and 10 m to 200 m (M41-4). This was done with a rosette sampler (Multi Wasserschöpfer MWS) using several 10 l NISKIN™ bottles at each depth (see Tabs. 1; 2).

Sites

The sample sites of this study are located in the eastern and western equatorial and tropical Atlantic (Fig.1). Sites CB1 and CB20 were located off Cape Blanc (CB) in the Mauritian upwelling area, sites CV2 and CV19 are situated south of the Cape Verde Islands within the Guinea Dome. We sampled the water column in the western part of the Guinea Basin at four different sites (EET15 through EET18) in a south-north transect (Eastern Equatorial Transect, EET). Sites WET10 through WET7 and WET11 through WET14 are situated in the oligotrophic western Atlantic, south of or on the equator (Western Equatorial Transect, WET). In the Western Tropical Atlantic (WTA; about 4° - 8° N and 31° - 40° W) samples were taken from four sites (WTA3 through WTA6).

Methods

Treatment of the samples onboard as well as the sample preparation followed procedures especially developed for this study. The method for the onboard filtration of seawater was influenced by techniques developed over several years by the working group (e.g. Kerntopf, 1997). The preparation of plankton samples for the quantitative study of calcareous dinoflagellates underwent several modifications during the work on material from cruise M38-1.

Onboard filtration

The seawater was pre-filtered through a 100 µm mesh-sieve and was then filtered through 5 µm polycarbonate filters (diameter: 50 mm) - using a vacuum pump system - until about 100 ml of the sample remained. This was stored together with the 5 µm filters in 250 ml NALGENE™ polycarbonate flasks. The polycarbonate filters are very smooth. Controls have

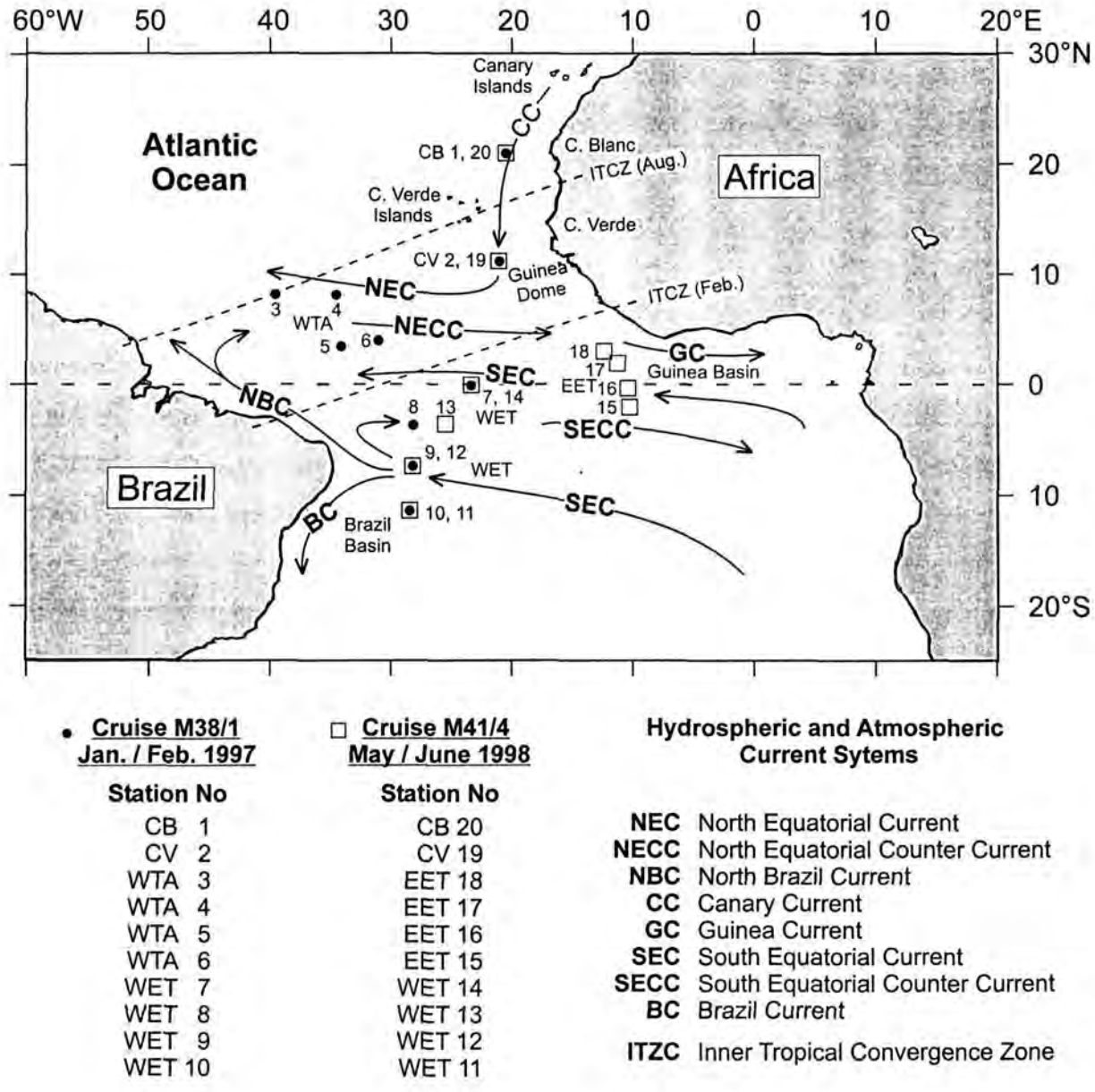

Fig.1: Hydrographic and atmospheric settings. Filled circles and open squares indicate sample sites from M38-1 and M41-4 respectively (see key for details). Modified largely after Peterson and Stramma (1991).

shown that mostly small particles, such as green algae and diatoms, remain on the filter when the sample is shaken; other particles are washed off into the rest of the sample. The seawater samples were fixed with 3 - 4 % formaldehyde at a final concentration of 2 %.

Sample preparation

A portion of the fixed seawater sample was filtered through a 0.8 µm cellulose-acetate filter (diameter: 13 mm). The sample was rinsed with 1 ml artificial seawater (hw Meersalz, Wiegand GmbH, Krefeld; 34 PSU; pH 8.6). The samples were dehydrated in an ethanol series and the filters were then mounted on microscope slides with a low viscosity resin (Spurr's resin; see also Janofske, 1996) and covered with a cover slip.

The use of Spurr's resin in this case was problematical and lead to the destruction of several sample slides. We abandoned the use of Spurr's resin along with the dehydration process. In the modified method, samples were simply rinsed with 1 ml artificial seawater. One millilitre of ethanol was added for ten minutes to remove the salt water. After rinsing with artificial seawater some samples (Tab.1, 2) were additionally treated with the DNA fluorochrome 4',6-diamidino-2-phenylindole (DAPI; Dann et al., 1979) to stain the nucleus. The stain was made up in a buffered solution containing 0.1 M TRISMA-base (titrated with HCL to pH 7.4) and 0.1 M NaCl. To 1 mg of DAPI, 2 ml of buffer was added. DAPI-buffer solution (2 µl) was added to 1 ml of artificial seawater. The mixture was then allowed to react with the sample for fifteen minutes. Samples were finally rinsed with 1 ml ethanol and the filters were mounted on microscope slides with glycerine jelly and covered with a cover slip. Samples were insulated from air with varnish.

Sample evaluation

Samples were studied with a Zeiss Axiophot light microscope. The entire slide content was counted. Three slides per sample were investigated for cruise M38-1. The three different counts per sample were each calculated to the total content of *T. heimii* shells per 100 l seawater. The three counts were used to calculate an arithmetic mean per 100 l of sea water (Tab. 1). The final of the three sample sets of cruise M38-1 was additionally stained with DAPI and used for the distinction between empty *T. heimii* shells and shells with cell content (Fig.2). The material was viewed under ultra-violet light (Zeiss filter set 01, extinction BP 365, emission LP 377); the cell content was evident by the DAPI-stained nucleus. Counts were calculated to 100 l of seawater. For cruise M41-4 one slide per sample was counted. The samples were stained with DAPI and allowed differentiation between *T. heimii* shells with and without cell content (Tab. 2; Fig.3). In the following text, total *T. heimii* content will be referred to as '*T. heimii* shells', whereas *T. heimii* shells with cell content will be referred to as '*T. heimii* cells'. The *T. heimii* cells were not examined on their viability. We assume the major portion of the *T. heimii* cells to have been alive at the time of sampling because their

nature is vegetative and generally metabolically and photosynthetically active (Tangen et al., 1982; Inouye and Pienaar, 1983). The content of non-calcified *T. heimii* cells was not established: The gymnoid planospores lack identifying thecal plates. Non-calcified aplanospores are also in short supply of easily identifiable features. It is extremely difficult to even relate the aplanospores by lightoptic means to the Dinophyceae when viewed outside a clonal culture.

Additional measurements

Temperature and salinity data (courtesy of the division of Marine Geology, Universität Bremen, Figs. 2, 3) were measured with a CTD system (Conductivity, Temperature, Depth). Since no CTD data were available for site WTA6 (Fig.1), World Ocean Atlas 1994 data (CD-ROM Data Set, National Oceanographic Data Center, Washington D.C.) averaged over three to five years were substituted. All salinity data are given in practical salinity units (psu) (Practical Salinity Scale 1978; UNESCO 1981).

Results

T. heimii occurred throughout the entire investigated area but in horizontally and vertically varying amounts (Figs.2 and 3).

Horizontal distribution

Cruise M38-1; January/February 1997

Maximum occurrences (mean of the entire depth profile) of *T. heimii* shells during this cruise (Fig.2) were observed in the WTA at ~4°N (WTA6). Samples show a decrease of *T. heimii* shells toward the north of this area (~8°N; WTA3, WTA4). The stations in the WET from the Brazil Basin (~11°S) toward the equator (~23°W) yield no distinct differences in *T. heimii* shell counts. Similar high occurrences of *T. heimii* shells as recorded in the WTA were observed only off CB. The abundance of *T. heimii* shells in the CB area is, on average, twelve times higher than at the Cap Verde station.

Fig.2: Distribution of *Thoracosphaera heimii*, cruise M38-1, January / February 1997 and measured CTD data. Open bars show content of *T. heimii* shells, black bars indicate *T. heimii* shells with cell content per 100 l of seawater in the given depth. Arrows indicate arithmetic mean of total *T. heimii* content of the entire depth profile. **Temperature:** graph with open squares. **Salinity:** graph with filled circles. Symbols on both graphs indicate sampled water depth.

Fig. 2

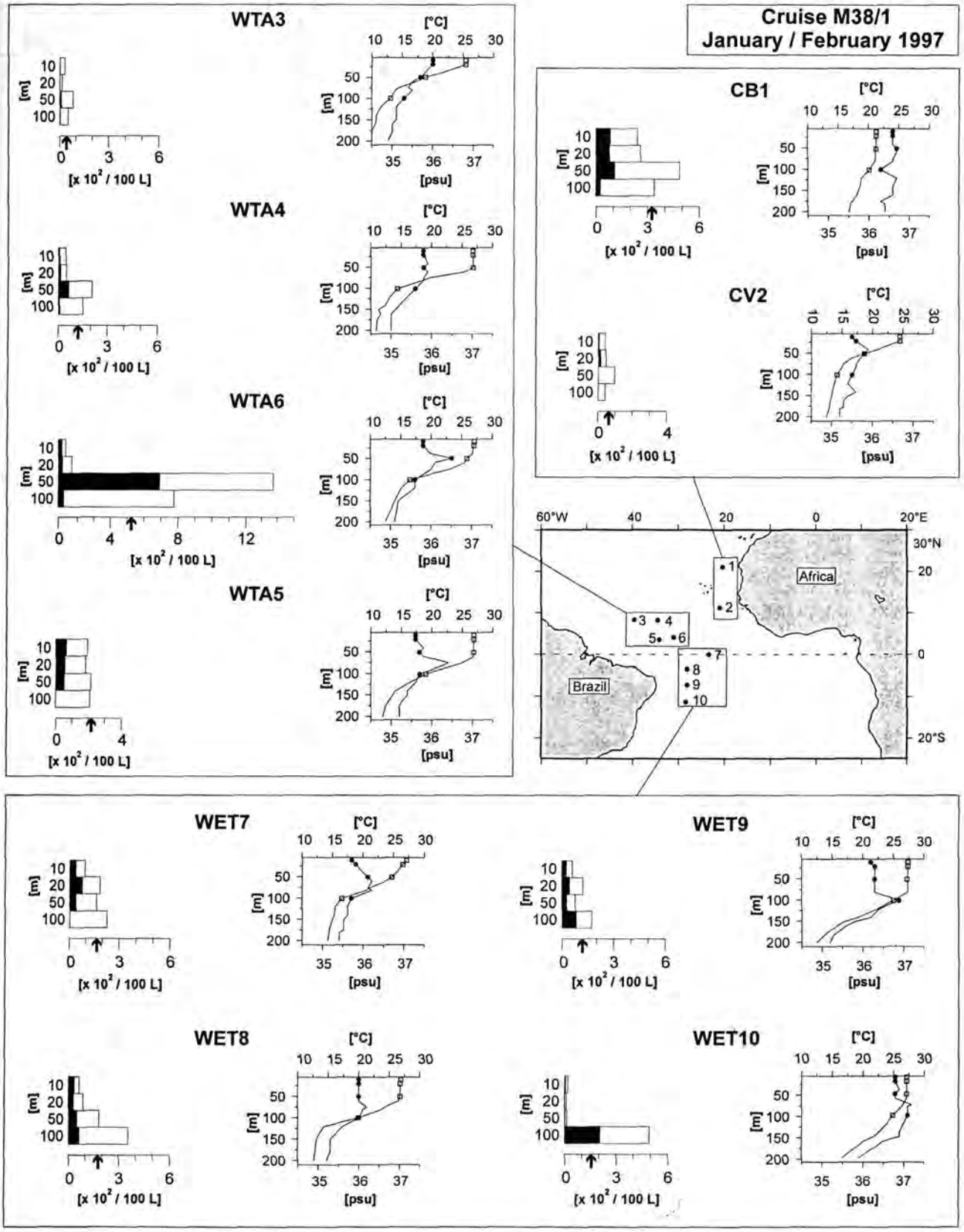
Cruise M38/1
January / February 1997
WTA3
WTA4
WTA6
WTA5
CB1
CV2
WET7
WET8
WET9
WET10
[m]
[°C]
[psu]
[x 10² / 100 L]
60°W
40
20
0
20°E
30°N
20
0
20°S
Africa
Brazil
1
2
3
4
5
6
7
8
9
10

Fig. 3

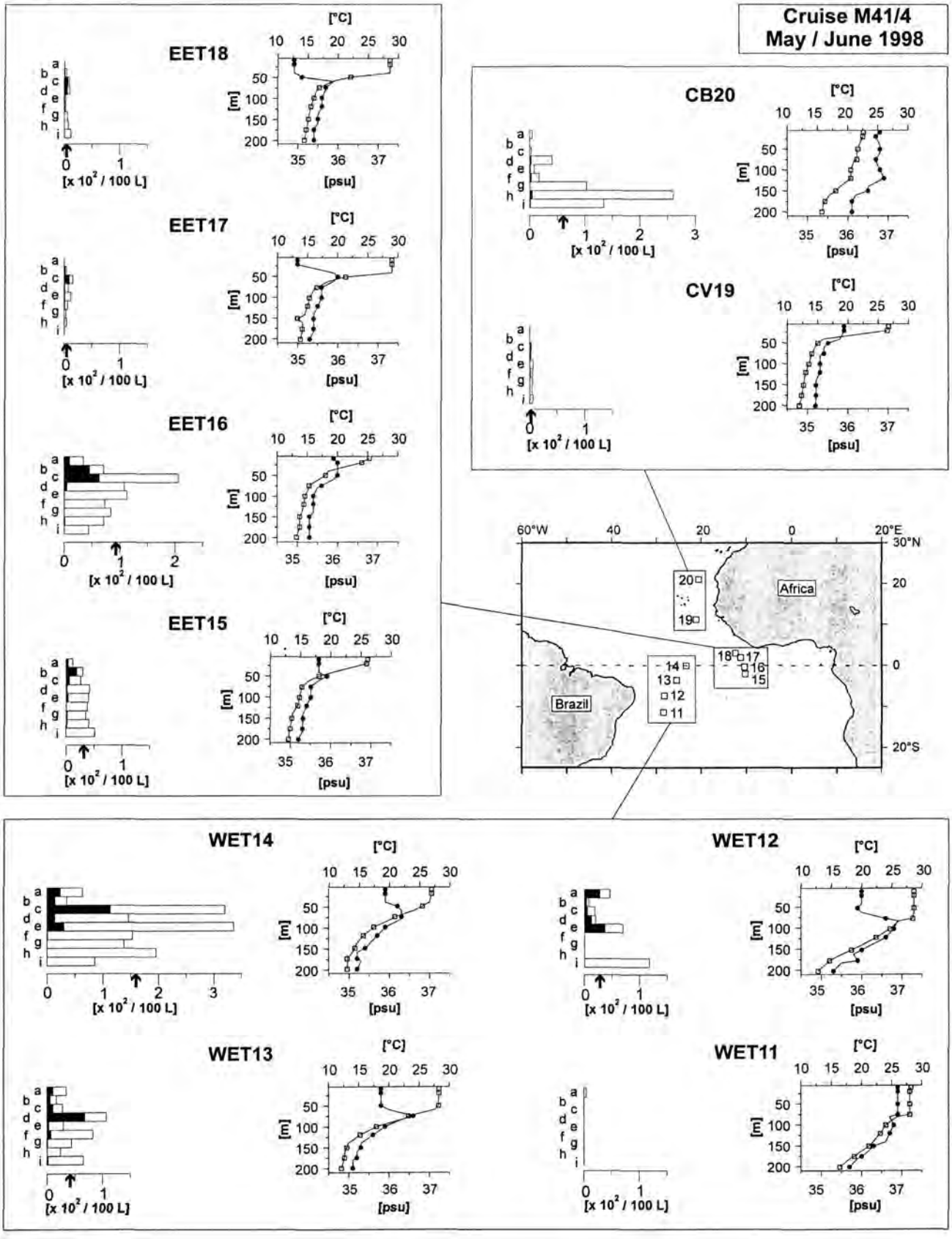
Cruise M41/4
May / June 1998
EET18
EET17
EET16
EET15
CB20
CV19
WET14
WET13
WET12
WET11
[°C]
[m]
[psu]
[x 10² / 100 L]
60°W
40
20
0
20°E
30°N
20
0
20°S
Africa
Brazil
20
19
18
17
16
15
14
13
12
11

Cruise M41-4; May/June 1998

Highest *T. heimii* shell abundances (arithmetic mean of the entire depth profile) were observed at stations south of or on the equator in the western as well as in the eastern investigated areas (Fig.3). In contrast to the situation in the WET during January/February 1997 samples from cruise M41-4 show a general increase of *T. heimii* shell abundances toward the equator. Counts rise from almost absent in the central Brazil Basin (~11°S, 28°W) to the highest abundance recorded during cruise M41-4 over the equator (~23°W). Again, the station off CB yielded relatively high *T. heimii* shell counts, about eighteen times greater than occurrences at the CV station. In the EET across the equator (2°S – 3°N; Western Guinea Basin), highest *T. heimii* shell counts were observed on the equator (~11°W, EET16). Somewhat lower, but still relatively high contents, were recorded south of the equator (~2°S; EET15). Both stations north of the equator showed extremely low values.

Vertical distribution

In most cases there are far greater differences in vertical distribution than in most horizontal distribution patterns (Figs.2, 3). In the depth profiles, samples show a tendency toward higher *T. heimii* shell abundances in a water depth of 50 to 100 m (M38-1 and M41-4) or even 150 to 200 m (M41-4). Additional counts show that *T. heimii* cells (when present) follow largely a similar trend to the depth distribution of *T. heimii* shell counts (M38-1; M41-4). However, in samples from cruise M41-4, which reach further down into the water column, *T. heimii* cells are rare to absent in depths below 100 to 120 m.

T. heimii cells were observed in a temperature range between 14.4°C to 27.3°C and a salinity range from 35.5 psu to 37.1 psu during cruise M38-1. In samples taken during M41-4, shells with cell content occurred within temperature and salinity ranges from 13.3°C to 28.7°C and 34.9 psu to 36.8 psu.

Fig.3: Distribution of *Thoracosphaera heimii*, cruise M41-4, May / June 1998. Open bars show content of *T. heimii* shells, black bars indicate *T. heimii* shells with cell content per 100 l of seawater. Arrows indicate arithmetic mean of total *T. heimii* content of the entire depth profile. **Water depth [m]** a = 10, b = 20, c = 50, d = 75, e = 100, f = 120, g = 150, h = 175, i = 200. **Temperature** : graph with open squares. **Salinity**: graph with filled circles. Symbols on both graphs indicate sampled water depth.

Maximum abundances of *T. heimii* cells were counted in samples taken from 18.8°C to 26.8°C and 35.6 to 37.1 psu (M38-1). For M41-4, highest abundances of *T. heimii* cells were counted in samples from 18°C to 25.9°C and 35.1 psu to 36.8 psu. These maxima were observed during both cruises mostly in depths from 50 m to 100 m with two exceptions at 20 m (CV2, EET15). However, it should be kept in mind that sampling during M38-1 (10 m to 100 m) usually did not include the last appearance of *T. heimii* cells in the depth profile. This leads to some doubt that the entire distribution range of these cells has been sampled during that cruise.

The position of the maximum *T. heimii* cell occurrences in the water column does not seem to be linked to the time of day (Tabs. 1; 2).

Discussion

Horizontal distribution

In areas where seasonally comparable data were available (WET, CB, CV) *T. heimii* showed higher occurrences during the cooler of the two studied seasons (January/February) (Figs. 2; 3).

At the sites of the WET *T. heimii* is generally less abundant in the samples taken during a time of comparatively increased windstress (May/June; Philander and Pacanowski. 1986) than during a time of low windstress (January/February; Philander and Pacanowski. 1986) in the area. The only exception is the site on the equator. Here, counts revealed approximately the same *T. heimii* shell abundances during both seasons. This is also the only site in the transect where the measured SST is not lower in January/February but is roughly the same in both seasons.

Romero et al. (in press) have determined total particle, opal and diatom fluxes for two sediment trap moorings positioned in the western equatorial Atlantic. Locations of these sites coincide roughly with the two northernmost stations in the WET of the present study. Whereas Romero et al. (in press) observed no distinct temporal pattern during the sampling period in the region, *T. heimii* seems to react to seasonal changes south of the area.

Cruise M38-1 stations in the WET yielded no significant lateral differences in *T. heimii* contents. On the other hand, *T. heimii* contents in samples retrieved during M41-4 in the WET rise with the transition from the open ocean oligotrophic area of the subtropical gyre to the more productive area of the equatorial Atlantic (Longhurst, 1993; Monger et al., 1997). There may be a connection between these interannual variations in *T. heimii* occurrences in the area and the seasonal movement of the ITCZ. By May/June, the influence of the ITCZ has caused

a northward shift of the SEC (Philander and Pacanowski, 1986) and its oligotrophic conditions (Longhurst, 1993). This may have caused the zoning in *T. heimii* occurrences in the WET during M41-4.

While the mean *T. heimii* shell abundances in January/February off CB and CV, similar to the situation in the WET, are clearly higher than those recorded in May/June it is more difficult to link this to any seasonality. In the area off CB, in contrast to observations in the WET, low *T. heimii* shell occurrences coincide with a decrease in trade wind speeds during late spring (Fischer et al. 1996). This contrasts with observations by Höll et al. (1999). They postulated that an increase of calcareous dinoflagellates coincides with relatively stratified conditions of the upper water column, which would mean a decrease of Trade Wind speeds for the area in the present study. Fischer and Wefer (1996) have described a seasonal flux pattern from sediment traps (positions coincide with the location of sites CB1 and CB20 of the present study) with maxima in winter-spring and summer. Fischer et al. (1996) have also shown year-to-year variations of 62 % from the same locality. Therefore, the differences in *T. heimii* occurrences could be the reflection of such annual variations.

Similar low *T. heimii* shell abundances as recorded off CV can be observed at the northern WTA sites (WTA3 and WTA4) in January/February and in May/June in the EET (EET17 and EET18) (Figs. 2; 3). However, even the low values off CV show clear differences between site values taken in winter and late spring. As in the seasonal comparisons presented so far, higher counts have been recorded in the cooler season (winter SST: 22°C - 23°C; spring SST: 25°C - 26°C; Mittelstaedt, 1991). During this time, increased upwelling occurs in the area (November - February, Mittelstaedt, 1991).

Vertical distribution

By comparing the recorded environmental data, temperature and salinity with the vertical distribution of *T. heimii* cells, the maximum occurrences of such cells can be connected with the position of the lower border of the mixed layer and the upper part of the thermocline.

This shows in the WET of cruise M41-4. Temperatures measured at the M41-4 WET sites show a thinning of the mixed layer toward the equator. The vertical distribution of *T. heimii* cells fits into this trend as well: the maximum occurrences follow the first temperature incline and stay just below the mixed layer and in the uppermost part of the thermocline. In terms of distribution of such cells, results from M38-1 for this area show no distinct trends. The two exceptions are the deep *T. heimii* cell peak (100 m) at the southernmost station and the absence of *T. heimii* cells at the same depth at the equator station. One might argue, with the

50 m to 100 m interval missing from M38-1 stations, that the true *T. heimii* cell maximum may have been overlooked in the evaluation. Nevertheless, there are no maxima below a significant decline of the temperature curve, and the *T. heimii* cell peaks of M38-1 seem to hug the lower border of the mixed layer.

Whenever the lower temperatures of the upper thermocline coincide with a rise in salinities an occurrence of distinct *T. heimii* cell maxima can be observed (Figs. 2; 3). This shows most in M41-4 sites WET11-14 and EET18. During cruise M38-1, the depth where these two factors coincide was not always sampled. Where data from this point are available there are clear maxima of *T. heimii* cells (WTA6, WET9, WET10). On the other hand, samples taken below such a rise in salinities often lack *T. heimii* cells altogether (WTA4, WTA5, WET7).

Off CB, the position of the thermocline was approximately the same at the time of sampling in both seasons. A similar pattern in depth distribution of *T. heimii* cells off CB in Jan. / Feb. (as seen at other sites during both cruises) was observed. However, the CB station of M41-4 does not yield a peak of such cells at or below the lower boundary of the mixed layer. In fact, shells with cell content are almost absent in the May/June samples. Empty *T. heimii* shells, however, are relatively abundant but occur in relevant numbers only at a depth of about 75 m or below 150 m. It is possible that these are the remnants and sinking detritus of an earlier, elevated production of *T. heimii* shells higher in the water column or some lateral transport of *T. heimii*, but that is purely speculation.

T. heimii prefers the oceanographic conditions provided by the lower boundary of the mixed layer and the upper thermocline. It has been suggested by Dale (1992a) that one of the possible advantages gained by the inclusion of a sinking stage into the life-cycle of the 'Thoracosphaerids' may be the removal of the cell from relatively higher levels of predation in the biologically more active photic zone. Thus, the organism would gain access to nutritionally richer waters usually found slightly deeper in the water column. This seems a very likely hypothesis, especially in view of the fact that *T. heimii* does indeed seem to favour lower levels in the water column. Whether this strategy, temperature, or a combination of both and further unknown factors (such as predation) lead to the distinct depth distribution of *T. heimii* cells remains to be seen.

It could be argued that the *T. heimii* cells are merely accumulated above or within the water layers with a relatively higher specific density of the lower mixed layer and upper thermocline. Together with the fact that almost all of the *T. heimii* shells passing this layer are empty (Fig.2), this argument also hints at the possibility that the species uses this layer of relatively higher density to keep its position in the water column.

The time of day does not seem to have any relation to the position of the *T. heimii* cell maxima in the water column. Sites sampled in the morning (e.g. WTA4, EET16), noon (CV19), evening (e.g. CB1, WTA6) or night (e.g. WET8, WET14) show no distinct peculiarities that could be related to local time. A diurnal migration cycle of *T. heimii* as has been observed for dinoflagellates (e.g. Eppley, 1968) seems very unlikely under the circumstances, but cannot be ruled out entirely.

Light is one of the major environmental factors not discussed in the present study. We undertook light intensity measurements in the water column during cruise M41-4 in May / June 1998. There is a manuscript in preparation in which a possible relationship between *T. heimii* cell depth distribution and light intensities (cruise M41-4) and reactions of *T. heimii* clones to different light intensities in laboratory experiments are being compared.

The distribution patterns of calcareous dinoflagellates observed by Höll et al. (1999), i.e. that contents are generally higher in the relatively more oligotrophic region in the west and lower in the highly productive area in the east, cannot be recreated within the limitations of the data set available for this study. Although cruise M38-1 sites show the highest values in the southern part of the WTA region (WTA6) during the time of year when productivity in the area (January to March; Longhurst, 1993) is lowest, the second highest occurrence of *T. heimii* in the upwelling area off CB (CB1) was observed at the same time (Fig.2).

While counts from sites in the WET and the southern WTA are uniformly high for cruise M38-1, matching the data presented by Höll et al. (1999), there are no data on the situation in the EET for this season. On the other hand, such data are available from cruise M41-4. In this case, they seem to suggest that *T. heimii* does indeed have higher occurrences in the western equatorial Atlantic than in the east. Nonetheless, with the short period represented by the samples, such assumptions have to be made very carefully.

It is true that the samples taken with a rosette sampler represent the conditions of a very short moment on a specific day in the water column. However, the fact that maximum occurrences of *T. heimii* cells were recorded near the lower boundary of the mixed layer or the upper part of the thermocline in so many different regions and in two different seasons is an unlikely coincidence. The question whether the seemingly seasonal variations of *T. heimii* abundances between stations are truly a reflection of an annual pattern can only be satisfactorily solved by the examination of sediment trap material. Studies of such samples would certainly yield valuable results.

Conclusions

The calcareous vegetative-coccoid stage of *Thoracosphaera heimii* was observed at all sites throughout the entire investigated area with a high variability in both horizontal and vertical distribution.

We noted similar high abundances of *T. heimii* in the oligotrophic western equatorial Atlantic Ocean and in high productivity areas such as off Cap Blanc and in the eastern equatorial Atlantic Ocean.

Highest counts of *T. heimii* shells with cell content have been observed in water depths from 50 m to 100 m. The major fraction of the environmental signal of *T. heimii* can be assumed to represent these deeper levels of the upper water column.

Distinct maxima in vertical distribution of *T. heimii* shells with cell content coincide with relatively lower temperatures and relatively higher salinities than surface conditions. A positive reaction of *T. heimii* to cooler SST seems to be reflected in seasonal variations as well, but work on sediment trap material is required to clear this point.

Acknowledgements

Financial support was provided by the Deutsche Forschungsgemeinschaft (Wi 725/7) and the SFB 261. We are thankful to the Arbeitsgruppe Meeresgeologie, Fachbereich Geowissenschaften especially Gerd Fischer for providing the CTD data. Thanks are due to the crew of the *RV Meteor* and cruise participants of *Meteor* cruises M38-1 1997 and M41-4 1998. We are indebted to Gerard Versteegh and J. Mutterlose for critical remarks and discussion of an earlier version of the manuscript. This study would not have been possible without the help of Anja Meyer during sample preparation and the onboard help of Nicole Zatloukal, Angelika Freesemann, Ines Flatter and Bärbel Hönisch. We also thank Bettina and Adam Price for correction of the English text.

References

Carton, J.A., 1989. Estimate of sea level in the tropical Atlantic Ocean using GEOSAT altimetry. J. Geophys. Res., 94: 8029-8039.

Chepurin, G. and Carton, J.A., 1997. The hydrography and circulation of the upper 1200 meters in the tropical North Atlantic 1982-1991. J. Mar. Res. 55,633-670

Dale, B., 1986. Life cycle strategies in oceanic dinoflagellates. UNESCO Tech. Papers. Mar. Sci., 49: 65-72.

Dale, B., 1992a. Dinoflagellate Contribution to the Open Ocean Sediment Flux. In: Dale, B., Dale, A., (eds.), Dinoflagellate Contributions to the Deep Sea. Ocean Biocoenosis Series ed., Woods Hole Oceanographic Institution, Woods Hole, 5: pp. 1-32.

Dale, B., 1992b. Thoracosphaerids: Pelagic Fluxes. In: Honjo S (ed.), Dinoflagellate Contributions to the Deep Sea, Ocean Biocoenosis Series ed., Woods Hole Oceanographic Institution, Woods Hole, Massachusetts, 5: pp. 33-43.

Dale, B. and Dale, A.L., 1992. Ocean Biocoenensis Series. Dinoflagellate Contributions to the Deep Sea. Woods Hole Oceanographic Institution, Woods Hole, Massachusetts, 5: pp. 1-75.

Dann, O., Bergen, G., Demant, E. and Volz, G., 1979. Trypanocide des 2-phenyl-benzofurans, 2-phenyl-indens und 2-phenyl-indols. Ann. Chem., 749: 68.

Eppley, R.W., Holm-Hansen, O. and Strickland, J.D.H., 1968. Some observations on the vertical migration of dinoflagellates. J. Phycol., 4(4): 333-340.

Fischer, G., Donner, B., Ratmeyer, V., Davenport, R. and Wefer, G., 1996. Distinct year-to-year particle flux variations off Cape Blanc during 1988-1991: Relation to $\delta^{18}O$-deduced sea surface temperatures and trade winds. J. Mar. Res., 54: 1-27.

Fischer, G. and Wefer, G., 1996. Long-term observation of particle fluxes in the Eastern Atlantic: Seasonality, changes of flux with depth and comparison with the sediment record. In: Wefer, G., Berger, W.H., Siedler, D.J., Webb, D.J. (eds.), The South Atlantic: Present and Past Circulation. Springer-Verlag, Berlin, Heidelberg, pp.325-344.

Hagen, E. and Schemainda, R., 1984. Der Guineadom im ostatlantischen Stromsystem. Beiträge zur Meereskunde, 51: 5-27.

Höflich, R.W., 1984. Climate of the South Atlantic Ocean. In: van Loon, H. (ed.), World Survey of Climatology, Vol. 15, Climate of the Oceans. Elsevier, Amsterdam, pp. 1-191.

Höll, C., 1998. Kalkige und organisch-wandige Dinoflagellaten-Zysten in Spätquartären Sedimenten des tropischen Atlantiks und ihre palökologische Auswertbarkeit. Ber. Fachber. Geowiss., Universität Bremen, 127: pp.121.

Höll, C., Zonneveld, K.A.F. and Willems, H., 1998. On the ecology of calcareous dinoflagellates: The Quaternary eastern Equatorial Atlantic. Mar. Micropaleont., 33: 1-25.

Höll, C., Karwath, B., Rühlemann, C., Zonneveld, K.A.F. and Willems, H., 1999. Palaeoenvironmental information gained from calcareous dinoflagellates: The Late Quaternary eastern and western tropical Atlantic Ocean in comparison. Palaeogeogr.

Palaeoclimatol. Plaeoecol., 146: 147-164

Inouye, I. and Pienaar, R.N., 1983. Observations on the life cycle and microanatomy of *Thoracosphaera heimii* (Dinophyceae) with special reference to its systematic position. S. Afr. J. Bot., 2: 63-75.

Janofske, D., 1996. Ultrastructure types in Recent "calcispheres". Bulletin de l'Institut océanographique, Monaco, 14 (4): 295-305.

Kerntopf, B., 1997. Dinoflagellate Distribution Patterns and Preservation in the Equatorial Atlantic and Offshore North-West Africa. PhD Thesis. Ber. Fachber. Geowiss., 103: 137 pp.

Lewis, J., Dodge, J.D. and Powell, A.J., 1990. Quaternary dinoflagellate cysts from the upwelling system offshore Peru, Hole 686B, ODP LEG 112. In Suess R, von Huene et al. (eds.), Proceedings of the Ocean Drilling Program, Scientific Results, 112: 323-328

Longhurst, A., 1993. Seasonal cooling and blooming in tropical oceans. Deep-Sea Res., 40: 2145-2165.

Longhurst, A., Sathyendranath, S., Platt, T. and Caverhill, C., 1995. An estimate of global primary production in the ocean from satellite radiometer data. J. Plankton. Res., 17: 1245-1271.

Matthiessen, J., 1995 Distribution patterns of dinoflagellate cysts and other organic-walled microfossils in recent Norwegian-Greenland Sea sediments. Mar. Micropaleont., 24: 307-334.

Mittelstaedt, E., 1991. The ocean boundary along the Northwest African coast: Circulation and oceanographic properties at the sea surface. Prog. Oceanogr., 26: 307-355.

Monger, B., McClain, C. and Martugudde, R., 1997. Seasonal phytoplankton dynamics in the eastern tropical Atlantic. J. Geophys. Res., 102: 12389-12411.

Petterson, R.G. and Stramma, L., 1991. Upper-level circulation in the South Atlantic Ocean. Prog. Oceanog., 26: 1-73.

Philander, S.G.H. and Pacanowski, R.C., 1986. A model of seasonal cycle in the tropical Atlantic ocean. J. Geophys. Res., 91: 14192-14206.

Romero, O.E., Lange, C.B., Fischer, G., Treppke, U.F. and Wefer, G., in press. Variability in export production documented by downwards fluxes and species composition of marine planktonic diatoms: Observations from the tropical and equatorial Atlantic. In: Fischer G, Wefer G (eds.), The Use of Proxies in Paleoceanography – Examples from the South Atlantic. Springer-Verlag, Berlin, Heidelberg.

Tangen, K., Brand, L.E., Blackwelder, P.L. and Guillard, R.R., 1982. *Thoracopsheara heimii*

Lohmann KAMPTNER is a dinophyte: observations on its morphology and life cycle. Mar. Micropaleont., 7: 193-212.

UNESCO, 1981. International Oceanographic Tables. UNESCO Technical Papers in Marine Science, 3: 39.

Van Camp, L., Nykjaer, L., Mittelstaedt, E. and Schlittenhardt, P., 1991. Upwelling and boundary circulation off Northwest Africa as depicted by infrared and visible satellite observations. Prog. Oceanog., 26: 357-402.

Voituriez, B., 1981. Les sous-courants équatoriaux nod et sud et la formation des dômes thermiques tropicaux. Oceanol. Acta., 4: 497-506.

Voituriez, B. and Herbland, A., 1977. Étude de la production pélagique de la zone équatorial de l'Atlantique à 4°W. Cahier ORSTROM, Série Océanographie 15: 313-331.

Wall, D., Dale, B., Lohmann, G.P. and Smith, W.K., 1977. The environmental and climatic distribution of dinoflagellate Cysts in modern marine sediments from regions in the North and South Atlantic Oceans and adjacent seas. Mar. Micropaleont., 2: 121-200.

Table 1: Cruise M38-1, January / February 1997.

Station	GeoB No.	Sample Depth [m]	Time local	Time UTC	Sample Volume [L]	Studied Volume [L]	(A) *T. heimii* content / 100L	(B) *T. heimii* content / 100L	(C) *T. heimii* C. / 100L	*T. heimii* shells / 100 [L]	*T. heimii* cells / 100 [L]
CB1	4302	10	17:20	18:20	43	16.1	*1852	*2826	2584	2421	832
		20			41	14.7	*2333	*1924	3549	2602	775
		50			41	19.6	*4509	6731	3363	4868	1070
		100			44	18.9	3025	4142	3028	3399	258
CV2	4303	10	01:30	02:30	42	31.0	*462	461	290	405	70
		20			40	14.5	*458	*557	326	447	143
		50			38	18.1	*1680	957	226	954	40
		100			39	29.1	426	533	232	397	0
WTA3	4305	10	06:20	08:20	40	19.0	*326	*587	0	305	0
		20			40	9.5	*240	*153	34	142	0
		50			40	17.6	*1232	998	263	831	101
		100			40	22.3	618	608	289	505	14
WTA4	4310	10	09:00	07:00	40	30.0	*679	492	260	470	90
		20			40	16.0	*967	*299	216	495	130
		50			37	15.5	*2997	*1966	1310	2091	655
		100			40	18.2	1135	2082	1370	1529	89
WTA5	4311	10	04:50	06:50	40	18.9	*2231	*1818	1880	1977	678
		20			40	14.6	*2050	*1942	1537	1843	574
		50			38	16.3	*2582	*2023	1900	2169	529
		100			38	25.5	2188	1908	2255	2118	0
WTA6	4316	10	23:20	01:20	40	22.2	*434	*452	513	467	239
		20			38	18.1	*1179	*754	586	840	254
		50			38	14.6	*15335	*12577	10488	12800	6085
		100			28	23.5	6955	6462	7521	6979	359
WET7	4318	10	04:30	07:30	20	9.8	*1085	*890	801	925	367
		20			30	14.8	*2652	*1310	1555	1839	788
		50			28	14.3	*1566	*2295	1049	1637	399
		100			28	21.4	2905	2248	1596	2250	11
WET8	4319	10	02:45	04:45	40	13.0	*831	*532	594	653	368
		20			40	19.0	*1242	*548	890	894	331
		50			28	12.8	*2304	*1682	1508	1832	512
		100			38	21.8	4276	3390	3024	3564	669
WET9	4320	10	03:10	05:10	40	22.2	*734	*822	281	613	258
		20			40	20.1	*1815	*777	1106	1233	452
		50			38	25.5	*1238	560	550	783	300
		100			38	29.2	2020	1548	1640	1736	830
WET10	4321	10	05:10	07:10	40	10.5	119	239	201	187	55
		20			40	9.0	79	51	175	102	22
		50			38	11.9	116	154	74	115	15
		100			38	9.0	4733	5054	4983	4924	2033

Local time: begin of sampling; sampling time approx. 45 min. *Samples prepared in an ethanol dehydration series and embedded in Spurr's resin. All others embedded in glycerine jelly. C – samples were additionally stained with DAPI. **A B and C**: total content of *Thoracosphaera heimii* of count A, B and C calculated to 100 l of seawater, respectively. *T. heimii* shells: arithmetic mean of A, B, C. *T. heimii* cells: *T. heimii* shells with cell content per 100 l of seawater calculated from D. series counts.

Table 2

Station	GeoB No.	Sample Depth [m]	Time local	Time UTC	Sample Volume [L]	Studied Volume [L]	*T. heimii* shells / 100 [L]	*T. heimii* cells /100 [L]
WET11	5201	10	03:00	06:00	28	4.9	40	0
		20			29.2	8.8	0	0
		50			29.6	7.3	0	0
		75			29.4	5.2	0	0
		100			27.6	4.7	0	0
		120			29.6	4.8	0	0
		150			37.2	6.4	0	0
		175			29	4.1	0	0
		200			37	2.8	0	0
WET12	5202	10	02:10	05:10	38.6	8.2	464	281
		20			39	10.0	80	40
		50			39.1	9.0	188	55
		75			38.6	10.0	201	130
		100			38	10.0	702	371
		120			31.5	10.0	0	0
		150			38.6	10.0	0	0
		175			30.4	10.0	0	0
		200			39	2.8	1178	0
WET13	5203	10	09:10	12:10	38.6	10.0	350	110
		20			36.4	10.0	170	60
		50			28.2	10.0	280	110
		75			30.4	7.2	1068	680
		100			27.7	6.1	294	33
		120			28.2	11.0	830	73
		150			39.2	10.0	441	10
		175			31.2	8.3	242	0
		200			39.4	9.2	653	22
WET14	5204	10	03:10	06:10	36.4	5.0	637	239
		20			38.2	7.6	356	145
		50			28.6	2.8	3207	1140
		75			29.2	10.0	1461	140
		100			37.5	10.0	3364	310
		120			29.8	10.0	1532	10
		150			38.6	10.0	1382	0
		175			28.2	7.3	1959	0
		200			38.6	8.3	858	0
EET15	5205	10	04:30	06:30	36.8	10.0	120	40
		20			37.6	10.0	299	189
		50			38.6	10.0	260	60
		75			37.8	10.0	420	20
		100			38.3	10.4	404	38
		120			29.4	10.0	381	0
		150			37.6	10.0	351	20
		175			28.8	10.0	411	20
		200			37.8	10.0	521	0
EET16	5206	10	08:15	10:15	37	6.1	346	99
		20			37.6	3.9	710	457
		50			34	2.5	2052	631
		75			38	10.0	1080	50
		100			38.8	10.0	1131	0
		120			30.2	10.0	730	0
		150			37	10.0	842	0
		175			30.2	10.0	711	10
		200			37.8	10.0	440	0
EET17	5207	10	07:00	09:00	38.3	8.7	0	0
		20			38.5	10.0	40	20
		50			17.3	6.5	155	93
		75			38.1	10.0	70	10
		100			38.5	10.0	120	10
		120			30.2	10.0	60	10
		150			38.5	10.0	30	0
		175			29.5	10.0	40	0
		200			40	10.0	0	0
EET18	5208	10	08:30	10:30	38.2	5.0	0	0
		20			38.8	10.0	40	10
		50			32.2	10.0	90	70
		75			39.2	10.0	100	60
		100			38.5	10.0	30	10
		120			31.2	10.0	20	0
		150			39	10.0	60	0
		175			30.8	10.0	70	0
		200			40.2	10.0	120	0
EET19	5209	10	12:45	15:45	39	4.6	0	0
		20			40.5	4.6	0	0
		50			37.5	3.6	28	28
		75			39.4	4.7	21	21
		100			39	10.0	60	0
		120			30.8	10.0	50	10
		150			38.3	10.0	50	0
		175			39.3	10.0	40	0
		200			39	6.8	59	0
EET20	5210	10	14:20	16:20	40.2	2.3	44	0
		20			38.2	1.7	0	0
		50			37.2	3.5	29	0
		75			29.4	3.7	406	27
		100			38.2	10.0	80	10
		120			30	10.0	170	30
		150			38	10.0	1031	0
		175			31.4	10.0	2603	50
		200			38.6	10.0	1342	10

Cruise M41-4, May / June 1998. Local time: begin of sampling; sampling time approx. 1 hour. All samples stained with DAPI and embedded in glycerine jelly. *T. heimii* shells: total content of *Thoracosphaera heimii* calculated to 100 l of seawater. *T. heimii* cells: *T. heimii* shells with cell content per 100 litre of seawater.

3.3

ON THE ECOLOGY OF MARINE CALCAREOUS DINOFLAGELLATES: A FIELD AND LABORATORY STUDY OF *THORACOSPHAERA HEIMII*

(in preparation)

ON THE ECOLOGY OF MARINE CALCAREOUS DINOFLAGELLATES: A FIELD AND LABORATORY STUDY OF *THORACOSPHAERA HEIMII*

* Britta Karwath, Dorothea Janofske, Helmut Willems

Fachbereich-5 Geowissenschaften, Universität Bremen, Postfach 330 440, D-28334 Bremen, Germany. Fax: 0421/2184451

*e-mail corresponding author: karwath@micropal.uni-bremen.de

Abstract

Although information on living and fossil calcareous dinoflagellates in sediments has steadily increased over the last decades, their environmental affinities are largely unknown. Our main aim is to provide a data basis for the interpretation of the sedimentary signal of these organisms by surveying the species occurrence in the photic zone and thus to get an impression of the survival strategies used by the organisms. To this end we chose the phototrophic, calcareous dinoflagellate *Thoracosphaera heimii* as a first case study: The vertical distribution of *T. heimii* in the upper water column (10 m to 200 m) of the eastern and western equatorial Atlantic Ocean has shown highest quantities in water depths between 50 m to 100 m (Karwath et al., 2000a). These distribution data were compared to irradiance, temperature, density and chlorophyll *a* measurements. Results show strong peaks in the species' abundance within the deep chlorophyll maximum (DCM). To get an impression of *T. heimii*'s reaction to different irradiances we exposed two strains to light intensities from 10 $\mu Em^{-2}s^{-1}$ (photosynthetically active radiation, PAR) to 800 $\mu Em^{-2}s^{-1}$. The laboratory studies have shown that *T. heimii* is highly adaptable to both high and low irradiances. *T. heimii* is also able to produce as many or even more cells under 40 $\mu Em^{-2}s^{-1}$ (about 1 % PAR of surface irradiance in the waters examined) as under 500 $\mu Em^{-2}s^{-1}$ (about 10 m water depth under clear skies in the field) under the same nutritional conditions. *T. heimii* may not exclusively inhabit the DCM, but it is well adapted to an existence within deeper levels of the euphotic zone.

Keywords: actuopalaeontology, culture experiments, deep chlorophyll maximum, growth, irradiance, nannoplankton

Introduction

Dinoflagellates are a group of unicellular eukaryotic organisms which represents one of the major (marine) phytoplankton groups. So far, research has mostly focused on toxic and bioluminescent dinoflagellates and the fossilisable organic remains of dinoflagellates, which are generally regarded as the preserved walls of cyst stages. Research includes, among other topics, studies on (palaeo-) productivity, (palaeo-) environment and (palaeo-) oceanography (e.g. Wall et al., 1977; Lewis et al., 1990; Matthiessen, 1995; Höll, 1998). In contrast, information is rare on dinoflagellate taxa with calcareous skeletal elements of which in particular the biology and ecology are largely unknown.

Calcareous dinoflagellates have often been neglected in plankton studies due to their size of about 10 µm to 60 µm. They are too small to be included in foraminifera research and too large for nannoplankton studies. In palynological studies the use of acids during preparation automatically excludes calcareous dinoflagellates from consideration. During the last decade observations made on this group have hinted at a far more important role for calcareous dinoflagellates than formerly recognised (Dale, 1992a, b; Kerntopf, 1997; Höll et al., 1998, 1999).

Whereas organic-walled dinoflagellate cysts are predominant in boreal regions (Dale and Dale, 1992), in the subtropics and tropics the assemblages of fossilisable dinoflagellate remains are mainly composed of calcareous dinoflagellates (Dale, 1992a; Höll., 1998). The high flux rates of calcareous dinoflagellates in the subtropics and tropics (Dale, 1992a, b) suggest that they may form an important contribution to the ocean carbon flux.

Calcareous dinoflagellate associations in the tropics and subtropics are often overwhelmingly dominated by the phototrophic species *Thoracosphaera heimii* (Kerntopf, 1997; Höll et al., 1998, 1999; Dale, 1992b). This prevalence of *T. heimii* in the calcareous dinoflagellate associations can be explained by the species' ability to produce large numbers of calcareous spheres in a relatively short period of time. Its position within the Dinophyceae is unique: most of the cells in a culture of *T. heimii* form a calcareous skeleton (Tangen et al., 1982). This calcareous wall has been referred to as a „shell" rather than the more usual term „cyst" to stress the predominance of the calcareous, vegetative-coccoid life-stage of the species (Inouye and Pienaar, 1983).

In spite of the abundance of *T. heimii* and, in most cases, the prevalence over other calcareous dinoflagellates, little is known so far about its environmental affinities. In one of the first studies on this topic, Höll et al. (1999) have compared the content of calcareous dinoflagellate remains in two sediment cores, one from below the highly productive eastern Atlantic equatorial divergence zone and another from the low productivity area of the western tropical Atlantic. In that study, *T. heimii* shows increased accumulation rates in the low productivity western South Atlantic and lower accumulation rates in the higher productivity region in the eastern South Atlantic. Furthermore, enhanced production of calcareous dinoflagellates in these cores could be correlated to periods of reduced palaeoproductivity probably related to relatively stratified conditions of the upper water column. The study suggested *T. heimii* accumulation rate as a proxy for productivity and / or stratification.

In view of these findings - and to improve on the data-base available for the interpretation of *T. heimii* occurrences in the sediment - it is important to take a closer look at the recent environmental affinities. We aim to provide a basis for the determination of the role of *T. heimii* in the water column and to test the hypothesis of Höll et al. (1999) by making a survey of the species' occurrence in the photic zone to get an impression of the survival strategies used by the organism.

Recent studies on living *T. heimii* address the influence of temperature on growth and cell size (Karwath et al., 2000b) and the spatial distribution of *T. heimii* in the upper 200 m of the water column in the tropical and equatorial Atlantic (Karwath et al., 2000a). The highest quantities of *T. heimii* shells with cell content were observed in water depths between 50 m to 100 m just below the mixed layer and the upper part of the thermocline (Karwath et al., 2000).

The present study deals with the position of *T. heimii* in the water column in the photic zone as estimated from vertical spectral irradiance, density and chlorophyll *a* profiles. The results are compared to growth experiments of two *T. heimii* strains in culture.

The photic and euphotic zone

The photic zone is the illuminated surface layer of the oceans. This layer is typically a few tens or hundreds of metres deep (Tett, 1990). The Sunlight penetrates the water to varying depths: the penetration depends upon the intensity and angle of radiation, the amount of surface reflection and the transparency of the water (Dawson, 1966; Kirk, 1983).

The euphotic zone is defined as the region in which there is sufficient light for photosynthesis, i.e. the zone above 1 % subsurface PAR (photosynthetically active radiation) (Kirk, 1983). In the rest of this contribution, the term irradiance refers to photon irradiance (in

μE = $\mu mol\ m^{-2}s^{-1}$) between wavelengths of 400 nm - 700 nm (PAR). Within the stratified ocean a distinct peak of chlorophyll concentration is normally found close to the bottom of the euphotic zone. This deep chlorophyll maximum (DCM), which is also a biomass maximum (Lindholm, 1992), lies either a little above or below the depth at which downward irradiance is 1 % of the subsurface value (Kirk, 1983). The DCM is widespread across the world's oceans (e.g. Shulenberger, 1978; Lindholm, 1992; Pollehne, 1993). In terms of total primary production, the DCM makes a significant contribution in those waters where it occurs (Kirk, 1983).

Material and Methods

Laboratory Studies

Cultures

Strains GeoB79 and GeoB86 were isolated from plankton samples taken in 20 m water depth in the equatorial and tropical South Atlantic (GeoB79: 07°30.01'S, 28°11.2'W; GeoB86: 03°52.1'S, 25°39.5'W) during *RV Meteor* cruise M38-1 in 1997. The strains were maintained at the University of Bremen Dept. of Geosciences in polystyrene culture plates (CellWells) and 250 ml Erlenmeyer flasks at 20°C. Light in the growth chamber with irradiance of 80 $\mu Em^{-2}s^{-1}$ (Licor Li-250; Sensor: MQS S/N 007) was provided by cool white fluorescent tubes. Cultures were kept in f/2 culture medium (Guillard and Ryther, 1962) without silica. Media were prepared with artificial seawater (hw Meersalz, Wiegand GmbH, Krefeld).

Equipment

To be able to expose the *T. heimii* strains to different light intensities simultaneously a Light Gradient Box (LGB) was constructed. At the core of the LGB are four cool white fluorescent lamps, which are covered lengthways with different strengths of semi-transparent plastic film. The lamps are cooled by fans connected to the laboratory's air conditioning system to avoid heat build up in the box. Culture tubes are inserted in plastic foam and are illuminated from below. The entire construction is housed in an insulated box covered by close-fitting lids.

The configuration including the semi-transparent plastic film allows experiments under irradiances of 10 $\mu Em^{-2}s^{-1}$ to 500 $\mu Em^{-2}s^{-1}$. A slightly different setup, the plastic film at the bright end of the gradient has to be removed, allows experiments under higher irradiances (700 $\mu Em^{-2}s^{-1}$ and 800 $\mu Em^{-2}s^{-1}$)

Set-up and realisation

F/2 culture medium was used for all experiments (Exp#1: GeoB79; Exp#2: GeoB86). Temperature in the LGB was set at room temperature (22.5°C). Cultures were subjected to light intensities between 10 $\mu Em^{-2}s^{-1}$ and 800 $\mu Em^{-2}s^{-1}$ in a 12h : 12h L/D cycle (see Tab.1 for further details). The maximal light intensity in the room during measurements was 12 $\mu Em^{-2}s^{-1}$.

Table 1: Set up of *Thoracosphaera heimii* growth experiments.

experiment No	strain	light intensity [$\mu Em^{-2}s^{-1}$]	culture medium 30 ml	[psu]	[pH]	initial cell density $*ml^{-1}$
#1	GeoB79	10, 20, 30, 40, 70, 100, 130, 160, 200, 500	f/2	34	8.28	2.9×10^3
		700, 800	f/2	36.3	8.47	7.6×10^4
#2	GeoB86	10, 20, 30, 40, 70, 100, 130, 160, 200, 500	f/2	34	8.28	4.2×10^3
		700, 800	f/2	36.3	8.47	6.1×10^4

Culture growth was monitored by daily *in vivo* chlorophyll *a* measurements. They were carried out with a laboratory fluorometer (TD-700, Turner Designs). Before placing the tubes in the fluorometer, cultures were mixed with a vortex stirrer. The results equal raw fluorescence data (RFD) relating to standard culture also measured *in vivo* prior to the experiment. RFD were used to calculate exponential growth rates in divisions per day for *T. heimii* after Brand and Guillard (1981) and Guillard (1973). Final yield was calculated twice from two different data sets after Sorokin (1973) $(X_1 - X_0) * V^{-1}$. In the first yield calculation ($yield_{RFD}$) X_0 equals RFD after inoculation, X_1 equals RFD on the last day of exponential growth and V is the culture media volume (30 ml). For the second yield calculation ($yield_{CC}$) we used cell counts, where X_0 = initial cell density and X_1 = cell density on the last day of exponential growth. X_1 was calculated from RFD and the according cell count from the final day of the experiments and the RFD from the last day of exponential growth.

Cell numbers were established with a Thoma counting device (chamber depth 0.1 mm). Cells were counted in all squares with several refills (n = 5). During the count, we distinguished between *T. heimii* cells with or without calcareous walls. Counts were taken at the beginning and end of the light experiments. To get an impression of how a culture

develops during growth, one reference culture of each strain was kept in a growth chamber at 20°C under light irradiation of 80 $\mu Em^{-2}s^{-1}$. These cultures were monitored in regular intervals to relate RFD to cell counts and to establish the percentage of different cell types at different stages of culture development (Figs.5a, b; 6a – d).

Salinity and temperature measurements for each culture tube in the LGB as well as in the growth chamber were taken in a two-week cycle. Evaporated water was refilled twice a week with demineralised autoclaved water to stabilise salinities.

Field Studies

Seawater Samples

The plankton samples examined in the present study were taken during an Atlantic cruise of the *R/V Meteor* in May/June 1998 (cruise M41-4). The cruise was carried out within the scope of the SFB 261 project "Der Südatlantik im Spätquartär: Rekonstruktion von Stoffhaushalt und Stromsystemen" at the Bremen University. Sample sites are shown in Fig.1.

Surface water samples were included into this study to give an impression of the *T. heimii* content in surface waters, even though the sites do not coincide with station positions of the depth profiles. These samples were retrieved from the water column at 5 m depth with the ship's membrane pump. The 10 µm to 100 µm fraction of the surface samples was separated onboard with a filtration unit operated by the pump's pressure. The sample volume was measured with a water meter. During sample preparation, a portion of the fixed seawater sample was passed through a 0.8 µm cellulose acetate filter and rinsed with 1 ml of artificial seawater. The samples were additionally treated with the DNA fluorochrome 4´,6-diamidino-2-phenylindole (DAPI; Dann et al., 1979) to stain the nucleus. To remove the saltwater the samples were rinsed with ethanol. The filters were mounted on microscope slides with glycerine jelly and covered with a cover slip. Samples were insulated from air with varnish.

Seawater samples from the depth profiles (10 m to 200 m; Karwath et al., 2000a) were taken with a rosette sampler (Multi Wasserschöpfer MWS) using several 10 litre NISKIN™ bottles at each depth. The pre-filtered 5 µm – 100 µm fraction of the fixed seawater samples was treated in the same fashion as the surface samples. For further details on sample treatment and preparation see Karwath et al. (2000a).

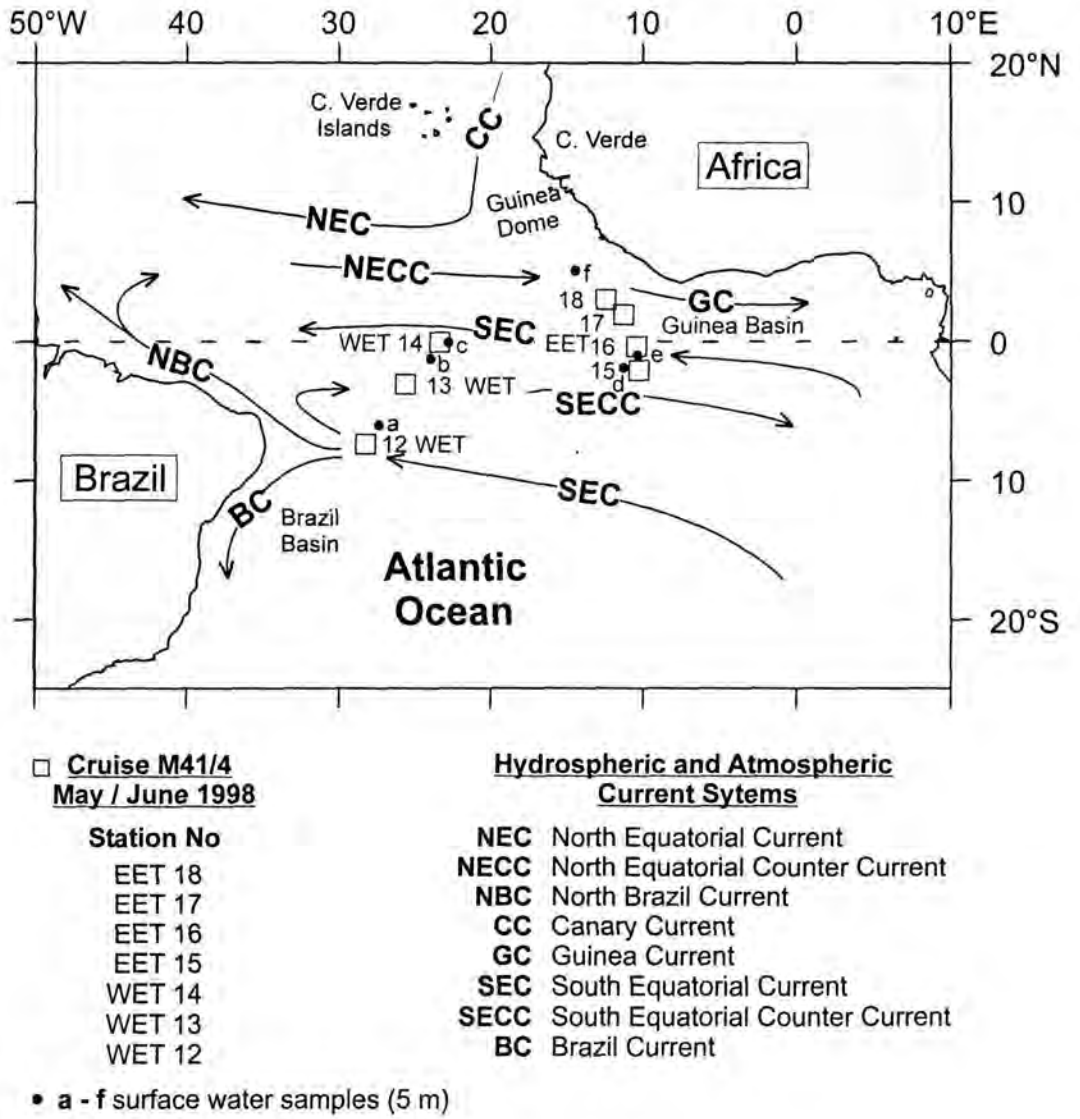

Fig.1: Hydrographic settings (modified largely after Peterson and Stramma, 1991). Symbols indicate sample sites from cruise M41/1 in May / June 1998. Open squares mark the location of the depth profiles (10 m to 200 m water depth), filled circles show the position of the surface water samples (5 m) (modified after Karwath et al., 2000a).

Sample evaluation

Samples were studied with a Zeiss Axiophot light microscope (LM). The entire slide content was counted. To identify *T. heimii* shells with cell content the material was viewed under ultra-violet light (Zeiss filter set 01, extinction BP 365, emission LP 377); the cell content was evident by the DAPI-stained nucleus. Counts were calculated to 100 l of seawater (Tab.2; 10 m to 200 m samples see Karwath et al., 2000a).

Table 2: Cruise M41-4, May / June 1998.

Station	Sample Volume [L]	Studied Volume [L]	calcified cells / 100 [L]	empty shells / 100 [L]
a	338	20.2	0	10
b	240	19.7	15	41
c	92	20.0	25	100
d	205	20.0	15	20
e	163	20.1	15	35
f	398	19.5	0	0

Content of *Thoracosphaera heimii* per 100 litres of seawater in surface samples (5 m water depth).

Light measurements

Monitoring of the apparent optical properties of the upper water column in vertical profiles (Figs.8, 9 and 10) was carried out with a MER-2040 Profiling Spectroradiometer (Biospherical Instruments, San Diego, USA). The spectral irradiance was measured with a PAR broadband sensor. Profiles were measured down to 1 % PAR-limit and thus to the lower boundary of the euphotic zone. Real-depth data were given by a pressure transducer. Initial processing and recording of the data was performed using software provided by Biospherical Instruments. Irradiance plots contain one metre averages of the measured profile data, the calculation procedure was included in the program package. Irradiance profiles were measured from the 23rd of May to the 3rd of June 1998 between about 07:00 LST and 11:00 LST (Local Solar Time). LST was calculated by subtraction of 4 min per 1°W of the station position.

Additional Measurements

Temperature, salinity and fluorescence data (courtesy of the division of Marine Geology, Bremen University, Figs.8, 9 and 10) were taken with a self-contained SBE 19 profiler equipped with a conductivity-temperature-depth probe and a CHELSEA fluorometer. All sensors were calibrated prior to the cruise by the manufacturer. Density (D = kg m^{-3}) was calculated from temperature and salinity using the standard NICMM equation (e.g. UNESCO report, 1981; Pond and Pickard, 1983):

$$D = (1000+(1.455*(S-0.03)/1.805)) - (0.00655 * (T-4+(0.4*(S-0.03)/1.805))^2)$$

where T is the temperature and S the salinity at the given water depth.

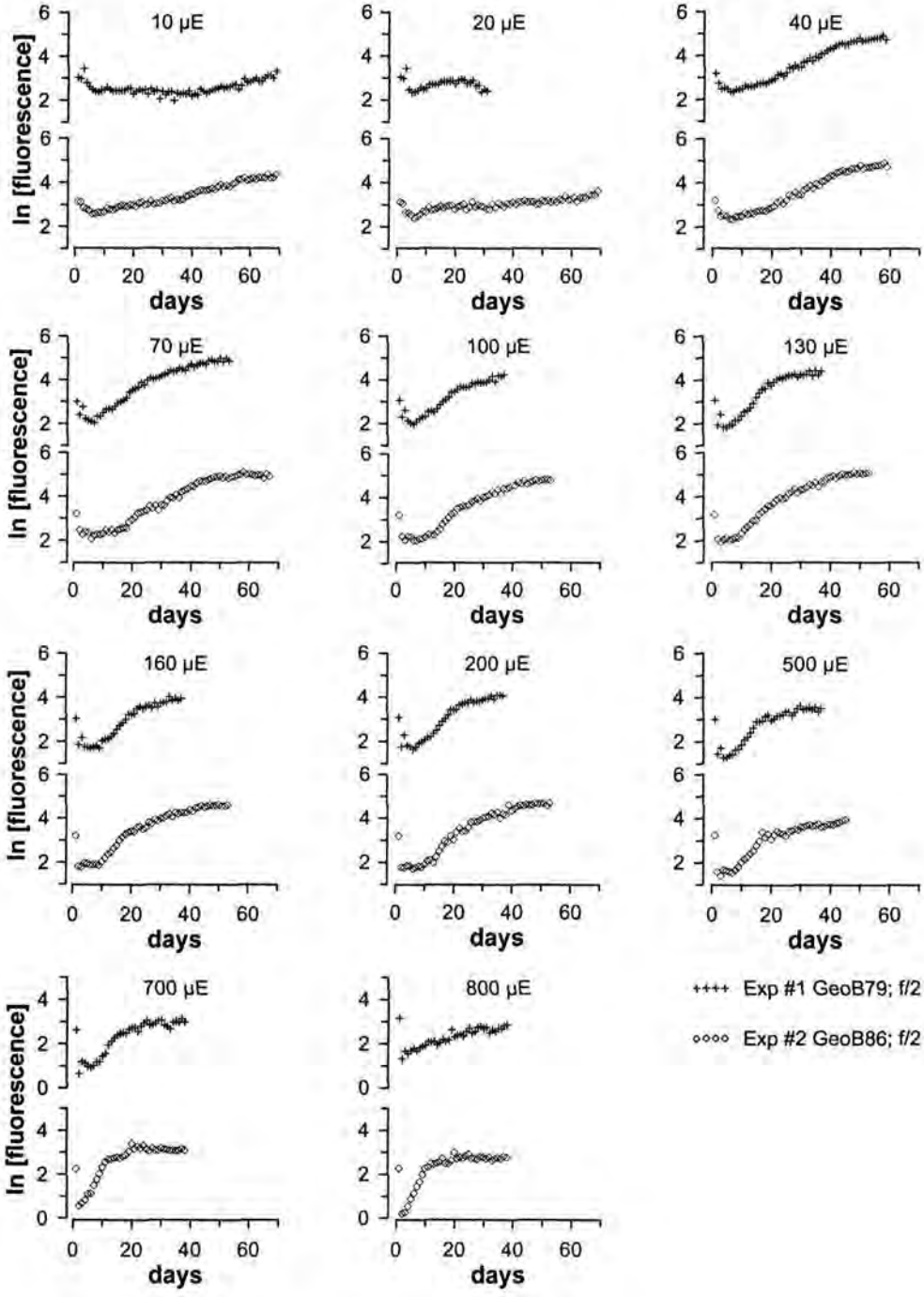

Fig.2: Growth of *Thoracosphaera heimii* in culture experiments. Irradiance is given in µE = $\mu Em^{-2}s^{-1}$ (PAR, 400 nm to 700 nm).

Results

Laboratory Studies

Culture growth

Growth occurred under all tested light conditions (Fig.2). RFD values measured on the day of inoculation and the second day of the experiments lie closer together at the dark end of the

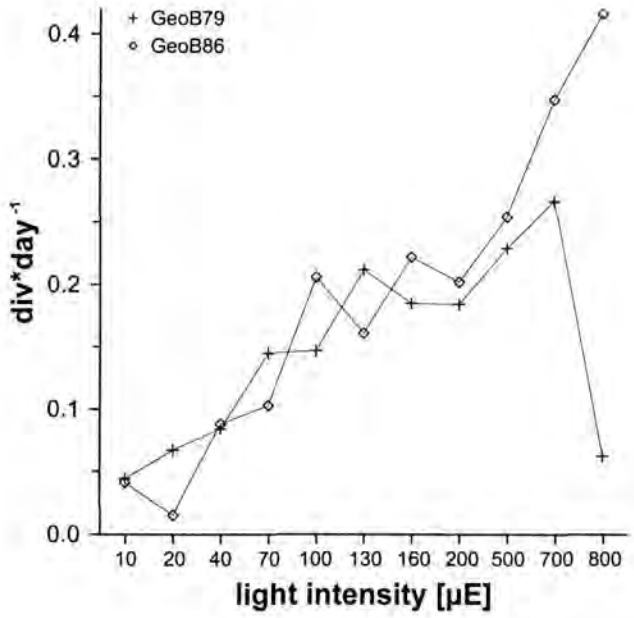

Fig.3: Growth rates of *T. heimii* within different light intensities (10 $\mu Em^{-2}s^{-1}$ to 800 $\mu Em^{-2}s^{-1}$; PAR, 400 nm to 700 nm) during exponential phase calculated from fluorescence data.

light gradient and drift further apart towards the bright end of the gradient. In general, the lag-phases of the growth curves shorten from low towards high light intensities. Maximal duration of the lag-phase (40 days) was observed at 10$\mu Em^{-2}s^{-1}$ (GeoB79), the minimal duration (2 days) at 700 $\mu Em^{-2}s^{-1}$ and 800 $\mu Em^{-2}s^{-1}$ (GeoB86).

Growth rates varied from 0.015 $div*day^{-1}$ (GeoB86, 20$\mu Em^{-2}s^{-1}$) to 0.416 $div*day^{-1}$ (GeoB86, 800 $\mu Em^{-2}s^{-1}$). Maximal growth rates during exponential phase (0.229 $div*day^{-1}$ to 0.416 $div*day^{-1}$) were obtained from 500 $\mu Em^{-2}s^{-1}$ to 800 $\mu Em^{-2}s^{-1}$. In the experiments, growth rates of *T. heimii* rise with increasing light intensities (exception 800 $\mu Em^{-2}s^{-1}$, GeoB86) (Fig.3). This upward trend levels out to some extent from 70 $\mu Em^{-2}s^{-1}$ to 200 $\mu Em^{-2}s^{-1}$ (GeoB79) or 100 $\mu Em^{-2}s^{-1}$ to 200 $\mu Em^{-2}s^{-1}$ (GeoB86).

Yield

During Exp#1 and Exp#2 cultures kept at 10 $\mu Em^{-2}s^{-1}$ and 20 $\mu Em^{-2}s^{-1}$, respectively, did not reach the declining and stationary phase within the time frame of the experiments (68 days). No final yield was calculated for these cultures. Under light intensities from 10 $\mu Em^{-2}s^{-1}$ to 200 $\mu Em^{-2}s^{-1}$, the final yield data calculated from both chlorophyll measurements ($yield_{RFD}$) and cell counts ($yield_{cc}$) follow largely the same trends (Fig.4). From 500 $\mu Em^{-2}s^{-1}$ to 800 $\mu Em^{-2}s^{-1}$ the curves diverge remarkably: the $yield_{RFD}$ curve declines, whereas the

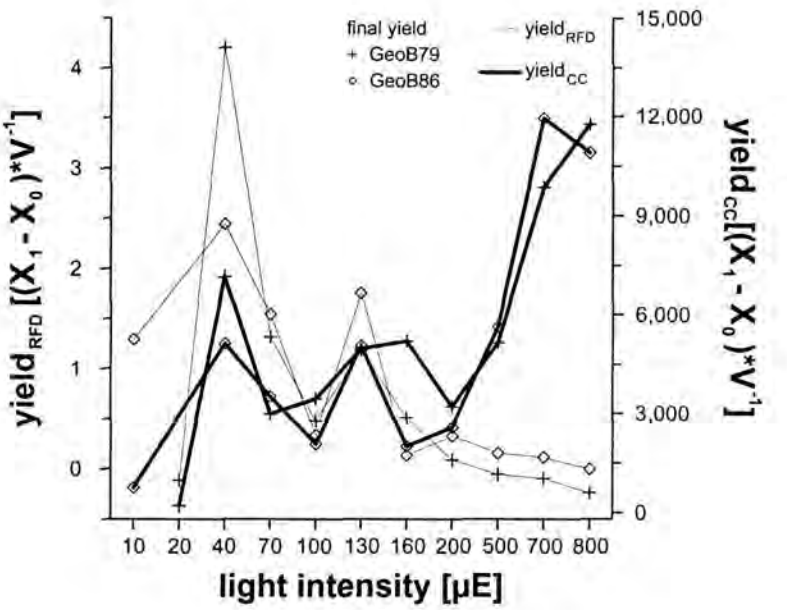

Fig.4: Final yield of *Thoracosphaera heimii*. Yield$_{RFD}$: X_0 = fluorescence after inoculation; X_1 = fluorescence on the last day of exponential growth. Yield$_{CC}$: X_0 = initial cell density; X_1 = cell density on the last day of exponential growth (calculated from fluorescence data and the according cell count from the final day of the experiment and the fluorescence of exponential growth). V = culture media volume (30 ml).

yield$_{cc}$ curve shows a sharp rise for both strains. Highest final yield$_{RFD}$ was observed at 40 µEm^{-2}s^{-1} (GeoB79, GeoB86), the minimum yield$_{RFD}$ was observed at 20 µEm^{-2}s^{-1} (GeoB79). Yield$_{cc}$ reached maximum values at 700 µEm^{-2}s^{-1} and 800 µEm^{-2}s^{-1} and minimum values at 10 µEm^{-2}s^{-1} and 20 µEm^{-2}s^{-1}. A relatively level area of the curves can be made out from 40 µEm^{-2}s^{-1} to 200µEm^{-2}s^{-1}.

Cell counts vs. *RFD*

Figures 5a and 5b compare the cell counts and the RFD measurements of the final day of each experiment. During Exp#1 (Fig.5a) cell counts from cultures kept under irradiation from 10 µEm^{-2}s^{-1} to 40 µEm^{-2}s^{-1} follow roughly the same trend as the RFD values. But whereas the cell counts from 40 to 160 µEm^{-2}s^{-1} are more or less stable and rise from 200 µEm^{-2}s^{-1} to 800 µEm^{-2}s^{-1}, the RFD values show a continuous decline between 40 µEm^{-2}s^{-1} and 800 µEm^{-2}s^{-1}. In Exp#2 (Fig.5b) cell counts and RFD values follow similar trends from 10 µEm^{-2}s^{-1} to 200 µEm^{-2}s^{-1}. Cell counts vary only slightly from 500 µEm^{-2}s^{-1} to 800 µEm^{-2}s^{-1} while the RFD measurements decline from 200 µEm^{-2}s^{-1} onwards.

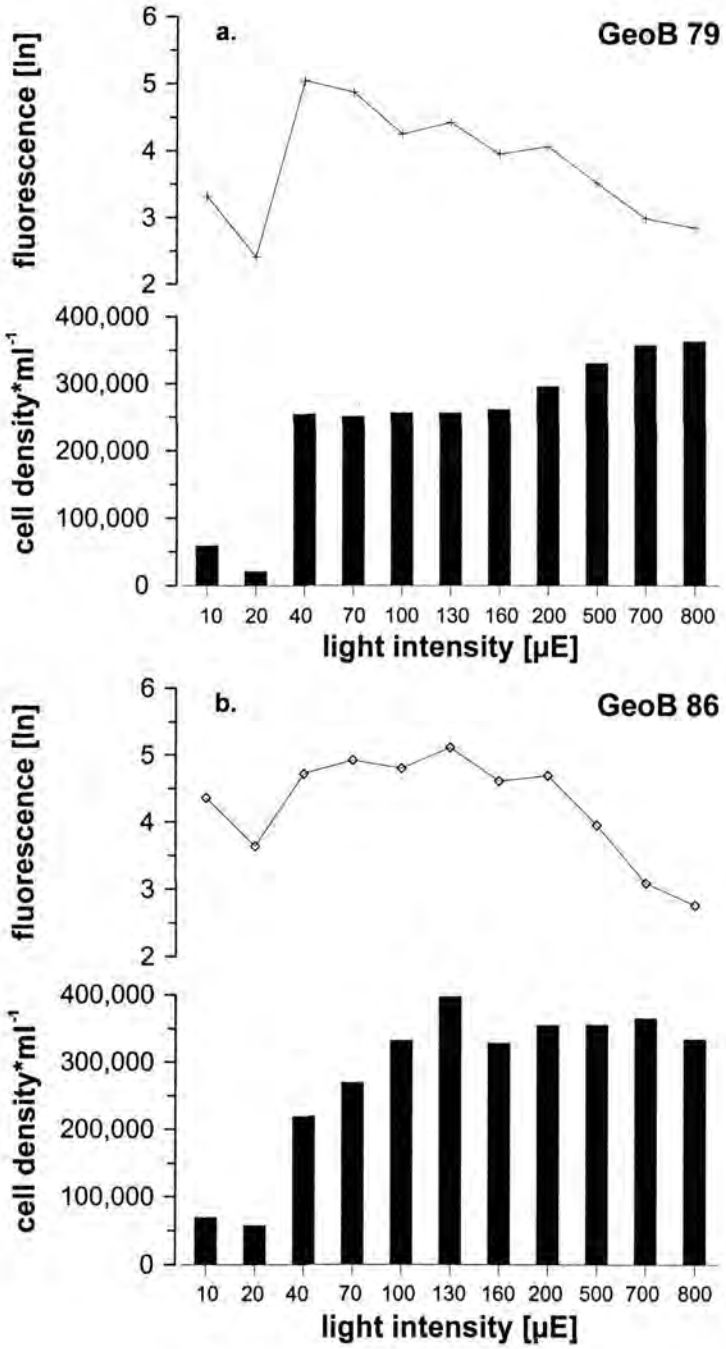

Fig.5: Comparison of the cell counts from fluorescence measurements on the final day of the experiments. a: Exp#1; b: Exp#2.

Culture development

Growth and cell type distribution of the reference cultures are shown in Figs.6a and b. The fluorescence data show a standard sigmoidal growth curve. The exponential growth phase started after 5 days in both cultures and lasted 17 days (0.166 div*day^{-1}) and 7 days (0.321 div*day^{-1}) for clones GeoB79 and GeoB86, respectively. The final $yield_{RFD}$ ($yield_{CC}$) of GeoB79 was 5.4 (3904) [$(X_1-X_o)*V^{-1}$] and 3.57 (4708) [$(X_1-X_o)*V^{-1}$] for GeoB86.

The percentage of calcified cells rose during the exponential and declining growth phase, or stayed constant in the declining phase (GeoB86). In the stationary phase of culture development the portion of calcified cells decreased again. Non-calcified cells did not show the bell-shaped distribution curve of the calcified cells but followed a sigmoidal distribution curve.

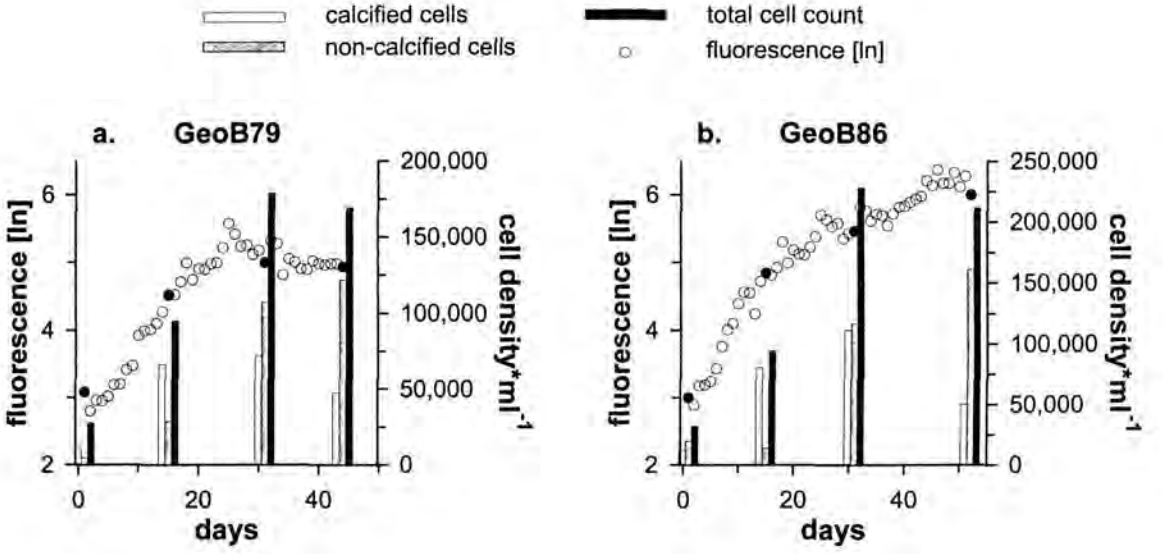

Fig.6: Growth and cell type distribution of *Thoracosphaera heimii* in reference cultures. Filled circles show the fluorescence on the day on which the cell counts were taken. a: Exp#1; b: Exp#2.

Culture growth in comparison with cell type distribution of cultures grown in 700 $\mu Em^{-2}s^{-1}$ and 800 $\mu Em^{-2}s^{-1}$ from Exp#1 and Exp#2 are shown in Figs.7a - d. In general, the cell types in these cultures from Exp#1 and Exp#2 follow similar distribution patterns as the ones in the reference cultures. The exception is GeoB79 (800 $\mu Em^{-2}s^{-1}$). In this culture the numbers of calcified cells did not exceed those of the non-calcified cells in the exponential or declining growth phase.

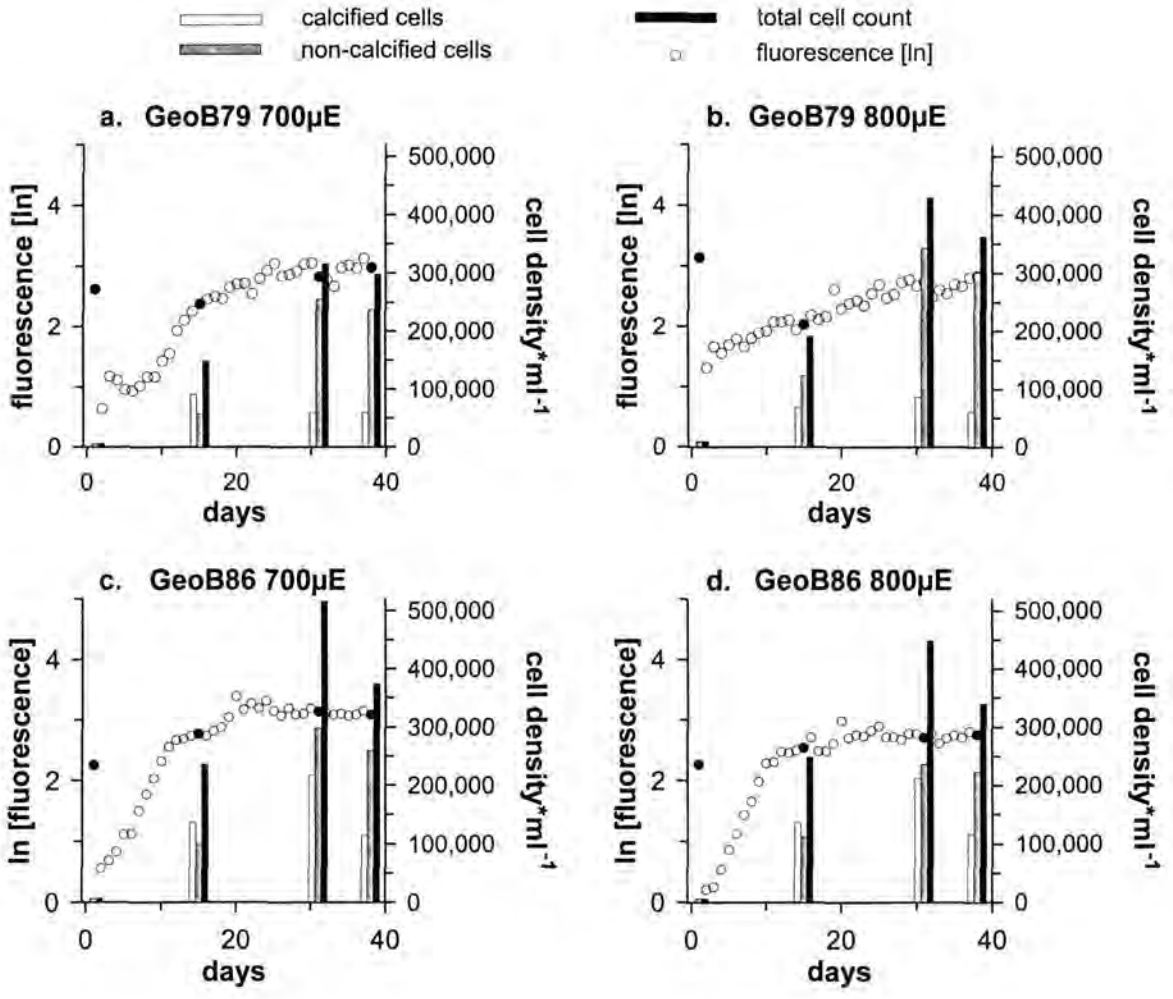

Fig.7: Growth and cell type distribution of *Thoracosphaera heimii* in cultures grown under high irradiances. Filled circles show the fluorescence on the day on which the cell counts were taken. a, b: Exp#1; c, d: Exp#2.

Field Studies

Distribution of *T. heimii* shells in the depth profiles in comparison with irradiance measurements, water temperature, chlorophyll *a* distribution and density are shown in Figs.8, 9 and 10.

Light measurements

Irradiance measurements were taken under clear skies (WET12, EET15, EET16), partial clouds (WET13, WET14, EET17) and overcast (EET18) weather conditions (for station positions see Fig.1). LST are shown in Figs.8, 9, and10. The maximal average irradiance in the upper first metre of the water column was 1400 $\mu Em^{-2}s^{-1}$ (WET14), the minimal average irradiance in the uppermost metre was 300 $\mu Em^{-2}s^{-1}$ (EET18). The 1 % PAR boundary of the euphotic zone lay between 10 $\mu Em^{-2}s^{-1}$ (EET18) and 43 $\mu Em^{-2}s^{-1}$ (EET15) in 20 m (EET15) to 80 m (WET12) water depth. In the WET the 1 % PAR limit shallows towards the equator (Fig.8). Irradiance measurements in the EET showed, with the exception of station EET15, depths of the euphotic zone between 50 m to 60 m (Fig.9). The shallow 1 % PAR limit at station EET15 relates to the early time of day and thus the low sun angle.

Seawater Samples

T. heimii shells in the surface samples are low in abundance in the entire material investigated (Tab.2). A detailed description of the vertical and horizontal distribution of *T. heimii* shells of cruise M41-4 in correlation to temperature, salinity and seasons is given in Karwath et al. (2000a).

T. heimii maxima were recorded from 30 $\mu Em^{-2}s^{-1}$ (EET16) to 48 $\mu Em^{-2}s^{-1}$ (EET17) and were situated close to the depth of the 1 % PAR limit. At stations, where the sampling depth coincided closely with the lower boundary of the euphotic zone, a significant maximum of *T. heimii* shells was recorded in the profile. In two cases (WET12, 13) the *T. heimii* maximum was situated below the 1 % PAR limit. At station WET12 the 1 % PAR limit (33 $\mu Em^{-2}s^{-1}$) lay in 81 m, the *T. heimii* maximum in 100 m water depth. The sample taken closest (75 m) to the lower boundary of the euphotic zone at WET12 showed no especially high *T. heimii* values. Station WET13's *T. heimii* maximum (75 m) was recorded just below the 1 % PAR limit (70 m, 30 $\mu Em^{-2}s^{-1}$). Aside from this, significant abundances of *T. heimii* below the euphotic zone occur only at WET14 (75 m and 100 m).

Temperature data from stations WET12 through EET18 show a well developed mixed surface layer. Shortly below this zone, a deep chlorophyll maximum (DCM) is established at

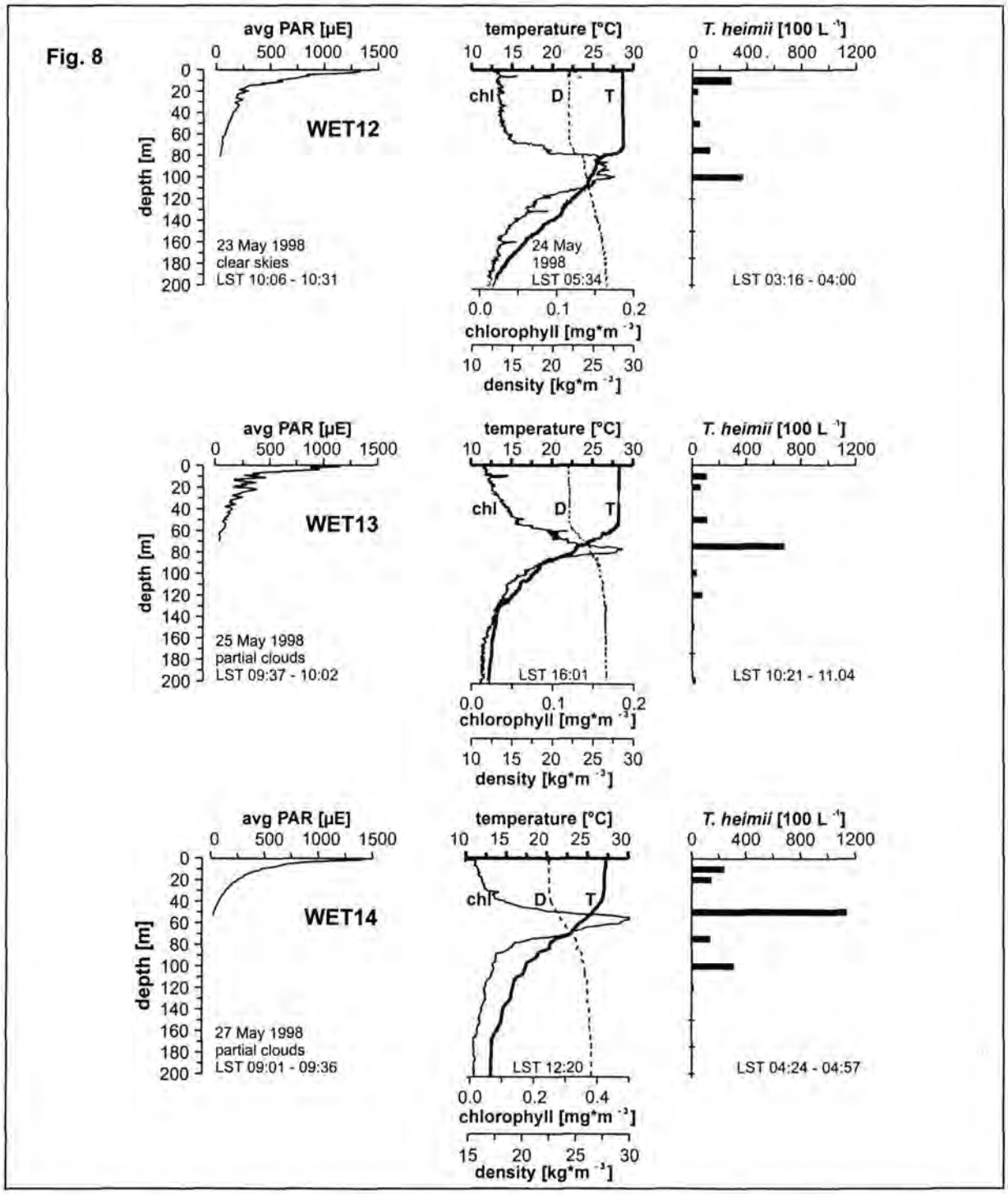

Fig.8: Distribution of *Thoracosphaera heimii* in depth profiles of the Western Equatorial Transect (Karwath et al., 2000a) in comparison with irradiance measurements, water temperature (T), chlorophyll *a* (chl) and density (D). Irradiance plots contain one metre averages of the measured profile data in $\mu Em^{-2}s^{-1}$ = $\mu mol\ m^{-2}s^{-1}$ between wavelengths of 400 nm to 700 nm (PAR). Density was calculated from salinity and temperature data using the standard NICMM equation. Bars show calcified cells of *T. heimii* per 100 litres of seawater.

Fig.9: Distribution of *Thoracosphaera heimii* in depth profiles of the Eastern Equatorial Transect (Karwath et al., 2000a). See Fig.8.

Fig. 9

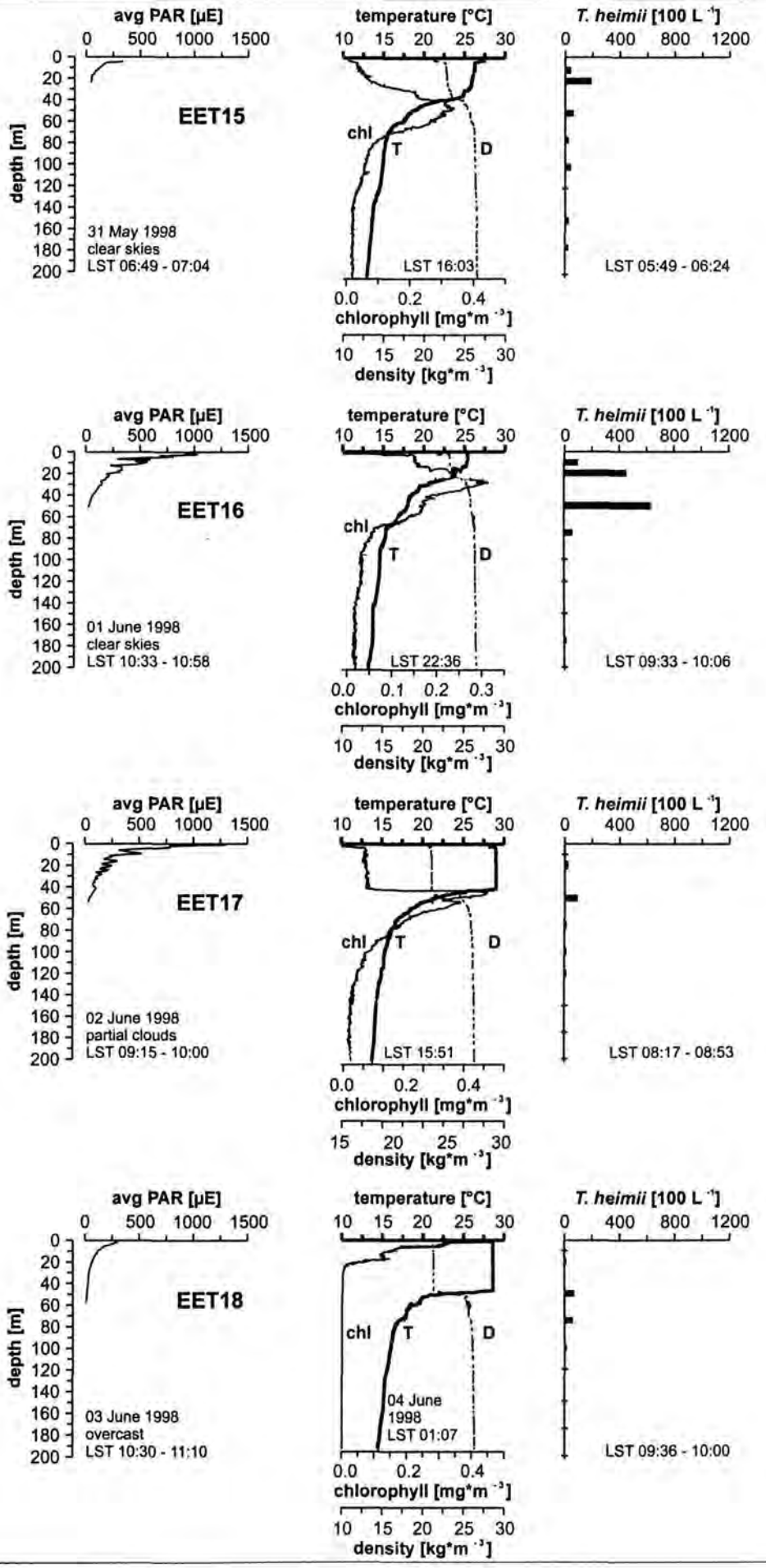
avg PAR [µE]
temperature [°C]
T. heimii [100 L⁻¹]
depth [m]
EET15
31 May 1998
clear skies
LST 06:49 - 07:04
chl
T
D
LST 16:03
LST 05:49 - 06:24
chlorophyll [mg*m⁻³]
density [kg*m⁻³]
EET16
01 June 1998
clear skies
LST 10:33 - 10:58
LST 22:36
LST 09:33 - 10:06
EET17
02 June 1998
partial clouds
LST 09:15 - 10:00
LST 15:51
LST 08:17 - 08:53
EET18
03 June 1998
overcast
LST 10:30 - 11:10
04 June
1998
LST 01:07
LST 09:36 - 10:00

all stations either around 35 m or 75 m water depth. The thickness of the DCM varies between 30 m at WET12 and 10 m recorded at WET13. The lowest chlorophyll *a* content in the DCM was observed at EET15, the highest chlorophyll *a* content in this layer was recorded at station WET14. Highest *T. heimii* contents were observed wherever the sampling depth coincided with the DCM. The exception to this is station EET15: the *T. heimii* maximum at this station lies above the DCM in 20 m depth. At station EET16 sampling depth did not coincide with the position of the DCM in the water column. At this station the observed *T. heimii* maximum (50 m) lies below the DCM.

Discussion

Laboratory Studies

Towards the dark end of the light gradient the *T. heimii* cultures have far longer acclimation times than cultures grown under high irradiation. This coincides with less decrease of RFD values from the first to the second day of the experiments in low irradiance, and increasing differences in cultures kept in the bright end of the gradient. Here the question arises, does the decrease in RFD represent a diminishing cell number or less production of chlorophyll *a* ?. In view of the divergent curves of $yield_{CC}$ and $yield_{RFD}$ from 500 $\mu Em^{-2}s^{-1}$ to 800 $\mu Em^{-2}s^{-1}$ (Fig.4), the latter seems to be the case, at least for this area of the gradient. After the first part of the experiments had been completed (cultures from 10 $\mu Em^{-2}s^{-1}$ to 500 $\mu Em^{-2}s^{-1}$) a direct comparison of RFD to cell counts (Figs.5a, b) hinted at this problem. During the subsequent growth experiments under irradiation of 700 $\mu Em^{-2}s^{-1}$ and 800 $\mu Em^{-2}s^{-1}$ we took the opportunity to check on this by subsampling the cultures (Fig.7a - d). In the comparison of the data derived from cell counts and the RFD from the same day, it is striking that the high RFD values on the first day are caused by very few cells. During the later course of culture development it takes many times the initial cell density to even reach the RFD values of the first day. On the other hand, the reference cultures, which did not have to adjust to different light conditions, do not show the pattern that has been observed in cultures from 700 $\mu Em^{-2}s^{-1}$ and 800 $\mu Em^{-2}s^{-1}$. The higher light intensity means that the cells do not need so much chlorophyll anymore and light saturation is achieved at much lower light levels. It is common amongst the algae that as the light intensity decreases during growth, the content of their photosynthetic pigments increases (Kirk and Tilney-Basset, 1978). The use of RFD for the growth rate calculation of *T. heimii* during the experiments instead of cell counts seems to be problematical in view of the shift of relative chlorophyll *a* content per cell over the entire gradient. But since the rates are calculated from data of the exponential growth phase after the

lag phase, and thus after acclimation to ambient light intensities, the slope of the exponential part of the curve should show the growth rate of the culture.

The growth rates of *T. heimii* observed during the experiments (0.015 – 0.416 div*day^{-1}) fall for the most part within the range of low rates typical of dinoflagellates (0.16 – 1.28 div*day^{-1}; Tang, 1996). They coincide roughly with the rates reported by Karwath et al. (0.08 – 0.38 div*day^{-1}, 14°C – 27°C, 100 µEm^{-2}s^{-1}; 2000b) but are well below the mean division rate established for *T. heimii* by Brand and Guillard (1981) (0.577 div*day^{-1} ; n = 20; 15°C). Control experiments conducted by Brand and Guillard (1981) have shown that the measurements taken with the fluorometer each day do not affect its reproduction rate.

In comparison of the growth rates with the final yields ($yield_{RFD}$ and $yield_{CC}$) over the gradient, the response of *T. heimii* is changing between 200 µEm^{-2}s^{-1} and 500 µEm^{-2}s^{-1}. From 40 µEm^{-2}s^{-1} to 200 µEm^{-2}s^{-1} the cultures show rising growth rates and both $yield_{RFD}$ and $yield_{CC}$ are decreasing. From 500 µEm^{-2}s^{-1} to 800 µEm^{-2}s^{-1}, however, the growth rates and $yield_{CC}$ increase but $yield_{RFD}$ decreases. Somewhere between 200 µEm^{-2}s^{-1} and 500 µEm^{-2}s^{-1} lies the point where the light intensity is such that the cells start to reduce their chlorophyll *a* content.

The cultures kept under 10 µEm^{-2}s^{-1} and 20 µEm^{-2}s^{-1} for which the final yield could be calculated show very low growth rates accompanied by low $yield_{RFD}$ and $yield_{CC}$ values. So, again somewhere between 20 µEm^{-2}s^{-1} and 40 µEm^{-2}s^{-1} is a point where shade adaptation is getting problematical and *T. heimii* has trouble acclimating to the low irradiances but is still able to do so.

A statement about which light intensity has the highest yield of calcareous cells cannot be made with the data available since the percentage of such cells changes during the course of culture development (Figs.6a, b and 7a - d): the counts made on the final day of the experiments reflect different stages in the individual culture development, ranging from exponential to dying / death phase.

Field Studies

Maximum occurrences of *T. heimii* coincide with the position of the DCM within the water column. We have to mention here that the distribution patterns of *T. heimii* are unlikely to have been caused simply by cell accumulations above a density gradient: *T. heimii* maxima occur in some cases together with the DCM below the pycnocline (WET12, WET13, EET16, EET17).

The only exception where the DCM was sampled without finding a *T. heimii* maximum was station EET15. At this sample site the *T. heimii* maximum lay above the DCM and coincided with the 1 % PAR boundary which was very shallow due to the early time of day. The maximum occurrences of *T. heimii* at the other stations not only fall within the DCM but are also very close to the 1 % PAR limit during day-time. Here the question might arise whether the organism truly prefers the DCM or if it migrates, within limits, with the diurnal movement of the 1 % PAR boundary.

Within the photic zone there is a given time at a particular depth for a photosynthetic species, where the light intensity is optimal for photosynthesis. To be able to move with this zone of optimal light conditions is a clear advantage for the species. Such migrational abilities are a common feature among the dinoflagellates and are well documented (e.g. for *Cachonina niei*, *Ceratium furca*, *Prorocentrum micans*; Eppley et al., 1968; Olsson and Graneli, 1991). Migration rates of these species vary from 1 m to 2 m per hour. *Cachonica niei*, e.g., covers a vertical distance of up to 10 m twice each day (Eppley et al., 1968).

Such an activity of daily movement seems to be precluded by *T. heimii*'s characteristics of its life-cycle: even though the organism possesses motile cells, the majority of its stages, including the dominant vegetative-coccoid one, are non-motile (Tangen et al., 1982; Inouye and Pienaar, 1983). The motile stage is active from only 3 min up to several hours (Inouye and Pienaar, 1983). If the behaviour of the species is not totally different in the field, (laboratory effects were kept to a minimum: Inouye and Pienaar (1983) conducted their life-cycle analyses with unialgal cultures isolated from samples which were taken weekly and returned to the laboratory within 4 to 6 hours) the low mean division rates of *T. heimii* (see 4.1) would not allow a high enough production of swarmers to travel several tenths of metres per day to follow the 1 % PAR limit. It is more likely that *T. heimii* is one of the dinoflagellate species that use their locomotive abilities to move themselves to and remain at a particular depth, rather than for regular diurnal up and down migration (e.g. *Ceratium hirudinella*; Heaney and Talling, 1980).

In our cultures, *T. heimii* shows higher activity, i.e. it forms relatively more swarmers, in the morning than during other times. Should this also be the case in the field, it may be that the organism uses this time of day to regain height that might have been lost during the rest of the day and the night. We cannot make any definite statements about the distribution of the non-calcified *T. heimii* cells in the water column. The gymnoid planospores lack thecal plates needed for identification and the non-calcified aplanospores are also in short supply of easily identifiable features. It is extremely difficult to even relate the aplanospores by lightoptic

means to the Dinophyceae when viewed outside a clonal culture. But the already mentioned dominance of non-motile stages within the life cycle makes a strong vertical separation of more than a few metres of the different cell types rather unlikely.

The problem of sinking below the zone of optimal irradiance should not be too dangerous for *T. heimii*. The species is able to adapt at least to light intensities around 10 $\mu Em^{-2}s^{-1}$ (this study) and is also able to withstand long periods of darkness. Griffith and Chapman (1988) exposed several dinoflagellate species (*T. heimii*, *Gonyoulax polyedra*, *Ensiculifera loeblichii* and *Scrippsiella trochoidea*) to prolonged darkness. The three motile dinoflagellates did not survive three days exposure to darkness and did not appear to respond to the darkness with resting cysts. The predominantly vegetative-coccoid *T. heimii*, however, was able to withstand at least eight, but less than ten weeks of darkness with long term recovery. In this regard *T. heimii*'s response was closer to that of the also tested coccolithophore *Coccolithus pelagicus*, which survived for the same length of time under similar conditions.

The laboratory studies have not only shown that *T. heimii* is capable of shade adaptation, but that the species is also able to quickly adapt itself to relatively high irradiances as well. *T. heimii* shows high growth rates and high $yield_{CC}$ under such high light intensities. Nevertheless, in the field *T. heimii* maxima were observed at irradiance levels of under 45 $\mu Em^{-2}s^{-1}$. In the laboratory experiments *T. heimii* showed not only a peak of chlorophyll *a* production at 40 $\mu Em^{-2}s^{-1}$, but an elevated production of cells ($yield_{CC}$) as well. However, cultures kept under 40 $\mu Em^{-2}s^{-1}$ exhibited no peak within the growth rate curve. *T. heimii* is able to produce under the same nutritional conditions as much, or, in the case of GeoB79, even more cells under relatively low irradiance of 40 $\mu Em^{-2}s^{-1}$ as under 500 $\mu Em^{-2}s^{-1}$. In the measured irradiance profiles 500 $\mu Em^{-2}s^{-1}$ correspond roughly to depths around 10 m or less under clear skies.

Keeping in mind that the mixed layer in the stratified ocean is nutrient depleted, and that within the area of the thermocline nutrients can enter this layer from the nutrient richer waters from below (e.g. Goldman, 1988; Platt et al., 1989), it is not astonishing that *T. heimii* produces maxima in these deeper levels of the water column. Under optimal conditions in the laboratory *T. heimii* may be able to produce more cells under high irradiances, but in the open ocean the nutrients, and thus the energy for such high growth rates, are not available.

Dinoflagellates are common constituents of the DCM (Taylor, 1987). *T. heimii*, however, is the only DCM species among the dinoflagellates known so far that leaves a calcareous fossil record. In subtropic and tropic oceans, several coccolithophore species are also characteristic for the lower photic zone. The most common of these species is *Florisphaera*

profunda (Okada and Honjo, 1973; Winter et al, 1994). The habitat of *F. profunda* is restricted to temperatures above 10°C (Okada and McIntyre, 1979). *F. profunda* has been established as an effective tool for Quaternary palaeoceanography. The abundance of *F. profunda* relative to surface-dwelling coccolithophore species may be used to estimate palaeo-waterdepth (Li and Okada, 1985) nutricline dynamics (Molfino et al., 1989; Molfino and McIntyre, 1990a,b), and mean water transparency (Ahagon et al., 1993). It would be interesting to compare the temporal and spatial distributions of *T. heimii* and *F. profunda* to determine similar and complementary applications in palaeoceanography.

T. heimii may not exclusively inhabit the DCM, but it shows a strong preference for this ecological niche and all in all the organism seems to be well adapted to life at the lower edge of the euphotic zone. Investigations of sediment cores from the equatorial and tropical Atlantic (Höll et al., 1999) have shown that calcareous dinoflagellates correlate to periods of reduced palaeoproductivity probably related to stratified conditions in the upper water column. This conclusion seems to be validated (at least for *T. heimii*) by the present findings, since a DCM needs a well-stratified water column for its formation (Kirk, 1983). Now work is needed to evaluate the ecological survival strategies of the remaining pelagic calcareous dinoflagellates to allow a better interpretation of their sedimentary signal.

Conclusions

The maximum occurrences of *Thoracosphaera heimii* in the waters examined in this study coincide with the position of the deep chlorophyll maximum (DCM). *T. heimii* shows shade adaptive abilities in both laboratory and field observations. It is not, however a shade species *sensu strictu* as it also occurs in surface waters as well, though far less abundant, and is tolerant of high irradiance levels in laboratory experiments.

The hypothesis of Höll et al. (1999) that *T. heimii* is a possible proxy for productivity and / or stratification could be validated. *T. heimii* is the only calcareous dinoflagellate known so far to form a preservable stage within the DCM (this study), a layer that needs a relatively stable water column for its formation (Kirk, 1983). The resultant sedimentary signal of *T. heimii* could have applications as an indicator of nutricline fluctuations and thus paleoproductivity of the lower photic zone.

Acknowledgements

Financial support was provided by the Deutsche Forschungsgemeinschaft (Wi 725/7) and the SFB 261. We are indebted to the Arbeitsgruppe Meeresgeologie, Fachbereich

Geowissenschaften especially Gerhard Fischer and Volker Ratmeyer for providing the CTD data. Thanks are due to the crew of the *RV Meteor* and cruise participants of *Meteor* cruise M41-4 1998. This study would not have been possible without the help of Anja Meyer during sample preparation as well as the experiments and the onboard help of Angelika Freesemann, Ines Flatter and Bärbel Hönisch. We also thank Bettina and Adam Price for correction of the English text.

References

Brand, L.E. and Guillard, R.R.L., 1981. A method for the precise determination of acclimated phytoplankton and reproduction rates. J. Plankton Res., 3 (2): 193-201.

Dale, B., 1992a. Dinoflagellate Contribution to the Open Ocean Sediment Flux. In: B. Dale and A. Dale (eds.), Dinoflagellate Contribution to the Deep Sea, Ocean Biocoenosis Series ed., Vol. No. 5. Woods Hole Oceanographic Institution, Woods Hole, pp. 1-32.

Dale, B., 1992b. Thoracosphaerids: Pelagic Fluxes. In: S. Honjo (ed.), Dinoflagellate Contribution to the Deep Sea, Ocean Biocoenosis Series ed., Vol. 5. Woods Hole Oceanographic Institution, Woods Hole, Massachusetts, pp. 33-43.

Dale, B. and Dale, A.L., 1992. Ocean Biocoenensis Series, 5: Dinoflagellate Contributions to the Deep Sea. Woods Hole Oceanographic Institution, Woods Hole, Massachusetts, 75 pp.

Dann, O., Bergen, G., Demant, E. and Volz, G., 1979. Trypanocide des 2-phenyl-benzofurans, 2-phenyl-indens und 2-phenyl-indols. Ann. Chem. 749: 68.

Dawson, E.Y., 1966. Marine Botany – An Introduction. Holt, Rinehart and Winston, Inc., 371 pp.

Eppley, R.W., Holm-Hansen, O. and Strickland, J.D.H., 1968. Some observations on the vertical migration of dinoflagellates. J. Phycol. 4(4): 333-340.

Goldman, J., 1988. Spatial and temporal discontinuities of biological processes in pelagic surface waters. In: Rothschild, B.J. (ed.), Toward a theory on biological-physical interactions in the world ocean. Kluwer Academic, pp. 273-296.

Griffith, K. and Chapman, D.J., 1988. Survival of phytoplankton under prolonged darkness: implications for the Cretaceous-Tertiary boundary darkness hypothesis. Palaeogeogr., Palaeoclimatol., Paleoclimatol.. 67: 305-314.

Guillard, R.R.L., 1973. Division rates. In: Stein, J.R. (ed.) Handbook of Phycological Methods Cambridge University Press, pp.289-311.

Guillard, R.R.L. and Ryther, J.H., 1962. Studies of marine planktonic diatoms. I. *Cyclotella*

nana Hustedt and *Detonula confervacea* Cleve, Can. J. Microbiol., 8: 229-239.

Heaney, S.I. and Talling, J.F., 1980. Dynamic aspects of dinoflagellate distribution patterns in a small productive lake. J. Ecol., 68: 75-94.

Höll, C., 1998. Kalkige und organisch-wandige Dinoflagellaten-Zysten in Spätquartären Sedimenten des tropischen Atlantiks und ihre palökologische Auswertbarkeit. Berichte, Fachbereich Geowissenschaften, Universität Bremen, 127: pp.121.

Höll, C., Zonneveld, K.A.F. and Willems, H., 1998. On the ecology of calcareous dinoflagellates: The Quaternary eastern Equatorial Atlantic. Mar. Micropaleont., 33: 1-25.

Höll, C., Karwath, B., Rühlemann, C., Zonneveld, K.A.F. and Willems, H., (1999). Palaeoenvironmental information gained from calcareous dinoflagellates: The Late Quaternary eastern and western tropical Atlantic Ocean in comparison. Palaeogeogr. Palaeoclimatol. Palaeoecol. 146: 147-164.

Inouye, I. and Pienaar, R.N., 1983. Observations on the life cycle and microanatomy of *Thoracosphaera heimii* (Dinophyceae) with special reference to its systematic position. S. Afr. J. Bot., 2: 63-75.

Karwath, B., Janofske, D., Tietjen, F. and Willems, H., 2000b. Temperature effects on growth and cell size in the marine calcareous dinoflagellate *Thoracosphaera heimii*. Mar. Micropaleont., 39: 43-51.

Karwath, B., Janofske, D. and Willems, H., 2000a. Spatial distribution of the calcareous dinoflagellate *Thoracosphaera heimii* in the upper water column of the tropic and equatorial Atlantic. Int. Journ. Earth Sciences 88 (4): 668-679.

Kerntopf, B., 1997. Dinoflagellate Distribution Patterns and Preservation in the Equatorial Atlantic and Offshore North-West Africa. Ber. Fachber. Geowiss., 103: 137pp.

Kirk, J.T.O., 1983. Light and photosynthesis in aquatic ecosystems. Cambridge University Press, 401pp.

Kirk, J.T.O. and Tilney-Bassett, R.A.E, (1978). The plastids. Second edition, Amsterdam: Elsevier.

Lewis, J., Dodge, J.D. and Powell, A.J., 1990. Quaternary dinoflagellate cysts from the upwelling system offshore Peru, Hole 686B, ODP LEG 112. In Suess R, von Huene et al. (eds.), Proceedings of the Ocean Drilling Program, Scientific Results, 112: 323-328

Li, W.-T. and Okada, H., 1985. Relations between floral composition of calcareous nannofossils and paleoceanographic environment observed in three piston cores

obtained from the equatorial Pacific, East China Sea and Japan Sea. Bull. Yamagata Univ., Nat. Sci., 11: 177-191 (in Japanese with English abstract).

Lindholm, T., 1992. Ecological role of depth maxima of phytoplankton. Arch. Hydrobiol. Beih. Ergebn. Limnol., 35: 33-45.

Matthiessen, J., 1995. Distribution patterns of dinoflagellate cysts and other organic-walled microfossils in recent Norwegian-Greenland Sea sediments. Mar. Micropaleont., 24: 307-334.

Molfino, B, McIntyre, A. and Campbell, D., 1989. Equatorial Atlantic nutricline variations aligned with the Younger Dryas. Trans. Amer. Geophys. Union., 70 (43): 1134.

Molfino, B. and McIntyre, A., 1990a. Precessional forcing of nutricline dynamics in the Equatorial Atlantic. Science, 249: 766-769.

Molfino, B. and McIntyre, A., 1990b. Nutricline variation in the Equatorial Atlantic coincident with the Younger Dryas. Paleoceanography, 5: 997-1008.

Olsson, P. and Graneli, E., 1991. Observations on diurnal vertical migration and phased cell division for three coexisting marine dinoflagellates. J. Plankton Res., 13 (6): 1313-1324.

Okada, H. and McIntyre, A., 1979. Seasonal distribution of modern coccolithophores in the western North Atlantic Ocean. Mar. Biol. 54: 319-328.

Okada, H. and Honjo, S., 1973. The distribution of oceanic coccolithophorids in the Pacific. Deep-Sea Res., 20: 355-374.

Petterson, R.G. and Stramma, L., 1991. Upper-level circulation in the South Atlantic Ocean. Prog. Oceanog., 26: 1-73

Platt, T., Harrison, W.G., Lewis, M.R., Li, W.K.W., Sathyendranath, S., Smith, R.E. and Venezia, A.F., 1989. Biological production of the oceans: the case for a consensus. Mar. Ecol. Prog. Ser., 52: 77-88.

Pollehne, F., Klein, B. and Zeitzschel, B., 1993. Low light adaptation and export production in the deep chlorophyll maximum layer in the northern Indian Ocean. Deep-Sea Res. II, 40 (3): 737-752.

Pond, S., Pickard, G.L., 1983. Introductory dynamical oceanography. Pergamon Press, Oxford.

Shulenberger, E., 1978. The deep chlorophyll maximum and mesoscale environmental heterogeneity in the western half of the North Pacific central gyre. Deep-Sea. Res., 25: 1193-1208.

Sorokin, C., 1973. Dry weight, packed cell volume and optical density. In: Stein, J.R. (ed.), Handbook of Phycological Methods. Cambridge University Press, pp. 321-343.

Tang, E.P.Y., 1996. Why do dinoflagellates have lower growth rates?. J. Phycol., 32: 80-84.

Tangen, K., Brand, L.E., Blackwelder, P.L. and Guillard, R.R., 1982. *Thoracopsheara heimii* (Lohmann) KAMPTNER is a dinophyte: observations on its morphology and life cycle. Mar. Micropaleont., 7: 193-212.

Taylor,F.J.R., 1987. General and marine ecosystems. In: Taylor F.J.R. (ed.), The biology of dinoflagellates, Botanical Monographs vol. 21, Blackwell Scientific Publications, pp. 399-502.

Tett, P., 1990. The photic zone. In: Campbell, A.K., Whitfield, M. and Maddock, L. (eds.) Light and Life in the Sea, Cambridge University Press, pp. 59-87.

UNESCO, Tenth Report of the Joint Panel on Oceanographic Tables and Standards, 1981. Unesco Technical Papers in Marine Science, 36.

Wall, D., Dale, B., Lohmann, G.P., Smith, W.K., 1977. The environmental and climatic distribution of dinoflagellate cysts in modern marine sediments from regions in the North and South Atlantic Oceans and adjacent seas. Mar. Micropaleont., 2: 121-200.

Winter, A., Jordan, R.W. and Roth, P.H., 1994. Biogeography of living coccolithophores in ocean waters. In: Winter, A. and Siesser, W.G. (eds.), Coccolithophores, Cambridge University Press, pp 107-177.

3.4

OCEANIC CALCAREOUS DINOFLAGELLATES OF THE EQUATORIAL ATLANTIC OCEAN: CYST-THECA RELATIONSHIP, TAXONOMY AND ASPECTS ON ECOLOGY

(submitted)

OCEANIC CALCAREOUS DINOFLAGELLATES OF THE EQUATORIAL ATLANTIC OCEAN: CYST-THECA RELATIONSHIP, TAXONOMY AND ASPECTS ON ECOLOGY

*Dorothea Janofske and Britta Karwath

Fachbereich-5 Geowissenschaften, Universität Bremen, Postfach 330 440, D-28334 Bremen, Germany. Fax: 0421/2184451

*e-mail corresponding author: janofske@micropal.uni-bremen.de

Keywords: Atlantic Ocean, biomineralization, calcareous cyst, Calciodinelloideae, crystallography, *Calciodinellum albatrosianum*, dinoflagellates, *Leonella granifera, Pernambugia tuberosa*

Abstract

Culturing experiments on dinoflagellates from the Atlantic Ocean revealed the cyst-theca relationship of three species of calcareous dinoflagellate cysts previously recorded only from sediment samples: *Calciodinellum albatrosianum* (Kamptner) n. comb., *Leonella granifera* (Fütterer) n. gen. and *Pernambugia tuberosa* (Kamptner) n. gen. Consideration of the morphological features of both the cellulosic theca and the calcareous cyst led to description of two new genera and emendation of taxa. Morphological and crystallographic ultrastructure of the calcareous layer of the cyst wall are the main focus of the description. A first investigation of both the horizontal and vertical distribution of the calcareous cyst stages in surface water samples from the equatorial Atlantic Ocean connects the three species with oceanic conditions and SST >22°C and with both oligotrophic as well as upwelling conditions.

Introduction

Dinoflagellates are a group of unicellular eukaryotic organisms which represent one of the major marine phytoplankton groups. The life history of dinoflagellates includes a motile stage with two different flagella and in 10% of the 2000 extant species, a non-motile cyst stage is included (Dale, 1983; Anderson et al., 1985; Head, 1996). Skeletal elements are a typical feature of this group (= Pyrrhophyta Pascher 1914) although preservation in recent and fossil sediments is dependent on the material used. Cellulose which is generally used for the skeletal elements of the motile stages during the life cycle (theca) is not fossilisable due to rapid microbial decay. The wall of the cyst stage generally contains more resistant material such as an organic sporopollenin-like material (dinosporin, Fensome et al., 1993) and/or calcareous elements (calcite, Wall et al., 1970).

About 200 marine dinoflagellate species are known to produce cysts (173 with organic-walled cysts: Head, 1996; 30 with calcareous cysts: unpubl. observ.). The cyst-theca relationships were usually determined by incubation of cysts with cell content ("living cysts") obtained from sediment samples. Until now extensive incubation experiments were carried out exclusively with sediment material from neritic environments (Baldwin, 1987; Blanco, 1989a, 1989b, 1989c; Bolch and Hallegraeff, 1990; Ellegaard et al., 1994; Evitt and Davidson, 1964; Hallegraeff and Bolch, 1992; Lewis, 1991; Nehring, 1994; Nehring, 1995; Sonneman and Hill, 1997; Wall, 1965; Wall and Dale, 1966; Wall and Dale, 1968a, 1968b).

In tropical-subtropical oceanic environments organic-walled dinoflagellate cysts are very rare (Dale, 1992) to absent (Kerntopf, 1997). The "oceanic assemblages" of organic-walled cysts from recent oceanic sediments are supposed to represent the result of long distance transport from more coastal regions rather than from oceanic dinoflagellate production (Dale, 1992). On the other hand "calcispheres", calcareous hollow spherical objects which are obviously skeletal remains of organisms, are abundant in plankton samples (Kerntopf, 1997), sediment trap material (Dale and Dale, 1992) and sediment samples (Kamptner, 1963; Kamptner, 1967; Karwath, 1995; Kerntopf, 1997; Höll et al., 1997; Höll et al., 1999). Together with the calcareous skeletal remains of foraminifers and coccolithophorids they produce a major part of the calcium carbonate in marine sediments (i.e. Wefer et al., 1994). These "calcispheres" were first described as coccolithophorids (Kamptner, 1963; Kamptner, 1967) and were later assumed to be the cyst stages of dinoflagellates (Fütterer, 1976; Fütterer, 1977; Dale and Dale, 1992; Karwath, 1995; Kerntopf, 1997; Höll et al., 1997).

During the last years (1994 - 1998) on several cruises of *RV Meteor* (M29-2 and 3, M34-3 and 4, M38-1 and 2, M41-1 through 4) plankton samples were taken from the oceanic surface

waters of the equatorial Atlantic Ocean with incubation and culturing of dinoflagellates on board and in the laboratory at the University of Bremen. "Calcispheres" with cell content were abundant in oceanic surface waters and, after incubation, they all proved to be calcareous dinoflagellate cysts. Although there was a diverse association of motile thecate dinoflagellates which survived the sampling procedure (see also Kerntopf, 1997) and the transport to Bremen, most of the cultures we suceeded to establish were small, phototrophic peridinoid taxa which in most cases produced sooner or later a calcareous cyst stage. Organic-walled dinoflagellate cysts were not observed and even the thecal equivalents were extremely rare during this work.

This study presents the cyst-theca relationship and the required systematic revision of the three most abundant calcareous dinoflagellate species - apart from *Thoracosphaera heimii* (Lohmann) Kamptner - described first as *Thoracosphaera albatrosiana* Kamptner, *Thoracosphaera granifera* Fütterer and *Thoracosphaera tuberosa* Kamptner. Preliminary results of the distribution of these three species in the water column down to 200 m water depth are given.

Material and Methods

Cultures

Plankton samples were obtained during several cruises of *RV Meteor*, either with a membrane pump on board from a water depth of 4.5 m or at stations with NISKIN™ bottles mounted on a rosette sampler from different depths (App.1). Single specimens were isolated as motile cell or calcareous cyst on board with a micropipette and placed in a culture plate for incubation. The origin of the strains of *Calciodinellum albatrosianum*, *Leonella granifera* and *Pernambugia tuberosa* is given in Fig.1 (see also App.1). At the University of Bremen culture plates were placed in growth chambers and kept at a temperature of 24°C, with a photoperiod of 12 : 12 L : D, and an irradiance of 90 $\mu E\ m^{-2} \cdot s^{-1}$ provided by cool-white fluorescent tubes. As medium on board the medium K without silica (Keller et al., 1987), in the laboratory both, medium K and medium f/2 without silica (Guillard and Ryther, 1962) was used. Media were prepared with artificial seawater (hw Meersalz, Fa. Wiegand GmbH, Krefeld, Germany) and adjusted to a salinity of 35 psu.

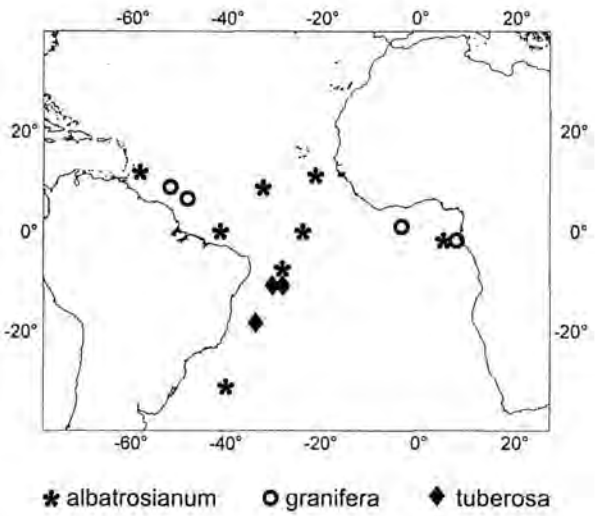

Fig.1: Locality map of the strains of *Calciodinallum albatrosianum*, *Leonella granifera* and *Pernambugian tuberosa*.

Sediment samples

One sediment sample (1608-9/0-1 cm, 00°03.6'S, 10°50.7'W, water depth 4581 m) was collected with a multicorer during the cruise M20-1 (1991/1992) of *RV Meteor* (Kerntopf, 1997). The sample Challenger 338 is surface sample material used also by Kamptner (1967), which was collected during the cruise of the steamship "Challenger" (1873 - 1876) at station 338 (21°15'S, 14°7'W) from a water depth of 3432 m.

Preparation

Lightmicroscopic (LM) observations were carried out with a Zeiss Axiophot with polarization equipment. Motile cells and calcareous cysts were observed in normal light and in polarised light with a gypsum plate for determination of interference colours and extinction patterns (Montresor et al., 1997). For LM micrographs (Pl.4, Figs.40 - 43, 45 - 48, 50 – 53; p. 122) the specimens were placed in a drop of medium on a microscopic slide and covered with a cover slip.

For thin sectioning (Pl.4, Figs.44, 49, 54; p.122) with a rotation microtome (Leica 2055 Autocut, steel blade) 1 ml of culture material was fixed with formaldehyde at a final concentration of 2 % for 1 hr. Following preparation steps were carried out by centrifuging. After medium rinses, the sample was dehydrated in a graded ethanol series. After dehydration the sample was embedded first in a 1:1 mixture of ethanol and a low-viscosity resin (Spurr, 1969; 10 g ERL-4206, 7 g DER 736, 26 g NSA, 0.2 g DMAE) and finally in pure resin in an Eppendorf cup (Eppendorf Micro Test Tubes, 2.0 ml). After polymerisation of the resin at

70°C for 24 hrs, thin sections with a thickness of 3 µm were made. The sections were placed on microscopic slides, embedded in Spurr's resin and covered with a cover slip.

For scanning electron microscope (SEM) observations, three different preparation techniques were used:

Sediment samples were rinsed in tap water adjusted to pH 7.8 - 8 to prevent dissolution of the calcareous material; the < 5 µm fraction was separated by hydraulic sedimentation. Cysts were selected from the dry sediment and fixed on the gelatinous side of a piece of developed photographic film by wetting with water. The film strip was fixed on a SEM stub after the specimens were air-dried. (Pl.1, Figs.12, 13 (p. 106); Pl.2, Figs.25, 26 (p. 113); Pl.3, Fig.39 (p. 120)).

1 ml of culture material with vegetative cells and cysts was fixed with formaldehyde at a final concentration of 2 % for 1 hr. Following preparation steps were carried out by centrifuging. The culture was rinsed in medium and dehydrated in a graded ethanol series. After dehydration the sample was treated first with a 1:1 mixture of ethanol and hexamethyldisilazane (HMDL) and finally with pure HMDL (Nation, 1983). For SEM observations 10 µl of the sample were given on a circular coverslip fixed on a SEM stub and air-dried.(Pl.2, Figs.21 – 23 (p. 113), Pl.3, Figs.34 – 38 (p.120)).

Culture material with vegetative cells and cysts was placed in a filter holder (Swinnex) provided with a polycarbonate membrane with 5 µm pore diameter. Preparation liquids were changed with the aid of a plastic syringe connected to the filter holder. The material was fixed in formaldehyde at a final concentration of 2 % for 1 hr and rinsed in medium. The sample was dehydrated in a graded acetone series. After critical point drying (CPD) of the whole filter holder, the membrane was removed and fixed on a SEM stub. (Pl.1, Figs.3 – 11 (p. 106); Pl.2, Figs. 15 – 20, 24 (p. 113); Pl.3, Figs. 28 – 33 (p. 120)).

All SEM samples were sputter-coated with gold and observed with a CamScan CS 44.

For additional data on thecal plate pattern the culture material was treated with Calcofluor according to Fritz and Triemer (1985). Fluorescence investigations were carried out with a Zeiss Axiophot with UV-light source and the Zeiss 01 filter set (extinction BP 365, emission LP 377).

A detailed description of the preparation techniques used for the determination of cyst distribution pattern (Fig.55 - 57) is given in Karwath et al. (2000).

The samples are deposited at the University of Bremen (Fachgebiet Historische Geologie/Paläontologie, Fachbereich Geowissenschaften).

Rationale for the crystallographic analysis

Optical mineralogical methods (i.e. Nesse, 1991) were used to identify the orientation of optic axes of the calcite crystals in the calcareous cyst wall layer(s) in dinoflagellates (Janofske, 1992; Janofske, 1996; Montresor et al., 1997).

Calcite is an uniaxial, optically negative mineral with a very high birefringence ($\delta = 0.179$, $n_\omega = 1.658$, $n_\varepsilon = 1.486$). The observation of a calcite crystal in orthoscopic illumination in polarised light results in a total extinction of the light when the *c*-axis (principal section) of the crystal is parallel to the light. In sections parallel or at various angles to the *c*-axis, the orientation of the *c*-axis can be identified by using a gypsum plate. This accessory plate is a first-order red plate, with the slow ray (n_γ) at 45°, which is inserted into the light path between the specimen and the analyzer. When the direction of the *c*-axis of calcite crystals corresponds to the slow ray (0°<*c*-axis<90° or 180°<*c*-axis<270°), a decrease of one wavelength of red ligth will produce a yellow interference color. When the direction of the *c*-axis corresponds to the direction of the fast ray (n_α) of the gypsum plate (90°<*c*-axis<180° or 270°<*c*-axis<360°), an increase of one wavelength of red light produces blue interference colors. With the *c*-axis oriented exactly at 0°/180° or at 90°/270°, a purple color indicates extinction. These intensive interference colors are more clearly visible when the calcite crystal is thinner that 5 μm. The yellow-green colors produced by calcite crystals thicker than 5 μm change only slightly when the crystal is rotated in the polarised light microscope, although the extinction pattern is always recognizable.

Average weight

The average volume of cysts was calculated using $V = 4/3\ \pi\ r^3$ with outer and inner diameter reduced by the amount of porosity and the volume of the operculum (see App.2). The operculum was estimated to come to 1/3 in *Calciodinellum albatrosianum* and 2/5 in *Pernambugia tuberosa*; the volume of the operculum of *Leonella granifera* and *Thoracosphaera heimii* (Tangen et al., 1982, Inouye and Pienaar, 1983) was calculated using $V = \pi\ r^2\ h$. Volumes were converted to masses by multiplying by the density of calcite (2.7102 g/cm³, Roberts et al., 1974).

Results

Taxonomy

Order Peridiniales Haeckel 1894

Family Peridiniaceae Ehrenberg 1831

Subfamily Calciodinelloideae Fensome, Taylor, Norris, Sarjeant, Wharton et Williams 1993

Genus *Calciodinellum* Deflandre 1949

Emended diagnosis

Calciodinelloid dinoflagellate. Motile stages with plate tabulation pattern po, x, 4', 3a, 7'', 6c (t + 5c), 6s, 5''', 2''''. Non-motile stages (cysts) have one calcareous wall layer. Crystals of the calcareous cyst wall layer are orientated with their crystallographic optic axis (c-axis) tangential to the cyst surface. Paratabulation patterns are always present. The operculum includes plates 2' - 4' and 1a - 3a.

Emenda diagnosis

Dinoflagellatum calciodinelloideum. Cellulae motiliter formula laminarum po, x, 4', 3a, 7'', 6c (t + 5c), 6s, 5''', 2'''' habent. Cellulae non-motiliter (cystae) unum corium calcarium habent. Cristalla corii calcarii de axe optico (c-axis) tangentialiter ad superficiem cystae directa sunt. Paratabulatio propria est. Operculum laminas apicales et intercalares adaequat.

Typespecies: *Calciodinellum operosum* (Deflandre, 1949) emend. Montresor, Janofske et Willems 1997

***Calciodinellum albatrosianum* (Kamptner 1963) n. comb.**

Fig.2; Pl.1, Figs.3 – 13 (p. 106), Pl.4, Figs. 40 – 44 (p. 122)

Basionym: *Thoracosphaera albatrosiana* Kamptner, 1963, p. 177 - 178, Pl. 5, Fig.30

Synonym:

Thoracosphaera albatrosiana, Kamptner, 1963, p. 177 - 178, Pl. 5, Fig.30

? *Thoracosphaera rela,* Kamptner, 1967, p. 158, Pl. 19, Figs.107, 108

Thoracosphaera reliana, Kamptner, 1967, p. 159, Pl. 20, Figs.109, 110, Pl. 21, Figs.111, 112, Pl. 22, Figs.113, 114

Thoracosphaera ricoseta, Kamptner, 1967, p. 159 , Pl. 13, Fig.87

Orthopithonella albatrosiana, Keupp, 1984, p. 13, Figs.8: 7 - 8

Sphaerodinella albatrosiana, Keupp and Versteegh, 1989, p. 209 - 210, Pl. 1, Figs.9, 11

Emended diagnosis

Epitheca slightly conical, hypotheca rounded. Epitheca equal in size with hypotheca. Motile stages with plate tabulation pattern po, x, 4', 3a, 7", 6c (t + 5c), 6s, 5"', 2"". Non-motile calcareous stages (cysts) are spherical with one calcareous layer which consists of numerous elements arranged rosette-like around pores. Crystals of the calcareous cyst wall layer are orientated with their crystallographic optic axis (c-axis) tangential to the cyst surface and radial around the pores. Paratabulation patterns are present as an angular archeopyle; the operculum includes plates 2' - 4' and 1a - 3a and comprises about a third part of the cyst.

Emenda diagnosis

Cellula motilis epithecam paululum conicam et hypothecam rotundam habet. Epitheca et hypotheca magnitudine adaequant. Cellulae motiliter formula laminarum po, x, 4', 3a, 7", 6c (t + 5c), 6s, 5"', 2"" habent. Cellulae non-motiliter (cystae) calcariae sphaeroideae unum corium habent. Corium compositum est ex multi elementis calcariis, formam comparabilis rosettam circum poros habent. Cristalla corii calcarii de axe optico (c-axis) tangentialiter ad superficiem cystae et radialiter circum poros directa sunt. Paratabulatio forma archeopylae angulatae est. Operculum laminas apicales et intercalares adaequat et tertia pars cystae est.

Description

Motile stage: The vegetative cells are rounded, with a mean length of 20 µm (range 17 - 27 µm) and a mean width of 17 µm (range 14 - 24 µm). The epitheca is slightly conical and the hypotheca is rounded; they are nearly equal in length (Pl.1, Figs.3, 5, p. 106). The cingulum is about 3.5 µm wide and displaced about half a girdle width (Pl.1, Fig.4, p. 106). The large nucleus is located in the central part of the cell; the living motile cells are light brown in colour (Pl.4, Fig.40, p. 122).

Plate tabulation (Fig.2): The plate tabulation formula is po, x, 4', 3a, 7", 6c (t + 5c), 6s, 5"', 2"". The thecal plates are relatively thin and smooth with small pores scattered over their surface. In the pre- and post-cingular plates the pores line the edges along the cingulum (Pl.1, Fig.4; p. 106).

The pore plate (po) is nearly circular and surrounded by a low elevated rim. The canal plate (x) is pentagonal in shape with an arrow-like angle pointing towards the pore plate (po) (Pl.1, Fig.6; p. 106). Plate 1' is extremely wide (about 6 µm) and shows an ortho configuration. The 2' - 4' plates are all irregularly polygonal because their shortest edges

contact the pore plate (po). The plates 2' and 4' are larger than plate 3'. In the intercalary series, plates 1a and 3a are pentagonal and nearly equal in size. Plate 2a is large and hexagonal. In the precingular series, the largest plates are 1" and 7". Plates 2", 3", 5", 6" and 7" are pentagonal. Plates 1" and 4" are trapezoid.

The cingular series consists of six plates. Plates 2c – 6c are about equal in size, but 1c (= transitional plate t) is much smaller (Pl.1, Fig.4; p. 106). The suture between 3c and 4c is located dorsally but the suture between 4c and 5c is displaced and in contact with the cingular border of plate 5" (Pl.1, Fig.5; p. 106).

The sulcus is ventral and extends into the hypotheca. It consists of six plates: an anterior sulcal (as), a left sulcal (ls), a right sulcal (rs), a posterior sulcal (ps), an anterior flagellar pore plate (af) and a posterior flagellar pore plate (pf) (Fig.2; Pl.1, Fig.4; p. 106 4). The anterior sulcal (as) adjoining 7", 1', t, af and rs, is trapezoid with extensions inserted between rs and af and between af and t. The suture between 1' and 1" contacts the suture between as and t. The right sulcal (rs) is rhombic in shape and in touch with the cingular plate 6c, 5"', ps and as. It overlaps af, ls and pf. The left sulcal (ls) is ellipsoid in shape and in touch with ps, t, af and pf. The posterior sulcal (ps) is the largest sulcal plate and is bordered by 5"', 2"", 1"", 1"', ls, pf and rs. The contact of ps with 1"' is a long extension which ends in a contact to the cingular plate t. The anterior flagellar pore plate (af) is located between as, ls and t and is slightly overlapped by rs. The posterior flagellar pore plate (pf) is located between ps and ls and is mostly overlapped by rs. The transversal flagellum emerges in an opening between af and rs, the longitudinal flagellum emerges where pf is overlapped by rs.

In the postcingular series, plates 1"', 2"' and 4"' are rectangular, 3"' is pentagonal (Pl.1, Fig.5; p. 106) and plate 5"' is also pentagonal with the shortest edge in touch with the right sulcal (rs). The two antapical plates 1"" and 2"" are pentagonal and of approximately equal size but the dorsal border of 1"" is shorter than the dorsal border of 2"" (Pl.1, Figs.5, 6; p. 106).

Cyst stage: The calcareous cysts are spherical with a mean diameter of 25.5 µm (range 20.5 - 35 µm). The cyst wall has a mean thickness of 1.8 µm (range 1.5 - 2.7) and consists of one layer of numerous calcite crystals. The porosity of the calcareous cyst wall layer is estimated with 33.3 % (App.2).The crystals are coalesced forming rosette-like structures on the surface around the pores (Pl.1, Fig.13; p. 106). Each crystal is orientated with its crystallographic optic axis (c-axis) exactly tangential to the cyst surface and exactly radial around the pores (Fig.2). The optic signs can be seen clearly in polarized light where the cyst

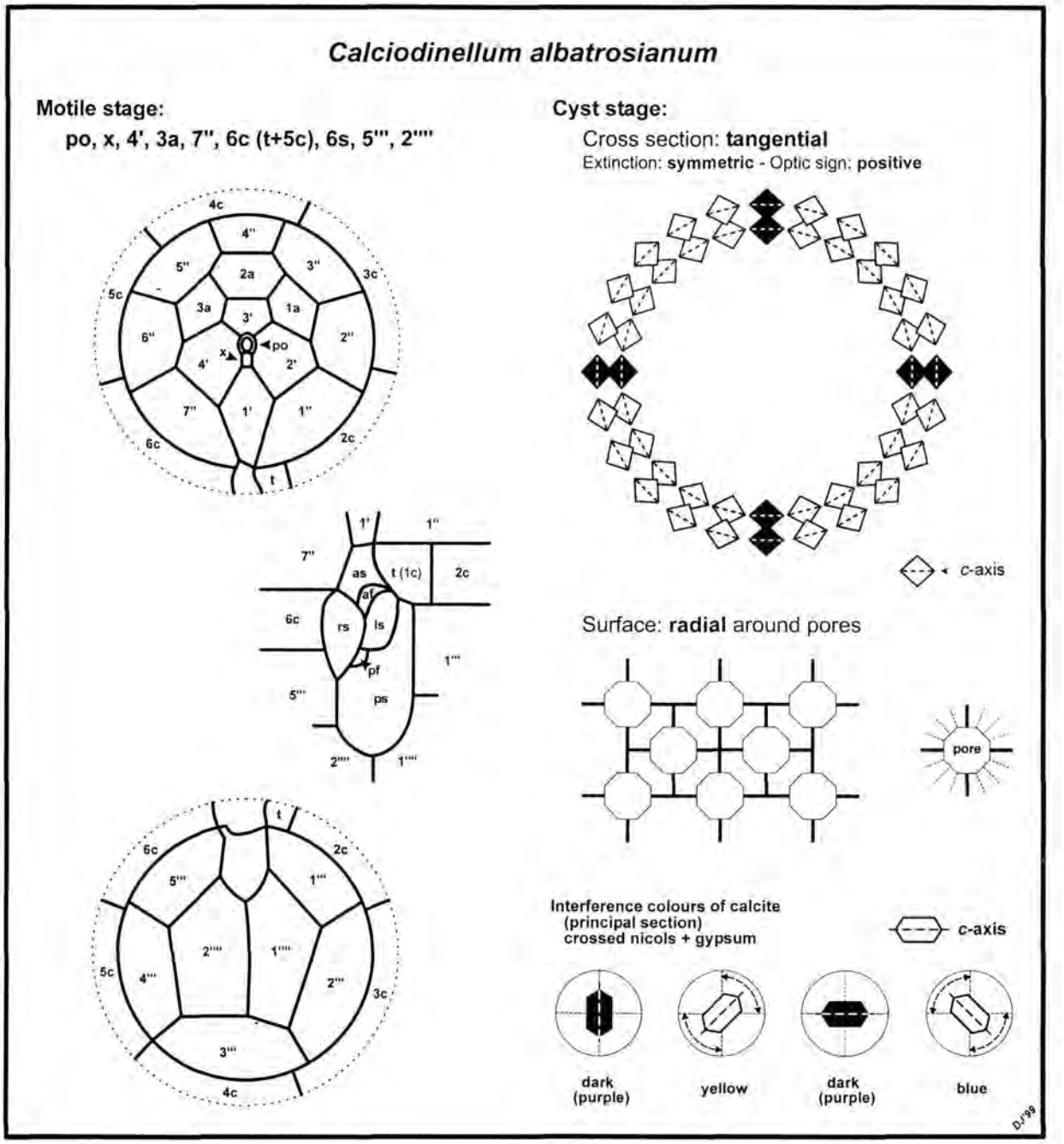

Fig.2: Schematic diagram of the characteristic morphological features of *Calciodinellum albatrosianum*

shows a diffuse symmetric extinction cross (Pl.4, Fig.42; p. 122). Using an accessory filter (gypsum plate), the resulting interference colours show blue colours in the first and the third quadrant and yellow colours in the second and fourth quadrant (Fig.2; Pl.4, Figs.42, 44; p. 122; Janofske, 1996) indicated by a strictly tangential orientation of the c-axes. Focusing on

the surface of the cyst (Pl.4, Fig.43; p.122), the typical net-like pattern is visible which is caused by the radial orientation of the c-axes around the pores (Fig.2); dark/purple areas are not the pores but the extinct crystals. Such patterns were already described before (Kamptner, 1967; Young, 1998) but are not possible with an angle of 120° of the c-axes to one another as given by Kamptner (1967).

The operculum comprises about 1/3 of the cyst and has always an angular outline; the operculum represents the 2' - 4' and 1a - 3a paraplates (Pl.1, Figs.8, 9, 12; p. 106). The crystals at the borders of archeopyle and operculum form continuous rims giving a preformed archeopyle (Pl.1, Figs.8, 9; p. 106). Paratabulation in *C. albatrosianum* cysts appears exclusively by the angular outline of the archeopyle/operculum.

Living cysts are dark brown in colour; a red accumulation body was not observed. The living cyst is surrounded by a very delicate organic layer (Pl.1, Figs.7, 8; p. 106) which is rapidly destroyed after the excystment process (Pl.1, Figs.9, 10; p. 106) and is generally damaged even by the critical point preparation process (Pl.1, Fig.11; p. 106). Under the calcareous wall layer lies another sheet of organic material (Fig.10). Cysts found in sediments are always without any organic residues (Pl.1, Figs.12, 13; p. 106).

After inoculation, the development of the culture starts with reproduction of the motile stages. Cyst production occurs about one week after inoculation. Indication for sexual reproduction during the life cycle such as the fusion of gametes or planozygotes were not observed; the encystment process could not be connected to a sexual phase in the life cycle of *C. albatrosianum*. The living cysts show intense red colours in epi-fluorescence caused by the autofluorescence of chlorophyll *a*.

The cysts produced in cultures are generally larger but have thinner calcareous walls than those found in the sediment (App.2). The average weight of cysts described from the sediment (Kamptner, 1963; Kamptner, 1967; Fütterer, 1977) was calculated to 3.9 ng (without operculum), those produced in cultures have a mean weight of 3.4 ng (without operculum).

Stratigraphic range: Late Paleocene (Keupp, 1984; Kohring, 1993a) to Recent

Record: The cyst of *Calciodinellum albatrosianum* is known from fossil strata of the Pacific Ocean, the Atlantic Ocean, the Mediterranean area and central Europe (Kamptner, 1963; Fütterer, 1977; Keupp, 1984; Keupp and Versteegh, 1989; Keupp et al., 1991; Keupp and Kohring, 1993; Kohring, 1993a, 1993b; Keupp et al., 1994; Kohring, 1997) as well as from recent sediments of the Atlantic Ocean (Kamptner, 1967; Fütterer, 1976; Karwath, 1995;

Kerntopf, 1997; Höll et al., 1997; Höll et al., 1999), the Mediterranean Sea (Meier, 1999) and the Arabian Sea (Gulf of Aden: M31-3, unpubl. observ.). The cyst of *C. albatrosianum* was described from plankton samples of the equatorial Atlantic Ocean (Kerntopf, 1997) and from sediment trap material of the Atlantic and the Pacific Ocean (Dale, 1992).

Discussion

Until now merely the calcareous cyst stage of *Calciodinellum albatrosianum* n. comb. was known. The cyst of *C. albatrosianum* was first described as *Thoracosphaera albatrosiana* from fossil strata of the equatorial Pacific Ocean (Kamptner, 1963: ST 61/562.0 - 563.5). *Thoracosphaera rela*, *Thoracosphaera reliana* and *Thoracosphaera ricoseta* (Kamptner, 1967) from surface sediments of the equatorial Atlantic Ocean are considered to be specimens of *C. albatrosianum*, too (Fütterer, 1976). SEM observations have shown an orthogonal ultrastructure of the calcareous crystals which implied a radial orientation of the crystallographic c-axis. Based on these observations *Orthopithonella albatrosiana* (Keupp, 1984) and later *Sphaerodinella albatrosiana* (Keupp and Versteegh, 1989) were established. Lightmicroscopic analysis confirmed the tangential orientation of the c-axes to the cyst surface (Kamptner, 1967; Janofske, 1996). Tangential crystallographic ultrastructure together with a large archeopyle which reflects paratabulation pattern are characters of the genus *Calciodinellum*. As also the plate tabulation of the motile stage of *C. albatrosianum* is identical to the motile stage of *Calciodinellum operosum* (Montresor et al., 1997), we propose *Calciodinellum albatrosianum* n. comb.

Paratabulation patterns such as ridges on the cyst surface were previously discussed for *C. albatrosianum* by several authors. The possible occurence of transitional stages extending from a spherical smooth kryptotabulate morphotype to a sculptured holotabulate morphotype within a single species were discussed (Keupp et al., 1991; Montresor et al., 1997; Kerntopf, 1997). But, in fact, paratabulation patterns in the form of ridges on the cyst surface were never observed in culture material of *C. albatrosianum* during this study. Certainly such paratabulation patterns are characteristic for another yet undescribed species from the Atlantic Ocean (strain GeoB*120) where ridges which reflect plate tabulation are always present.

The extant genus *Scrippsiella* Balech ex Loeblich III is characterised by a plate formula po, x, 4', 3a, 7", 6c (t + 5c), 6s, 5"', 2"", tangential crystallographic orientation and an operculum comprising apical and intercalary plates as well, but indications for paratabulation patterns are missing (Janofske and Willems, subm.).

Plate 1

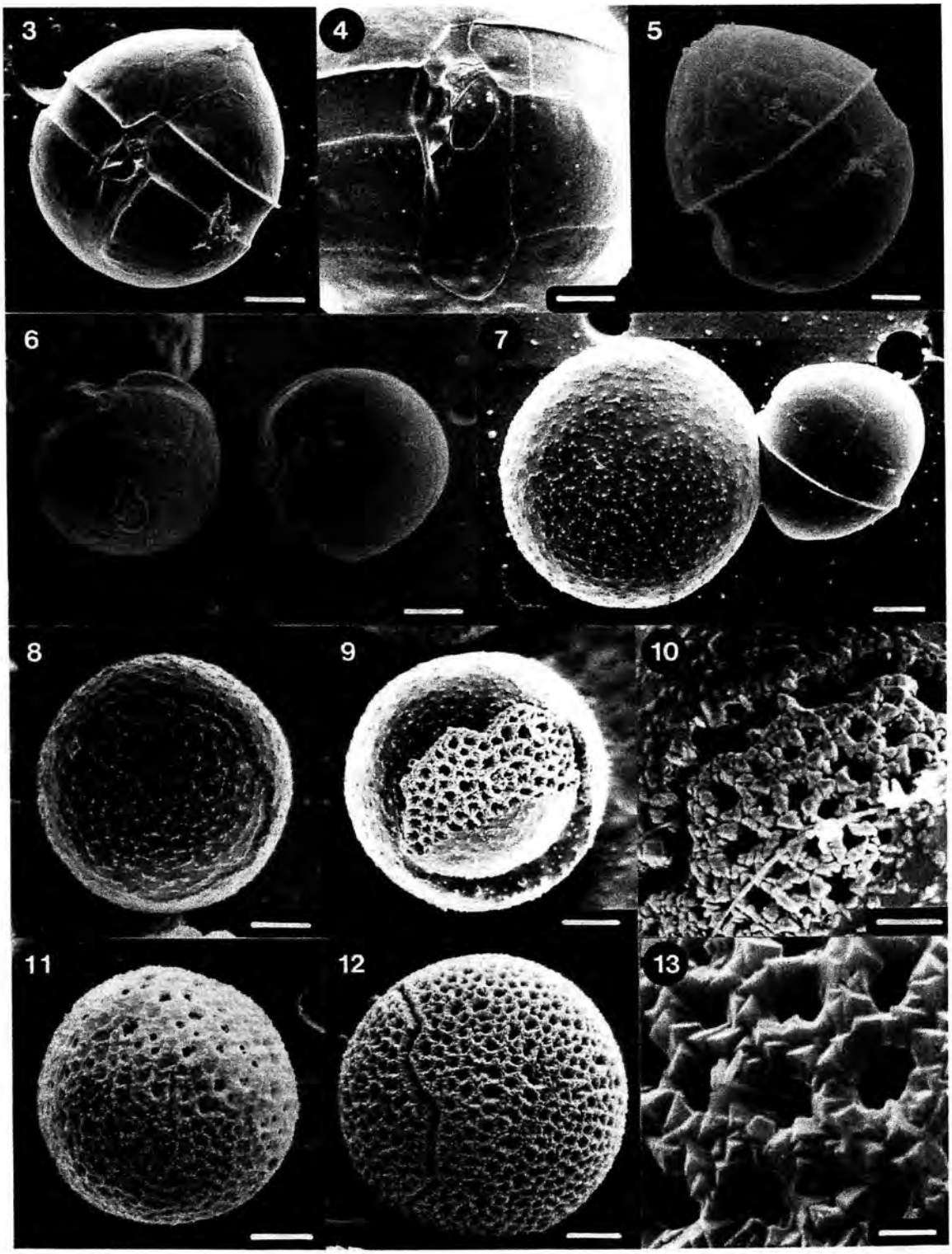

Plate 1: SEM micrographs of *Calciodinellum albatrosianum* n. comb.

Fig. 3: Theca: ventral view. Strain M 34-*26/4. - CPD. Scale bar 5 µm.

Fig. 4: Theca: sulcal area. Strain M 34-*26/4. - CPD. Scale bar 3 µm.

Fig. 5: Theca: dorsal view. Strain M 34-*26/4. - CPD. Scale bar 3 µm.

Fig. 6: Theca: apical and antapical view. Strain M34-*26/4. - CPD. Scale bar 5 µm.

Fig. 7: Cyst stage and motile stage. Strain M 34-*26/4. - CPD. Scale bar 5 µm.

Fig. 8: Calcareous cyst. Strain M 34-*26/4.- CPD. Scale bar 5 µm.

Fig. 9: Calcareous cyst. Strain M 34-*26/5.- CPD. Scale bar 5 µm.

Fig. 10: Detail of calcareous cyst from culture. Strain M 34-*26/4.- CPD. Scale bar 2 µm.

Fig. 11: Calcareous cyst. Strain M 34-*26/4.- CPD. Scale bar 5 µm.

Fig. 12: Calcareous cyst from sediment. M 20/1, 1608-9/0-1 cm. - Air-dried. Scale bar 5 µm.

Fig. 13: Detail of calcareous cyst from sediment. M 20/1, 1608-9/0-1 cm. - Air-dried. Scale bar 1 µm.

Genus *Leonella* n. gen.

Diagnosis

Calciodinelloid dinoflagellate. Motile stages with plate tabulation pattern po, x, 4', 3a, 7", 6c (t + 5c), 6s, 5"', 2"". Non-motile stages (cysts) have one calcareous wall layer. Crystals of the calcareous cyst wall layer are orientated with their crystallographic optic axis (c-axis) radial to the cyst surface. The operculum includes apical plates.

Diagnosis

Dinoflagellatum calciodinelloideum. Cellulae motiliter formula laminarum po, x, 4', 3a, 7", 6c (t + 5c), 6s, 5"', 2"" habent. Cellulae non-motiliter (cystae) unum corium calcarium habent. Cristalla corii calcarii de axe optico (c-axis) radialiter ad superficiem cystae directa sunt. Operculum laminas apicales adaequat.

Type species: *Leonella granifera* (Fütterer 1977) n. gen.

Derivatio nominis: Sierra Leone Rise, equatorial South Atlantic Ocean (type locality, Fütterer, 1977)

***Leonella granifera* (Fütterer 1977) n. gen.**

Fig.14; Pl.2, Figs.15 – 26 (p. 113); Pl.4, Figs.45 – 49 (p. 122)

Basionym: *Thoracosphaera granifera* Fütterer 1977, p. 715, Pl. 2, Figs.1, 4, 7

Synonym:

Thoracosphaera granifera, Fütterer, 1977, Pl. 2, Figs.1 - 12

Obliquipithonella granifera, Kohring, 1993*a*, p. 71, Pl. 40, Figs.a - f

Orthopithonella granifera, Keupp and Kohring, 1993, p. 29 - 30, Pl. 2, Figs.9 - 15

Emended diagnosis

Epitheca and hypotheca rounded. Epitheca equal in size with hypotheca. Motile stages with plate tabulation pattern po, x, 4', 3a, 7", 6c (t + 5c), 6s, 5"', 2"". Non-motile calcareous stages (cysts) are spherical with one calcareous layer which consists of numerous elements. Elements are very tiny, primarily tetraedrical coalescing crystals. Crystals of the calcareous cyst wall layer are orientated with their crystallographic optic axis (c-axis) radial to the cyst surface. The small operculum is circular and includes apical plates.

Emenda diagnosis

Cellula motilis epithecam et hypothecam rotundam habet. Epitheca et hypotheca magnitudine adaequant. Cellulae motiliter formula laminarum po, x, 4', 3a, 7", 6c (t + 5c), 6s, 5"', 2"" habent. Cellulae non-motiliter (cystae) calcariae sphaeroideae unum corium habent. Corium compositum est ex multi elementis calcariis. Elementa minuta proprie quattuor latera habent et coniuncta sunt. Cristalla corii calcarii de axe optico (c-axis) radialiter ad superficiem cystae directa sunt. Operculum parvum orbiculatum est et laminas apicales adaequat.

Description

Motile stage: The vegetative cells are rounded, with a mean length of 14 µm (range 13 - 17 µm) and a mean width of 11.5 µm (range 10.5 - 13 µm). The epitheca and the hypotheca are rounded; they are nearly equal in length (Pl.2, Fig.15; p. 113). The cingulum is about 3 µm wide and displaced about half a girdle width (Pl.2, Fig.16; p. 113). The large nucleus is located to the posterior part of the cell; the living motile cells are light brown in colour (Pl.4, Fig.45; p. 122).

Plate tabulation (Fig.14): The plate tabulation formula is po, x, 4', 3a, 7", 6c (t + 5c), 6s, 5"', 2"". The thecal plates are very delicate and are difficult to obtain even by the critical point preparation process. The surface of the thecal plates is smooth with few small pores scattered over their surface. In the pre- and post-cingular plates the pores line the edges along the cingulum (Pl.2, Figs.16, 17; p. 113).

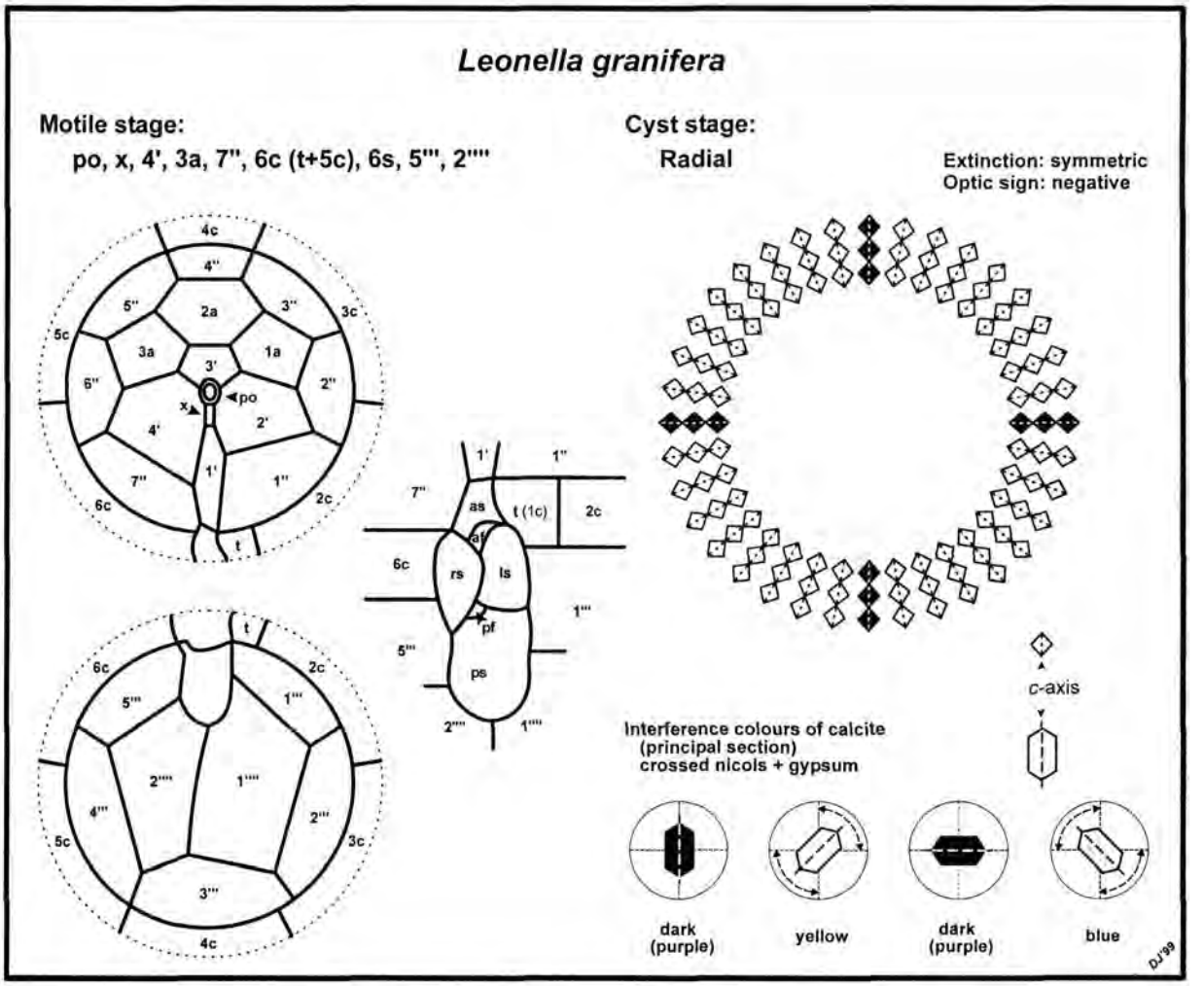

Fig.14: Schematic diagram of the characteristic morphological features of *Leonella granifera* n. gen. For abbreviations see text.

The pore plate (po) is nearly circular and surrounded by a low elevated rim (Pl.2, Fig.18, arrow; p. 113). The canal plate (x) is rectangular and located ventrally, just anterior to the 1' plate. Plate 1' is narrow in width (about 2 μm) and shows an ortho configuration. The 2' - 4' plates are all irregularly polygonal because their shortest edges are contacting the pore plate (po). The plates 2' and 4' are larger than plate 3'. In the intercalary series, plates 1a and 3a are pentagonal and nearly equal in size and plate 2a is large and hexagonal. The largest plate in the precingular series is 1". Plates 2", 3", 5", 6" and 7" are pentagonal but the plates 1" and 4" are trapezoid.

The cingular series consists of six plates of which 2c – 6c are about equal in size, but 1c (= transitional plate t) is much smaller (Pl.2, Fig.16; p. 113). The two sutures between 3c and 4c and between 4c and 5c are located dorsally (Pl.2, Fig.17; p. 113).

The sulcus is ventral and extends into the hypotheca. It consists of six plates: an anterior sulcal (as), a left sulcal (ls), a right sulcal (rs), a posterior sulcal (ps), an anterior flagellar pore plate (af) and a posterior flagellar pore plate (pf) (Fig.14; Pl.2, Fig.16; p. 113). The anterior sulcal (as) adjoining 7", 1', t, af and rs, is trapezoid with an extension inserted between af and t. The suture between 1' and 1" contacts the suture between as and t. The right sulcal (rs) is rhombic in shape and in touch with the cingular plate 6c, 5"', ps and as. It overlaps af, ls and pf. The large left sulcal (ls) (Pl.2, Figs.16, 20; p. 113) is ellipsoid in shape and in touch with ps, 1"', t, af and pf. The posterior sulcal (ps) is the largest sulcal plate and is bordered by 5"', 2"", 1"", 1"', ls, pf and rs. The anterior flagellar pore plate (af) is located between as and ls and is slightly overlapped by rs. The posterior flagellar pore plate (pf) is located between ps and ls and is mostly overlapped by rs. The transversal flagellum emerges in an opening between af and rs, the longitudinal flagellum emerges where pf is overlapped by rs.

In the postcingular series, plates 1"', 2"' and 4"' are rectangular but 3"' is pentagonal (Pl.2, Fig.17; p. 113). Plate 5"' is also pentagonal with the shortest edge in touch with the right sulcal (rs). The two antapical plates 1"" and 2"" are pentagonal and of approximately equal size. The dorsal border of 2"" is shorter than the dorsal border of 1"" (Pl.2, Figs.17, 19; p. 113).

Cyst stage: The calcareous cysts are spherical with a mean diameter of 22 µm (range 18 - 27 µm). The cyst wall has a mean thickness of 1.8 µm (range 1.2 - 2.5 µm) and consists of one layer of numerous tiny calcite crystals. The crystals are primarily tetraedrical with a mean size of 0.1 µm and appear on the cyst surface arranged in rows which in turn form more or less triangular clusters (Pl.2, Fig.26; p. 113). Vertically the crystals can form irregular columns (Pl.2, Figs.23, 26: arrow; p. 113); the porosity of the calcareous cyst wall layer is estimated with 50 % (App.2). Mineralisation obviously takes place in clusters which can be seen in less mineralized specimens (Pl.2, Fig.23; p. 113). This ultrastructure can give the cyst a undulated surface. (Pl.2, Fig.26; p. 113). All crystals are coalesced with each other and form a very solid cyst wall layer despite the high porosity.

Each tiny crystal is orientated with its crystallographic optic axis (c-axis) exactly radial to the cyst surface (Fig.14). The optic signs can be seen clearly in polarised light where the cyst shows a sharp symmetric extinction cross (Pl.4, Fig.47; p. 122). Using an accessory filter

(gypsum plate), the resulting interference colours show yellow colours in the first and the third quadrant and blue colours in the second and fourth quadrant (Fig.14; Pl.4, Figs.47 - 49; p. 122; Janofske, 1996) indicated by a strictly radial orientation of the c-axes. Focusing on the surface of the cyst, the fine-grained ultrastructure of the cyst is visible (Pl.4, Fig.48; p. 122).

The small operculum is circular and has a mean diameter of 7 µm (range 5 - 10 µm). Paratabulation patterns are not recognizable.

Living cysts are dark brown in colour; a red accumulation body was not observed. The living cyst is surrounded by a thin organic layer (Pl.2, Figs.21 - 23; p. 113) which shows intense light blue fluorescence when stained with Calcofluor indicating cellulose, carboxylated polysaccharides or callose as material (Hughes and McCully, 1975). Cysts found in sediments are always without any organic residues (Pl.2, Figs.25, 26; p. 113).

The calcareous cyst stage is obviously the dominant life stage of *L. granifera*. After inoculation of the culture at first the number of calcareous cyst stages is increasing. Not until the culture ages, more and more motile stages are visible particularly 2 to 3 hours after the beginning of the light photoperiod. Indication for sexual reproduction during the life cycle such as the fusion of gametes or planozygotes were not observed; the encystment process could not be connected to a sexual phase in the life cycle of *L. granifera*. The living cysts show intense red colours in epi-fluorescence caused by the autofluorescence of chlorophyll *a*.

The cysts produced in cultures are generally larger and have thicker calcareous walls than those found in the sediment (App.2). The average weight of cysts described from the sediment (Fütterer, 1977) was calculated to 1.8 ng (without operculum), those produced in cultures have a mean weight of 3.1 ng (without operculum).

Stratigraphic range: Oligocene (Keupp and Kohring, 1994) to Recent

Record: The cyst of *Leonella granifera* is known from fossil strata of the Atlantic Ocean (Fütterer, 1977) and the Mediterranean area (Keupp and Kohring, 1993; Kohring, 1993a, 1993b; Keupp et al., 1994; Keupp and Kohring, 1994; Kohring, 1997) and from recent sediments of the Atlantic Ocean (Karwath, 1995; Kerntopf, 1997; Höll et al., 1997; Höll et al., 1999) and the Arabian Sea (Gulf of Aden: M31-3, unpubl. observ.). The cyst of *L. granifera* was described from plankton samples of the equatorial Atlantic Ocean (Kerntopf, 1997) and from sediment trap material of the Atlantic and the Pacific Ocean (Dale, 1992).

Discussion

Leonella granifera was first described as *Thoracosphaera granifera* from fossil strata of the equatorial South Atlantic Ocean (DSDP Leg 41, Site 366, Pliocene/Pleistocene, Fütterer, 1977). Interpreting crystal morphology as being equivalent to crystallographic orientation, Kohring (1993a) wrongly named this species *Obliquipithonella granifera* but corrected it later to *Orthopithonella granifera* (Keupp and Kohring, 1993).

The extant genus *Thoracosphaera* is characterised by a tangential crystallographic orientation of the calcareous crystals (Kamptner, 1967), the fossil genus *Obliquipithonella* by an oblique crystallographic orientation (Keupp and Mutterlose, 1984) and the fossil genus *Orthopithonella* is characterised by radial crystallographic orientation with paratabulation pattern reflected by the archeopyle/operculum (typespecies *Orthopithonella gustafsoni* Keupp and Mutterlose, 1984). Until now a taxon of calcareous dinoflagellate cysts with radial crystallographic orientation of the calcareous crystals and a small operculum without any paratabulation pattern was not described from fossil or recent strata. Therefore we propose *Leonella* as a new genus with so far only one species *Leonella granifera* n. gen.

Plate 2: SEM micrographs of *Leonella granifera* n. gen.

Fig.15: Theca: ventral view. Strain GeoB 38. - CPD. Scale bar 3 µm.

Fig.16: Theca: sulcal area. Strain GeoB 38. - CPD. Scale bar 1 µm.

Fig.17: Theca: dorsal view. Strain GeoB 38. - CPD. Scale bar 5 µm.

Fig.18: Theca: apical view. Note the apical pore complex (arrow) Strain GeoB 38. - CPD. Scale bar 3 µm.

Fig.19: Theca: antapical view. Strain GeoB 38. - CPD. Scale bar 3 µm.

Fig.20: Theca: hypotheca. Strain GeoB 38. - CPD. Scale bar 3 µm.

Fig.21: Calcareous cyst. Strain GeoB 38. - HMDL. Scale bar 3 µm.

Fig.22: Archeopyle and attached operculum of calcareous cyst. Strain GeoB 132. - HMDL. Scale bar 5 µm.

Fig.23: Detail of a less mineralized calcareous cyst from culture. Strain GeoB 132. - HMDL. Scale bar 2 µm.

Fig.24: Cyst stage and motile stage. Strain GeoB 38. - CPD. Scale bar 5 µm.

Fig.25: Calcareous cyst from sediment. M 20/1, 1608-9/0-1 cm - Air-dried. Scale bar 5 µm.

Fig.26: Detail of calcareous cyst from sediment. M 20/1, 1608-9/0-1 cm. - Air-dried. Scale bar 2 µm.

Plate 2

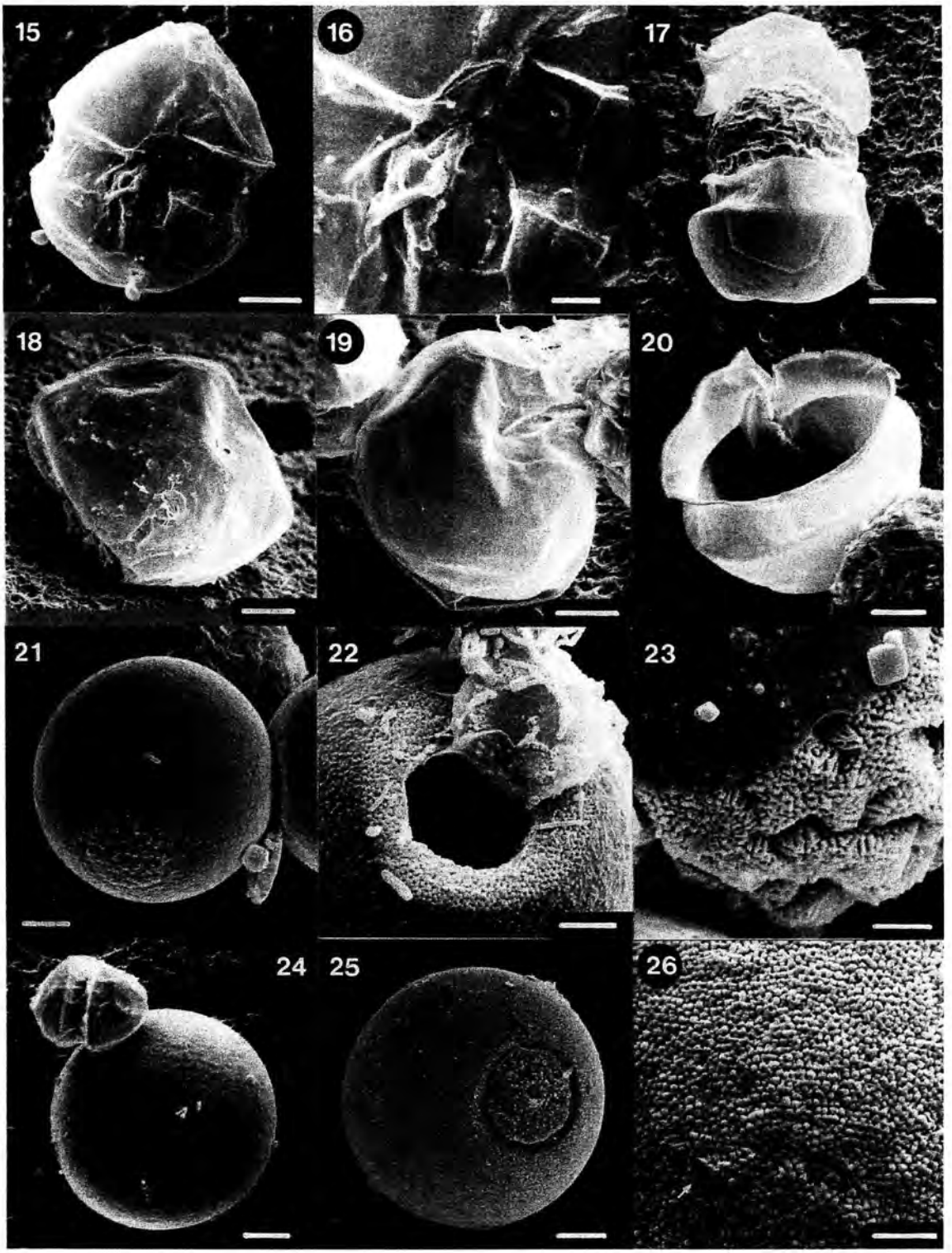

Genus *Pernambugia* n. gen.

Diagnosis

Calciodinelloid dinoflagellate. Motile stages with plate tabulation pattern po, x, 4', 3a, 7", 5c (t + 4c), 6s, 5"', 2''''. Non-motile stages (cysts) have a single calcareous wall layer. Crystals of the calcareous cyst wall layer are orientated with their crystallographic optic axis (c-axis) irregularly oblique to the cyst surface. The operculum includes apical and intercalary plates.

Diagnosis

Dinoflagellatum calciodinelloideum. Cellulae motiliter formula laminarum po, x, 4', 3a, 7", 5c (t + 4c), 6s, 5"', 2'''' habent. Cellulae non-motiliter (cystae) unum corium calcarium habent. Cristalla corii calcarii de axe optico (c-axis) incomposite obliquiter ad superficiem cystae directa sunt. Operculum laminas apicales et intercalares adaequat.

Type species: *Pernambugia tuberosa* (Kamptner 1963) n. gen.

Derivatio nominis: Pernambugo Abyssal Plain, off Brazil, Atlantic Ocean (source area of strains of the type species *P. tuberosa*)

***Pernambugia tuberosa* (Kamptner 1963) n. gen.**

Fig.27; Pl.3, Figs.28 – 39 (p. 120); Pl.4, Figs. 50 – 54 (p. 122).

Basionym: *Thoracosphaera tuberosa* Kamptner, 1963, p. 179 - 180, Pl. 4, Fig.26

Synonym:

Thoracosphaera tuberosa, Kamptner, 1963, p. 179 - 180, Pl. 4, Fig.26

Thoracosphaera candora, Kamptner, 1967, p. 157; Pl. 17, Figs.100, 102, Pl. 18, Figs.105, 106

Thoracosphaera narena, Kamptner, 1967, p. 158, Pl. 15, Figs.96, 97, Pl. 16, Figs.98, 99, Pl. 16, Figs.101, 103

Thoracosphaera sp. 3, Fütterer, 1977, p. 717, Pl. 8, Figs.3, 6

Sphaerodinella tuberosa, Keupp and Versteegh, 1989, p. 209 - 210

Emended diagnosis

Epitheca slightly conical with a small apical horn, hypotheca rounded. Epitheca equal in size with hypotheca. Motile stages with plate tabulation pattern po, x, 4', 3a, 7", 5c (t + 4c), 6s, 5"', 2''''. Non-motile calcareous stages (cysts) are spherical with one calcareous layer

which consists of numerous elements. Elements are large and rhomboedric or bulky in shape. Crystals of the calcareous cyst wall layer are orientated with their crystallographic optic axis (c-axis) irregularly oblique to the cyst surface. The operculum includes apical and intercalary plates and comprises two fifth of the cyst.

Emenda diagnosis

Cellula motilis epithecam paululum conicam cum cornu apicali humili et hypothecam rotundam habet. Epitheca et hypotheca magnitudine adaequant. Cellulae motiliter formula laminarum po, x, 4', 3a, 7", 5c (t + 4c), 6s, 5"', 2"" habent. Cellulae non-motiliter (cystae) calcariae sphaeroideae unum corium habent. Corium compositum est ex multi elementis calcariis magnis, formam comparabilis rhombum vel truncum habent. Cristalla corii calcarii de axe optico (c-axis) incomposite obliquiter ad superficiem cystae directa sunt. Operculum laminas apicales et intercalares adaequat et duplex quinta pars cystae est.

Description

Motile stage: The vegetative cells are rounded, with a mean length of 15.5 µm (range 13 - 18 µm) and a mean width of 12 µm (range 10.5 - 15 µm). The epitheca is slightly conical with a small apical horn and the hypotheca is rounded. Epi- and hypotheca are nearly equal in length (Pl.3, Figs.28, 30; p. 120; Pl.4, Fig.50; p. 122). The cingulum is about 3 µm wide and displaced about half a girdle width (Pl.3, Fig.29; p. 120). The large nucleus is located in the central part of the cell; the living motile cells are light brown in colour (Pl.4, Fig.50; p. 122).

Plate tabulation (Fig.27): The plate tabulation formula is po, x, 4', 3a, 7", 5c (t + 4c), 6s, 5"', 2"". The thecal plates are thin and smooth with few small pores scattered over their surface. In the pre- and post-cingular plates the pores line the edges along the cingulum (Pl.3, Figs.29, 31; p. 120).

The pore plate (po) is nearly circular and surrounded by a low elevated rim (Pl.3, Figs.28, 30; p. 120). The canal plate (x) is pentagonal in shape with an arrow-like angle pointing towards the pore plate (po). Plate 1' is medium in width (about 2.6 µm) and shows an ortho configuration. The 2' - 4' plates are all irregularly polygonal because their shortest edges are in contact with the pore plate (po). The plates 2' and 4' are larger than plate 3'. In the intercalary series, plates 1a and 3a are pentagonal and nearly equal in size. Plate 2a is large and hexagonal. In the precingular series, the largest plates are 1" and 7". Plates 2", 3", 5", 6" and 7" are pentagonal but the plates 1" and 4" are trapezoid.

The cingular series consists of five plates of which 3c – 5c are about equal in size, but 2c and especially 1c (= transitional plate t) are smaller (Pl.3, Fig.29; p. 120). The suture between 3c and 4c is located dorsally nearly equivalent to the suture between 3" and 4" (Pl.3, Fig.30; p. 120). The suture between 4c and 5c is located lateral and is in contact to the cingular border of plate 6" (Pl.3, Fig.31; p. 120).

The sulcus is ventral and extends into the hypotheca. It consists of six plates: an anterior sulcal (as), a left sulcal (ls), a right sulcal (rs), a posterior sulcal (ps), an anterior flagellar pore plate (af) and a posterior flagellar pore plate (pf) (Figs.27; Pl.3, Fig.29; p. 120). The anterior sulcal (as) adjoins 7", 1', t, af and rs; it is trapezoid with extensions inserted between rs and af and between af and t. The right sulcal (rs) is rhombic in shape and in touch with the cingular plate 5c, 5"', ps and as. It overlaps af, ls and pf. The left sulcal (ls) is ellipsoid in shape and is in touch with ps, t, af and pf. The posterior sulcal (ps) is the largest sulcal plate and is bordered by 5"', 2"", 1"", 1"', ls, pf and rs. The contact of ps with 1"' is a long extension which ends in a contact to the cingular plate t. The anterior flagellar pore plate (af) is located between as, t and ls and is slightly overlapped by rs. The posterior flagellar pore plate (pf) is located between ps and ls and is mostly overlapped by rs. The transversal flagellum emerges in an opening between af and rs, the longitudinal flagellum emerges where pf is overlapped by rs.

In the postcingular series, plates 1"', 2"' and 4"' are rectangular, 3"' is pentagonal and plate 5"' is pentagonal with the shortest edge in touch with the right sulcal (rs). The two antapical plates 1"" and 2"" are pentagonal and of approximately equal size (Pl.3, Fig.32; p. 120).

Cyst stage: The calcareous cysts are spherical with a mean diameter of 27 µm (range 19.5 - 32.5 µm). The cyst wall has a mean thickness of 3.2 µm (range 2.4 - 4.5 µm) and consists of one layer of large calcite crystals. The crystals are generally rhomboedric in shape (Pl.3, Figs.34 – 36, 39; p. 120) but they are mostly incomplete, often hollow rhomboedrons (skeletal crystals). Morphotypes with triradiate grooved crystals (Pl.3, Fig.37; p. 120) or with plate-like crystals occur (Pl.3, Fig.28; p. 120). Top and edges of the calcareous elements at the outer surface are smooth (Pl.3, Figs.34, 35; p. 120). The calcareous elements are loosely attached but coalescing to form a solid cyst wall layer; the porosity of the calcareous cyst wall layer is estimated with 33,3 % (App.2).

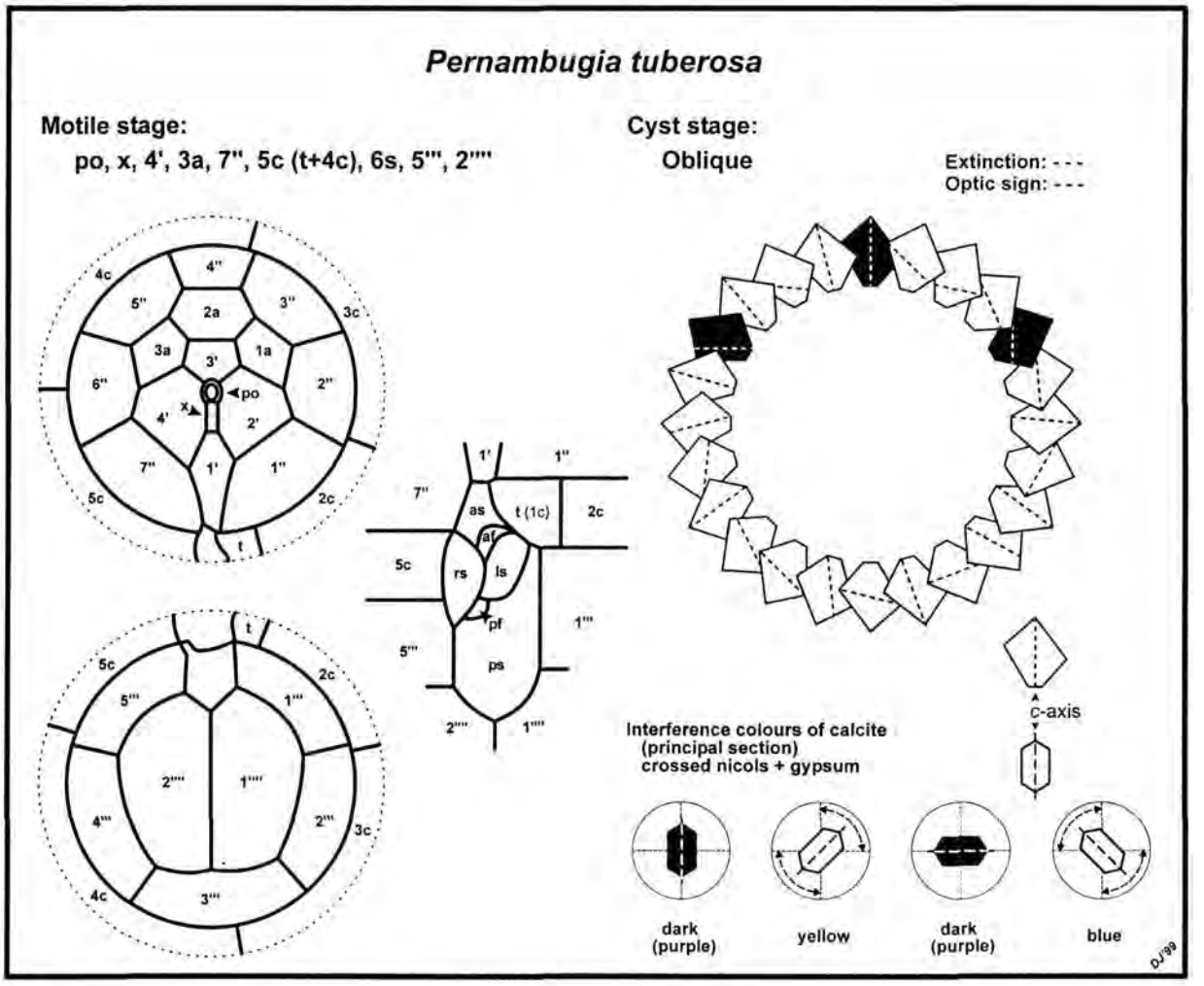

Fig.27: Schematic diagram of the characteristic morphological features of *Pernambugia tuberosa* n. gen. For abbreviations see text.

The crystallographic optic axes (c-axis) of the calcareous elements are arranged irregularly oblique to the cyst surface (Fig.27). Whole cysts in LM observation have the yellow-green colors produced by overlapping of optic signs and calcite crystals thicker than 5 µm (Pl.4, Figs.52, 53; p. 122). The optic signs can be seen clearly only in thin sections in polarised light with accessory filter (gypsum plate), when the calcareous elements each show their individual optic sign (Pl.4, Fig.54; p. 122) (Janofske, 1996). Focusing on the surface of the cyst, the rhomboedric morphology of the crystals becomes visible; optic signs are not distinguishable because of the thickness of the calcareous elements (Pl.4, Fig.53; p. 122).

The very large operculum is circular and comprises about 2/5 of the cyst (Pl.3, Figs.34, 37, 38; p. 120). Paratabulation patterns are not recognizable.

Living cysts are dark brown in colour with a large red accumulation body (Pl.4, Figs.50 - 53; p. 122). The living cyst is surrounded by a thin organic layer (Pl.3, Figs.37, 38; p. 120). A continuous organic layer can be found at the inner surface of the cyst even after the excystment process (Pl.3, Figs.35, 36; p. 120). Organic material is visible as (mucus?) threads between the crystals (Pl.3, Figs.34 - 36; p. 120). Cysts found in sediments are always without any organic residues (Pl.3, Fig.39; p. 120).

Cyst production occurs immediately after inoculation of the culture. In the beginning the motile stages and the cyst stages are equal in number, in aged cultures the calcareous cysts stages are dominant. Indication for sexual reproduction during the life cycle such as the fusion of gametes or planozygotes were not observed; the encystment process could not be connected to a sexual phase in the life cycle of *P. tuberosa*. The living cysts show intense red colours in epi-fluorescence caused by the autofluorescence of chlorophyll *a*.

The cysts produced in cultures are generally larger and have thicker calcareous walls than those found in the sediment (App.2). The average weight of cysts described from the sediment (Kamptner, 1967, Fütterer, 1977) was calculated to 4.2 ng (without operculum), those produced in cultures have a mean weight of 7.1 ng (without operculum).

Stratigraphic range: Pleistocene (Kamptner, 1963; Fütterer, 1977) to Recent

Record: Cysts of *Pernambugia tuberosa* are known from fossil strata of the equatorial Pacific Ocean (Kamptner, 1963) and the Atlantic Ocean (*Thoracosphaera* sp. 3, Fütterer, 1977) as well as from recent sediments of the Atlantic Ocean (as *Thoracosphaera candora*, *Thoracosphaera narena* in Kamptner, 1967; "*Sphaerodinella*" *tuberosa* in Karwath, 1995: Pl. 1, Fig.G - H, pl. 3, Fig.E - H, Pl. 4, Fig.D, E - F, Pl. 5, Fig.A - D and in Kerntopf, 1997: Pl. 28, Fig.5 - 8, Pl. 29, Fig.1 - 2, 5 - 6). The cyst of *P. tuberosa* was observed in sediment trap material of the Pacific Ocean (Dale, 1992: pl. 1.3, Fig.13 - 16, 18 - 19).

Discussion

Pernambugia tuberosa n. gen. was first described as *Thoracosphaera tuberosa* from fossil strata of the equatorial Pacific Ocean (ST 61/562,0 - 563,5, Middle Pleistocene, Kamptner, 1963). The holotype was described as "... a third part of a sphere ..." and is a single operculum. The holotype has a circular outline with a diameter of 28 µm and a wall thickness

of 3.3 µm (Kamptner, 1963) just like the specimen from culture GeoB*61 (Fig.36), which is 27 µm in diameter with a wall thickness of 3.2 µm. *Thoracosphaera candora* and *Thoracosphaera narena* (Kamptner, 1967) obtained from surface sediments of the equatorial Atlantic Ocean are considered to be specimens of *P. tuberosa*, too (Fütterer, 1976). SEM observations showed an orthogonal ultrastructure of the calcareous crystals which implied a radial orientation of the crystallographic c-axis. Based on these observations *Sphaerodinella tuberosa* (Keupp and Versteegh, 1989) was established. Lightmicroscopic analysis confirmed the oblique orientation of the c-axes to the cyst surface (Kamptner, 1967; Janofske, 1996).

The plate formula of *Pernambugia tuberosa* fits the plate formula of the genus *Pentapharsodinium* Indelicato et Loeblich 1986 emend Montresor 1993 but differs concerning the number, morphology and arrangement of the sulcal plates and the position of the suture between 3c and 4c which in *P. tuberosa* is not in the middle of the dorsal part of the cell (Montresor et al., 1993). The genus *Thoracosphaera* is characterised by a tangential crystallographic orientation of the calcareous crystals (Kamptner, 1967). Until now a dinoflagellate taxon with calcareous cysts showing irregularly oblique crystallographic orientation of the calcareous crystals and a large operculum without any paratabulation pattern was not described from fossil or recent strata. Therefore the new genus *Pernambugia* is proposed with so far only one species *Pernambugia tuberosa* n. gen.

The specimens with rhomboedric-orthogonal ultrastructure, a large angular archeopyle which reflects paratabulation pattern and a tangential crystallographic orientation which were described as *Thoracosphaera tuberosa* (Fütterer, 1976; Fütterer, 1977; Dale, 1992: Pl. 1.3, Fig.17), as *Sphaerodinella tuberosa* (Keupp and Versteegh, 1989: Pl. I, Figs.10, 13; Keupp et al., 1991; Kohring, 1993*a*: Pl. 10, Figs.g - p, Pl. 41, Figs e - g) and as *"Sphaerodinella" tuberosa* (Karwath, 1995: Pl. 3, Figs.A - H, Pl. 4, Figs.A - C; Kerntopf, 1997: Pl. 27, Figs.1 - 6, Pl. 28, Figs.1 - 4, Pl. 29, Figs.7, 8; Janofske, 1996: Pl. I, Fig.3; Höll et al., 1997; Höll et al., 1999) are not *P. tuberosa*, but a yet undescribed species of the genus *Calciodinellum*.

Plate 3

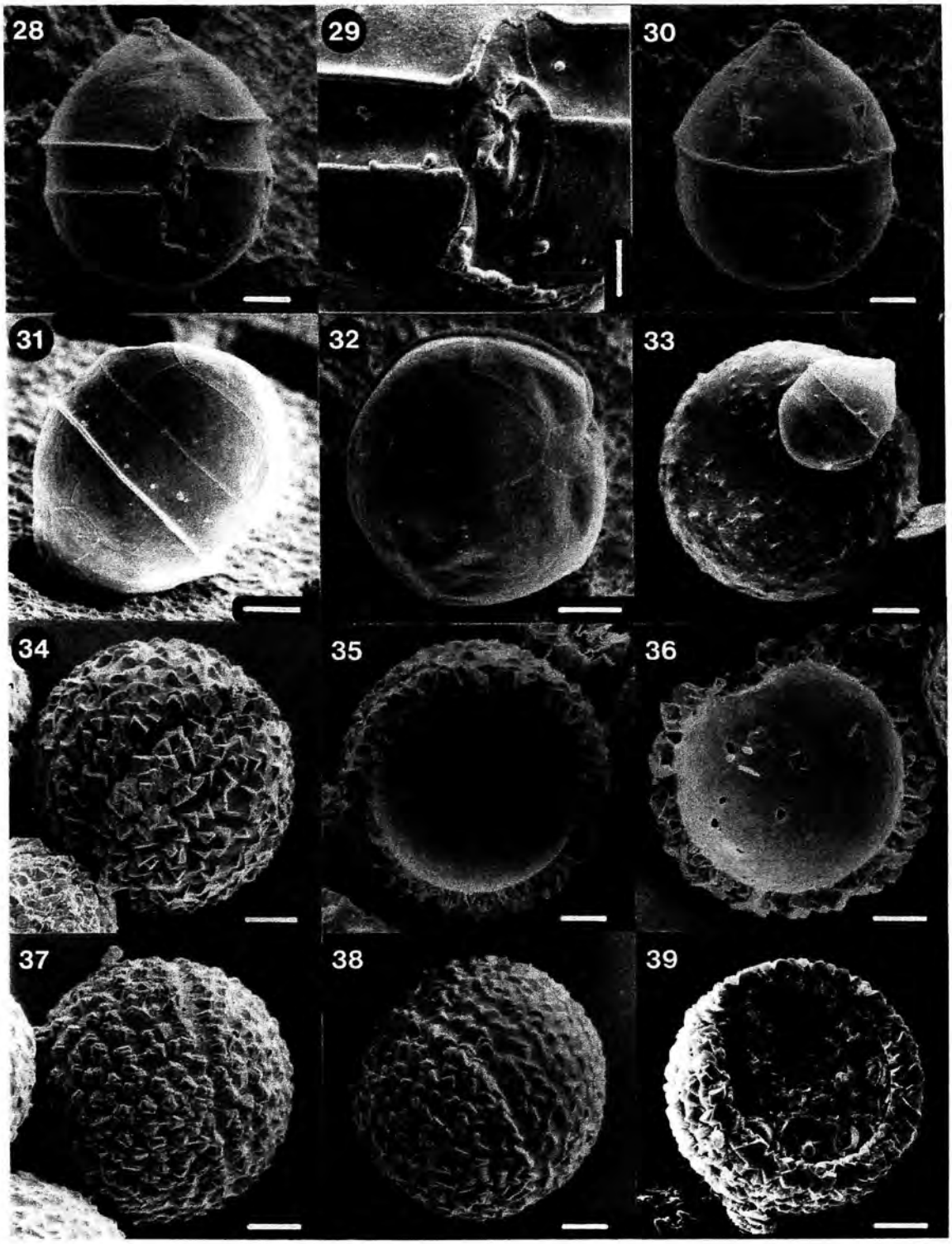

Plate 3: SEM micrographs of *Pernambugia tuberosa* n. gen.

Fig.28: Theca: ventral view. Strain GeoB*61. - CPD. Scale bar 3 µm.

Fig.29: Theca: sulcal area. Strain GeoB*61. - CPD. Scale bar 2 µm.

Fig.30: Theca: dorsal view. Strain GeoB*61. - CPD. Scale bar 3 µm.

Fig.31: Theca: lateral view. Strain GeoB*61. - CPD. Scale bar 3 µm.

Fig.32: Theca: antapical view. Strain GeoB*61. - CPD. Scale bar 3 µm.

Fig.33: Cyst stage and motile stage. Strain GeoB*61. - CPD. Scale bar 5 µm.

Fig.34: Calcareous cyst, rhomboedric-orthogonal morphotype. Strain GeoB*61. - HMDL. Scale bar 5 µm.

Fig.35: Empty calcareous cyst. Strain GeoB*61. - HMDL. Scale bar 5 µm.

Fig.36: Operculum. Strain GeoB*61. - HMDL. Scale bar 5 µm.

Fig.37: Calcareous cyst, morphotype with grooved crystals. Strain GeoB*61. - HMDL. Scale bar 5 µm.

Fig.38: Calcareous cyst, morphotype with plate-like crystals. Strain GeoB*61. - HMDL. Scale bar 5 µm.

Fig.39: Calcareous cyst from sediment. Challenger 338 - Air-dried. Scale bar 5 µm.

Ecology

For a first investigation of both the horizontal and vertical distribution of the cyst stages of *Calciodinellum albatrosianum*, *Leonella granifera* and *Pernambugia tuberosa*, plankton samples were taken from the upper water column of the equatorial and tropical Atlantic Ocean (water depths 10 - 200 m) during the cruise M41-4 (May/June 1998) of *RV Meteor* (App.3). Four sites in the western Atlantic Ocean off Brazil represent oligotrophic conditions; six sites in the eastern Atlantic Ocean off Africa are influenced by upwelling conditions. A detailed description of the oceanographic situation is given in Karwath et al. (2000). The plankton samples were checked for calcareous dinoflagellates; the number of empty cysts and of cysts with cell content were counted using LM with polarization and epifluorescence equipment according to Karwath et al. (2000). Only one site was found void of the three cyst species (WET11, SST 28.2°C). Throughout the samples the measured salinity data show only insignificant variation (range 34.9 to 36.9 psu).

C. albatrosianum cysts occur at all sites except WET11 and at all depths down to 200 m. Living specimens or rather cysts with cell content were present down to 175 m within a temperature range from 13 to 29°C and a salinity range from 34.9 to 36.8 psu; associations with 100 % cysts with cell content are found in depths of 75 m, 100 m and 175 m in the west and from 10 m to 50 m in the east. Maximum abundances of living cysts are present in the

Plate 4

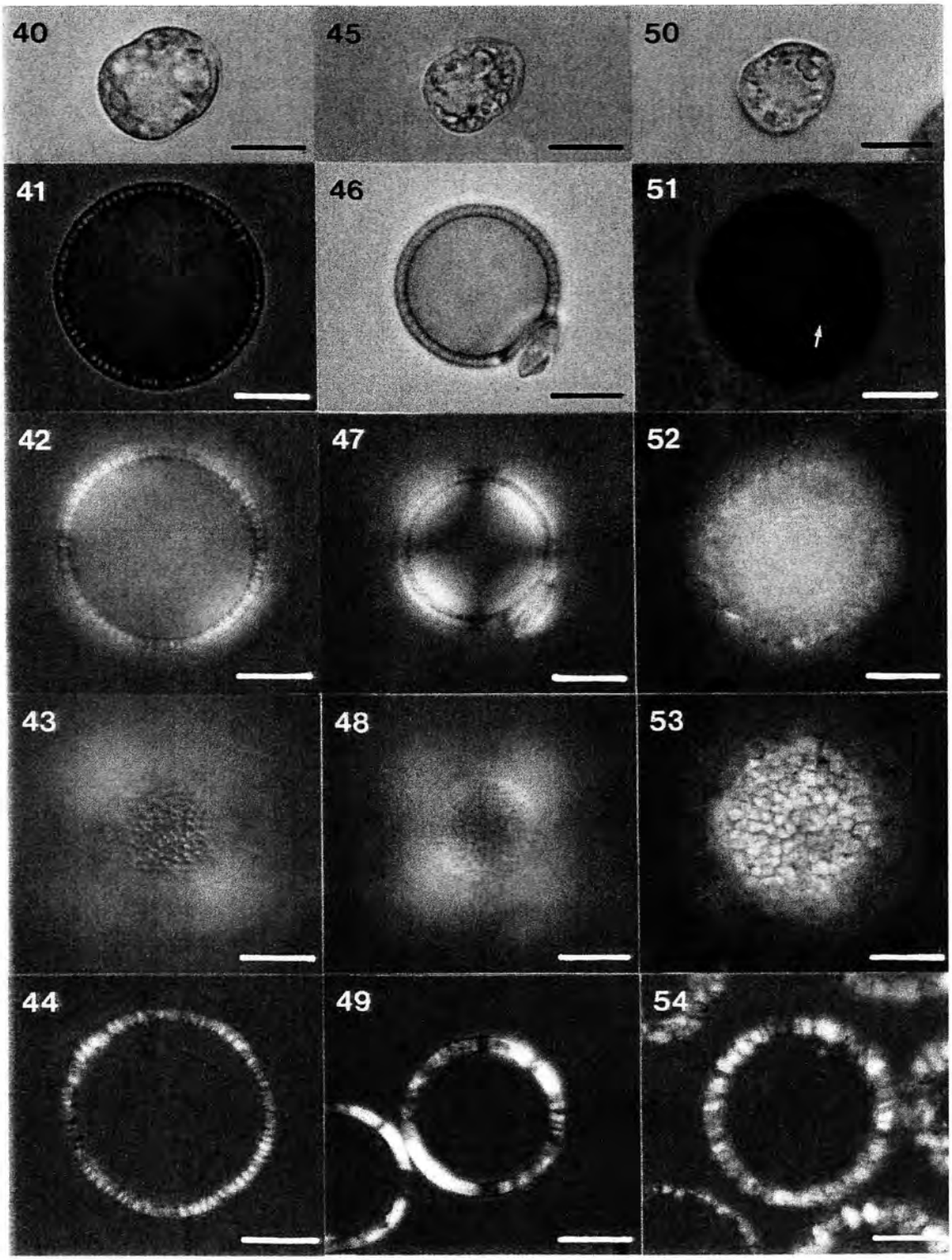

Plate 4: LM micrographs. All figures equal magnification, scale bars represent 10 µm.

Fig.40 – 44: *Calciodinellum albatrosianum* n. comb.

Fig.40: Motile stage. Strain M 34-*26/4.

Fig.41: Cyst stage, empty. Strain M34-*26/5.

Fig.42: Cyst stage: cross-section. Strain M34-*26/5. Same specimen as Fig. 41. - Polarised light and gypsum plate.

Fig.43: Cyst stage: surface. Strain M34-*26/5. Same specimen as Fig. 41. - Polarised light and gypsum plate.

Fig.45: Cyst stage: thin section. Strain M34-*26/5. - Polarised light and gypsum plate.

Fig.45 – 49: *Leonella granifera* n. gen.

Fig.45: Motile stage. Strain GeoB 38.

Fig.46: Cyst stage, empty with attached operculum. Strain GeoB 39.

Fig.47: Cyst stage: cross-section. Strain GeoB 39. Same specimen as Fig. 41. - Polarised light and gypsum plate.

Fig.48: Cyst stage: surface. Strain GeoB 39. Same specimen as Fig. 41. - Polarised light and gypsum plate.

Fig.49: Cyst stage: thin section. Strain GeoB 38. - Polarised light and gypsum plate.

Fig.50 – 54: *Pernambugia tuberosa* n. gen

Fig.50: Motile stage. Strain GeoB*61.

Fig.51: Cyst stage. Strain GeoB*61. Note the red accumulation body (arrow).

Fig.52: Cyst stage: cross-section. Strain GeoB*61. Same specimen as Fig. 41. - Polarised light and gypsum plate.

Fig.53: Cyst stage: surface. Strain GeoB*61. Same specimen as Fig. 41. - Polarised light and gypsum plate.

Fig.54: Cyst stage: thin section. Strain GeoB*61. - Polarised light and gypsum plate.

west (WET14: 175 m/13°C) and in the east (EET18: 10 m/28.6°C + 75 m/16.9°C) (App.3; Fig.55).

L. granifera cysts occur at all sites except WET11 and at all depths down to 200 m. Cysts with cell content were present from 10 m to 150 m depth within a temperature range from 13 to 28.7°C and a salinity range from 34.9 to 36.9 psu; associations with 100 % cysts with cell content are found in depth from 10 m to 50 m. Maximum abundances of living cysts are found in the west (WET12: 100 m/24.7°C), in the equatorial eastern part (EET16: 20 m/24°C) as well as north of the Cape Verde Islands (CB 20: 75 m/21.5°C) (App.3; Fig.56).

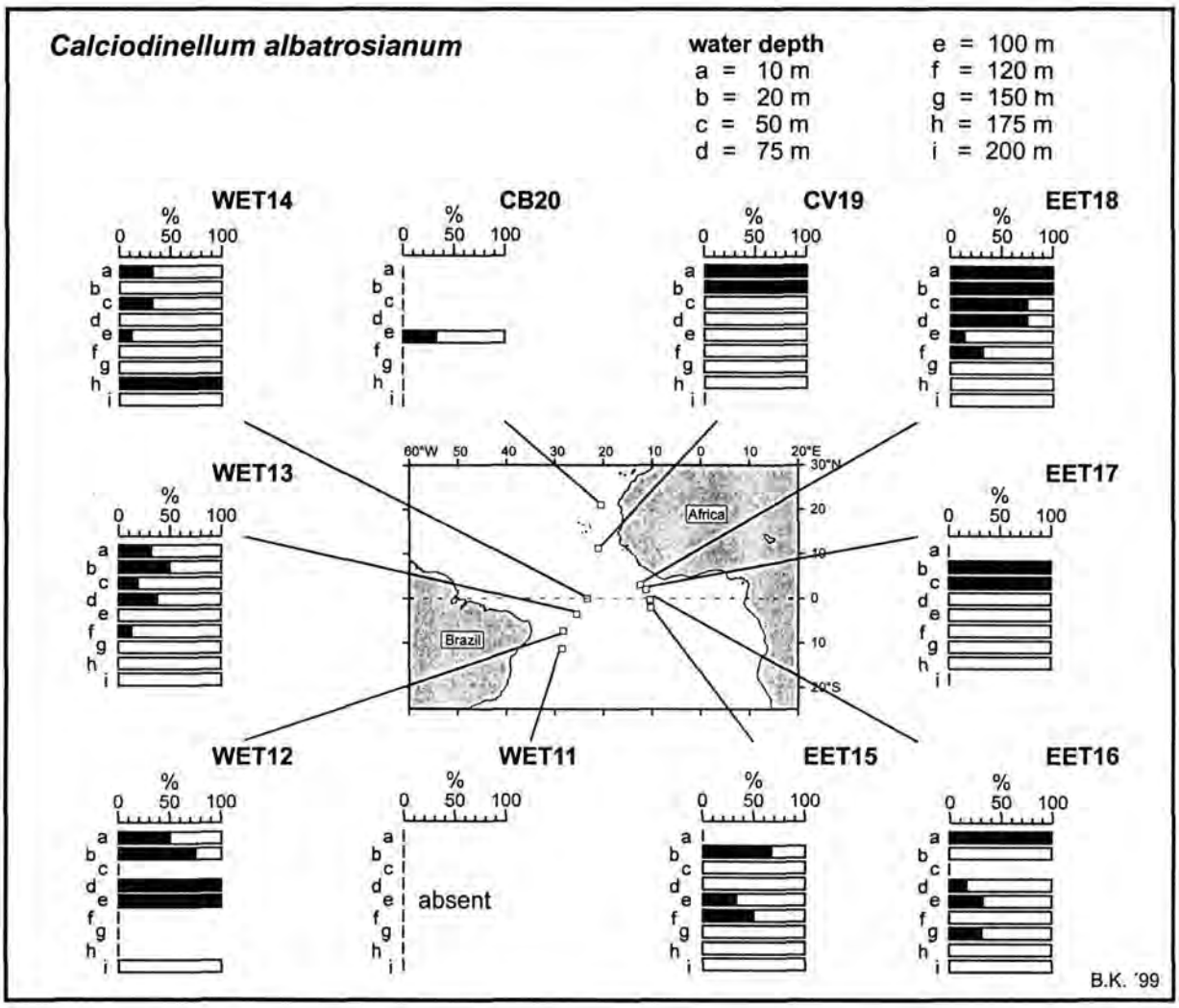

Fig.55: Distribution of *Calciodinellum albatrosianum* cyst stages in the water column, cruise M41-4, May/June 1998. Open bars show total content of cysts, black bars indicate cysts with cell content.

P. tuberosa cysts were found only at four sites. Cysts with cell content occur at two sites; one in the west off Brazil (WET12: 50 m/28.7°C + 100 m/24.7°C) and one in the east off Africa (EET16: 150 m/13.7°C) (App.3; Fig.57).

Discussion

Extensive studies on plankton sample material from the Atlantic Ocean have proved that the "calcispheres" - calcareous spherical hollow biogenic particles - which were described before from fossil and recent sediments as *Thoracosphaera albatrosiana* Kamptner, *Thoracosphaera granifera* Fütterer and *Thoracosphaera tuberosa* Kamptner, are indeed the cyst stages of dinoflagellates as assumed earlier (Fütterer, 1976). The morphological features of both the cellulosic theca and the calcareous cyst led to revision in taxonomy with

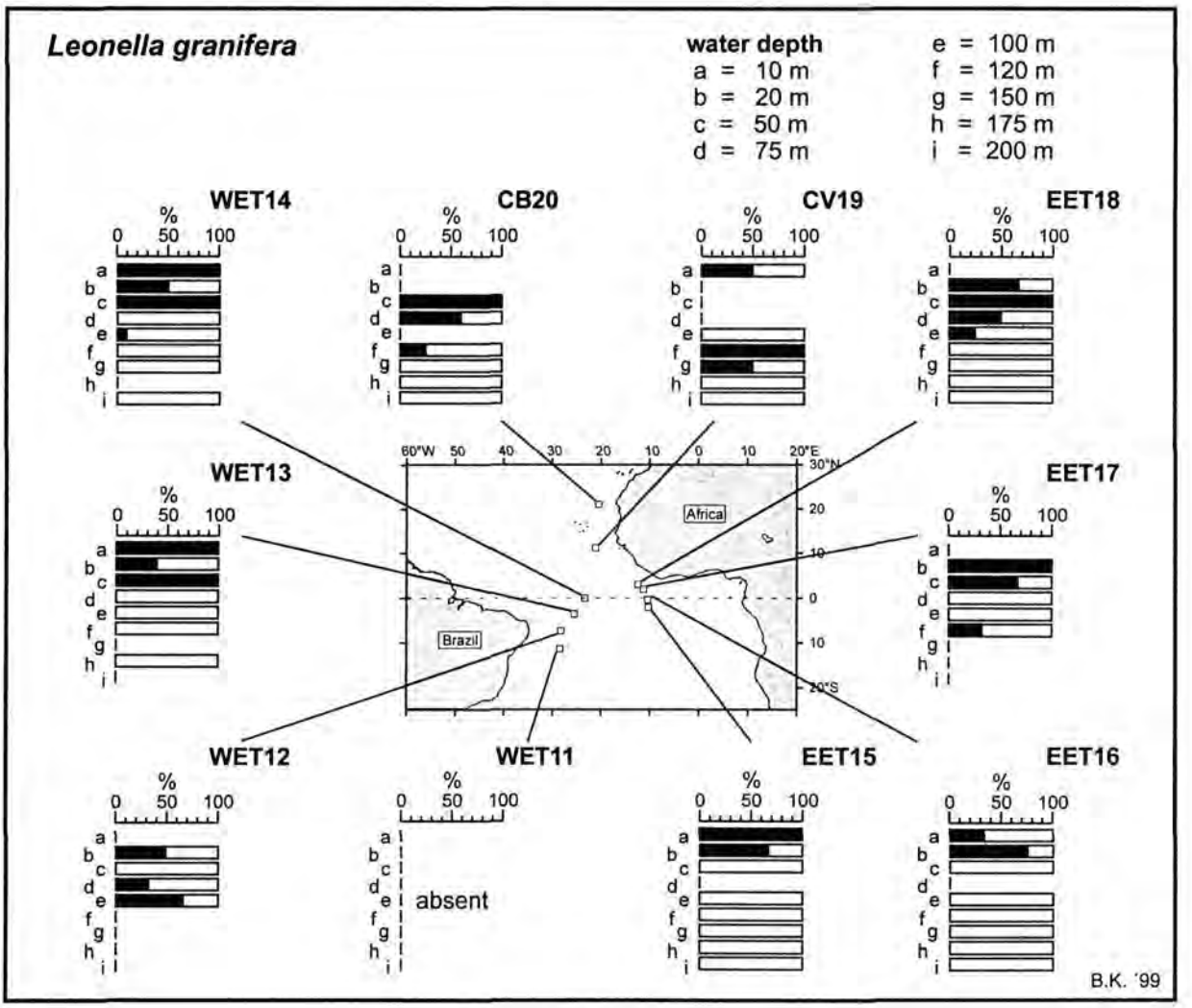

Fig.56: Distribution of *Leonella granifera* cyst stages in the water column, cruise M41-4, May/June 1998. For legend see Fig.55.

description of two new genera and the emendation of the taxa as follows: *Calciodinellum albatrosianum* (Kamptner) n. comb., *Leonella granifera* (Fütterer) n. gen. and *Pernambugia tuberosa* (Kamptner) n. gen.

The life cycle of the three species includes a small motile stage with a cellulosic theca and a larger non-motile cyst stage with a calcareous wall. The motile stages of the three species are very similar in size and shape and show only slight variation in sulcal and cingular plate arrangements. The spherical calcareous cyst equivalents differ remarkably concerning morphological and crystallographic ultrastructure of the calcite crystals, the size of the archeopyle and the existence of paratabulation patterns. In fact, the classification of the motile stages is difficult without detailed morphological studies, but the cysts are easily distinguished by their optical characters in the LM (Figs.40 - 54).

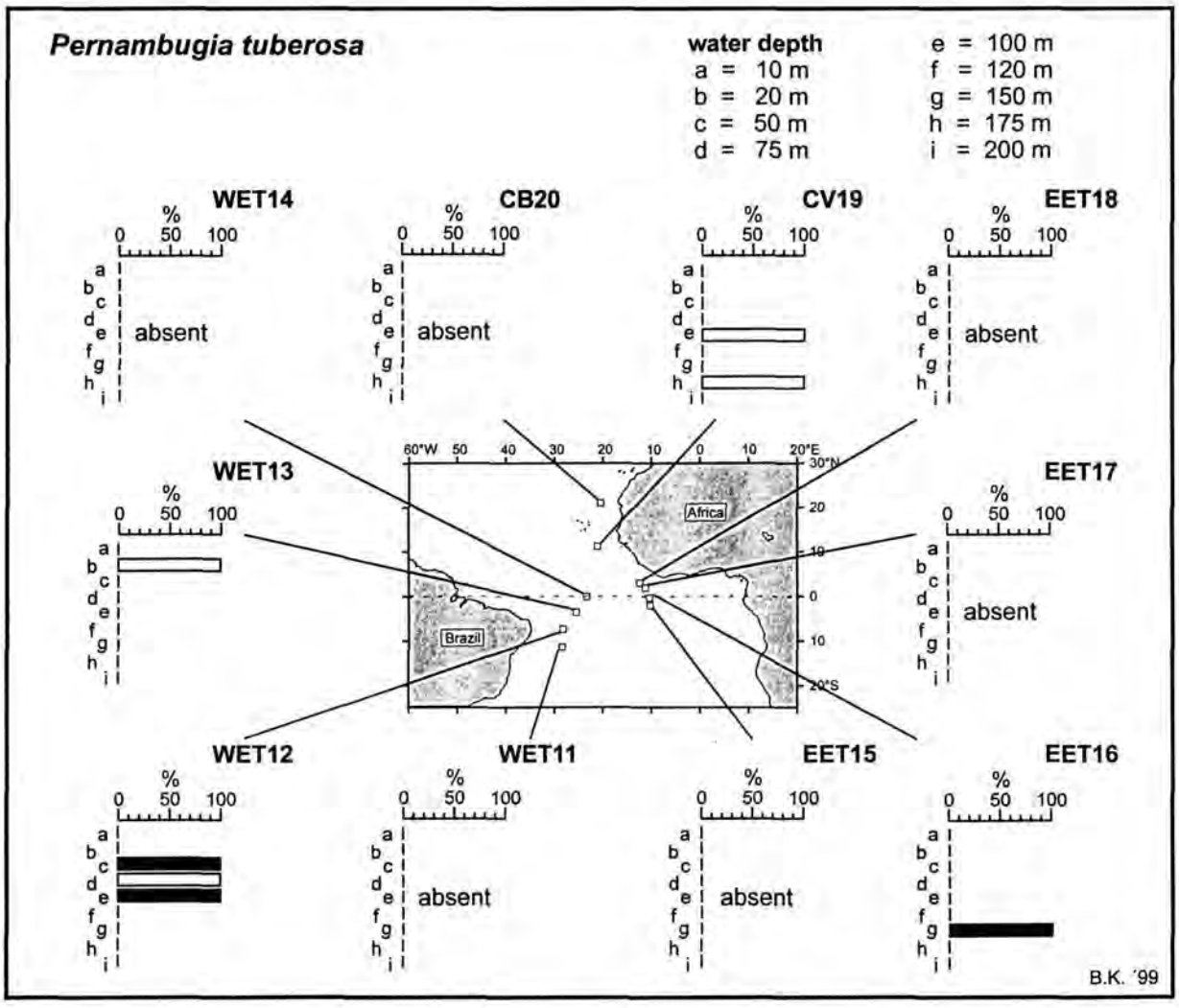

Fig.57: Distribution of *Pernambugia tuberosa* cyst stages in the water column, cruise M41-4, May/June 1998. For legend see Fig.55.

In cultures the cysts are produced constantly and may form 50 % or more of the living specimens of a culture (*C. albatrosianum*, *P. tuberosa*) or are even the dominant stage during the life cycle (*L. granifera*). The cyst stages are generally larger than the motile stages (Figs.7, 24, 33) and show the intense red autofluorescence of chlorophyll *a*, too. Since the calcareous cyst stages could not be connected to a sexual reproduction phase in the life cycle of these oceanic dinoflagellate species, they are definitely not hypnozygotes or resting cysts. Nevertheless, the calcareous cyst stage is obviously of importance for the organism which is expressed by the evolution of complex calcareous skeletal arrangements. A strictly tangential orientation of the crystal lattices to the cyst surface together with strictly radial orientation around the pores in case of *C. albatrosianum* or a strictly radial crystallographic orientation of countless tiny crystals in case of *L. granifera* are not formed by chance but indicate specific biomineralization processes. Biomineralization of calcareous skeletal elements is generally

regarded as a complex metabolic process which is induced and controlled by the organism (Addadi et al., 1990, Heuer et al., 1992). Morphological and crystallographic characters of skeletal elements are regarded as genetically fixed and are essential data for studies on taxonomy and phylogeny. Therefore the morphological and crystallographic ultrastructure of the calcareous layer of the cyst wall were the main focus for the description of the taxa.

From neritic environments the three species were never recorded. However, plankton samples, sediment trap material and surface sediment samples from oceanic tropical-subtropical environments are rich in (skeletal remains of) calcareous dinoflagellates (Dale, 1992, Kerntopf, 1997); apart from *Thoracosphaera heimii* the cysts of *C. albatrosianum*, *L. granifera* and *P. tuberosa* are characteristic components of these associations. Using the average weight data calculated in this study (App.2) the calcareous dinoflagellates contribute up to 1 % to the dry sediment (GeoB 2204-2, 295 cm: Höll et al., 1999).

In the upper water column of the equatorial and tropical Atlantic Ocean *C. albatrosianum* is the most abundant species, *L. granifera* is a widespread but rare species and *P. tuberosa* was found in larger numbers only in surface waters off Brazil (App.3, Figs.55, 56, 57). Sediment data show similar distribution patterns (Kerntopf, 1997; Höll et al., 1999); *P. tuberosa* was recorded in larger quantities only from a sediment core off Brazil (Karwath, 1995) and from a surface sediment sample in the central South Atlantic Ocean east of the Mid-Atlantic Ridge (Challenger 338, Kamptner, 1967).

The cysts of *C. albatrosianum*, *L. granifera* and *P. tuberosa* were found earlier to be present in subtropical-tropical surface water samples of the Atlantic Ocean connected with SST >24°C ("warm water cysts", Kerntopf, 1997). SST at all sites of M41-4 were >22°C (App.3) but cysts with cell content were present even in greater depth with temperatures of 13°C. Interestingly enough maximum abundances of living *C. albatrosianum* cysts were found at 175 m depth with 13°C as well as at 10 m depth with 28.6°C. Calcareous cysts with cell content were found within a temperature range from 13 to 29°C. Approximately one third of the plankton samples with living cysts derived from depths with temperatures <20°C. The distribution of the "warm water cyst" species is obviously controlled not by temperature alone but the oceanographic conditions which produce and maintain high SST.

Since throughout the samples the measured salinity data show only insignificant variation (range 34.9 to 36.9 psu), distribution patterns connected to salinity data could not be recognised. In culture, the calcareous dinoflagellates prefer low irradiance conditions (90 $\mu E \cdot m^{-2} \cdot s^{-1}$) so they should to be able to survive even in deeper water layers. Maximum abundances of calcareous dinoflagellate cysts with cell content were observed in the western

Atlantic Ocean off Brazil with oligotrophic conditions as well as in the eastern Atlantic Ocean off Africa which are influenced by upwelling conditions. Oceanic calcareous dinoflagellates such as *Calciodinellum albatrosianum*, *Leonella granifera* and *Pernambugia tuberosa* are obviously a group of organisms which are well adapted to a wide range of life conditions in the open ocean.

Acknowledgements

These studies could not have been done without the continuous support of Prof. Helmut Willems facilitating the work in the field and in the laboratory at the University of Bremen. Thanks are due to all the participants of the cruises on board of *RV Meteor* for sampling and isolation of dinoflagellates, Monika Kirsch for careful maintenance of the cultures in Bremen, Angelika Freesemann and Sebastian Meier for excellent preparation of the material and Mark Koehler, Nicole Zatloukal and Anja Meyer for the photographic work. Sediment sample material (Challenger 338) was provided by Jeremy R. Young (The Natural History Museum, London).

Field work was carried out within the scope of the SFB 261 "The South Atlantic in the Late Quaternary: Reconstruction of Material Budget and Current Systems" at the Department of Geoscience/University of Bremen. This research was supported by the Deutsche Forschungsgemeinschaft (Wi 725/7) and the University of Bremen (FNK 05/818/6).

References

Addadi, L., Berman, A., Moradian-Oldak, J. and Weiner, S., 1990. Tuning of Crystal Nucleation and Growth by Proteins: Molecular Interactions at Solid-Liquid Interfaces in Biomineralization. *Croat. Chem. Acta*, 63: 539-544.

Anderson, D.M., Lively, J.J., Reardon, E.M. and Price, C.A., 1985. Sinking characteristics of dinoflagellate cysts. *Limnol. Oceanogr.*, 30: 1000-1009.

Baldwin, R., 1987. Dinoflagellate resting cysts isolated from sediments in Marlborough Sounds, New Zealand. N. Z. J. Mar. Freshwater Res., 21: 543-553.

Blanco, J., 1989a. Quistes de Dinoflagelados de las costas de Galicia. I. Dinoflagelados Gonyaulacoides. Scient. Mar., 53: 785-796.

Blanco, J., 1989b. Quistes de Dinoflagelados de las costas de Galicia. II. Dinoflagelados Peridinoides. Scient. Mar., 53: 797-812.

Blanco, J., 1989c. Quistes de Dinoflagelados de las costas de Galicia. III. Dinoflagelados Gymnodinioides. Scient. Mar., 53: 813-819.

Bolch, C.J., and Hallegraeff, G.M. 1990. Dinoflagellate Cysts in Recent Marine Sediments from Tasmania, Australia. Bot. Mar., 33: 173-192.

Dale, B., 1983. Dinoflagellate resting cysts: "benthic plankton". In: Fryxell, G.A., (ed.) Survival strategies of the algae, 69-144. Cambridge University Press, Cambridge.

Dale, B., 1992. Dinoflagellate Contributions to the Open Ocean Sediment Flux. Ocean Biocoen. Ser., 5: 1-31.

Dale, B. and Dale, A.L., 1992. Dinoflagellate contribution to the Deep Sea. Ocean Biocoen. Ser., 5: 76 pp.

Ellegaard, M., Christensen, N.F. and Moestrup, O., 1994. Dinoflagellate cysts from Recent Danish marine sediments. Eur. J. Phycol., 29: 183-194.

Evitt, W.R. and Davidson, S.E., 1964. Dinoflagellate studies. I. Dinoflagellate cysts and thecae. Stanford Univ. Publ. (Geol. Sci.), 10: 1-12.

Fensome, R.A., Taylor, F.J.R., Norris, G., Sarjeant, W.A.S., Wharton, D.I. and Williams, G.L., 1993. A classification of living and fossil dinoflagellates. Micropaleontology, spec. publ., 7: 351 pp.

Fritz, L. and Triemer, R.E., 1985. A rapid simple technique utilizing Calcofluor White M2R for the visualization of dinoflagellate thecal plates. J. Phycol., 21: 662-664.

Fütterer, D., 1976. Kalkige Dinoflagellaten ("Calciodinelloideae") und die systematische Stellung der Thoracosphaeroideae. N. Jb. Geol. Paläont. Abh., 151: 119-141.

Fütterer, D., 1977. Distribution of calcareous dinoflagellates in Cenozoic sediments of site 366, Eastern North Atlantic. In: Lancelot, Y. and Seibold et al., E., (eds.)Deep Sea Drilling Project: Initial Reports, 709-737.

Guillard, R.R.L. and Ryther, J.H., 1962. Studies on marine planktonic diatoms. I. Cyclotella nana Hustedt and Detonula confervacea (Cleve) Gran. Can. J. Microbiol., 8: 229-239.

Hallegraeff, G.M. and Bolch, C.J., 1992. Transport of diatom and dinoflagellate resting spores in ships' ballast water: implications for plankton biogeography and acquaculture. J. Plankton Res., 14: 1067-1084.

Head, M.J. 1996., Modern dinoflagellate cysts and their biological affinities. In Palynology: principles and applications. (Jansonius, J. and McGregor, D.C., editors), 1197-1248.

Heuer, A.H., Fink, D.J., Laraia, V.J., Arias, J.L., Calvert, P.D., Kendall, K., Messing, G.L., Blackwell, J., Rieke, P.C., Thompson, D.H., Wheeler, A.P., Veis, A. and Caplan, A.I., 1992. Innovative Material Processing Strategies: A Biomimetic Approach. Science, 255: 1098-1105.

Höll, C., Karwath, B., Rühlemann, C., Zonneveld, K.A.F. and Willems, H., 1999. Palaeoenvironmental information gained from calcareous dinoflagellates: the late Quaternary eastern and western tropical Atlantic Ocean in comparison. Palaeogeogr. Palaeoclimatol. Palaeoecol., 146: 147-164.

Höll, C., Zonneveld, K.A.F. and Willems, H., 1997. On the ecology of calcareous dinoflagellates: the Quaternary Eastern Equatorial Atlantic. Mar. Micropaleont., 33: 1-25.

Hughes, J. and McCully, M.E., 1975. The use of an optical brightener in the study of plant structure. Stain Technol., 50: 319-329.

Inouye, I. and Pienaar, R.N., 1983. Observations on the life cycle and microanatomy of Thoracosphaera heimii (Dinophyceae) with special reference to its systematic position. S. Afr. J. Bot., 2: 63-75.

Janofske, D., 1992. Kalkiges Nannoplankton, insbesondere Kalkige Dinoflagellaten-Zysten der alpinen Ober-Trias: Taxonomie, Biostratigraphie und Bedeutung für die Phylogenie der Peridiniales. Berliner geowiss. Abh., E, 4: 53 pp.

Janofske, D., 1996. Ultrastructure types in Recent "calcispheres". Bull. Inst. océanogr. Monaco, 14: 295-303.

Janofske, D. and Willems, H., subm.. *Scrippsiella trochoidea* and *Scrippsiella regalis* nov. comb. (Peridiniales, Dinophyceae) - a comparison. J. Phycol.,

Kamptner, E., 1963. Coccolithineen-Skelettreste aus Tiefseeablagerungen des Pazifischen Ozeans. Ann. Naturhist. Mus. Wien, 66: 139-204.

Kamptner, E., 1967. Kalkflagellaten-Skelettreste aus Tiefseeschlamm des Südatlantischen Ozeans. Ann. Naturhistor. Mus. Wien, 71: 117-198.

Karwath, B., 1995. Verteilung kalkiger Dinoflagellaten der letzten 170 000 Jahre im westlichen Brasil-Becken (Südatlantik, Kern GeoB 2204-2). Unpubl. Dipl.Arb., FB Gowissenschaften, Universität Bremen, 109 pp.

Karwath, B., Janofske, D. and Willems, H., 2000. Spatial distribution of the calcareous dinoflagellate Thoracosphaera heimii in the upper water column of the tropical and equatorial Atlantic Ocean. Int. Journ. Earth Sciences 88 (4): 668-679.

Keller, M.D., Selvin, R.C., Claus, W. and Guillard, R.R.L., 1987. Media for the culture of oceanic ultraphytoplankton. J. Phycol., 23: 633-638.

Kerntopf, B., 1997. Dinoflagellate distribution patterns and preservation in the Equatorial Atlantic and offshore North-West Africa. Ber. FB Geowiss. Univ. Bremen, 103: 136 pp.

Keupp, H., 1984. Revision der kalkigen Dinoflagellaten-Zysten G. DEFLANDRES, 1948. Pal. Z., 58: 9-31.

Keupp, H., Bellas, S.M., Frydas, D. and Kohring, R., 1994. Aghia Irini, ein Neogenprofil auf der Halbinsel Gramvoússa/NW-Kreta. Berliner geowiss. Abh., E 13: 469-481.

Keupp, H. and Kohring, R., 1993. Kalkige Dinoflagellatenzysten aus dem Obermiozän von El Mehdi (Algeria). Berliner geowiss. Abh., E 9: 25-43.

Keupp, H. and Kohring, R., 1994. Kalkige Dinoflagellaten-Zysten aus dem Rupelton (Mittel-Oligozän) des Mainzer Beckens und der Niederrheinischen Bucht. Mainzer geowiss. Abh., 23: 159-184.

Keupp, H., Monnet, B. and Kohring, R., 1991. Morphotaxa bei kalkigen Dinoflagellaten-Zysten und ihre problematische Systematisierung. Berliner geowiss. Abh., A 134: 161-185.

Keupp, H. and Mutterlose, J., (1984). Organismenverteilung in den D-Beds von Speeton (Unterkreide, England) unter besonderer Berücksichtigung der kalkigen Dinoflagellaten. Facies, 10: 153-178.

Keupp, H. and Versteegh, G., 1989. Ein neues systematisches Konzept für kalkige Dinoflagellaten-Zysten der Subfamilie Orthopithonelloideae Keupp 1987. Berliner geowiss. Abh., A 106: 207-219.

Kohring, R., 1993a. Kalkdinoflagellaten aus dem Mittel- und Obereozän von Jütland (Dänemark) und dem Pariser Becken (Frankreich) im Vergleich mit anderen Tertiär-Vorkommen. Berliner geowiss. Abh., E 6: 164 pp.

Kohring, R., 1993b. Kalkdinoflagellaten-Zysten aus dem unteren Pliozän von E-Sizilien. Berliner geowiss. Abh., E, 9: 15-23.

Kohring, R., 1997. Calcareous dinoflagellate cysts from the Blue Clay formation (Serravallian, Late Miocene) of the Maltese Islands. N. Jb. Geol. Paläont. Mh., 1977: 151-164.

Lewis, J., 1991. Cyst-theca Relationships in Scrippsiella (Dinophyceae) and Related orthoperidinoid Genera. Bot. mar., 34: 91-106.

Meier, S., 1999. Die kalkigen Dinoflagellaten-Zysten des Mittelmeeres (M 40/4): Analyse der Assoziationen und Verbreitung. Unpubl. Dipl.-Arb., FB Geowissenschaften, Universität Bremen, 53 pp.

Montresor, M., Janofske, D. and Willems, H., 1997. The cyst-theca relationship in Calciodinellum operosum emend. (Peridiniales, Dinophyceae) and a new approach for the study of calcareous cysts. J. Phycol., 33: 122-131.

Montresor, M., Zingone, A. and Marino, D., 1993. The calcareous resting cyst of Pentapharsodinium tyrrhenicum comb. nov. (Dinophyceae). J. Phycol., 29: 223-230.

Nation, J.L., 1983. A new method using Hexamethyldisilazane for preparation of soft insect tissues for scanning electron microscopy. Stain Technol., 58: 347-351.

Nehring, S., 1994. Spatial distribution of dinoflagellate resting cysts in recent sediments of Kiel Bight, Germany (Baltic Sea). Ophelia, 39: 137-158.

Nehring, S., 1995. Dinoflagellate resting cysts as factors in phytoplankton ecology of the North Sea. Helgol. Meeresunters., 49: 375-392.

Nesse, W.D., 1991. Introduction to Optical Mineralogy., 2nd. edition. Oxford University Press, New York.

Roberts, W.L., Rapp, G.R.J. and Weber, J., 1974. Encyclopedia of Minerals., Van Nostrand Reinhold, New York.

Sonneman, J.A. and Hill, D.R.A., 1997. A Taxonomic Survey of Cyst-producing Dinoflagellates from Recent Sediments of Victorian Coastal Waters. Bot. Mar., 40: 149-177.

Spurr, A.R., 1969. A low-viscosity epoxy-resin embedding medium for electron microscopy. J. Ultrastr. Res., 26: 31-43.

Tangen, K., Brand, L.E., Blackwelder, P.L. and Guillard, R.R.L., 1982. Thoracosphaera heimii (Lohmann) Kamptner is a dinophyte: observations on its morphology and life cycle. Mar. Micropaleont., 7: 193-212.

Wall, D., 1965. Modern hystrichospheres and dinoflagellate cysts from the Woods Hole region. Grana Palynol., 6: 297-314.

Wall, D. and Dale, B., 1966. "Living fossils" in western Atlantic Plankton. Nature, 211: 1025-1026.

Wall, D. and Dale, B., 1968a. Modern dinoflagellate cysts and evolution of the Peridiniales. Micropaleontology, 14: 265-304.

Wall, D. and Dale, B., 1968b. Quaternary calcareous dinoflagellates (Calciodinellideae) and their natural affinities. J. Paleont., 42: 1395-1408.

Wall, D., Guillard, R.R.L., Dale, B., Swift, E. and Watabe, N., 1970. Calcitic resting cysts in Peridinium trochoideum (Stein) Lemmermann, an autotrophic marine dinoflagellate. Phycologia, 9: 151-156.

Wefer, G., Beese, D., Berger, W.H., Buschhoff, H., Cepek, M., Diekamp, V., Fischer, G., Holmes, E., Kemle von Mücke, B., Kerntopf, B., Lange, C., Mulitza, S., Otto, S., Plugge, R., Ratmeyer, V., Rühlemann, C., Schmidt, W., Schwarze, M., Wallmann, K.

and Zabel, M., 1994. Report and preliminary results of Meteor Cruise M 23/3 Recife - Las Palmas, 21.3. - 12.4.93. Ber. FB Geowiss. Univ. Bremen, 44: 71 pp.

Young, J.R., 1998. Neogene. In: Bown, P.R., (ed.) Calcareous Nannofossil Biostratigraphy, 225-265. Chapman and Hall, London.

Appendix 1: Data of the strains of *Calciodinellum albatrosianum*, *Leonella granifera* and *Pernambugia tuberosa* at the Department of Geoscience at the University of Bremen (GeoB).

Strain No.	Locality	Temperature	Salinity	Water Depth	Cruise /Date
Calciodinellum albatrosianum					
M 34 -*12	30°31.4' S 40°11.3' W	24.2°C	33.69 psu	Surface water	M 34/3 8.3.96
M 34 - 17	00°00' 41°03.1' W	28.1°C	34.3 psu	Surface water	M 34/4 2.4.96
M 34 -*26/4 M 34 -*26/5	12°15.8' N 58°20.2' W	27.1°C	33.46 psu	Surface water	M 34/4 12.4.96
GeoB*31	11°28.9' N 21°01.0' W	24.5°C	35.5 psu	- 10 m	M 38/1: 4303-4 1.2.97
GeoB 34	08°30.06' N 32°27.33' W	26.2°C	no data	Surface water	M 38/1 4.2.97
GeoB*123	01°47.53' S 08°25.30' E	29.7°C	32.56 psu	Surface water	M 41/1 14.3.98
GeoB*144	00°12.74' S 23°36.21' W	26.7°C	36.04 psu	Surface water	M 41/4 26.5.98
GeoB 149	07°45.28' S 28°14.99' W	28.5°C	36.12 psu	Surface water	M 41/4 22.5.98
Leonella granifera					
GeoB 38	06°56.9' N 47°54.1' W	26.4°C	35.5 psu	Surface water	M 38/2 28.3.97
GeoB 39	08°42.3' N 51°49.5' W	26.3°C	35.2 psu	Surface water	M 38/2 29.3.97
GeoB*121	01°19.33' N 02°41.18' W	29.6°C	34.59 psu	Surface water	M 41/1 23.2.98
GeoB 132	02°4.31' S 08°37.63' E	22.9°C	32.5 psu	- 40 m	M 41/1: 4909-2 4.3.98
GeoB 145 GeoB 148	02°18.85' S 08°04.07' E	26.6°C	31.7 psu	- 20 m	M 41/1: 4910-1 4.3.98
Pernambugia tuberosa					
GeoB*61 GeoB*73 GeoB*74	11°32.2' S 28°34.5' W	27.6°C (SST)	no data	- 100 m	M 38/1: 4321-9 27.2.97
GeoB*136	18°36.31' S 34°26.90' W	no data	no data	Surface water	M 41/2 13.4.98
GeoB*146	11°44.71' S 30°0.25' W	26.9°C	33.6 psu	Surface water	M 41/4 20.5.98

Clonal cultures with asterisk (*).

Appendix 2: Average weight [ng] of oceanic calcareous dinoflagellates from sediment and culture material.

	Calciodinellum albatrosianum		*Pernambugia tuberosa*		*Leonella granifera*		*Thoracosphaera heimii*	
Source	Sediment *1, *2, *4	Culture	Sediment *2, *4	Culture	Sediment *4	Culture	Sediment *2, *3, *4	Culture *5, *6
Size [µm]	24.3	25.94	23.65	27.73	18.75	22.24	16.3	15
Wall thickness [µm]	2.1	1.5	2.86	3.53	1.5	1.8	1	1
Operculum	1/3	1/3	2/5	2/5	6.5 µm	7.12 µm	5.16 µm	6 µm
Porosity	33.3 %		33.3 %		50 %		25 %	
Average weight [ng] with operculum	5.9	5.1	7.1	11.8	1.9	3.2	1.5	1.25
Average weight [ng] without operculum	3.9	3.4	4.2	7.1	1.8	3.1	1.45	1.2

Measured density of calcite 2.7102 g/cm³ (Roberts *et al.*, 1974).

*1 - Kamptner, 1963
*2 - Kamptner, 1967

*3 - Fütterer, 1976
*4 - Fütterer, 1977

*5 - Tangen *et al.*, 1982
*6 - Inouye & Pienaar, 1983

Appendix 3: Calcareous dinoflagellate data of cruise M 41-4, May/June 1998; tot / 100 litres - total content of calcareous cysts calculated to 100 litres of seawater; wcc / 100 litres - calcareous cysts with cell content per 100 litres of seawater.

Station	Sample Depth [m	*C. albatrosianum* tot / 100 [L]	*C. albatrosianum* wcc /100 [L]	*P. tuberosa* tot / 100 [L]	*P. tuberosa* wcc /100 [L]	*L. granifera* tot / 100 [L]	*L. granifera* wcc /100 [L]	Temp. °C	Salinity psu
WET11	10	-	-	-	-	-	-	28.2	36.9
	20	-	-	-	-	-	-	28	36.9
	50	-	-	-	-	-	-	28	36.9
	75	-	-	-	-	-	-	28	36.9
	100	-	-	-	-	-	-	24	36.8
	120	-	-	-	-	-	-	23.1	36.7
	150	-	-	-	-	-	-	21.2	36.3
	175	-	-	-	-	-	-	18.8	36
	200	-	-	-	-	-	-	16.4	35.7
WET12	10	73	37	-	-	-	-	28.7	36
	20	40	30	-	-	20	10	28.7	36
	50	-	-	22	22	11	-	28.7	35.9
	75	10	10	10	-	60	20	28.5	36.6
	100	40	40	20	20	120	80	24.7	36.8
	120	-	-	-	-	-	-	22.4	36.6
	150	-	-	-	-	-	-	18.3	36
	175	-	-	-	-	-	-	14.7	35.9
	200	107	-	-	-	-	-	12.8	35.3
WET13	10	90	30	-	-	20	20	28.3	35.8
	20	40	20	10	-	50	20	28.3	35.8
	50	100	20	-	-	10	10	28.2	35.8
	75	111	42	-	-	28	-	23.2	36.6
	100	82	-	-	-	16	-	17.9	35.9
	120	73	9	-	-	9	-	15.2	35.6
	150	70	-	-	-	-	-	13	35.3
	175	24	-	-	-	24	-	12.6	35.2
	200	33	-	-	-	-	-	12.1	35.1
WET14	10	60	20	-	-	20	20	27	35.9
	20	13	-	-	-	26	13	27	35.9
	50	107	36	-	-	36	36	25.5	36.2
	75	50	-	-	-	10	-	20.9	36.3
	100	80	10	-	-	110	10	17.4	35.9
	120	40	-	-	-	40	-	15.7	35.7
	150	100	-	-	-	50	-	14.3	35.4
	175	164	164	-	-	-	-	13	35.2
	200	97	-	-	-	24	-	13	35.2
EET15	10	0	-	-	-	10	10	26.1	35.7
	20	60	40	-	-	30	20	25.9	35.7
	50	10	-	-	-	10	-	18	35.9
	75	10	-	-	-	-	-	15.2	35.5
	100	58	19	-	-	19	-	14.8	35.5
	120	20	10	-	-	20	-	14.5	35.4
	150	40	-	-	-	40	-	13.5	35.3
	175	10	-	-	-	10	-	13.3	35.3
	200	70	-	-	-	20	-	13	35.2

Station	Sample Depth [m	*C. albatrosianum* tot / 100 [L]	*C. albatrosianum* wcc /100 [L]	*P. tuberosa* tot / 100 [L]	*P. tuberosa* wcc /100 [L]	*L. granifera* tot / 100 [L]	*L. granifera* wcc /100 [L]	Temp. °C	Salinity psu
EET16	10	16	16	-	-	49	16	25.3	35.9
	20	51	-	-	-	101	76	24	36
	50	-	-	-	-	39	-	18	36
	75	60	10	-	-	-	-	15.3	35.6
	100	30	10	-	-	10	-	14.6	35.4
	120	20	-	-	-	20	-	14.4	35.4
	150	30	10	10	10	30	-	13.7	35.3
	175	10	-	-	-	30	-	13.7	35.3
	200	30	-	-	-	20	-	13.2	35.3
EET17	10	-	-	-	-	-	-	29	35
	20	10	10	-	-	10	10	29	35
	50	15	15	-	-	46	31	21.3	36
	75	30	-	-	-	30	-	16.5	35.6
	100	30	-	-	-	30	-	15.3	35.6
	120	30	-	-	-	30	10	15	35.5
	150	50	-	-	-	-	-	13.3	35.4
	175	10	-	-	-	-	-	14.1	35.4
	200	0	-	-	-	-	-	13.8	35.3
EET18	10	80	80	-	-	-	-	28.6	34.9
	20	20	20	-	-	30	20	28.6	34.9
	50	40	30	-	-	30	30	22.1	35.1
	75	80	60	-	-	60	30	16.9	35.7
	100	70	10	-	-	40	10	16	35.6
	120	30	10	-	-	10	-	15.5	35.6
	150	30	-	-	-	10	-	15.1	35.5
	175	30	-	-	-	30	-	14.7	35.4
	200	20	-	-	-	30	-	14.4	35.4
CV19	10	22	22	-	-	43	22	26.7	35.9
	20	44	44	-	-	-	-	26.5	35.9
	50	56	-	-	-	-	-	15	35.5
	75	43	-	-	-	-	-	14	35.4
	100	20	-	10	-	20	-	13.5	35.3
	120	20	-	-	-	10	10	13	35.3
	150	60	-	-	-	20	10	12.6	35.2
	175	40	-	10	-	10	-	12.3	35.2
	200	-	-	-	-	15	-	12	35.2
CB20	10	-	-	-	-	-	-	22.6	36.8
	20	-	-	-	-	-	-	22.5	36.7
	50	-	-	-	-	29	29	21.7	36.8
	75	-	-	-	-	135	81	21.5	36.7
	100	60	20	-	-	-	-	20.5	36.8
	120	-	-	-	-	40	10	20.5	36.9
	150	-	-	-	-	70	-	18	36.5
	175	-	-	-	-	40	-	16.2	36.1
	200	-	-	-	-	10	-	15.7	36.1

3.5

PALAEOENVIRONMENTAL INFORMATION GAINED FROM CALCAREOUS DINOFLAGELLATES: THE LATE QUATERNARY EASTERN AND WESTERN TROPICAL ATLANTIC OCEAN IN COMPARISON

(Palaeogeography, Palaeoclimatology, Palaeoecology 146: 147-164. 1999)

PALAEOENVIRONMENTAL INFORMATION GAINED FROM CALCAREOUS DINOFLAGELLATES: THE LATE QUATERNARY EASTERN AND WESTERN TROPICAL ATLANTIC OCEAN IN COMPARISON

Christine Höll[1], Britta Karwath[1], Carsten Rühlemann[2], Karin A. F. Zonneveld[1], Helmut Willems[1*],

[1] Historische Geologie/ Paläontologie, Fachbereich-5 Geowissenschaften, Universität Bremen, Postfach 330 440, 28334 Bremen, Germany. Fax: 0421/2184451

[2] Meeresgeologie, Fachbereich-5 Geowissenschaften, Universität Bremen, Postfach 330 440, 28334 Bremen, Germany

[*] e-mail corresponding author: willems@micropal.uni-bremen.de

Abstract

The environmental preferences of calcareous dinoflagellates have been investigated over the last 140 ka by comparing material from two sediment cores: one from the highly productive equatorial divergence of the eastern Atlantic Ocean and the other from the low productivity western tropical Atlantic Ocean. Pronounced differences in palaeoproductivity between the two sediment cores are indicated by high and variable organic carbon accumulation rates in the east, in contrast to relatively constant and low values in the west. Calcareous dinoflagellates show just the opposite pattern: high accumulation rates in the west and lower in the east. At the equatorial divergence, temporal variations of calcareous dinoflagellate and organic carbon accumulation rates show, for the most part, an inverse relationship. High calcareous dinoflagellate content coincides with low organic carbon accumulation rates and vice versa. In the investigated region and time interval, enhanced production of calcareous dinoflagellates can be correlated to periods of reduced palaeoproductivity probably related to relatively stratified conditions of the upper water column.

Keywords: Calcareous dinoflagellates, Tropical Atlantic Ocean, Palaeoenvironment, Late Quaternary

Introduction

Calcareous dinoflagellates are often neglected in micropaleontological investigations due to their size (on average: 16-26 µm in diameter); they are too small to be detected in foraminiferal studies and too large for nannoplankton investigations. Therefore, information about their (palaeo)environmental preferences is extremely limited. Dale (1992a, b) has shown that dinoflagellate cyst assemblages of the subtropical to tropical Atlantic and Pacific oceans are overwhelmingly dominated by calcareous forms, suggesting that they may form an important contribution to the oceanic carbon flux.

Cysts of organic-walled dinoflagellates have been frequently used to obtain palaeoenvironmental and palaeoceanographic information (e.g. Lewis et al., 1990; Matthiessen, 1991; de Vernal et al., 1992; Marret, 1994; Versteegh, 1995). To determine the usefulness of calcareous dinoflagellates to palaeoenvironmental investigations, it is important to study their environmental preferences. In one of the first studies on the palaeo-ecology of calcareous dinoflagellates, Höll et al. (1998) have demonstrated that higher values of calcareous dinoflagellates in Late Quaternary sediments of the eastern Equatorial Atlantic Ocean correlate with periods of reduced palaeoproductivity related to relatively stratified surface water conditions. Thus, higher calcareous dinoflagellate production may be expected in regions with oligotrophic surface water conditions. In order to validate this assumption, we compare the distribution patterns of the calcareous dinoflagellates from Core GeoB 2204-2, recovered from the oligotrophic western tropical Atlantic Ocean with those of Core GeoB 1105-4 derived from the highly productive divergence zone in the eastern equatorial Atlantic Ocean (Fig 1). Furthermore, the calcareous dinoflagellate data from both cores are related to the corresponding total organic carbon accumulation rate, which is used as a proxy for palaeoproductivity. Changes in accumulation rates of calcareous dinoflagellates are discussed in terms of palaeoproductivity and related factors.

Oceanographic setting of the tropical Atlantic Ocean

The upper-level current system of the tropical Atlantic Ocean is characterised by the broad westward flow of the South Equatorial Current (SEC; Fig.1). The SEC is divided by the South Equatorial Counter Current (SECC) into a main southern stream and a smaller, faster flowing northern stream. Off Brazil at about 10°S, the southern branch of the SEC splits into the southward flowing Brazil Current (BC) and the northward flowing North Brazil Current (NBC). The eastward-flowing Equatorial Undercurrent (EUC) originates in the western

Equatorial Atlantic Ocean to finally become a surface current near the African continent (Peterson and Stramma, 1991).

The mixed surface water layer in the tropical Atlantic Ocean deepens from east to west (Hastenrath and Merle, 1987). Surface waters of the western tropical Atlantic Ocean (Core GeoB 2204-2; 1) are characterised, in comparison to those of the eastern region (Core GeoB 1105-4), by lower productivity, higher sea surface temperatures (SST) and lower seasonality (e.g. Houghton, 1991). This east-west contrast covaries with annual changes in wind and current intensities.

In boreal summer, the SE-trade winds are most intensive and the Intertropical Convergence Zone (ITCZ) reaches its northernmost position (Philander and Pacanowsi, 1986). During this time the SEC speed is at a maximum, leading to enhanced divergence, which entrains nutrients into the surface waters supporting high productivity. Concurrently, thermocline depth and SST are at their annual minimum in the eastern tropical Atlantic Ocean. Strong westward advection leads to piling up of SEC water in the western tropical Atlantic Ocean and, therefore, weakens the EUC (Katz and Garzoli, 1982). As a result, the thermocline deepens in the western tropical region. Despite these annual oceanological changes, SST remains nearly constant throughout the year in this western region (Merle, 1983).

In boreal winter, when the SE-trade winds are weak, the SEC speed is at its minimum and part of the tropical surface water piled up in the west flows back to the east in form of countercurrents (Richardson and Reverdin, 1987). In the eastern tropical Atlantic Ocean, the divergence is at its minimum, resulting in a relatively stratified surface water layer with less bio-productivity. The thermocline is relatively deep and SST is at its annual maximum. The thermocline in the western part shallows during this season, but remains deeper than in the eastern tropical Atlantic Ocean (Hastenrath and Merle, 1987). The eastward flow of the EUC is at its seasonal maximum.

Beneath the mixed surface water layer, South Atlantic Central Water (SACW) and, below, Antarctic Intermediate Water (AAIW; extending from about 400m to 1000-1200 m water depth; Tomczak and Huges, 1980; Reid, 1989) flow to the north. The North Atlantic Deep Water (NADW) flows to the south, between AAIW and the northward flowing Antartic Bottom Water (AABW). In the present context, the transition zone between NADW and AABW is of special interest, as it marks the depth of the lysocline (Bickert and Wefer, 1996). Carbonates deposited below the lysocline undergo dissolution, whereas they are preserved above. In the western tropical Atlantic Ocean the transition zone between these two deep water masses is situated at a depth of about 4000 m, deepening to a water depth of 4700 to

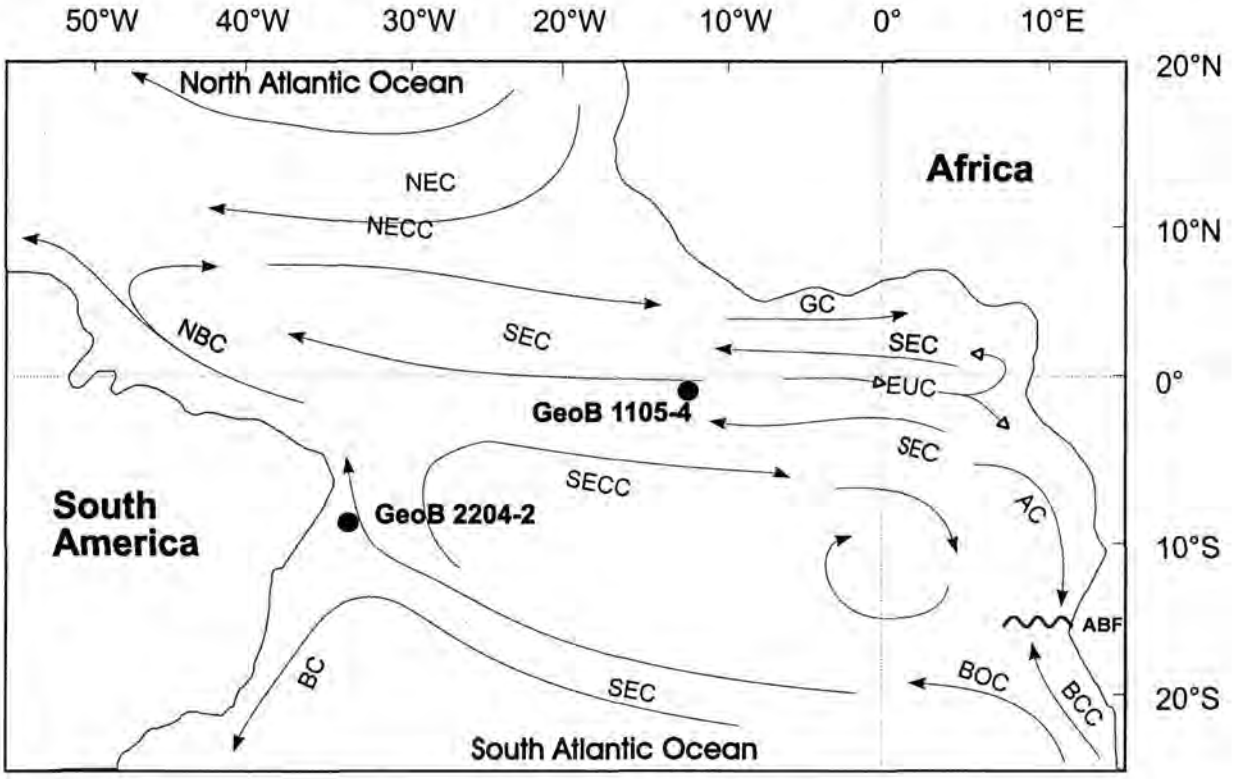

Fig.1: Position of cores GeoB 1105-4 and GeoB 2204-2 and schematic summary of sea surface currents of the tropical Atlantic Ocean (after Meinecke 1992, Schneider et al., 1996 and Rühlemann, 1996). NEC: North Equatorial Current; NECC: North Equatorial Counter Current; SEC: South Equatorial Current; SECC: South Equatorial Counter Current; EUC: Equatorial Under Current; GC: Guinea Current; AC: Angola Current; BCC: Benguela Coastal Current; BOC: Benguela Oceanic Current; BC: Brasil Current; NBC: North Brasil Current; ABF: Angola-Benguela Front. (Black arrows: surface currents; open arrows: Undercurrent).

4900 m in the eastern basins (Biscaye et al., 1976; Thunell, 1982; Fig.2). This asymmetry in bottom water extension was probably not present during glacial times, when the lysocline depth was reconstructed at 3800 m near the equator in both the eastern and western basins (Bickert and Wefer, 1996). Thus, both of our studied cores remained well above the lysocline.

Productivity variations in the Late Quaternary eastern and western tropical Atlantic Ocean

During the cold climatic periods of both, glacials and interglacials, reduced insolation intensity of the northern hemisphere may have weakened the SW-monsoon (Prell and Kutzbach, 1987), resulting in increased zonality of the SE-trade winds and thereby forcing an increase in SEC speed. This may have strengthened equatorial upwelling and seasonality and lowered SST in the eastern tropical Atlantic Ocean (Mix et al., 1986; McIntyre et al., 1989).

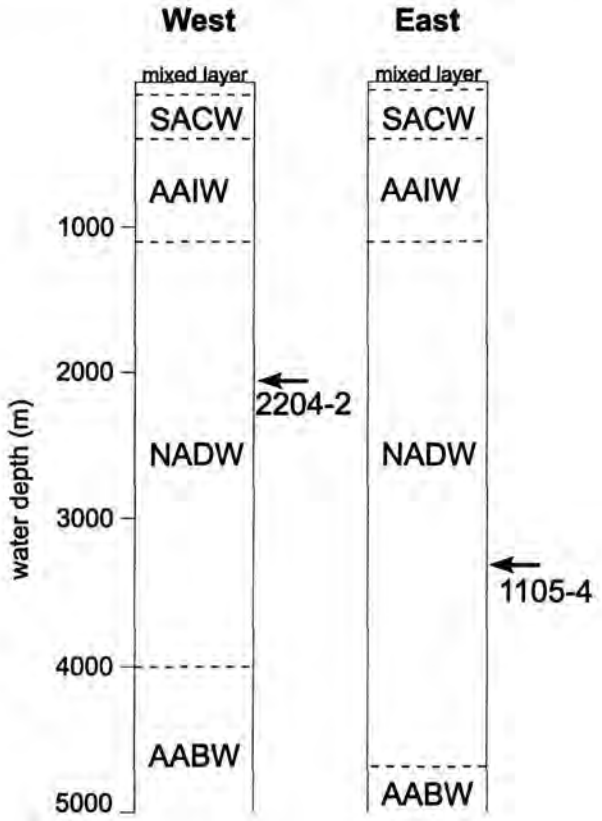

Fig.2: Schematic representation of water columns in the modern tropical western and eastern Atlantic Ocean with approximately depth of water masses (after various authors, see text). Mixed Layer: mixed surface water layer; SACW: South Atlantic Central Water; AAIW: Antarctic Intermediate Water; NADW: North Atlantic Deep Water; AABW: Antarctic Bottom Water.

In addition to the intensification of the equatorial divergence, an increase of zonal wind stress during glacial periods may have led to an ascent of the thermocline and nutricline in the eastern tropical Atlantic Ocean and a simultaneous deepening in the western tropical region, lowering nutrient concentrations in the upper water masses of the west (Rühlemann et al., 1996). The rise of the nutricline may also have enhanced palaeoproductivity in the east and reduced it in the west (Fig.3).

Besides oceanographic variations related to the changing tropical Atlantic wind field, reduced nutrient concentration of glacial subsurface waters may also have accounted for the east-west contrast in palaeoproductivity (Mulitza et al., 1998). Central and intermediate waters are assumed to be the primary nutrient-source in subtropical and tropical low productivity areas (Eppley, 1980). During cold climatic stages, deep water circulation might have switched to a mode in which subantarctic surface waters formed nutrient-rich deep waters rather than intermediate waters (Mulitza et al., 1998), while the upper part of the water column was largely composed of nutrient-poor central and intermediate waters of northern

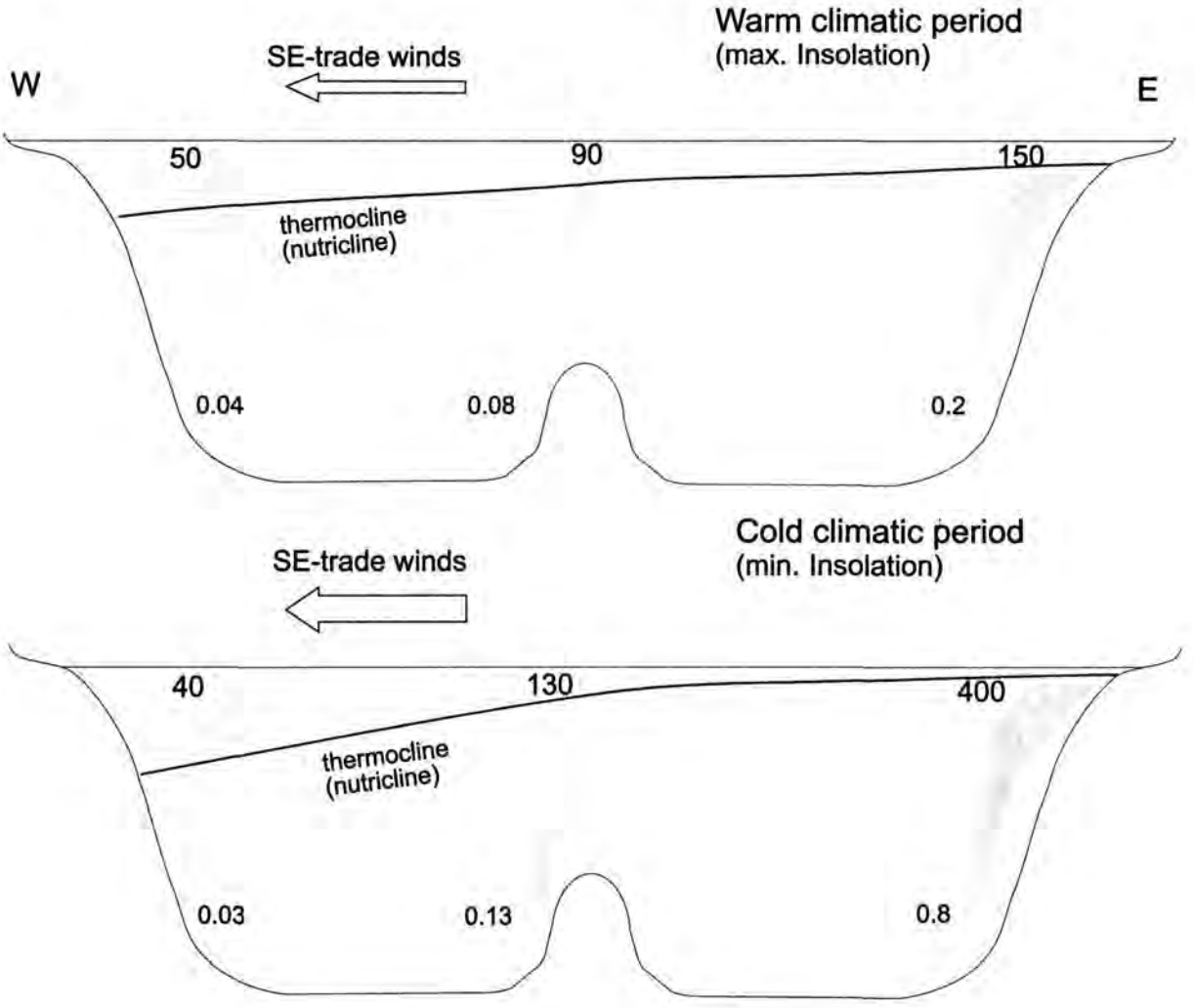

Fig.3: Schematic illustration of causes for contrary palaeoproductivity patterns in the eastern and western tropical Atlantic Ocean. The numbers indicate palaeoproductivity (above) and accumulation rates (below) in $gCm^{-2}a^{-1}$ (after Rühlemann, 1996).

origin (Boyle and Keigwin, 1987; Bickert and Wefer, 1996). The reduction in nutrient concentration of intermediate waters during glacials has possibly led to a decrease in productivity in the oligotrophic regions, whereas the contemporary increase in productivity in the highly productive upwelling areas was apparently sustained by the intensification of the wind-stress controlled divergence (Rühlemann, 1996).

Material

58 of the investigated samples originate from gravity Core GeoB 1105-4, recovered below the equatorial divergence in the western Guinea Basin (01°40′S, 12°26′W; water depth: 3225m), during "Meteor"-cruise M 9-4 (Wefer et al., 1989). From Core GeoB 2204-2,

recovered from the Brazilian continental slope (8°32'S, 34°01'W; water depth: 2072m) during „Meteor"-cruise M 23/3 (Bleil et al., 1994), 35 samples were examined.

The sediments of Core GeoB 1105-4 consist of light grey to dark grey nannofossil-foraminiferal-ooze and siliceous nannofossil-foraminiferal-ooze (Fig.4). The material of Core GeoB 2204-2 mainly consists of nannofossil ooze in the upper part and foraminiferal-nannofossil ooze in the lower part (Fig.4). The studied sediments of both cores were deposited between 141 ka to 6.7 ka BP (oxygen isotope stage 6.3 to 1). Age assessments of cores GeoB 1105-4 and GeoB 2204-2 are based on Wefer et al., (1996) and Dürkoop et al. (1997), respectively.

Methods

Preparation of calcareous dinoflagellates

The calcareous dinoflagellate preparation of Core GeoB 1105-4 follows the method described by Höll et al. (1998). For Core GeoB 2204-2, a slightly modified method has been used. Modification previous to further treatment consist of „freeze-drying" of samples in suspension (water plus a few drops of ammonia) for better separation of particles. Furthermore, 0.01 g of dry sediment was dissolved in 5 ml of ethanol (40%, a few drops of ammonia added to it) instead of 1 g in 100 ml used in Höll et al. (1998). The absolute numbers of individuals counted for both cores are given in App.1A, B.

Among the calcareous dinoflagellates, a differentiation has to be made between the shell of the coccoid, vegetative stage of *Thoracosphaera heimii* (Lohmann) Kamptner 1927 and the calcareous resting cysts of: *Sphaerodinella albatrosiana* (Kamptner) Keupp and Versteegh 1989, *Sphaerodinella tuberosa* (Kamptner) Keupp and Versteegh 1989, *Calciodinellum operosum* Deflandre 1947, *Orthopithonella granifera* (Fütterer) Keupp and Kohring 1993 and *Rhabdothorax* spp. Kamptner 1958. For convenience, this paper uses the term "calcareous dinoflagellates" for both the vegetative stage of *T. heimii* and the calcareous resting cysts. For general information on calcareous dinoflagellates see e.g. Montresor et al. (1997). Furthermore, a new taxonomic concept is currently in preparation (Janofske, Keupp and Willems, in prep.), which will include changes to the generic attribution of species presently included in *Sphaerodinella* and *Orthopithonella*.

Fig.4: Lithology and position of samples (used for calcareous dinoflagellate studies) of cores GeoB 1105-4 (Wefer et al., 1989) and GeoB 2204-2 (Bleil et al., 1994).

GeoB 1105-4

position: 01°40´S, 12°26´W ;
water depth: 3225m

GeoB 2204-2

position: 08°32´S, 34°01´W ;
water depth: 2072m

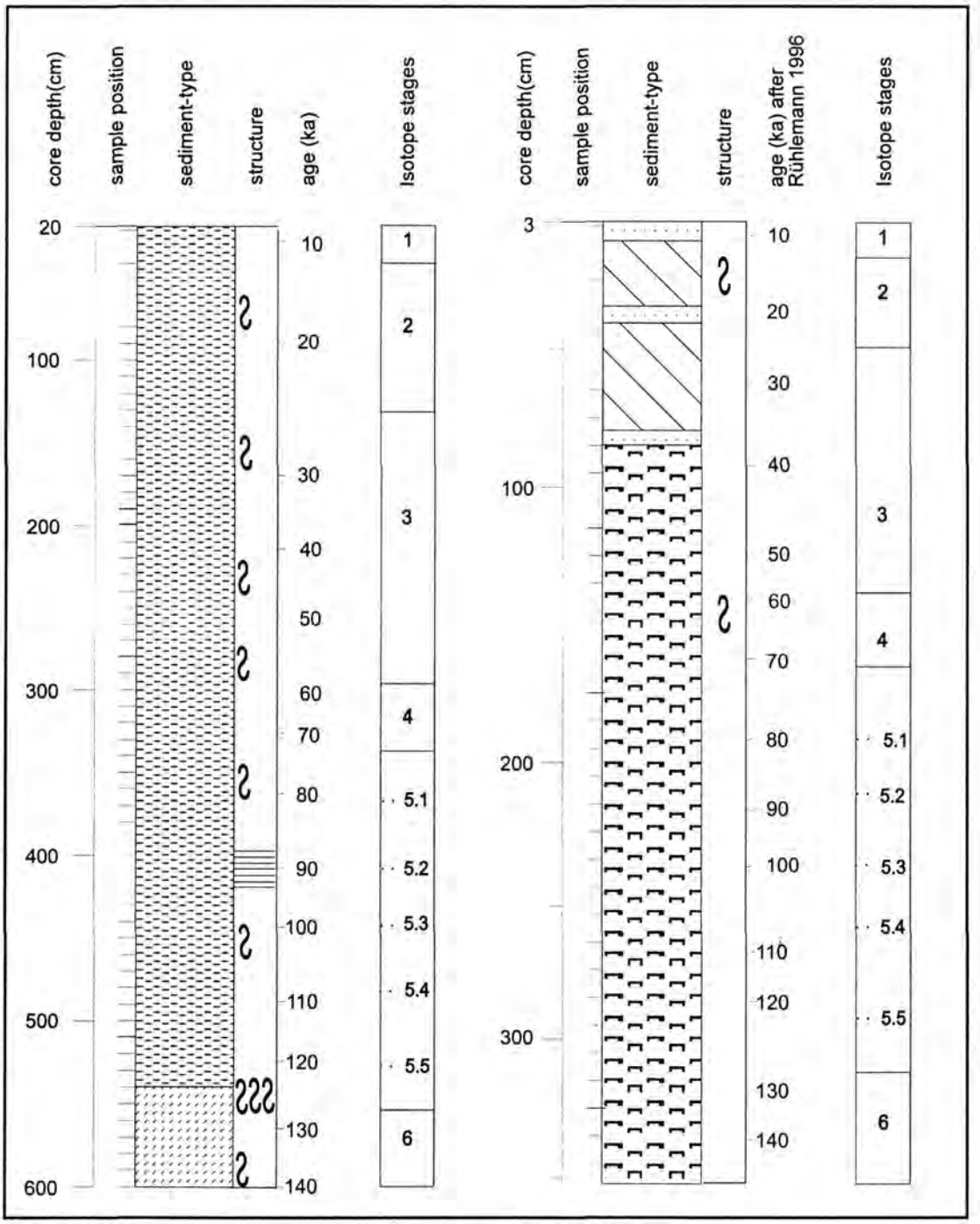

sediment-type:

- nannofossil ooze (amount of foraminifera 0-10%)
- foraminiferal-nannofossil ooze (amount of foraminifera 10-25%)
- nannofossil-foraminiferal ooze (NFO) (amount of foraminifera 25-50%)
- siliceous NFO
- sand

structure:

- laminated
- bioturbated
- strongly bioturbated
- glacial periods

Statistical and further methods

The multivariate ordination technique Redundancy Analysis (RDA, the canonical form of Principle Component Analysis (Jongman et al., 1987)) was used to determine the relationships between total organic carbon accumulation rate (TOC) and species distribution of calcareous dinoflagellates.

In a RDA diagram, a positive species score indicates increasing values of a species with TOC, whereas decreasing values of a species with TOC is indicated by a negative species score. The length of a species line indicates the importance of that species on the TOC gradient. Species, which are plotted close to the centre are not related to changes in TOC. TOC and fragment determination of planktic foraminifera are described in Rühlemann et al. (1996).

Accumulation rates have been calculated according the following equations:

calcDino accumulation rate (individuals per cm^2/ka) = calcDino/g * DBD * SR (1)

TOC accumulation rate = (TOC weight% / 100) * DBD * SR (2)

calcDino/g = calcareous dinoflagellates per gram of sediment
DBD = dry bulk density in g/cm^3
SR = sedimentation rate of the concerned core for the last 140 ka in cm/ka

In the RDA in this study, the accumulation rates of the calcareous dinoflagellates of both cores (data were log-transformed due to the dominance of *Thoracosphaera heimii*) were related to TOC accumulation rates.

Results

A comparison of the calcareous dinoflagellate associations shows, on average, a 2.4-fold higher accumulation rate of *Thoracosphaera heimii* and more than ten-fold higher accumulation rate of the calcareous resting cysts between sediments of Core GeoB 2204-2 compared to GeoB 1105-4 (Fig.5). The average accumulation rate of *T. heimii* in Core GeoB 1105-4 is eighteen times greater than that of the calcareous cysts, whereas mean accumulation rate of *T. heimii* in Core GeoB 2204-2 is about four times higher than the mean accumulation rate of calcareous cysts.

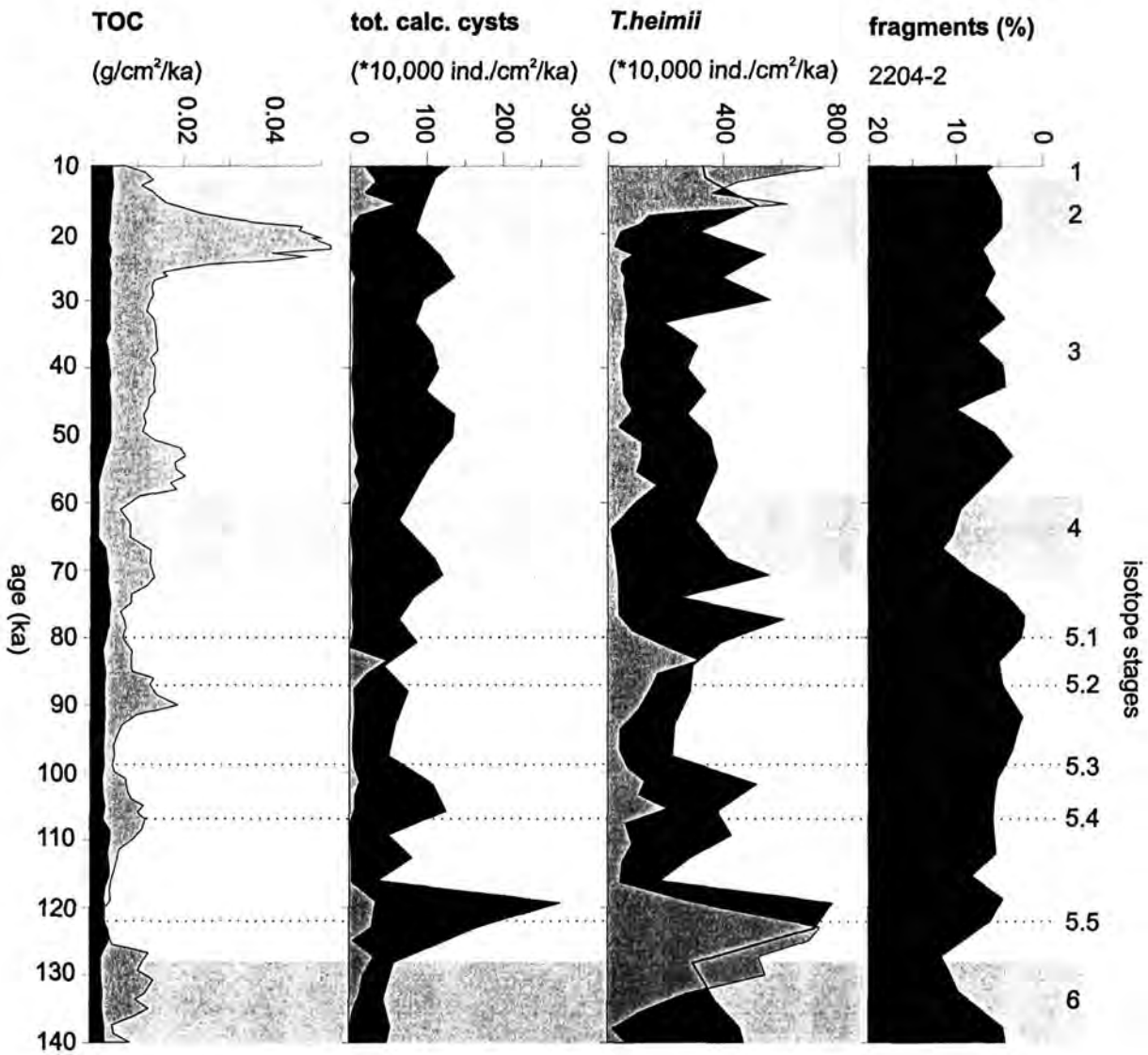

Fig.5: Accumulation rates of total organic carbon (TOC), calcareous resting cysts and *Thoracosphaera heimii* in cores GeoB 1105-4 and GeoB 2204-2; fragments of planktic foraminifera shells of GeoB 2204-2 in percent (scale is inverted due to easier comparison with other graphs) given for the last 140 ka. Fragments counted by W. Hale, data given in Rühlemann (1996). Light gray blocks indicate glacial intervals. Age and isotope stages after Wefer et al. (1996; GeoB 1105-4) and Dürkoop et al. (1997; GeoB 2204-2)

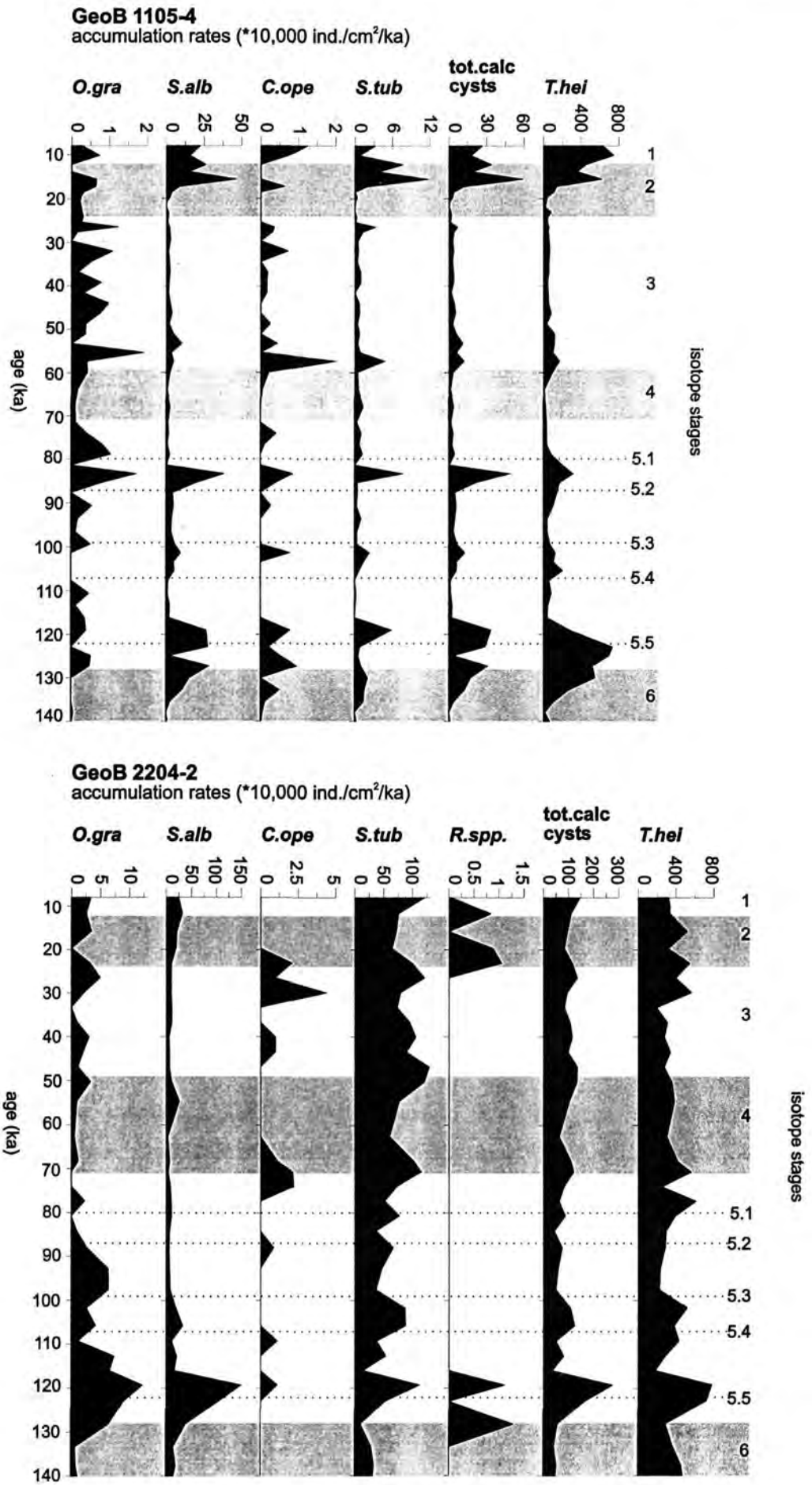
GeoB 1105-4
accumulation rates (*10,000 ind./cm²/ka)
O.gra
S.alb
C.ope
S.tub
tot.calc cysts
T.hei
age (ka)
isotope stages
GeoB 2204-2
accumulation rates (*10,000 ind./cm²/ka)
O.gra
S.alb
C.ope
S.tub
R.spp.
tot.calc cysts
T.hei
age (ka)
isotope stages

The species compositions of the two cores are slightly different; *S. albatrosiana* has the highest accumulation rate among the calcareous resting cysts in Core GeoB 1105-4, whereas *S. tuberosa* shows the highest accumulation rates of all the resting cysts in Core GeoB 2204-2 (Fig.6). The calcareous cyst *Rhabdothorax* spp. occurs only sparsely in Core GeoB 2204-2 and is nearly absent in Core GeoB 1105-4 (Fig.6, App.A, B).

Accumulation rates of both *T. heimii* and the calcareous resting cysts covary throughout Core GeoB 1105-4 (Figs.5, 6). Their maxima occur during deglaciations (transition from isotope stage 6 to 5 and 2 to 1). In Core GeoB 2204-2, maximum accumulation rates of *T. heimii* are reached mainly during glacial isotope stages 2, 4 and 6, with additional peaks during stage 5 (Figs.5, 6). A glacial/interglacial variation in the accumulation rates of the calcareous resting cysts of Core GeoB 2204-2 is less obvious.

The accumulation rate of TOC is much higher in Core GeoB 1105-4 than in GeoB 2204-2, with maximum values during isotope stages 2, high accumulation rate in stages 3 and 4 and further peaks during stage 5 and 6 (Fig.5). TOC accumulation rates in Core GeoB 2204-2 remained low throughout the last 140 ka, only showing minor fluctuations.

Table 1

	1. axis	2. axis
T.hei	-0.47	-0.55
S.tub	-0.59	-0.74
S.alb	-0.47	-0.57
O.gra	-0.17	-0.65
C.ope	-0.14	-0.19
*Rh.*spp.	-0.16	-0.27
TOC	1	0

Coordinates of species and environmental variable scores of RDA given for the first and second axis. Abbreviations: *T.hei* = *Thoracosphaera heimii*, *S.tub* = *S. tuberosa*, *S.alb* = *Sphaerodinella albatrosiana*, *O.gra* = *Orthopithonella granifera*, *C.ope* = *Calciodinellum operosum*, *R.*spp. = *Rhabdothorax* spp.; TOC = total organic carbon accumulation rate.

Fig.6: Accumulation rates of calcareous dinoflagellates (individuals/cm^2/ka) in cores GeoB 1105-4 and GeoB 2204-2. Grey blocks indicate glacial intervals. Age after Wefer et al. (1996; GeoB 1105-4) and Dürkoop et al. (1997; GeoB 2204-2). Abbreviations: *O.gra* = *Orthopithonella granifera*, *S.alb* = *Sphaerodinella albatrosiana*, *C.ope* = *Calciodinellum operosum*; *S.tub* = *S. tuberosa*, *R.*spp. = *Rhabdothorax* spp., tot.calc.cysts = total number of calcareous resting cysts, *T.hei* = *Thoracosphaera heimii*.

In the RDA, carried out on the combined data set of both cores, 17% of the variance in the data of the calcareous dinoflagellates is explained by the first axis, which represents the variable TOC, and 36% are explained by the 2. Axis (Tab.1). All calcareous dinoflagellate species are correlated with decreasing values of TOC (Fig.7; Tab.1). This implies that the accumulation rates of calcareous dinoflagellates increase with decreasing values of TOC.

Discussion

Differences in calcareous dinoflagellate accumulation rates between the western and eastern tropical Atlantic Ocean might be caused by several factors such as preservation, redeposition or production.

Preservation and redeposition

When comparing the total sediment accumulation rates of both investigated cores, we find a difference of 1g/cm^2/ka higher total sediment accumulation rate in the eastern tropical Atlantic Ocean (Tab.2). That means in the eastern tropical region we have altogether higher total sediment accumulation rates, but in the western area the calcareous dinoflagellate accumulation rates are much higher. This indicates, the contrast in calcareous dinoflagellate accumulation rates between the two region might partly be caused by dissolution of calcareous dinoflagellates in the eastern region. Bickert and Wefer (1996) have shown that dissolution of carbonate in Core GeoB 1105-4 occurred during intervals with high accumulation rates of organic carbon. However, based on statistical analyses, Höll et al. (1998) concluded that dissolution was probably a minor factor influencing the calcareous dinoflagellate association of Core GeoB 1105-4. The low percentages of fragmented planktic foraminifera shells (Fig.5) and the presence of aragonitic pteropod shells indicate excellent carbonate preservation in Core GeoB 2204-2 over the last 300 ka (Rühlemann, 1996). We therefore assume that dissolution was not a major factor responsible for the differences in calcareous dinoflagellate accumulation rates between the two sediment cores.

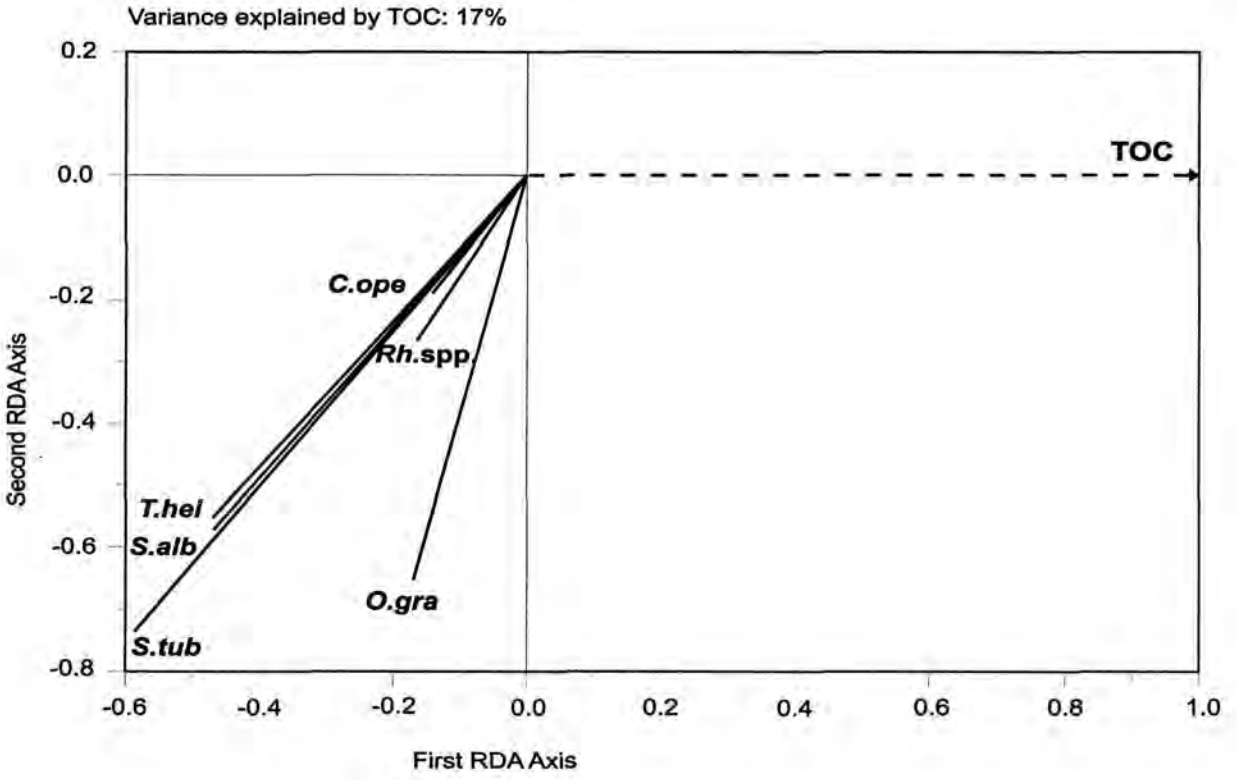

Fig.7: RDA diagram (combined data sets of cores GeoB 2204-2 and GeoB 1105-4) of species accumulation rates in relation to the variable TOC (dashed arrow). Scale of axes is given in standard deviations. For abbreviations of species names, see Fig. 6.

Table 2

a. AR tot = SR * DBD

AR tot	= accumulation rate of total sediment
SR	= sedimentation rate of concerned core for the last 140 ka in cm/ka
DBD	= dry bulk density in g/cm^3

b. AR tot average values for the last 140 ka:

GeoB 1105-4: 2.97 g/cm^2/ka

GeoB 2204-2: 1.9 g/cm^2/ka

Accumulation rates of the total sediment calculated according to the follwing equation **(a.)**. Average values of total sediment accumulation rates are given for both cores **(b.)**. Data for SR and DBD after Rühlemann (1996; Core GeoB 2204-2) and Meinecke (1992; GeoB 1105-4).

Redeposition appears not to be a significant factor influencing the association and concentration of the calcareous dinoflagellates in the eastern Equatorial Atlantic Ocean (GeoB 1105-4; Höll et al., 1998). Low amounts of reworked organic-walled dinoflagellate cysts of Tertiary age have been recorded in the sediments of Core GeoB 2204-2. During Tertiary the diversity of calcareous dinoflagellates species was higher compared to Late Quaternary (e.g. Keupp and Kohring, 1993, 1994; Kohring, 1993; Weiler, 1990). If reworked calcareous dinoflagellates of that age were present in the sediments of Core GeoB 2204-2, we could expect to find additional conspicuously different forms than the six recorded species (Fig.6; Append.1A). As this is not the case, we suggest that the calcareous dinoflagellate accumulation rates in the western tropical Atlantic have hardly been affected by redeposition.

Hence, we assume that redepostion did not cause the differences in fluxes between the two cores.

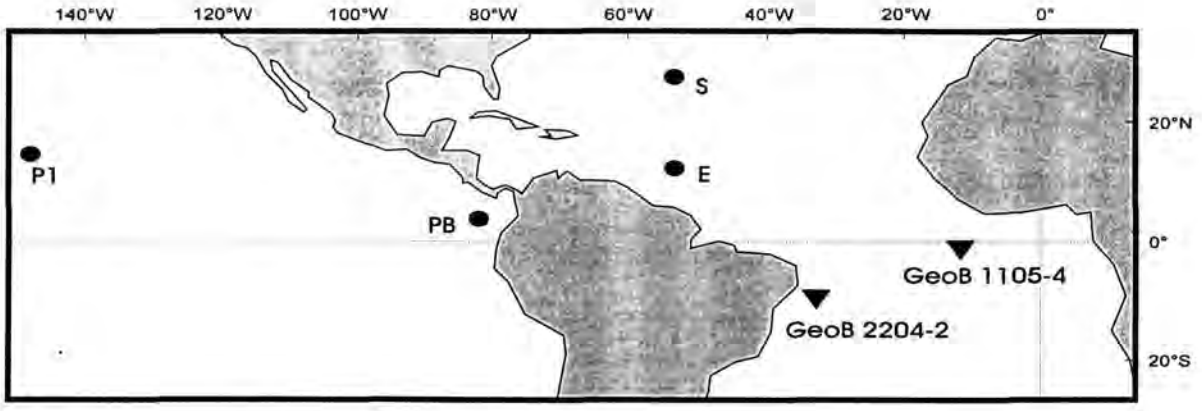

Station	Position	water depth (m) of sediment traps	T.hei+O.gra (per cm^2/ka)	others (per cm^2/ka)
E	13°30'N/54°00'W	389, 988, 3755, 5068	no data	$36*10^6$
S	31°33'N/55°55'W	976, 3694, 5369	$2*10^6$	$21*10^6$
PB	05°21'N/81°53'W	667, 1268, 2869, 3769, 3791	$112*10^6$	$11*10^6$
P1	15°21'N/151°29'W	2778, 4280, 5582	$44*10^6$	$5*10^6$
GeoB 1105-4	01°40'S/12°26'W		$2*10^6$	$9*10^4$
GeoB 2204-2	08°32'S/34°01'W		$4*10^6$	$9*10^5$

Productivity and other factors

If preservation and redeposition can be eliminated as the main factors causing the differences in calcareous dinoflagellate accumulation rates between both cores, we are left with the assumption, differences are caused by differential calcareous dinoflagellate production.

High calcareous dinoflagellate accumulation rates are inversely correlated with TOC accumulation rates (Figs.5, 7). Decreases in TOC accumulation rates in the eastern equatorial Atlantic and differences in TOC accumulation rates between the eastern and western tropical Atlantic can be related to decreases and differences in palaeoproductivity (Meinecke, 1992; Rühlemann, 1996, Wefer et al., 1996). Consequently, the present results suggests that enhanced production of calcareous dinoflagellates can be related to reduced primary productivity. Palaeoproductivity in the eastern Equatorial Atlantic Ocean apparently decreased during warm climatic periods with reduced upwelling intensity, when the wind-driven equatorial divergence was diminished (Schneider et al., 1995, 1996; Wefer et al., 1996). Based on planktic foraminiferal assemblages, Mix and Morey (1996) assumed that the equatorial upwelling intensity was weakest during ice melting periods. This is supported by our data of Core GeoB 1105-4, which show maximum accumulation rates of calcareous dinoflagellates at the transitions from isotope stage 6 to 5 and 2 to 1 (Figs.5, 6). In the oligotrophic western tropical Atlantic Ocean, where productivity is very low due to a constantly deep nutricline throughout the year (Fig.3), and relatively stratified surface waters compared to the eastern equatorial region, the accumulation rates of calcareous dinoflagellate cysts are much higher than in the eastern Equatorial Atlantic Ocean (Fig.5). This is also valid for the accumulation rates of *T. heimii*, except at transitions from isotope stage 6 to 5 and 2 to 1 (Fig.5).

During cold climatic periods, the nutricline deepens further in the western tropical Atlantic Ocean, resulting in less productivity in the surface waters. Furthermore, at those times central and intermediate waters (the primary nutrient-source in tropical low productivity regions; Eppley, 1980) were probably reduced in nutrient concentration, and thus possibly responsible

Fig.8: Positions of sediment traps (S, E, PB, P1) after Dale (1992a, b) and core positions (GeoB 1105-4, GeoB 2204-2). Sediment trap data (Dale, 1992a, b): Mean values of individuals/cm^2/ka are given for one station including sediment trap data of different water depths. Others include: *Sphaerodinella albatrosiana*, *Calciodinellum operosum*, cysts of *Scrippsiella* (= *Rhabdothorax* spp.), Bicarinate-type, ?calcareous cyst sp., unidentified calcareous cysts. For abbreviations of species names, see Fig. 6.

Plate 1

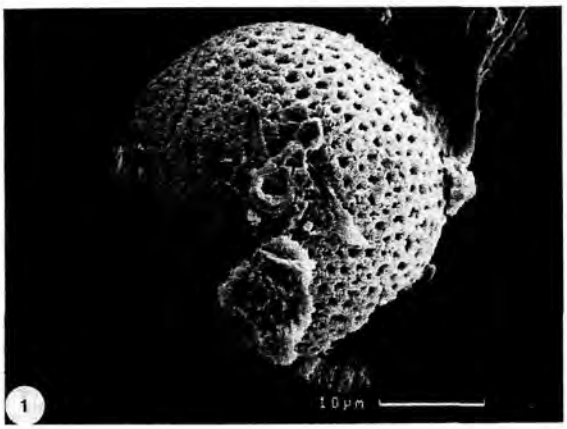

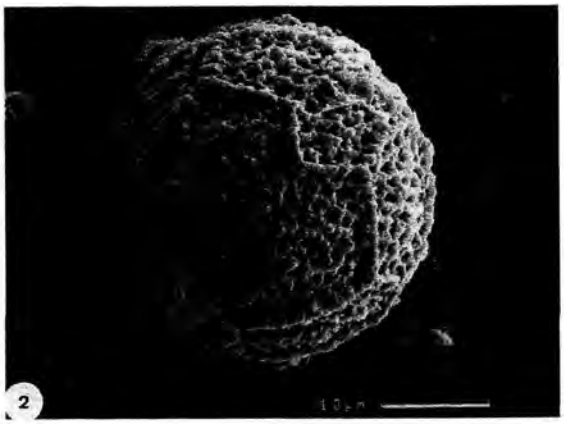

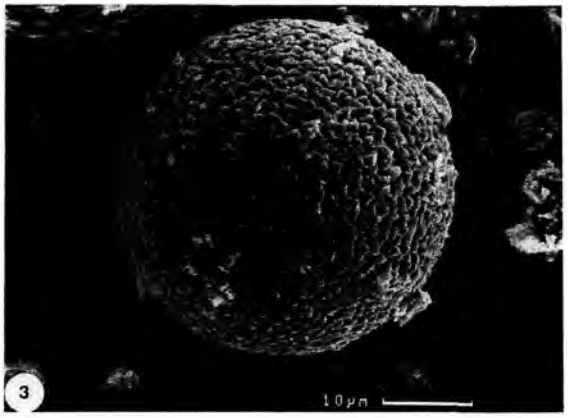

for even lower productivity in comparison to warm climatic periods. During those cold climatic periods, the accumulation rates of *T. heimii* in Core GeoB 2204-2 increases slightly (Fig.6), whereas that pattern is less obvious for the calcareous resting cysts.

Beside productivity, another striking environmental difference between the eastern and western tropical Atlantic is the contrast in stratification of the upper water masses, with a relatively more stable stratification in the west. This suggests increasing calcareous dinoflagellate production can probably be related to relatively stratified, oligotrophic surface waters. If this correlation with productivity and/or stratification is a general relationship, we should expect to find it in regions other than the tropical Atlantic Ocean. To date, information about flux rates of recent calcareous dinoflagellates is restricted to a few studies (Dale, 1992a,b). In these investigations, sediment trap material was studied for its calcareous dinoflagellate content at four locations in the North Atlantic and Pacific oceans (Fig.8). For better comparison of calcareous dinoflagellate data of the different stations, mean values of flux rates have been calculated for the sediment trap data at different water depths at each station (Fig.8). Note: Dale (1992b) included in „thoracosphaerids" not only *T. heimii*, but also *O. granifera* (previously *Thoracosphaera granifera*), not a vegetative stage (D. Janofske, pers. comm.).

Stations E, S and P1 are all situated in low productivity regions, whereas station PB (Panama Basin) is probably influenced by the higher productive waters of the equatorial divergence in the Pacific Ocean. Based on our work, we would expect to find higher fluxes of calcareous dinoflagellates at the stations situated in the low productivity areas. In fact, at station PB only the fluxes of the calcareous cysts are lower than at the Atlantic Ocean stations (Fig.8). But the fluxes are higher than at station P1 which is situated in the low productivity area south-east of Hawaii in the Pacific Ocean. However, contrary to expectations, the fluxes of *T. heimii* and *O. granifera* at station PB reach the highest values of all stations. To a certain

Plate 1: SEM photographs of calcareous dinoflagellates. Orientation is given only when possible. Scale bar shown.

1. *Sphaerodienella albatrosiana*. Lateral view. Suture of apical archaeopyle can be seen on the left side of the photograph. Sample: 2204-2, 55 cm.
2. *Calciodinellum operosum*. Antapical view. Sample: 2204-2, 55 cm.
3. *Sphaerodinella tuberosa*. Sample: 2204-2, 145 cm.
4. *Orthopithonella granifera*. View showing the operculum. Sample: 2204-2, 295 cm.
5. *Thoracosphaera heimii*. View showing the operculum. Sample: 2204-2, 55 cm.

extent, these discrepancies from our findings might be explained by the fact that the sediment trap material only reflects a period of maximally five months of production in the second half of one year and not all seasonal variations are included in the data, also they give insight to only one temporal window, which might neglect special annual variations (e.g. such as El Niño events). Furthermore, only less than 20 % of the variation within the data of the calcareous dinoflagellates of the studied cores can be explained by TOC (Fig.7), suggesting that, besides productivity and related stratification of the upper water masses, other factors are influencing their accumulation rates. In addition, during periods with reduced palaeoproductivity in the tropical eastern Atlantic Ocean, when enhanced accumulation rates of calcareous dinoflagellates occurred, sea surface temperatures (SST) were apparently higher than during periods with intensified upwelling (Sikes and Keigwin, 1994; Billups and Spero, 1996; Wefer et al., 1996). The western tropical region in comparison shows low seasonality in modern SST (Merle, 1983), which is thought to be valid also for the Late Quaternary, with a seasonal SST variation not greater than 2.5°C (Dürkoop et al., 1997). The correlation of estimated SST and seasonality based on planktic foraminifera with calcareous dinoflagellate data of the eastern Equatorial Atlantic Ocean has shown no significant relationship (Höll et al., 1998). This could be due to the lack of reliability of the estimations, or may suggest that other factors such as nutrient content or water stratification are more important than temperature and/or seasonality for the calcareous dinoflagellate association in the eastern equatorial Atlantic. In other oceanic regions, temperature is thought to play a more prominent role (Zonneveld et al., in press).

Besides the differences in calcareous dinoflagellate flux, differences within the associations are also conspicuous. The entire calcareous dinoflagellate association does not necessarily have to be dominated by *T. heimii* or by „thoracosphaerids", respectively, as has been observed in cores GeoB 1105-4 and 2204-2 (Fig.6). At station S, the „other" calcareous dinoflagellate species dominate the association (Fig.8; Dale, 1992a). The dominating resting cyst in Core GeoB 1105-4 is *S. albatrosiana*, whereas it is *S. tuberosa* in Core GeoB 2204-2. This might indicate a preference of S. *tuberosa* for rather more oligotrophic, stratified waters. Unfortunately, Dale (1992a) did not count *S. tuberosa* separately in his trap samples and only provided a photograph of one specimen (?*Thoracosphaera tuberosa*, Dale, 1992a: plate 1.3), recorded at station P1. It is not clear to the authors whether this species was simply not observed or was included in one of the species groups. Therefore we cannot directly compare our observations on the named species with the data of Dale (1992a).

In general, different production-limiting factors might be important for each calcareous species. Factors such as salinity, light intensity and water depth could also have an important influence on the distribution and flux rates of calcareous dinoflagellates. For the Late Quaternary tropical Atlantic Ocean, we can assume that enhanced production of calcareous dinoflagellates can be correlated to reduced palaeoproductivity and probably relatively stable stratification of the surface waters. These findings can only be partially supported by sediment trap data of the North Atlantic and Pacific oceans, which indicates that in other oceanic regions the distribution patterns of the calcareous dinoflagellates might be controlled by other factors.

Conclusion

A stratigraphic study of calcareous dinoflagellates in the western and eastern tropical Atlantic Ocean during the last 140 ka shows much higher accumulation rates of calcareous forms in the oligotrophic western region. The assemblage of the calcareous dinoflagellates in both sediment cores is dominated by *Thoracosphaera heimii*. Increases of calcareous dinoflagellate production from the eastern to the western tropical Atlantic Ocean can be related to relatively stratified oligotophic conditions of the upper water column in the west. The calcareous dinoflagellate associations and accumulation rates of both cores are probably not significantly affected by dissolution and/or redepostion.

Acknowledgements

We are thankful to the Sonderforschungsbereich 261 at the University of Bremen (Contribution no. 92) for making the core material available to us. Thanks are due to Dr. Dorothea Janofkse for critical reading of the manuscript, Annemiek Vink for correcting the English, and Anne Meyer for development of the photographs. Furthermore, we would like to thank Dr. Rex Harland and Prof. Hans Thierstein for constructive reviews. This research was funded by the Deutsche Forschungsgemeinschaft in the Graduierten Kolleg project „Stoff-Flüsse in marinen Geosystemen“ with fellowships for C. Höll and K. Zonneveld.

References

Bickert, T. and Wefer, G., 1996. Late Quaternary Deep Water Circulation in the South Atlantic: Reconstruction from Carbonate Dissolution and Benthic Stable Isotopes. In: G. Wefer, W.H. Berger, G. Siedler and D.J. Webb (Editors), The South Atlantic: Present and Past Circulation. Springer Verlag, Berlin, Heidelberg, pp. 599-620.

Billups, K. and Spero, H.J., 1996. Reconstructing the stable isotope geochemistry and paleotemperatures of the equatorial Atlantic during the last 150,000 years: Results from individual foraminifera. Paleoc., 11(2): 217-238.

Biscaye, P.E., Kolla, V. and Turekian, K.K., 1976. Distribution of calcium carbonate in surface sediments of the Atlantic Ocean. J. Geophys. Res., 81: 2595-2603

Bleil, U., Spieß, V. and Wefer, G. (Editors), 1994. Geo Bremen SOUTH ATLANTIC 1993, Cruise No. 23, 4 February-12 April 1993, Meteor Berichte ed., Vol. 94-1. Universität Hamburg, Hamburg, 261 pp.

Boyle, E.A. and Keigwin, L., 1987. North Atlantic thermohaline circulation during the past 20,000 years linked to high-latitude surface temperature. Nature, 330: 35-40.

Dale, B., 1992a. Dinoflagellate Contribution to the Open Ocean Sediment Flux. In: S. Honjo (Editor), Dinoflagellate Contribution to the Deep Sea, Ocean Biocoenosis Series ed., Vol. No. 5. Woods Hole Oceanographic Institution, Woods Hole, pp. 1-32.

Dale, B., 1992b. Thoracosphaerids: Pelagic Fluxes. In: S. Honjo (Editor), Dinoflagellate Contibution to the Deep Sea, Ocean Biocoenosis Series ed., Vol. 5. Woods Hole Oceanographic Institution, Woods Hole, Massachusetts, pp. 33-44.

Deflandre, G., 1947. Calciodinellum nov.gen,. premier représentant d'une famille nouvelle de Dinoflagellé fossile à thèque calcaire. Comptes rendues des séances de l' Academie des Science Paris, 224: 1781-1782.

de Vernal, A., Londeix, L., Mudie, P.J., Harland, R., Morzadec-Kerfourn, M.-T., Turon, J.-L. and Wrenn, J.H., 1992. Quaternary organic-walled dinoflagellate cysts of the North Atlantic Ocean and adjacent seas: ecostratigraphy and biostratigraphy. In: M.J. Head and J.H. Wrenn (Editors), Neogene and Quaternary Dinoflagellate Cysts and Acritarchs. American Association of Stratigraphic Palynologists Foundation, Dallas, pp. 289-328.

Dürkoop, A., Hale, W., Mulitza, S., Pätzold, J. and Wefer, G., 1997. Late Quaternary variations of sea surface salinity and temperature in the western tropical Atlantic: Evidence from 18O of Globigerinoides sacculifer. Paleoceanography, 12 (6): 764-772.

Eppley, R.W., 1980. Autotrophic production of particulate matter.- In: Longhurst, A. (editor): Analysis of marine Ecosystems: 343-361, Academic Press, London.

Hastenrath, S. and Merle, J., 1987. Annual cycle of subsurface thermal structure in the tropical Atlantic. J. Phys. Oceanogr., 17: 1518-1538.

Höll, C., Zonneveld, K.A.F. and Willems, H., 1998. On the ecology of calcareous dinoflagellates: The Quaternary eastern Equatorial Atlantic. Mar. Micropaleont., 33: 1-25.

Houghton, R.W., 1991. The relationship of Sea Surface Temperature to thermocline depth at annual and interannual time scales in the tropical Atlantic. J. Geophys. Res., 96 (C8): 15,173-15,185.

Jongman, R.H.G., ter Braak, C.J.F. and van Tongeren, O.F.R. (Editors), 1987. Data analysis in community and landscape ecology. Centre for Agricultural Publishing and Documentation, Wageningen, 299 pp.

Kamptner, E., 1927. Beitrag zur Kenntnis adriatischer Coccolithophoriden. Archiv für Protistenkunde, 58: 173-184.

Kamptner, E., 1958/59. Betrachtungen zur Systematik der Kalkflagellaten, nebst Versuch einer neuen Gruppierung der Chrysomonadales. Archiv für Protistenkunde, 103 (1-2): 54-116.

Katz, E.J. and Garzoli, S., 1982. Response of the western equatorial Atlantic Ocean to an annual wind cycle. Journal of Marine Reseach, 40, Supplement: 307-327.

Keupp, H. and Versteegh, G., 1989. Ein neues systematisches Konzept für kalkige Dinoflagellaten-Zysten der Subfamilie Orthopithonelloideae Keupp 1987. Berliner geowiss. Abh., 106 (A): 207-219.

Keupp, H. and Kohring, R., 1993. Kalkige Dinoflagellatenzysten aus dem Obermiozän von El Medhi (Algerien). Berliner geowiss. Abh., (E) 9: 35-43.

Keupp, H. and Kohring, R., 1994. Kalkige Dinoflagellaten-Zysten aus dem Rupelton (Mittel-Oligozän) des Mainzer Beckens und der Niederrheinischen Bucht. Mainzer Geowiss. Mitt., 23: 159-184.

Kohring, R., 1993: Kalkdinoflagellaten aus dem Mittel- und Obereozän von Jütland (Dänemark) und im Pariser Becken (Frankreich) im Vergleich mit anderen Tertiär-Vorkommen. Berliner geowiss. Abh., (E) 6: 1-164.

Lewis, J., Dodge, J.D. and Powell, A.J., 1990. Quaternary dinoflagellate cysts from the upwelling system offshore Peru, Hole 686B, ODP LEG 112. In: E. Suess, R. von Huene, et al. (Editors), Proceedings of the Ocean Drilling Program, Scientific Results, Vol. 112.,, pp. 323-328.

Lyle, M., 1988. Climatically forced organic carbon burial in equatorial Atlantic and Pacific Oceans. Nature, 335: 529-532.

Marret, F., 1994. Evolution paleoclimatique et paleohydrologique de l'Atlantique Est-Equatorial et du proche Continent au Quaternaire terminal. Contribution palynologique (kystes de dinoflagellés, pollen et spores). Ph.D. Dissertation, L'Université Bordeaux I, 271 pp.

Martinson, D.G., Pisias, N.G., Hays, J.D., Imbrie, J., Moore, T.C. and Shackleton, N.J., 1987. Age Dating and the Orbital Theory of the Ice Ages: Development of a High-Resolution 0 to 300,000 y Chronostratigraphy. Quaternary Res., 27: 1-29.

Matthiessen, J., 1991. Dinoflagellate-Zysten im Spätquartär des europäischen Nordmeeres: Palökologie und Paläo-Ozeanographie. Ph.D. Dissertation, Geomar, Kiel, 104 pp. (Geomar Report 7)

McIntyre, A., Ruddiman, W.F., Karli, K. and Mix, A.C., 1989. Surface water response of the Equatorial Atlantic Ocean to orbital forcing. Paleoceanography, 4 (1): 19-55.

Meinecke, G., 1992. Spätquartäre Oberflächenwassertemperaturen im östlichen Äquatorialen Atlantik. Berichte, Fachbereich Geowissenschaften, Universität Bremen, 29: 181 pp.

Merle, J., 1983. Seasonal Variability of Subsurface Thermal Structure in the Tropical Atlantic Ocean. - IN: Hydrodynamics of the Equatorial Ocean. Elsevier Oceanogr. Ser., 36: 31-49.

Mix, A.C., Ruddiman, W.F. and McIntyre, A., 1986. Late Quaternary paleoceanography of the tropical Atlantic, 2: The seasonal cycle of sea surface temperatures, 0-20,000 years b.p. Paleoceanography, 1 (3): 339-353.

Mix, A.C. and Morey, A.E., 1996. Climate Feedback and Pleistocene Variations in the Atlantic South Equatorial Current. In: W.H. Berger, G. Wefer, G. Siedler and D.J. Webb (Editors), The South Atlantic: Present and Past Circulation. Springer Verlag, Berlin, Heidelberg, pp. 503-525.

Montresor, M., Janofske, D. and Willems, H., 1997. The cyst-theca relationship in Calciodinellum operosum emend. (Peridiniales, Dinophyceae) and a new approach for the study of calcareous cysts. J. Phycol., 33: 122-131.

Mulitza, S., Rühlemann, C., Bickert, T., Hale, W., Pätzold, J. and Wefer, G., 1998. Late Quaternary 13C gradients and carbonate accumulation in the western equatorial Atlantic. Earth Planet. Sci. Lett., 155: 237-249.

Peterson, R.G. and Stramma, L., 1991. Upper-level circulation in the South Atlantic Ocean. Prog. Oceanog., 26: 1-73.

Philander, S.G.H. and Pacanowsi, R.C., 1986. A Model of the Seasonal Cycle in the Tropical Atlantic Ocean. J. Geophys. Res., 91: 14,192-14,206.

Prell, W.L. and Kutzbach, J.E., 1987. Monsoon Variability over the past 150,000 Years. J. of Geophys. Res., 92(D7): 8411-8425.

Reid, J.L., 1989. On the total geostrophic circulation of the South Atlantic Ocean: Flow patterns, tracers, and transport. Prog. Oceanog., 23: 149-244.

Richardson, P.L. and Reverdin, G., 1987. Seasonal cycle of velocity in the Atlantic North Equatorial Countercurrents as measured by surface drifters, current meters, and ship drifts. J. Geophys. Res., 92: 3691-3703.

Rühlemann, C. 1996. Akkumulation von Carbonat und organischem Kohlenstoff im tropischen Atlantik: Spatquartäre Produktivitäts-Variationen und ihre Steuerungsmechanismen. Ber., Fachber. Geowiss., Univ. Bremen, 84: 139pp.

Rühlemann, C., Frank, M., Hale, W., Mangini, A., Mulitza, S., Müller, P.J. and Wefer, G., 1996. Late quaternary productivity changes in the western equatorial Atlantic: Evidence from 230Th-normalized carbonate and organic carbon accumulation rates. Mar. Geol., 135, 127-152.

Schneider, R., Müller, P.J. and Ruhland, G., 1995. Late Quaternary surface circulation in the east equatorial South Atlantic: Evidence from alkenone sea surface temperature. Paleoceanography, 10(2): 197-219.

Schneider, R.R., Müller, P.J., Ruhland, G., Meinecke, G., Schmidt, H. and Wefer, G., 1996. Late Quaternary Surface Temperatures and Productivity in the East-Equatorial South Atlantic: Response to changes in Trade/Monsoon Wind Forcing and Surface Water Advection. In: G. Wefer, W.H. Berger, G. Siedler and D.J. Webb (Editors), The South Atlantic: Present and Past Circulation. Springer Verlag, Berlin, Heidelberg, pp. 527-551.

Sikes, E.L. and Keigwin, L.D., 1994. Equatorial Atlantic sea surface temperature for the last 30kyr: A comparison of Uk'37, 18O and foraminiferal assemblage temperature estimates. Paleoceanography, 9(1): 31-45.

Thunell, R.C., 1982. Carbonate dissolution and abyssal hydrography in the Atlantic Ocean. Mar. Geol., 47: 165-180

Tomczak, M. and Huges, P., 1980. Three dimensional variability of the water masses and currents in the Canary current upwelling region. "METEOR" Forschungs-Ergebnisse, A21: 1-24.

Verardo, D.J. and McIntyre, A., 1994. Production and destruction: Control of biogenous sedimentation in the tropical Atlantic 0-300,000 years B.P. Paleoceanography, 9(1): 63-86.

Versteegh, G.J.M., 1995. Palaeoenvironmental changes in the Mediterranean and North Atlantic in relation to the onset of nortern hemisphere glaciations (2.5 Ma B.P.) -A palynological approach-. Ph.D. Dissertation, State University of Utrecht, Utrecht, 134 pp.

Wefer, G. and cruise participants, 1989. Bericht über die Meteor-Fahrt M 9-4, Dakar-Santa Cruz, 19.2.1989-16.3.1989. Ber., Fachber. Geowiss., Univ. Bremen, 7: 103pp.

Wefer, G., Berger, W.H., Bickert, T., Donner, B., Fischer, G., Kemle-von Mücke, S., Meinecke, G., Müller, P.J., Mulitza, S., Niebler, H.-S., Pätzold, J., Schmidt, H., Schneider, R.R. and Segl, M., 1996. Late Quaternary Surface Circulation of the South Atlantic: The Stable Isotope Record and Implications for Heat Transport and Productivity. In: G. Wefer, W.H. Berger, G. Siedler and D.J. Webb (eds.), The South Atlantic: Present and Past Circulation. Springer Verlag, Berlin, Heidelberg, pp. 461-502.

Weiler, H., 1990. Calcisphaeren aus oligozänen Schichten des Mainzer Beckens und des Oberrheingrabens., Mainzer geowiss. Mitt., 19: 9-48.

Zonneveld, K.A.F., Höll, C., Janofske, D., Karwath, B., Kerntopf, B., Rühlemann, C. and Willems, H. Calcareous dinoflagellate cysts as palaeo-environmental tools. Fischer, G. and Wefer, G. (eds.), Proxies in Paleoceanography, in press.

Appendix A. Calcareous dinoflagellate data of core GeoB 2204-2

sample	age (ka)	*T. hei*	*S. tub*	*S.alb*	*C. ope*	*O. gra*	*R.* spp.	tot. CD	tot.calc Cysts
5	7.7	382	146	29	0	4	0	561	179
15	11.7	402	90	38	0	3	1	533	132
25	15.8	612	85	25	0	4	0	726	114
35	19.7	361	73	22	0	0	1	456	96
45	23.1	519	95	10	2	3	1	629	111
55	26.5	402	122	10	1	5	0	539	138
65	29.9	512	72	9	4	2	0	599	87
75	33.3	190	71	11	0	0	0	272	82
85	36.7	327	100	12	0	1	0	440	113
95	40.1	275	105	6	1	3	0	390	115
105	43.5	343	90	7	1	2	0	443	100
115	46.9	253	118	6	0	1	0	378	125
125	50.3	333	112	10	0	3	0	458	125
135	54.6	423	85	29	0	1	0	538	115
145	62.6	647	128	7	0	1	0	783	136
155	68.3	364	89	6	1	1	0	461	97
165	70.7	521	107	4	2	0	0	634	113
175	74	231	66	8	2	0	0	307	76
185	77.3	542	46	9	0	2	0	599	57
195	80.7	397	78	11	0	0	0	486	89
205	84.2	336	42	8	0	1	0	387	51
215	88	327	76	7	1	3	0	414	87
225	92.8	261	52	8	0	7	0	328	67
235	97.6	247	40	9	0	7	0	303	56
245	101.8	602	101	23	0	3	0	729	127
255	105.8	458	106	40	0	5	0	609	151
265	109.3	385	34	10	1	1	0	431	46
275	112.7	274	51	20	0	7	0	352	78
285	116	167	13	15	0	6	0	201	34
295	119.3	699	101	134	1	11	1	946	248
305	123	641	47	93	0	8	0	789	148
315	128.2	453	16	61	0	10	2	542	89
325	133.4	555	43	22	0	1	0	621	66
335	137.7	592	43	25	0	1	0	661	69
345	144.1	652	37	10	0	2	0	701	49

Ages after Dürkoop et al. (1997). For investigation of calcareous dinoflagellates 0.01 g of dry sediment was dissolved in 5 ml ethanol (40%). Absolute counting of a slide containing 100 µl subsample. Sample: sample numbers are equivalent to core depth in cm. Abbreviations: *T.hei* = *Thoracosphaera heimii*, *S.tub* = *S. tuberosa*, *S.alb* = *Sphaerodinella albatrosiana*, *O.gra* = *Orthopithonella granifera*, *C.ope* = *Calciodinellum operosum*, *R.*spp. = *Rhabdothorax* spp.; CD = total number of calcareous dinoflagellates; tot. CalcCysts = total number of calcareous resting cysts.

Appendix B. Calcareous dinoflagellate data of core GeoB 1105-4 (after Höll et al., 1998)

sample	age (ka)	*weight(g)*	*vol(ml)*	*slide ml*	*T. hei*	*S. tub*	*S. alb*	*C. ope*	*O. gra*	*R.* spp.	tot. CD	tot.calc Cysts
21	6.67	1.04	100	0.05	713	6	33	2	0	0	754	41
30	10.22	1.06	100	0.05	1012	1	21	1	1	0	1036	24
40	12.26	1.00	100	0.05	592	10	34	0	0	0	636	44
50	13.94	1.02	100	0.05	481	5	20	0	0	0	506	25
60	15.60	1.10	100	0.05	949	18	71	0	1	0	1039	90
70	17.26	1.03	100	0.1	445	6	27	2	2	0	482	37
80	18.53	0.72	70	0.1	348	0	11	0	1	0	360	12
90	19.68	0.70	100	0.5	357	3	20	0	2	0	382	25
100	20.81	0.23	20	0.3	301	1	2	0	2	0	306	5
110	21.95	0.20	10	0.3	337	0	1	0	4	0	342	5
120	23.09	0.71	70	0.15	316	0	5	0	1	0	322	6
130	24.22	0.72	70	0.25	326	2	9	0	2	0	339	13
140	25.36	1.03	100	0,2	351	1	7	0	2	0	361	10
150	26.50	1.04	100	0.15	341	19	12	2	7	0	381	40
160	27.63	1.04	100	0.15	347	8	15	2	1	0	373	26
170	29.70	1.08	100	0.15	379	3	16	0	0	0	398	19
180	32.08	1.00	100	0.15	380	3	8	4	6	0	401	21
190	34.45	1.05	100	0.15	348	2	12	0	3	0	365	17
200	36.83	1.02	100	0.15	334	5	14	1	1	0	355	21
210	39.22	1.03	100	0.15	292	6	11	1	5	0	315	23
220	41.60	1.01	100	0.15	331	0	9	1	2	0	343	12
230	43.98	1.02	100	0.15	335	4	16	0	6	0	361	26
240	46.36	1.08	100	0.1	337	3	15	0	3	0	358	21
250	48.74	1.08	100	0.2	293	3	15	2	3	0	316	23
260	51.12	1.00	100	0.1	331	2	13	0	1	0	347	16
270	53.30	1.04	100	0.1	273	1	24	1	0	0	299	26
280	55.40	1.08	100	0.15	372	3	12	0	7	0	394	22
290	57.40	1.01	100	0.1	430	12	12	5	1	0	460	30
300	59.90	1.06	100	0.1	467	2	11	1	2	0	483	16
310	63.90	1.03	100	0.35	270	14	15	1	4	0	304	34
320	67.89	0.98	100	0.25	289	14	27	0	1	0	331	42
330	71.54	1.01	100	0.2	319	3	12	0	1	0	335	16
340	74.11	1.02	100	0.2	368	10	17	4	4	0	403	35
350	76.68	1.04	100	0.2	373	7	10	1	8	0	399	26
360	78.94	1.07	100	0.1	409	6	12	0	5	0	432	23
370	81.39	1.08	100	0.05	379	0	1	0	0	0	380	1
380	83.39	1.02	100	0.05	371	9	45	1	2	0	428	57
390	85.39	1.02	100	0.1	431	1	50	1	2	0	485	54
400	87.64	1.01	100	0.1	327	1	10	0	0	0	338	11
410	90.64	1.08	100	0.15	395	1	18	1	2	0	417	22
420	93.64	1.04	100	0.1	262	6	22	0	1	0	291	29
430	96.64	1.05	100	0.15	380	3	30	0	1	0	414	34
440	99.39	1.05	100	0.1	419	2	34	0	3	0	458	39
450	101.39	1.03	100	0.1	331	6	25	2	0	0	364	33
460	103.40	1.04	100	0.1	306	4	14	0	0	0	324	18
470	105.40	1.05	100	0.05	303	1	8	0	0	0	312	9
480	107.60	1.08	100	0.2	359	0	8	0	0	0	367	8
490	110.60	1.05	100	0.1	360	1	4	0	2	0	367	7
500	113.30	1.03	100	0.15	435	1	21	0	1	0	458	23

Appendix B. (continued)

sample	age (ka)	*weight(g)*	*vol(ml)*	*slide ml*	*T. hei*	*S. tub*	*S. alb*	*C. ope*	*O. gra*	*R.* spp.	tot. CD	tot.calc Cysts
510	116.20	1.04	100	0.15	357	0	18	0	3	0	378	21
520	119.10	1.05	100	0.05	724	15	68	2	1	0	810	86
530	122.90	1.11	100	0.05	1692	2	64	0.5	0	0	1758.5	66.5
540	124.90	1.05	100	0.05	1339	1	5	1	1	0	1347	8
550	127.30	1.02	100	0.05	1081	2	59	2	1	0	1145	64
560	130.00	0.92	100	0.05	1064	4	30	0	0	0	1098	34
570	132.80	1.01	100	0.05	530	3	21	1	0	0	555	25
580	135.50	1.09	100	0.1	479	6	11	0.5	0	0	496.5	17.5
590	137.90	1.08	100	0.15	330	0	1	1	1	0	333	3
600	140.40	1.06	100	0.1	627	2	5	0	0	0	634	7

Ages after Wefer et al. (1996). Abbreviations: weight (g) = gram of dry sediment used for counting of calcareous dinoflagellates; vol (ml)= ml of ethanol (40%) added to amount of sediment material used for counting; slide (ml): amount on slide counted for calcareous dinoflagellates. Further abbreviations see Appendix A.

4. Concluding Remarks

This dissertation is the result of roughly three years of research on calcareous dinoflagellates, concerning their response to changing environmental factors in culture experiments, their vertical and horizontal distribution in the upper water column of the equatorial and tropical Atlantic Ocean, their cyst-theca relationships and their occurrences within Quaternary sediments. During this time, the central aim has been to contribute to the data basis needed for the evaluation of the applicability of this phytoplankton group as palaeoenvironmental indicators.

The main attention has been focused on the vegetative-coccoid *T. heimii* due to its prominent position among the pelagic calcareous dinoflagellates (Dale, 1992a; Kerntopf, 1997; Höll, 1998). It has been attempted to gain an insight into the ecology of this species to get an impression of the potential use of *T. heimii* in palaeoceanographic reconstructions. The present study is the first comprehensive ecological investigation of *T. heimii* and combines results from laboratory experiments, the euphotic zone and the sediment record.

T. heimii is a cosmopolitic species of warm and temperate waters (Tangen et al., 1982), grows under a wide range of temperatures (14°C to 27°C; see chap. 3.1) and has been observed at all sites of the investigated area in the tropical and equatorial Atlantic Ocean. At first glance this makes the species an unlikely candidate for palaeoenvironmental work: the more restricted an organism is to particular environmental circumstances, the better it can be used to reconstruct its environment. Nevertheless, even though *T. heimii* may be able to adapt itself to environmental change, it has found its special niche. The occurrences of the calcareous stage of *T. heimii* in surface waters (5 m to 200 m depth) show a high variability in both horizontal and vertical distribution patterns. Pronounced maxima of living calcareous *T. heimii* stages occurred in depths between 50 m to 100 m and could be correlated to relatively lower temperatures and relatively higher salinities than surface conditions.

Further research has shown that *T. heimii* is well adapted but not totally restricted to the deep chlorophyll maximum (DCM). The adaptation of the species to the lower euphotic zone shows itself in the laboratory experiments by slow but persistent growth in relatively low temperatures: the species produces higher final yields under the same nutritional conditions when grown in low temperatures than in high temperatures. The response of *T. heimii* to varying light intensities also fits into the reaction of a species preferring to live in deeper levels of the euphotic zone, even though it does not show an avoidance of high irradiation. *T. heimii* is able to grow under both high and low PAR intensities, but, as with temperature, it is

able to produce as much or more cells under conditions that roughly coincide with the lower photic zone than under irradiances equalling surface water conditions.

Large daily migrational movements, as observed for other dinoflagellate species (e.g. for *Cachonina niei*, *Ceratium furca*, *Prorocentrum micans*; Eppley et al., 1968; Olsson and Graneli, 1991), are not observed for *T. heimii*. The locomotive abilities of this predominantly coccoid species are used to move itself to a certain depth and to hold its position within the water column.

As the only dinoflagellate known so far to form a calcareous stage within the DCM that can be preserved as a sedimentary signal, *T. heimii* could have applications as a tracer of nutricline fluctuations and thus of palaeoproductivity of the lower photic zone. Indirectly, since *T. heimii* has its highest occurrences in sediments beneath areas with oligotrophic surface conditions (see chap. 3.5; Vink et al., 2000) it is also possible to make assumptions about the conditions of the upper water layers as well.

For other calcareous dinoflagellates surveyed during the present study (*C. albatrosianum*, *L. granifera* and *P. tuberosa*, chap. 3.4) the distribution pattern in the vertical profiles of the upper water column is less clear. The horizontal distribution of these species, however, could be linked to SST above 22°C.

In the study on calcareous dinoflagellates in two sediment cores from the equatorial and tropical Atlantic Ocean (see chap. 3.5), the distribution of *T. heimii* can be explained by the species' ecology. The research has shown enhanced production of calcareous dinoflagellates (mostly *T. heimii*) during periods of reduced palaeoproductivity. These periods probably also relate to relatively stratified conditions of the upper water column. The "stratified conditions" are meant to describe open ocean oligotrophic conditions relative to upwelling conditions. Since a DCM needs a well stratified water column for its formation (Kirk, 1983), the increase of *T. heimii* during such periods is a reflection of the stability of this deep phytoplankton layer.

5. Perspectives

As with all scientific work, many more questions have arisen from the results of the present study:

What are the applications of T. heimii *in palaeoenvironmental research and how can they be developed further?*

1. *T. heimii* shows strong promise as a tool for the reconstruction of nutricline dynamics and thus palaeoproductivity, but the first detailed reconstruction has yet to be made. To do this, it would be helpful to have a reference value against which the reliability of the new proxy could be checked. Among the calcareous nannoplankton several coccolithophore species are also characteristic for the lower photic zone in subtropic and tropic oceans. The most common of these species adapted to life in the lower photic zone is *Florisphaera profunda* (Okada and Honjo, 1973; Winter et al., 1994). *F. profunda* has been recognised as a powerful tool for Quaternary palaeoceanography. The relative abundance level of the species may be used to determine nutricline dynamics (Molfino et al., 1989; Molfino and McIntyre, 1990a,b), palaeo-waterdepth (Li and Okada, 1985) and mean water transparency (Ahagon et al., 1993).

   It would be interesting to compare *T. heimii* to *F. profunda* both in the plankton and in the sediment to determine the different applications of the dinoflagellate as a new proxy in palaeoceanography.

2. Recent publications have linked high calcareous dinoflagellate occurrences (mostly *T. heimii*) to oligotrophic, relatively stratified conditions of the open ocean (see chap. 3.5; Vink et al., in press). They have also been described as a potential water mass tracer (Vink et al., in press). Another interesting approach would be to measure oxygen isotopes on *T. heimii*. To be able to make routine oxygen isotope measurements on *T. heimii* remains from the sediment, it is necessary to develop a standardised method to accumulate these tiny spheres sufficiently to reach the volume of carbonate presently required by the instruments. Dudley et al. (1980) have determined the oxygen isotopic composition of *T. heimii* grown in batch culture at known temperatures. The oxygen isotopic composition of *T. heimii* shells is strongly temperature dependent (~2.5‰ depleted in ^{18}O relative to equilibrium), which is promising for possible temperature reconstructions of the lower euphotic zone using this species.

What is the reaction of T. heimii *to seasonality?*

Information on the seasonality of *T. heimii* production, and of all other calcareous dinoflagellate species for that matter, is severely limited. To be able to make a statement about seasonal production of *T. heimii*, and of course the other calcareous dinoflagellate species, much work on sediment trap material is needed. During studies on calcareous nannoplankton, size is not the only reason for the exclusion of calcareous dinoflagellates, the

minimum size of *T. heimii* (9 µm) has led to at least a mention of this species, or of what is generally termed 'thoracosphaerids'. It was more the abundance of coccolithophores than the size of *T. heimii* which has led to the neglect of the calcareous dinoflagellate: where sometimes one litre of seawater is sufficient for coccolithophore studies, in some cases ten times as much or more material is needed to allow quantification of the calcareous dinoflagellate assemblage-dominating *T. heimii*. This way calcareous dinoflagellates have usually played a minor role in sediment trap studies on calcareous nannoplankton. A considerable demand for such data has arisen with the increasing interest in calcareous dinoflagellates and is urgently needed to understand the population dynamics in the field.

T. heimii *prefers a certain level in the water column as its habitat. Since this is the case, what specialisation may be used by the other oceanic calcareous dinoflagellate species?*

Aside from the results presented in this dissertation on *T. heimii* (see chap. 3.2 and 3.3) very little is known about the ecology of the other calcareous dinoflagellates. Whether they use the same survival strategy as *T. heimii* (i.e. employing their locomotive abilities to reach a certain depth and stay there), is not clear. In fact, the cyst-theca relationships have only recently been established for some species (Montresor et al., 1997; Janofske, subm.). Thus, detailed life-cycle analyses have not yet been made, and it is mostly not clear if sexual reproduction takes place, what the dominant life stages are, or to what end calcareous skeletons are being included into the life-cycle at all.

For *C. albatrosianum*, *L. granifera* and *P. tuberosa*, at least, no fusion of gametes or formation of planozygotes was observed. In culture, *L. granifera* is the one species closest to *T. heimii* as its calcareous cyst stage is clearly dominant (see chap. 3.4). But *T. heimii* still stands apart from the other species since it is the only calcareous dinoflagellate known so far where the motile stage is not reminiscent of *Scrippsiella* and lacks thecal plates altogether.

Be that as it may, the calcareous skeletons of pelagic dinoflagellates obviously have to play a different role than those formed by neritic calcareous or organic species: in a neritic environment the cysts are for reasons yet unknown often formed at certain times in the year, after which they sink to the bottom. When the resting period is over, excystment takes place and the motile stages move upward (Evitt, 1985). In an open ocean environment such a strategy would be completely useless. The pelagic calcareous dinoflagellates have to leave their cysts in the water column if they are to stay in the photic zone.

As with *T. heimii*, it is imperative to find out where in the water column and under what circumstances the calcareous cysts are formed to understand what the sedimentary record of

these organisms represents. In doing so, it might also be possible to ascertain if the abundance of *T. heimii* shells relative to calcareous dinoflagellate cysts is an indicator of change in the upper water column.

Using the laboratory methods established here, further experiments with calcareous dinoflagellates could be made that will give valuable insights into the mechanics and environmental conditions of cyst formation and the resultant cyst morphology.

Such research should be among the main focus points of future studies both within the plankton and in the laboratory if the calcareous dinoflagellates are to be developed as the useful tool in palaeoceanography they promise to be.

6. References

Ahagon , N., Tanaka, Y. and Ujiié, H., 1993. *Florisphaera profunda*, a possible indicator of late Quaternary changes in sea-water turbidity at the northwestern margin of the Pacific. Mar. Micropaleont., 22: 255-273.

Bjørnland, T., 1990. Chromatographic Separation and Spectrometric Characterization of Native Carotinoids from the Marine Dinoflagellate *Thoracosphaera heimii*. Biochem. Syst. Ecol., 18: 307-316.

Bleil, U., Spieß, V. and Wefer, G. (Editors), 1994. Geo Bremen SOUTH ATLANTIC 1993, Cruise No. 23, 4 Februar-12 April 1993, Meteor Berichte, Vol 94-1. Universität Hamburg, Hamburg, 261 pp.

Brand, L.E. and Guillard, R.R.L., 1981. A method for the precise determination of acclimated phytoplankton and reproduction rates. J. Plankton Res., 3 (2): 193-201.

Bütschli, O., 1885. Protozoa. In: Dr. H.G. Bronn's Klassen und Ordnungen des Thier-Reichs, wissenschaftlich dargestellt in Wort und Bild. C.F. Winter'sche Verlagsbuchhandlung, Leipzig, Heidelberg, Erster Band: pp. 865-1088.

Dale, B., 1992a. Thoracosphaerids: Pelagic Fluxes. In: Dinoflagellate Contribution to the Deep Sea. (Editor: Honjo, S.), Ocean Biocoenosis Series ed., Vol. 5. Woods Hole Oceanographic Institution, Woods Hole, Massachusetts, pp. 33-43.

Dale, B., 1992b. Dinoflagellate Contribution to the Open Ocean Sediment Flux. In: Dinoflagellate Contribution to the Deep Sea. (Editors: Dale, B. and Dale, A.), , Ocean Biocoenosis Series, Vol. No. 5. Woods Hole Oceanographic Institution, Woods Hole, pp. 1-32.

Dale, B. and Dale, A.L., 1992. Ocean Biocoenensis Series, 5: Dinoflagellate Contributions to the Deep Sea. Woods Hole Oceanographic Institution, Woods Hole, Massachusetts, 75 pp.

Dann, O., Bergen, G., Demant, E. and Volz, G., 1979. Trypanocide des 2-phenyl-benzofurans, 2-phenyl-indens und 2-phenyl-indols. Ann. Chem. 749: 68.

Dudley, W.C., Duplessy, Blackwelder, P.L., Brand, L.E. and Guillard, R.R.L., 1980. Coccoliths in Pleistocene-Holocene nannofossil assemblages. Nature, 285: 222-223.

Dürkoop,A., Hale, W., Mulitza, S. Pätzold, J. and Wefer, G., 1997. Late Quaternary variations of sea surface salinity and temperature in the western tropical Atlantic: Evidence from $\delta^{18}O$ of *Globigerinoides sacculifer*. Paleoceanography, 12 (6): 746-772.

Eppley, R.W., Holm-Hansen, O. and Strickland, J.D.H., 1968. Some observations on the vertical migration of dinoflagellates. J. Phycol. 4 (4): 333-340.

Evitt, W.R., 1985. Sporopollenin dinoflagellate cysts. American Association of Stratigraphic Palynologists Foundation, 333 pp.

Fensome, R.A., Taylor, F.J.R., Norris, G., Sarjeant, W.A.S., Wharton, D.I., Williams, G.L., 1993. A classification of living and fossil dinoflagellates. Micropaleontology, Spec. Publ., 7: 351 pp.

Fütterer, D., 1976. Kalkige Dinoflagellaten ("Calciodinelloideae") und die systematische Stellung der Thoracosphaeroideae. N. Jb. Geo. Paläont. Abh., 151 (2): 119-141.

Fütterer, D. 1977. Distribution of calcareous dinoflagellates in Cenozoic sediments of Site 366, eastern North Atlantic. Init. Repts. DSDP, 41: 709-737.

Geitzenauer, K.R., 1969. Coccoliths as late Quaternary palaeoclimatic indicators in the subantarctic Pacific Ocean. Nature, 223: 170-172.

Geitzenauer, K.R., Roche, M.B., McIntyre, A., 1977. Coccolith biogeography from the North Atlantic and Pacific Surface sediments. In: Ramsay, A.T.S. (Editor) Oceanic Micropaleontology. Academic Press, New York, 2, pp. 973-1008.

Gilbert, M.W. and Clark, D.L., 1982. Central Arctic Ocean paleoceanographic interpretations based on late Cenozoic calcareous dinoflagellates. Mar. Micropaleont., 7:385-401.

Guillard, R.R.L., 1973. Division rates. In: Handbook of Phycological Methods. (Editor: Stein, J.R.) Cambridge University Press, pp.289-311.

Guillard, R.R.L. and Ryther, J.H., 1962. Studies of marine planktonic diatoms. I. *Cyclotella nana* Hustedt and *Detonula confervacea* Cleve. Can. J. Microbiol., 8: 229-239.

Hansen, G., 1993. Light and electron microscopical observations of the dinoflagellate *Actiniscus pentasterias* (Dinophyceae). J. Phycol., 29: 486-499.

Hildebrand-Habel, T., Willems, H. and Versteegh, G.J.M., 1999. Variations in calcareous dinoflagellate associations from the Maastrichtian to Middle Eocene of the western

South Atlantic Ocean (São Paulo Plateau, DSDP Leg 39, Site 356). Rev. Palaeobot. Palynol., 00: 1-31.

Höll, C., 1998. Kalkige und organisch-wandige Dinoflagellaten-Zysten in Spätquartären Sedimenten des tropischen Atlantiks und ihre palökologische Auswertbarkeit. Berichte, Fachbereich Geowissenschaften, Universität Bremen, 127: pp.121.

Höll, C., Zonneveld, K.A.F. and Willems, H., 1998. On the ecology of calcareous dinoflagellates: The Quaternary eastern Equatorial Atlantic. Mar. Micropal., 33: 1-25.

Inouye, I. and Pienaar, R.N., 1983. Observations on the life cycle and microanatomy of *Thoracosphaera heimii* (Dinophyceae) with special reference to its systematic position. S. Afr. J. Bot., 2: 63-75.

Janofske, D., 1992. Kalkiges Nannoplankton, insbesondere Kalkige Dinoflagellaten-Zysten der alpinen Ober-Trias: Taxonomie, Biostratigraphie und Bedeutung für die Phylogenie der Peridiniales. Berliner geowiss. Abh., (E), 4: 53 pp.

Janofske, D., 1996. Ultrastructure types in Recent "calcispheres". Bull. Inst. Océanogr., Monaco, 14 (4): 295-305.

Jeffrey, S.W., Sielicki, M. and Haxo, F.T., 1975. Chloroplast pigment patterns in dinoflagellates. J. Phycol., 11: 374-384.

Jones, G.J., Nichols, P.D. and Johns, R.B., 1983. The Lipid Composition of *Thoracosphaera heimii*: Evidence for Inclusion in the Dinophyceae. J. Phycol., 19: 416-420.

Karwath, B., 1995. Verteilung kalkiger Dinoflagellaten der letzten 170 000 Jahre im westlichen Brasil-Becken (Südatlantik, Kern GeoB 2204-2) Unpubl. Dipl. Arb., Fachbereich Geowissenschaften, Universität Bremen, 109 pp.

Keller, D.K., Selvin, R.C., Claus, W. and Guillard, R.R.L., 1987. Media for the culture of oceanic ultraplankton. J. Phycol., 23: 633-638.

Kerntopf, B., 1997. Dinoflagellate distribution patterns and preservation in the Equatorial Atlantic and offshore North-West Africa. Ber. Fachber. Geowiss., 103: 137pp.

Keupp, H., Kohring, R. and Kowalski, F.-U., 1992. Neue Arten der Gattung *Ruegenia* WILLEMS 1992 (kalkige Dinoflagellaten-Zysten) aus Kreide und Tertiär. Berliner geowiss. Abh., (E) 3: 191-209.

Keupp, H., Bellas, S.M., Frydas, D. and Kohring, R., 1994. Aghia Irini, Ein Neogenprofil auf der Halbinsel Gramvoússa/NW-Kreta. Berliner geowiss. Abh., (E), 13: 469-481.

Kirk, J.T.O., 1983. Light and photosynthesis in aquatic ecosystems. Cambridge University Press, 401 pp.

Li, W.-T. and Okada, H., 1985. Relations between floral composition of calcareous nannofossils and paleoceanographic environment observed in three piston cores obtained from the equatorial Pacific, East China Sea and Japan Sea. Bull. Yamagata Univ., Nat. Sci., 11: 177-191 (in Japanese with English abstract).

McIntyre, A., 1967. Coccoliths as paleoclimatic indicators of Pleistocene glaciation. Science, 158: 1314-1317.

McIntyre, A., and Molfino, B., 1996. Forcing of Atlantic Equatorial and Subpolar Millennial Cycles by Precession. Science, 274: 1867-1870.

Molfino, B, McIntyre, A. and Campbell, D., 1989. Equatorial Atlantic nutricline variations aligned with the Younger Dryas. Trans. Amer. Geophys. Union., 70 (43): 1134.

Molfino, B. and McIntyre, A., 1990a. Precessional forcing of nutricline dynamics in the Equatorial Atlantic. Science, 249: 766-769.

Molfino, B. and McIntyre, A., 1990b. Nutricline variation in the Equatorial Atlantic coincident with the Younger Dryas. Paleoceanography, 5: 997-1008.

Montresor, M., Janofske, D. and Willems, H., 1997. The cyst-theca relationship in *Calciodinellum operosum* emend. (Peridiniales, Dinophyceae) and a new approach for the study of calcareous cysts. J. Phycol. 33: 122-131.

Monod, J., 1942. La Croissance des cultures bactériennes. Hermann et Cie, Paris, France.

Okada, H. and Honjo, S., 1973. The distribution of oceanic coccolithophorids in the Pacific. Deep-Sea Res., 20: 355-374.

Olsson, P. and Graneli, E., 1991. Observations on diurnal vertical migration and phased cell division for three coexisting marine dinoflagellates. J. Plankton Res., 13 (6): 1313-1324.

Roth, P.H. and Coulbourn, W.T., 1982. Floral and solution patterns of coccoliths in surface sediments of the North Pacific. Mar. Micropaleont., 7:1-52.

Rowan, R. and Powers, D.A., 1992. Ribosomal RNA sequences and the diversity of symbiotic dinoflagellates (zooxanthellae). Proc. Natl. Acad. Sci. USA, 89: 3639-3643.

Rühlemann, C., 1996. Akkumulation von Carbonat und organischem Kohlenstoff im tropischen Atlantik: Spätquatäre Produktivitäts-Variationen und ihre Steuerungsmechanismen. Berichte, Fachbereich Geowissenschaften, Universität Bremen, 84: pp. 139.

Sorokin, C., 1973. Dry weight, packed cell volume and optical density. In: Stein, J.R. (ed.), Handbook of Phycological Methods. Cambridge University Press, pp. 321-343.

Spurr, A.R., 1969. A low-viscosity epoxy-resin embedding medium for electron microscopy. J. Ultrastr. Res., 26: 31-43.

Tangen, K., Brand, L.E., Blackwelder, P.L. and Guillard, R.R., 1982. *Thoracopsheara heimii* (Lohmann) KAMPTNER is a dinophyte: observations on its morphology and life cycle. Mar. Micropaleont., 7: 193-212.

Tappan, H., 1980. The paleobiology of plant protists. W.H. Freeman and Company, San Francisco, 1028 pp.

Versteegh, G.J.M., 1993. New Pliocene and Pleistocene calcareous dinoflagellate cysts from southern Italy and Crete. Rev. Palaeobot. Palynol., 78:353-380.

Vink, A., Zonneveld, K.A.F. and Willems, H., 2000. Distributions of calcareous dinoflagellate cysts in surface sediments of the western equatorial Atlantic Ocean, and their potential use in palaeoceanography. Mar. Micropaleont., 38:149-180.

Wall, D. and Dale,B., 1968. Quaternary Calcareous Dinoflagellates (Calciodinellideae) and their natural affinities. J. Paleontol., 42 (6):1395-1408.

Wall, D., Dale, B. and Harada, K., 1973. Description of new fossil dinoflagellates from the Late Quaternary of the Black Sea. Micropaleontology, 19 (1):18-31.

Wall, D., Guillard, R.R.L., Dale, B., Swift, E. and Watabe, N., 1970. Calcitic resting cysts in *Peridinium trochoideum* (STEIN) LEMMERMANN, an autotrophic marine dinoflagellate. Phycologia 9 (2): 151-156.

Wefer, G. and cruise participants, 1989. Bericht über die Meteor-Fahrt M 9-4, Dakar-Santa Cruz, 19.2.1989 - 16.3.1989. Berichte, Fachbereich Geowissenschaften, Universität Bremen, 1: 103 pp.

Wefer, G., Berger, W.H., Bickert, T., Donner, B., Fischer, G., Kemle-von Mücke, S., Meineke, G., Müller, P.J., Mulitza, S., Niebler, H.-S., Pätzold, J., Schmidt, H. Schneider, R.R. and Segl, M., 1996. Late Quaternary Surface Circulation of the South Atlantic: The Stable Isotope Record and Implications for Heat Transport and Productivity. In: The South Atlantic Present and Past Circulation. (Editors: Wefer, G., Berger, W.H., Siedler, G. and Webb, D.J). Springer Verlag, Berlin Heidelberg: pp 461-502.

Willems, H., 1988. Kalkige Dinoflagellaten-Zysten aus der oberkretazischen Schreibkreide-Fazies N-Deutschlands (Coniac bis Maastricht). Senckenbergiana lethaea. 68 (5/6): 433-477.

Willems, H., 1992. Kalk-Dinoflagellaten aus dem Unter-Maastricht der Insel Rügen. Z. Geol. Wiss., 20 1(2): 155-178.

Winslow, C.E.A. and Walker, H.H., 1939. The earlier phases of the bacterial culture cycle. Bacterial. Rev., 3: 147-86.

Winter, A., Jordan, R.W. and Roth, P.H., 1994. Biogeography of living coccolithophores in ocean waters. In: Winter, A. and Siesser, W.G. (eds.), Coccolithophores, Cambridge University Press, pp 107-177.

Zonneveld, K.A.F., Höll, C., Janofske, D., Karwath, B., Kerntopf, B. and Willems, H., (in press). Calcareous dinoflagellate resting cysts as paleo–environmental tools. In: Fischer, G., Wefer, G. (eds.) Proxies in Paleoceanography. Springer-Verlag, Berlin, Heidelberg.